

IAEA

International Atomic Energy Agency

Passive Safety Systems in Water Cooled Reactors: An Overview and Demonstration with Basic Principle Simulators

PASSIVE SAFETY SYSTEMS
IN WATER COOLED REACTORS:
AN OVERVIEW AND DEMONSTRATION
WITH BASIC PRINCIPLE SIMULATORS

The following States are Members of the International Atomic Energy Agency:

AFGHANISTAN	GERMANY	PAKISTAN
ALBANIA	GHANA	PALAU
ALGERIA	GREECE	PANAMA
ANGOLA	GRENADA	PAPUA NEW GUINEA
ANTIGUA AND BARBUDA	GUATEMALA	PARAGUAY
ARGENTINA	GUYANA	PERU
ARMENIA	HAITI	PHILIPPINES
AUSTRALIA	HOLY SEE	POLAND
AUSTRIA	HONDURAS	PORTUGAL
AZERBAIJAN	HUNGARY	QATAR
BAHAMAS	ICELAND	REPUBLIC OF MOLDOVA
BAHRAIN	INDIA	ROMANIA
BANGLADESH	INDONESIA	RUSSIAN FEDERATION
BARBADOS	IRAN, ISLAMIC REPUBLIC OF	RWANDA
BELARUS	IRAQ	SAINT LUCIA
BELGIUM	IRELAND	SAINT VINCENT AND THE GRENADINES
BELIZE	ISRAEL	SAN MARINO
BENIN	ITALY	SAUDI ARABIA
BOLIVIA, PLURINATIONAL STATE OF	JAMAICA	SENEGAL
BOSNIA AND HERZEGOVINA	JAPAN	SERBIA
BOTSWANA	JORDAN	SEYCHELLES
BRAZIL	KAZAKHSTAN	SIERRA LEONE
BRUNEI DARUSSALAM	KENYA	SINGAPORE
BULGARIA	KOREA, REPUBLIC OF	SLOVAKIA
BURKINA FASO	KUWAIT	SLOVENIA
BURUNDI	KYRGYZSTAN	SOUTH AFRICA
CAMBODIA	LAO PEOPLE'S DEMOCRATIC REPUBLIC	SPAIN
CAMEROON	LATVIA	SRI LANKA
CANADA	LEBANON	SUDAN
CENTRAL AFRICAN REPUBLIC	LESOTHO	SWEDEN
CHAD	LIBERIA	SWITZERLAND
CHILE	LIBYA	SYRIAN ARAB REPUBLIC
CHINA	LIECHTENSTEIN	TAJIKISTAN
COLOMBIA	LITHUANIA	THAILAND
CONGO	LUXEMBOURG	TOGO
COSTA RICA	MADAGASCAR	TRINIDAD AND TOBAGO
CÔTE D'IVOIRE	MALAWI	TUNISIA
CROATIA	MALAYSIA	TURKEY
CUBA	MALI	TURKMENISTAN
CYPRUS	MALTA	UGANDA
CZECH REPUBLIC	MARSHALL ISLANDS	UKRAINE
DEMOCRATIC REPUBLIC OF THE CONGO	MAURITANIA	UNITED ARAB EMIRATES
DENMARK	MAURITIUS	UNITED KINGDOM OF GREAT BRITAIN AND NORTHERN IRELAND
DJIBOUTI	MEXICO	UNITED REPUBLIC OF TANZANIA
DOMINICA	MONACO	UNITED STATES OF AMERICA
DOMINICAN REPUBLIC	MONGOLIA	URUGUAY
ECUADOR	MONTENEGRO	UZBEKISTAN
EGYPT	MOROCCO	VANUATU
EL SALVADOR	MOZAMBIQUE	VENEZUELA, BOLIVARIAN REPUBLIC OF
ERITREA	MYANMAR	VIET NAM
ESTONIA	NAMIBIA	YEMEN
ESWATINI	NEPAL	ZAMBIA
ETHIOPIA	NETHERLANDS	ZIMBABWE
FIJI	NEW ZEALAND	
FINLAND	NICARAGUA	
FRANCE	NIGER	
GABON	NIGERIA	
GEORGIA	NORTH MACEDONIA	
	NORWAY	
	OMAN	

The Agency's Statute was approved on 23 October 1956 by the Conference on the Statute of the IAEA held at United Nations Headquarters, New York; it entered into force on 29 July 1957. The Headquarters of the Agency are situated in Vienna. Its principal objective is "to accelerate and enlarge the contribution of atomic energy to peace, health and prosperity throughout the world".

TRAINING COURSE SERIES No. 69

PASSIVE SAFETY SYSTEMS
IN WATER COOLED REACTORS:
AN OVERVIEW AND DEMONSTRATION
WITH BASIC PRINCIPLE SIMULATORS

INTERNATIONAL ATOMIC ENERGY AGENCY
VIENNA, 2019

COPYRIGHT NOTICE

All IAEA scientific and technical publications are protected by the terms of the Universal Copyright Convention as adopted in 1952 (Berne) and as revised in 1972 (Paris). The copyright has since been extended by the World Intellectual Property Organization (Geneva) to include electronic and virtual intellectual property. Permission to use whole or parts of texts contained in IAEA publications in printed or electronic form must be obtained and is usually subject to royalty agreements. Proposals for non-commercial reproductions and translations are welcomed and considered on a case-by-case basis. Enquiries should be addressed to the IAEA Publishing Section at:

Marketing and Sales Unit, Publishing Section
International Atomic Energy Agency
Vienna International Centre
PO Box 100
1400 Vienna, Austria
fax: +43 1 26007 22529
tel.: +43 1 2600 22417
email: sales.publications@iaea.org
www.iaea.org/books

For further information on this publication, please contact:

Nuclear Power Technology Development Section
International Atomic Energy Agency
Vienna International Centre
PO Box 100
1400 Vienna, Austria
Email: Official.Mail@iaea.org

PASSIVE SAFETY SYSTEMS IN WATER COOLED REACTORS:
AN OVERVIEW AND DEMONSTRATION WITH BASIC PRINCIPLE SIMULATORS
IAEA, VIENNA, 2019
IAEA-TCS-69
ISSN 1018-5518

© IAEA, 2019

Printed by the IAEA in Austria
April 2019

FOREWORD

The IAEA supports human capacity development in its Member States by providing educational materials and offering training courses on a wide range of nuclear related topics. The IAEA also maintains a series of basic principle simulators, which can be used in educational and training courses to build human capacity. Basic principle simulators can also be used to demonstrate the functionality of several reactor systems, including a variety of passive safety systems. The hands-on approach made possible by these simulators can help further trainees' practical and technical understanding of course material.

Passive concepts enhance overall system reliability, and thus play an important role in meeting the safety related design goals of advanced water cooled reactor technologies. As a result, passive safety systems are being included in many new reactor designs. In response to growing international interest, the IAEA has provided education and training in the fundamentals of passive safety in support of human capacity building efforts that may be of interest to Member States operating, constructing or planning the construction of reactors that utilize these technologies.

This publication is largely adapted from the lectures and course material presented at the National Training Course on Advanced Water Cooled Reactors (WCRs): Physics, Technology, Passive Safety and Basic Principle Simulators held by the IAEA and the Pakistan Institute of Engineering and Applied Sciences (PIEAS) in Islamabad 22–26 January 2018. The course covered the basics of reactor operation, natural circulation phenomena and modelling, and passive safety systems. The concepts taught in course lectures were reinforced with practical training exercises and demonstrations using the IAEA basic principle simulators. The training materials from the course were compiled, edited and supplemented to create this publication as a resource for conducting similar training courses, as a reference for education and training programmes, and for direct use by trainees.

The IAEA officers responsible for this publication were T. Jevremovic and M. Krause of the Division of Nuclear Power.

EDITORIAL NOTE

This publication has been prepared from the original material as submitted by the contributors and has not been edited by the editorial staff of the IAEA. The views expressed remain the responsibility of the contributors and do not necessarily reflect those of the IAEA or the governments of its Member States.

Neither the IAEA nor its Member States assume any responsibility for consequences which may arise from the use of this publication. This publication does not address questions of responsibility, legal or otherwise, for acts or omissions on the part of any person.

The use of particular designations of countries or territories does not imply any judgement by the publisher, the IAEA, as to the legal status of such countries or territories, of their authorities and institutions or of the delimitation of their boundaries.

The mention of names of specific companies or products (whether or not indicated as registered) does not imply any intention to infringe proprietary rights, nor should it be construed as an endorsement or recommendation on the part of the IAEA.

The authors are responsible for having obtained the necessary permission for the IAEA to reproduce, translate or use material from sources already protected by copyrights.

The IAEA has no responsibility for the persistence or accuracy of URLs for external or third party Internet web sites referred to in this publication and does not guarantee that any content on such web sites is, or will remain, accurate or appropriate.

CONTENTS

1. INTRODUCTION	1
1.1. BACKGROUND.....	1
1.2. OBJECTIVE.....	1
1.3. SCOPE	2
1.4. STRUCTURE.....	2
2. OPERATIONAL STATES AND ACCIDENT CONDITIONS IN WATER COOLED REACTORS.....	3
2.1. GENERIC DESIGN OF REACTOR SYSTEMS	3
2.1.1. Generic PWR design.....	3
2.1.2. Generic BWR design	7
2.1.3. SMR concept and application	10
2.1.4. Generic design safety systems	12
2.1.5. System evaluation within the PSA framework	14
2.2. OPERATIONAL STATES	16
2.2.1. Normal operation parameters.....	16
2.2.2. Example fuel pin temperature analysis	21
2.3. ACCIDENTS CONDITIONS	25
2.3.1. Accident classifications	25
2.3.2. Examples of accident progression	26
2.3.3. Lessons learned.....	30
3. NATURAL CIRCULATION	32
3.1. NATURAL CIRCULATION FLOW	32
3.1.1. Overview of natural circulation flow	32
3.1.2. Governing equations of single phase flow	34
3.1.3. Governing equations of two phase flow	41
3.2. CHALLENGES TO NATURAL CIRCULATION	55
3.2.1. Examples for loss of natural circulation flow	55
3.2.2. Examples calculations for thermal stratification.....	60
3.3. COMPUTATIONAL FLUID DYNAMICS MODELLING	75
3.3.1. Computational fluid dynamics concepts.....	75
3.3.2. CFD applications in reactor safety.....	88
3.3.3. Example CFD simulations	92
4. PASSIVE SAFETY SYSTEMS IN ADVANCED WATER COOLED REACTORS..	103
4.1. OVERVIEW AND ASSESSMENT OF PASSIVE SAFETY SYSTEMS.....	103
4.1.1. Design goals of advanced WCRs and passive safety systems.....	103

4.1.2.	Classification of passive safety systems	108
4.1.3.	Challenges to passive safety systems.....	109
4.1.4.	Examples of common passive safety systems	111
4.2.	EXAMPLES OF PASSIVE SAFETY IN ADVANCED REACTOR SYSTEM DESIGNS.....	119
4.2.1.	PWR design example: VVER-1000 (V-466B).....	120
4.2.2.	BWR design example: Economic Simplified Boiling Water Reactor	121
4.2.3.	SMR design example: NuScale Power Modular and Scalable Reactor.....	124
5.	SUMMARY.....	127
	APPENDIX I: PCTRAN TWO-LOOP PWR SIMULATOR.....	129
	APPENDIX II: ADVANCED PASSIVE PWR SIMULATOR	133
	APPENDIX III: INTEGRAL PRESSURIZED WATER REACTOR SIMULATOR.....	137
	REFERENCES	141
	ANNEX: OVERVIEW OF RELATED IAEA LITERATURE.....	145
	GLOSSARY	149
	ABBREVIATIONS	153
	CONTRIBUTORS TO DRAFTING AND REVIEW	155

1. INTRODUCTION

1.1. BACKGROUND

Accident mitigation is an important factor for nuclear reactor design and operation. One major concern following an accident is the reactor core's continuous production of decay heat after shutdown. Safety systems are used to remove this decay heat; however, many rely on movement of fluid or mechanical parts, access to external power, and operator action. As a result, certain events, such as a station blackout, may disable safety systems and compromise decay heat removal. The development and implementation of more robust, more reliable safety systems is an essential design goal of advanced water cooled reactor technologies.

Passive safety systems utilize passive processes such as natural circulation or evaporation, which occur without external power or force, to perform safety related functions including: reactivity control, decay heat removal, maintenance of water inventory, and containment cooling. Passive safety systems are implemented in many advanced WCR designs due to their capacity for enhancing safety and reliability by reducing the need for external interference. Additionally, passive systems are often less prone to disablement in the event of a station blackout or a beyond design basis accident capable of interrupting the power supply or operator signalling capability necessary for the functioning of an active system. In an idealized scenario, fully passive safety systems would create a 'walk away safe' reactor in which no external action or power source would be necessary to maintain safe conditions following a safety related event. Nevertheless, current state of the art passive safety systems may only remain independently operational for a few days in certain accident scenarios due to factors such as loss of coolant water. These systems, however, remain a significant improvement when compared to active safety systems, which rely on constant access to external power or operator action. Due to an increased use in advanced WCR designs, education and training on these passive systems and underlying phenomena are becoming more important.

Basic principle simulators offer an intimate approach for learning reactor operation and design fundamentals. The IAEA maintains a suite of simulators for several reactors, including a variety of WCR technologies, and distributes them freely to interested Member States. Users can simulate accident scenarios and familiarize themselves with the features of simulated reactors. These basic principle simulators can be used to contextualize various reactor phenomena and reactor components in an interactive format. Of specific relevance, these basic principle simulators may be used to demonstrate the functional purpose of safety systems.

1.2. OBJECTIVE

The objective of this publication is to teach advanced WCR passive safety concepts through lessons on the standard design, operational states and accident conditions in WCRs; the phenomena and modelling of natural circulation; and the application of passive safety systems to advanced WCR designs whilst supporting these lessons with examples created in PC based basic principle simulators.

1.3. SCOPE

The scope of this publication is to explain the underlying phenomena, modelling methodology, and application of passive safety systems in advanced WCR designs, that is in WCRs which achieve improvements over previous and/or existing designs through either ‘evolutionary’ or ‘innovative’ designs; evolutionary designs achieve improvements through small or moderate changes to existing designs, where innovative designs incorporate more radical conceptual changes [1]. Explanations and examples are limited to light water reactors (LWRs). Following an overview of standard LWR design and operation, this publication provides detailed explanations of natural circulation phenomena and flow modelling as they relate to passive safety systems in advanced WCRs. The publication further provides an overview of passive safety systems and examples of their applications in advanced LWR designs. Representative demonstrations from educational basic principle simulators are used to reinforce the presented concepts.

1.4. STRUCTURE

This publication contains three content sections, each of which consists of subsections for various lesson topics:

- (a) **Operational States and Accident Conditions in Water Cooled Reactors** provides relevant information on standard LWR design, normal operation, and accident scenarios.
- (b) **Natural Circulation** explains the concepts and governing equations of natural circulation flow.
- (c) **Passive Safety Systems in Advanced Water Cooled Reactors** provides an overview of the design goals of advanced reactors as well as discusses passive safety systems and their applications in various advanced reactor designs.

These are followed by a short summary of passive safety system use.

The appendices of this publication reinforce lesson concepts through representative example demonstrations of passive safety systems created using basic principle simulators.

2. OPERATIONAL STATES AND ACCIDENT CONDITIONS IN WATER COOLED REACTORS

Despite serious design efforts and implementation of safe operation practices, several accidents have occurred in WCRs. These accidents, however, are part of the driving force which motivates demand for further safety developments in the nuclear energy field. Giving context to discussion of phenomena and systems in later sections, generic designs and safety considerations of WCRs are presented and accident classifications described. Discussion of accidents are supplemented by example accident progressions taken from the Three Mile Island and Fukushima Daiichi accidents. The lessons learned from these accidents support the need for improvement of human capacity building and the use of advanced safety systems.

2.1. GENERIC DESIGN OF REACTOR SYSTEMS

First, generic pressurized water reactor (PWR) and boiling water reactor (BWR) designs are presented; small modular reactor (SMR) concepts are briefly explained. Also discussed are some of the safety systems typically used in WCRs and explanations of their function and purpose. These generic designs and safety system operation are essential background knowledge for understanding the phenomena, technology, and motivation involved in the development of passive safety systems for advanced WCRs.

2.1.1. Generic PWR design

The PWR is the most commonly used reactor for electricity generation worldwide and is based upon preliminary concepts pioneered by the US Navy. In this concept, water remains liquid throughout the entire primary loop (i.e. no boiling in the core during normal operation). This ensures that minimal radiation shielding is needed to protect staff and personnel. FIG. 1 shows a typical, full PWR system.

These systems consist of a primary and a secondary fluid system. The primary system has water flowing directly through the nuclear reactor core past the fuel rods, where it is heated to the design hot leg temperature (typically around 329 °C). This hot coolant is maintained at a pressure of around 15.5 MPa to prevent boiling. The hot coolant is then run through a steam generator where secondary water at approximately 6.9 MPa is boiled to steam. This steam is sent to the turbine system, after which it is condensed and pumped back into the steam generator. The primary loop water, after boiling the secondary water and being cooled to 292 °C, is then sent through the reactor coolant pumps back into the reactor pressure vessel. More detailed parameters can be found in Table 1 [2].

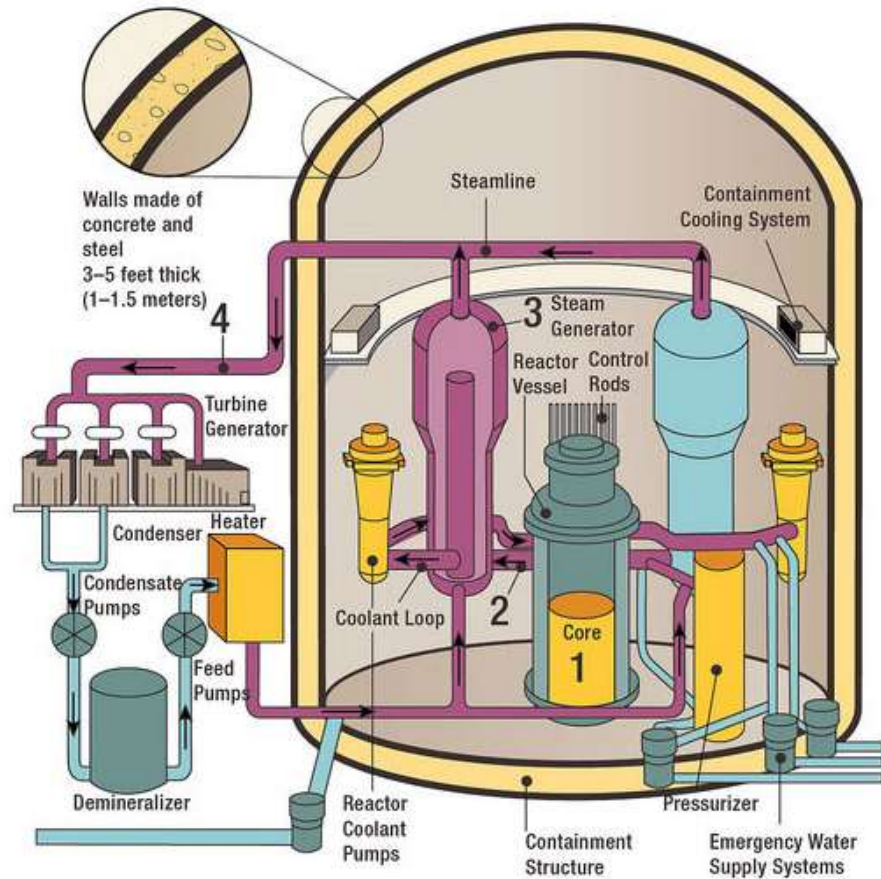


FIG. 1. Typical PWR system [3].

TABLE 1. BASIC OPERATING PARAMETERS OF A GENERIC PWR

CHARACTERISTIC	VALUE	CHARACTERISTIC	VALUE
POWER		REACTOR PRESSURE VESSEL	
Thermal output	3800 MW	Inside diameter	4.4 m
Electrical output	1300 MW	Total height	13.6 m
Efficiency	0.34	Wall thickness	22.0 cm
CORE		FUEL	
Length	4.17 m	Cylindrical fuel pellets	UO ₂
Diameter	3.37 m	Pellet diameter	8.19 mm
Specific power	33 kW/kg(U)	Rod outer diameter	9.5 mm
Power density	102 kW/L	Zircaloy clad thickness	0.57 mm
Av. Linear heat rate	17.5 kW/m	Rod lattice pitch	12.6 mm
Rod surface heat flux		Rods/assembly (17 × 17)	264
Average	0.584 MW/m ²	Assembly width	21.4 cm
Maximum	1.46 MW/m ²	Fuel assemblies in core	193
REACTOR COOLANT SYSTEM		Fuel loading	115 × 10 ³ kg
Operating pressure	15.5 MPa (2250 psia)	Initial enrichment % U-235	1.5/2.4/2.95
Inlet temperature	292 °C	Equil. Enrichment % U-235	3.2
Water flow to vessel	65.9 × 10 ⁶ kg/h	Discharge fuel burnup	33 GWd/Tu
STEAM GENERATOR		REACTIVITY CONTROL	
Number	4	No. control rod assemblies	68
Outlet steam pressure	1000 psia	Shape	Rod cluster
Outlet steam temp.	284 °C	Absorber rods per assembly	24
Steam flow at outlet	1.91 × 10 ⁶ kg/h	Neutron absorber	Ag-In-Cd
		Soluble poison shim	Boric acid H ₃ BO ₃

The three major components of the primary system are the reactor pressure vessel (RPV), the pressurizer, and the steam generators. A typical PWR RPV is illustrated in FIG. 2. The RPV has several water inlet nozzles, where coolant water from the reactor coolant pumps enters the outer annular region of the vessel. This water flows downward through the vessel until it reaches the bottom of the RPV where it turns 180° to flow past the core support assembly. This water flows past the fuel rods, where it is heated by fission energy, and then exits the core via the upper fuel assembly alignment plate. This hot water then enters the outlet plenum, where it is funnelled into water outlet nozzles and directed to steam generators. Note that for the PWR, the control rods are inserted through the top of the core, driven by the control rod drive mechanisms outside the RPV. The instrumentation tubes, however, are inserted into the bottom of the core through the bottom of the RPV. One of the challenges facing new reactor construction is the lack of current expertise in forging large high pressure single forging vessels, as is required in current designs for new PWRs.

The reactor core, found at the heart of the reactor pressure vessel, for this common design is comprised of 193 fuel assemblies arranged in a cylindrical pattern on top of the core bottom support plate. These assemblies, sketched in FIG. 3, contain 264 fuel rods arranged in a square 17×17 pattern, held in place by top and bottom nozzles and a series of grid spacers. The fuel rods slide into place within the top and bottom nozzles and are held by mechanical spring mechanisms located in the spacer grids along their length. In each fuel assembly, there are locations where fuel rods are replaced by control rod guide tubes. These guide tubes serve as a sleeve where control rods can be raised and lowered through the core to achieve the desired neutron absorption.

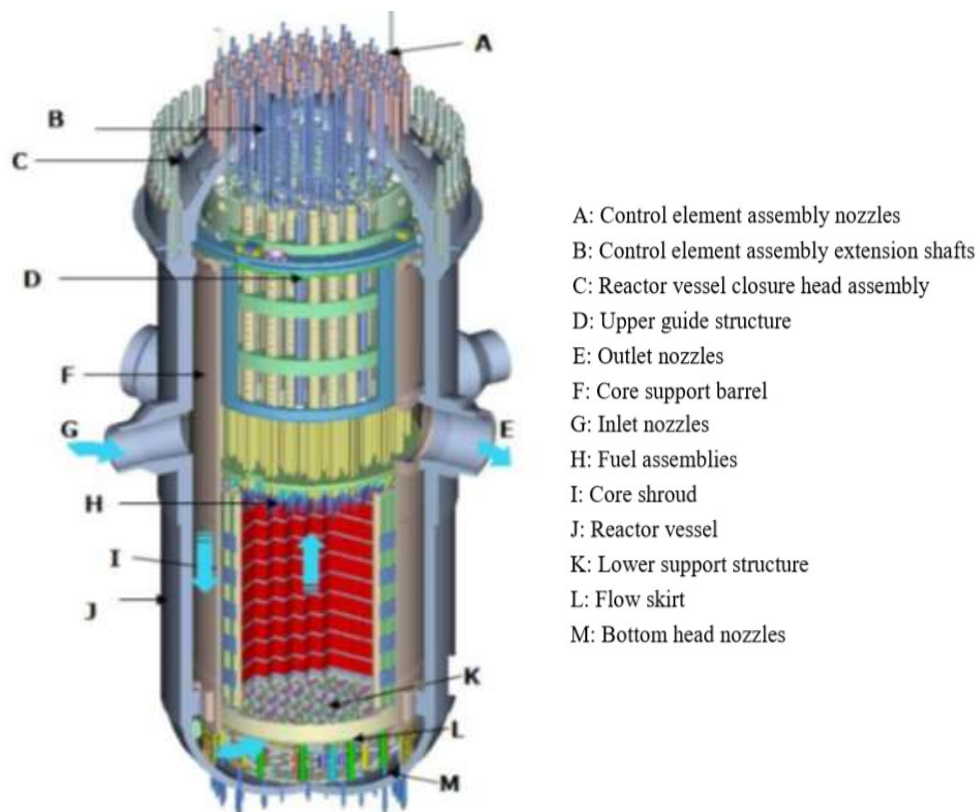


FIG. 2. Schematic of a PWR reactor pressure vessel, with key components labelled [4].

The steam generator component (illustrated in FIG. 3) primarily serves to provide sufficient heat exchange to facilitate boiling of the low pressure secondary water using the high pressure primary water. The primary water enters the steam generator in the bottom where it enters one leg of U shaped tubes and flows upward through the tube and back down the other leg where it exits the steam generator. As a note, the steam generator tubes are U shaped in order to prevent buckling stresses upon thermal expansion of the tubes. The secondary coolant flows on the shell side of the steam generator, and after undergoing phase transition, flows upwards through moisture separators and through the steam outlet to turbines.

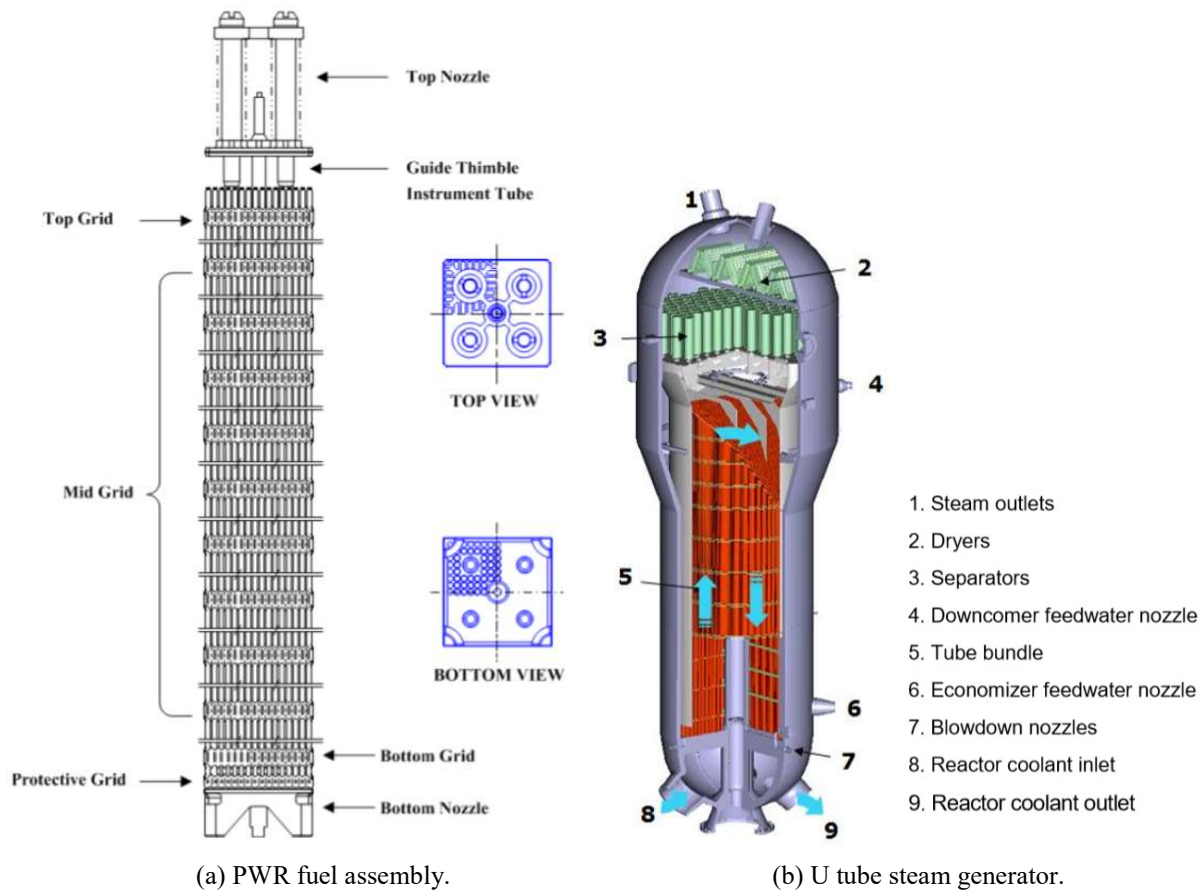


FIG. 3. Labelled sketches of PWR (a) fuel assembly and (b) U tube steam generator [4].

The primary system arrangement, illustrated in FIG. 4, is typically made up of the following components:

- (a) Two, three, or four loops of piping (depending on the PWR design);
- (b) Two, three, or four U tube steam generators;
- (c) Two, three, or four reactor coolant pumps;
- (d) One pressurizer;
- (e) One reactor pressure vessel.

Note in FIG. 4 the orientation and arrangement of the steam generators, including the secondary loop inlets. The reactor coolant pumps are located on the cold leg, typically after the steam generator, while the pressurizer is located on one of the hot legs.

The pressurizer serves as the key pressure regulating component in a PWR. There is typically both liquid water and steam inside the pressurizer. Spray nozzles and heater elements are used in the pressurizer to regulate reactor pressure by modifying the amount of steam inside the fixed volume of the pressurizer. For example, if the steam pressure in the reactor decreases, the pressurizer will increase pressure in the system by using the heaters to boil some of the water in the pressurizer into steam. This steam mass increases, in turn increasing the system pressure. If the reactor pressure increases beyond a setpoint, the spray nozzles spray cool water through the steam to condense it and decrease the total steam mass. This results in a reduction of the total pressure in the system. In this way, the pressurizer component, depicted in FIG. 4, controls pressure inside the PWR primary loop.

Although this lesson has described the systems, structures, and components for a typical PWR, there is very little uniformity from plant to plant. Additionally, there are many different PWR designs that are being developed and licensed for future operation. These designs vary greatly in concept and application, though all share the common features described above.

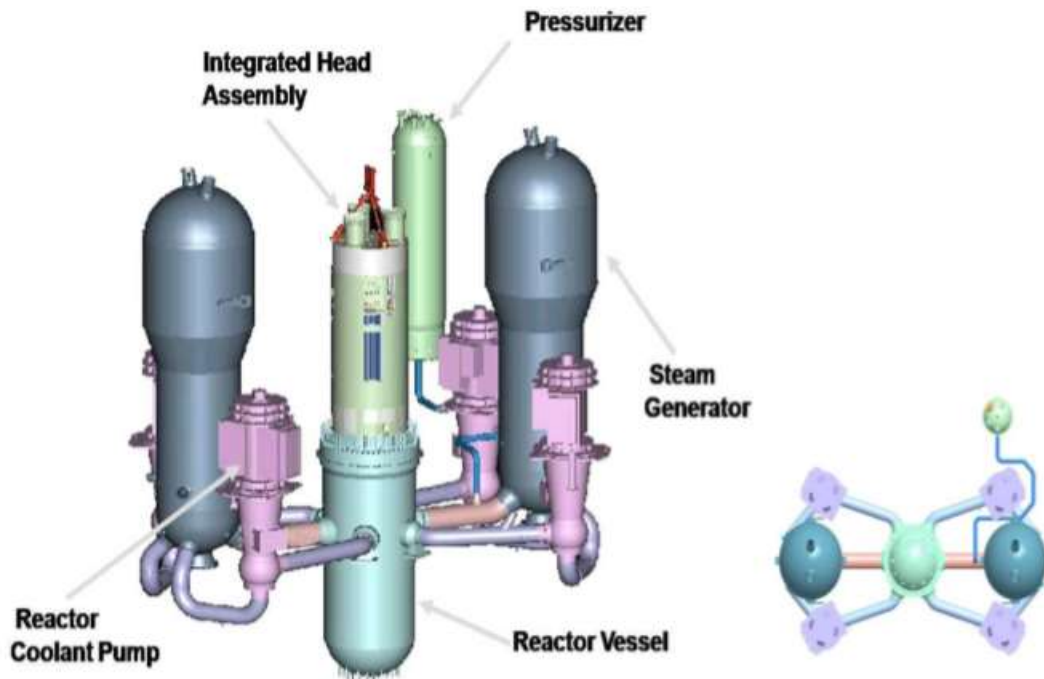


FIG. 4. Sketches of key components in a two loop PWR [4].

2.1.2. Generic BWR design

Boiling water reactors are most commonly identified by having a single coolant loop. This means that the coolant loop combines core cooling and power conversion functions. Unlike in a PWR, where the primary coolant is separated from the power conversion system, in a BWR the entire power conversion system becomes radioactive and requires shielding. Further, pressure disturbances anywhere in the system will affect core reactivity coefficients. A typical, full BWR system is shown in FIG. 5.

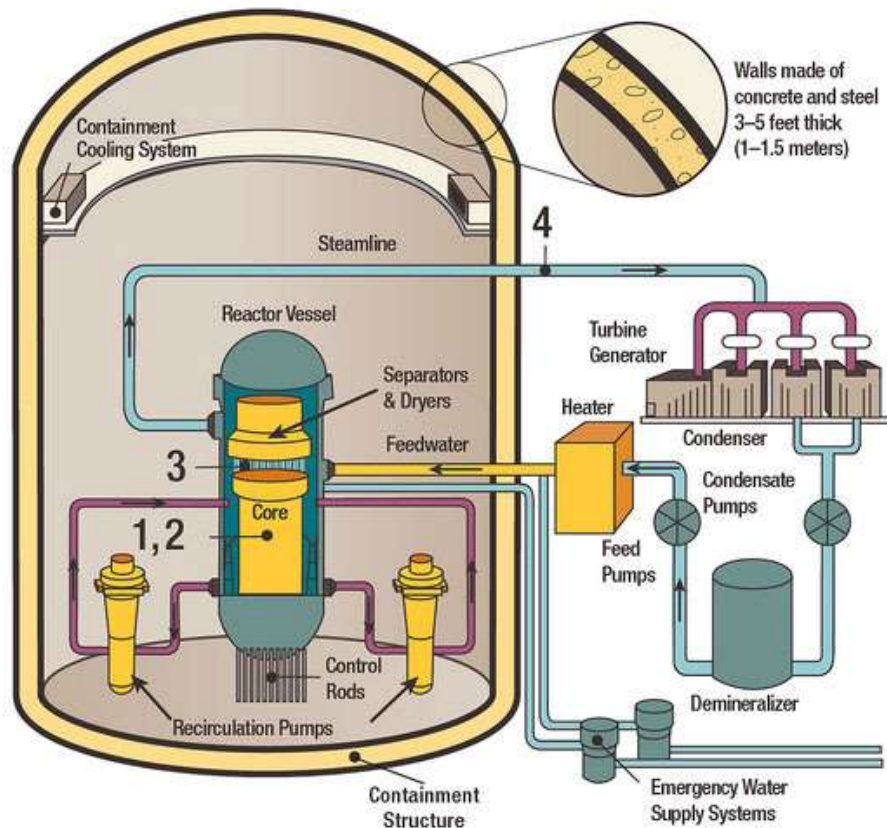


FIG. 5. Typical BWR system [5].

As with a PWR, the reactor is often cooled by light water, which flows inwards through feed water nozzles, then downward through the annular region external to the core barrel. This water then turns at the bottom of the vessel and flows upwards through the core to outlet piping. Both reactor concepts depend on the generation of heat in a nuclear core, the removal of this heat through a coolant, the moderation of the core through the coolant, and the generation of electricity by converting this heated coolant flow into mechanical work.

Unlike a PWR, the primary coolant in a BWR is also used as the working fluid for the power conversion system. The coolant, upon being heated by fuel rods, is a saturated steam–water two phase flow mixture, with many water droplets being entrained in the steam flow. Thus, of necessity, there is significant need for both steam separators and steam dryers in the top of the reactor vessel above the core. These serve the function of removing entrained water droplets so that the steam quality can reach the 99.9% value required for effective and long term turbine operation. Once dried, the primary coolant steam is transferred via the main steam line to the turbine generator, where it is used to drive a high pressure turbine and two to three low pressure turbines per loop. Between the high and low pressure turbines, reheating is used to optimize efficiency. The turbine effluent is then pumped through a demineralizer, where the water chemistry is controlled, and back into the reactor pressure vessel via the main feed lines. Recirculation jet pumps are used to maintain the flow through the primary coolant system. Key parameters for a standard BWR are given in Table 2 [2].

TABLE 2. KEY BWR PLANT PARAMETERS

OVERALL	
Total heat output	3293 MW
Electrical output	1100 MW
Vessel dome pressure	71.7 kg/cm ²
Main steam flow	6410 tons/hr
Feedwater temperature	215.5 °C
Turbine	TC6F 41 in
Reheat	No reheat
Overall efficiency	33.40%
NUCLEAR BOILER	
Reactor vessel	
Inner diameter	6.4 m
Outer diameter	22.1 m
Power density	50.0 kW/L
Fuel assemblies	764
Assembly configuration	8 × 8
Control rod materials	185 B ₄ C

The BWR has a substantially different core design than the PWR, primarily due to the fact that substantial water vapour may be present in the core throughout operation. This could contribute to flow instabilities, reactor feedback loops, and vibration challenges. Thus, BWR cores employ closed fuel assemblies, as depicted in FIG. 6. Because the fuel rod assemblies are enclosed in channels by an assembly wall, control rods are shaped as a cruciform instead of a rod, and this cruciform configuration fits between individual assemblies. Further, these control rods are inserted from the bottom of the core, rather than the top, since the top of the core has a large fraction of water vapour, and thus the control rods would be significantly less effective in this region.

As with a PWR, the BWR reactor vessel is enclosed in a containment structure, and flow passes from the reactor vessel to the turbine generators through containment penetrations, then from the feed pumps back into the reactor vessel through additional penetrations.

Finally, it is significant to note that due to the presence of water vapour in the core for BWRs, there is a strong need to adjust the vapour fraction to control reactivity feedbacks for short term control. This is accomplished in a BWR through the recirculation loop. This loop is driven by jet pumps, which can vary the water flow through the core, thus adjusting reactivity feedbacks during steady state operation. A schematic of a BWR jet pump is included in FIG. 7. This pump drives high pressure, high velocity water through a venture nozzle to create a suction flow of vessel water downward between the vessel wall and the core barrel wall, which then passes upward through the core.

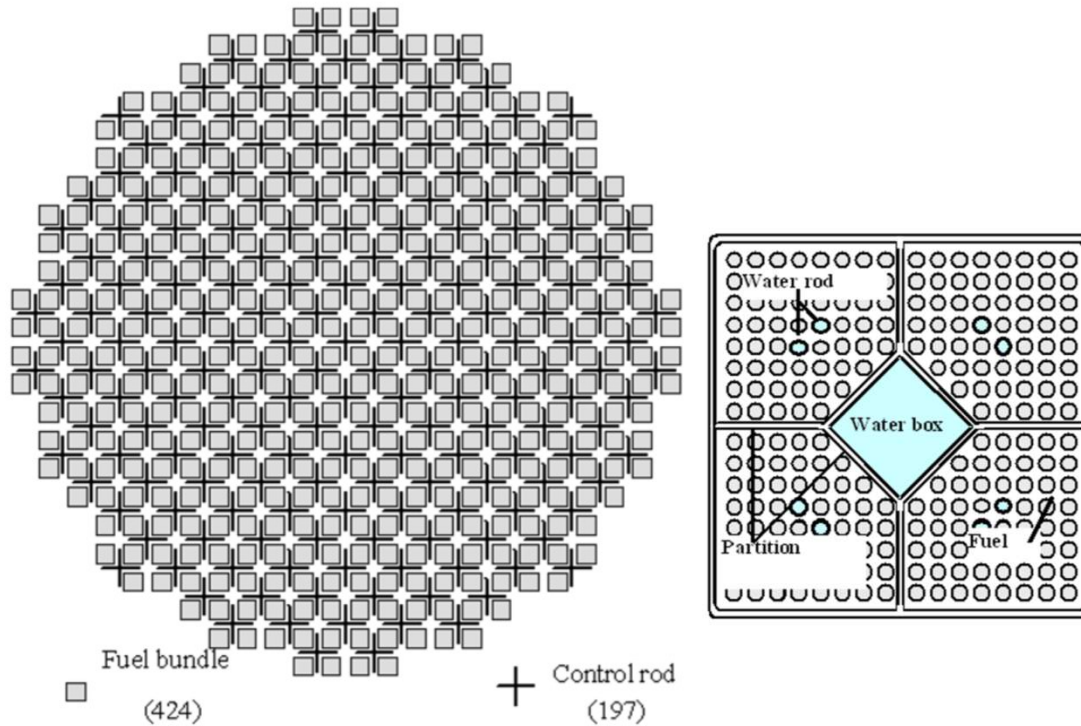


FIG. 6. Sketches of BWR fuel module with closed fuel channel assemblies and cruciform control rod [4].

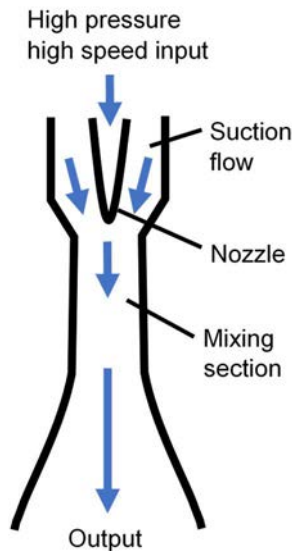


FIG. 7. BWR jet pump concept [2].

2.1.3. SMR concept and application

Small modular reactors are defined as reactors which produce a maximum of 300 MW(e) and which are designed for production in factories before being transported to plant sites. SMR designs use a variety of different coolants but, while much of the discussion applies to SMRs globally, the focus of this discussion will be on water cooled SMRs.

SMRs utilize very similar base concepts to those of large WCRs, however there are several advantages to their smaller size; in comparison to large reactors, SMRs typically have [6]:

- Improved power generation flexibility;
- Enhanced safety through inherent features resulting from scale (e.g. lower mass of fissile material);
- Economic affordability (initial capital, generating cost is likely higher);
- High suitability for non-electric applications;
- Valid deployment options for remote areas;
- Shortened plant construction time.

As a result, significant global interest has led to many new SMR designs in recent years. These systems vary greatly from one to the next, however many water cooled SMR designers have adopted integral reactor concepts where most or all primary system components are located within the reactor vessel, as shown in FIG. 8. By eliminating complex piping and other external systems, these designs further simplify the construction process.

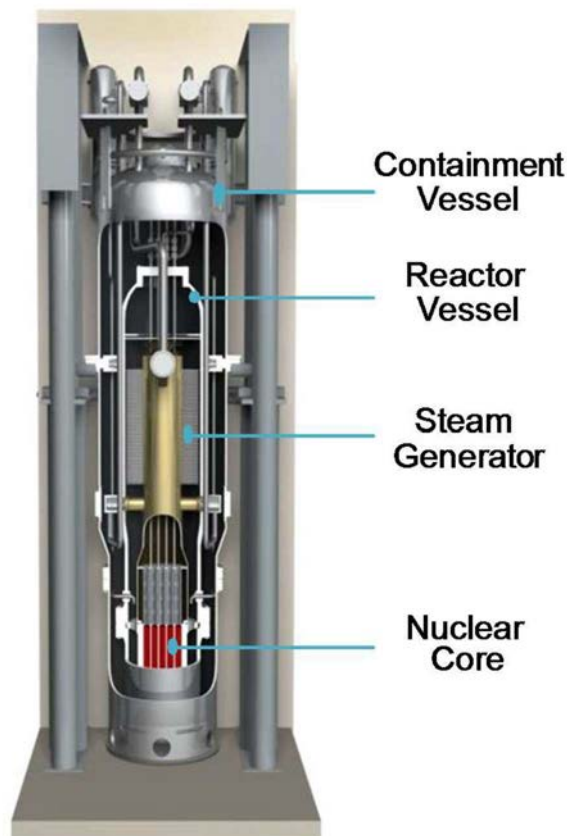


FIG. 8. Integral SMR layout of NuScale module [4].

The novelty of new SMR systems raise several issues, including how to deal with the following:

- Control room staffing at multi-unit sites;
- Defining emergency planning zones at multi-unit sites (source term definition);
- Developing codes and standards.

Further information on the development status and designs of specific SMRs are available from [7] and other IAEA publications.

2.1.4. Generic design safety systems

Safety systems ensure safe reactor shutdown, provide residual heat removal, and limit the consequences of anticipated operational occurrences and design basis accidents. There are seven safety systems which may be considered part of a generic nuclear plant design:

- (1) Reactor protection system (RPS);
- (2) Essential service water system (ESWS);
- (3) Emergency core cooling system (ECCS);
- (4) Emergency electrical system;
- (5) Containment system;
- (6) Standby gas treatment system;
- (7) Ventilation and radiation protection systems.

The functionality of each of these systems is described in the following paragraphs.

(1) Reactor protection system

The reactor protection system consists of two primary parts: control rods, and safety injection standby liquid control.

The control rods are composed of a material that has a high neutron cross section, typically boron or hafnium. Upon insertion into the core, the neutrons contributing to fission in the fuel are instead absorbed by the control rods, decreasing the multiplication factor of the core. By inserting the control rods completely and quickly, or in other words, by preventing the steady fission reactions via ‘scram’ of the control rods, the fission reaction can be reduced to subcritical levels and the number of fissions decreased to near zero.

In the case of a loss of coolant accident (LOCA), cooling in the primary system is lost through a leak. In this scenario, it is important to both BWR and PWR safety to be able to replenish water supply in an attempt to prevent core uncover. In a BWR, this occurs via a standby liquid control system, which contains water and dissolved boron (also known as boric acid) and is injected into the core in the case of a low water level. In a PWR boric acid is required to completely shut down the reactor, so large tanks of boric acid are on hand to provide safety injection to stop fission reactions within the core.

(2) Essential service water system

Many components inside the reactor (pumps, heat exchangers, structures, etc.) are cooled via heat exchange to low temperature cooling water. This water is essential for several decay heat removal systems. For this reason, the supply of ‘service water’ is an essential safety function to maintain the cooling capacity of safety systems. A cooling tower is often incorporated into this system to maximize heat rejection efficiency.

(3) Emergency core cooling system

The emergency core cooling system is the most direct defence against core heating and melting. It is a complex system with several subsystems, including:

- (i) A high pressure injection system, which is capable of injecting makeup water into the primary system in case of dropping liquid levels at high pressures. This subsystem is designed to automatically actuate when the coolant system drops below a predetermined liquid level within the primary coolant loop.
- (ii) An automatic depressurization system (ADS), which consists of a series of valves attached to the primary coolant system. These valves are designed to actuate and decrease the pressure in both PWRs and BWRs, with steam being vented into a liquid water pool.
- (iii) A low pressure injection system, which pumps coolant into the primary reactor loop once pressure has been decreased via an ADS.
- (iv) A containment cooling spray system, which is designed to spray cold coolant into the containment building to condense steam and decrease pressure within the containment.
- (v) Accumulators, containing pressurized coolant which is injected into the primary loop passively on loss of pressure (this system is discussed in more depth in a later chapter).
- (vi) In the case of a BWR, a spray system is used to directly spray cool liquid on the core to facilitate enhanced cooling of the core and reduce the amount of steam that is generated.

Note that each ECCS subsystem is required during one or several accident conditions, and a significant portion of licensing and design efforts is dedicated to the design, operation, and preservation of these ECCS subsystems.

(4) Emergency electrical system

Electrical energy is required to utilize the ECCS, ESWS, and RPS for currently operating systems. These active systems will fail in the case of loss of electrical power (such as station blackout) and thus a backup electrical system is required to facilitate pumps, valve actuation, and other minor mechanical functions. The emergency electrical systems consist of:

- (i) Diesel generators, which can provide AC power sufficient to power the safety systems and safely shut down the power plant upon initiation. It is required that multiple sets of generators with different locations and connections be included to provide redundancy of operation.
- (ii) Flywheels, which require additional mechanical energy to begin rotating (such as on pumps) but then continue to spin upon loss of electrical power, providing a continuous supply of power in the initial stages of an accident to ECCS and ESWS systems.
- (iii) Batteries, which are not sufficient to run pumps and other heavy equipment, but that provide sufficient DC power to actuate valves, run automatic control systems, and provide measurements regarding the state of the power plant.

(5) Containment system

The containment systems are physical barriers designed to prevent the release of radiation to the public. Though it is possible to breach a single containment system in accident scenarios, several containment systems are incorporated into light water reactors in order to prevent public dose via failure of individual containment system. The typical containment systems for water cooled reactors include:

- (i) Fuel cladding, which is the protective coating around the fuel designed to prevent release of fission products. A gas plenum within the fuel cladding is used to capture and store gaseous fission products.
- (ii) Reactor vessel, which is the pressure vessel immediately surrounding the nuclear core. This vessel is designed to withstand high pressures at high temperature to prevent rupture.
- (iii) Containment system, a physically closed structural barrier to prevent or control radioactive substance releases.
- (iv) In a BWR, a secondary containment is included around the primary coolant loop. This is because the radioactive coolant in a BWR extends all the way to the power generation system and would not be contained by only a reactor vessel.

(6) Standby gas treatment system

The standby gas treatment system filters and pumps air out of the containment building to maintain a slight negative pressure inside. This is to prevent leaking of radioactive gasses to the environment, which could contribute to a dose to the public.

(7) Ventilation and radiation protection systems

In circumstances where radioactive releases may occur, ventilation and release systems are designed to remove radiation from the air to minimize the impact on affected persons. This includes purification of control room air to protect operators, as well as purification of air leaving the containment to protect the public.

Ventilation systems also serve to ensure adequate atmospheric conditions within the reactor containment system are maintained to prevent damage to structures, systems or components; for example, vented release of gas from containment may prevent combustible hydrogen mixtures from forming under some severe accident conditions.

2.1.5. System evaluation within the PSA framework

Extensive system models are used in performance evaluations of safety systems and their impact on overall plant safety requires evaluation in a probabilistic safety analysis (PSA), also commonly referred to as probabilistic risk assessment (PRA), framework. FIG. 9 illustrates the methodology of a risk analysis for a nuclear system, structure or component. The following steps show an example procedure for PSA or PRA:

- (i) Identify initiating events for analysis (e.g. broken pipe, flood, failed pumps, fires, etc.).
- (ii) Perform a fault tree analysis — branching evaluation of event progressions.
- (iii) Evaluate and propagate reliabilities, probabilities, and impact of each event, ultimately determining core damage frequencies and radiation exposure amounts for each path. The dominant event chains are highlighted and tabulated for use in evaluating cumulative probabilities for damage and radioactive release in Table 3 [8]. In this table, each containment event tree sequence (CET SEQ) is assigned a release category (REL CAT) with a plant damage state (PDS) occurring with a calculated frequency (FREQ).
- (iv) Sum the probabilities for each chain along to the failure tree to determine overall core damage frequencies and exposure rates.

Reference [9] provides a detailed description of the development and application of a Level 1 PSA.

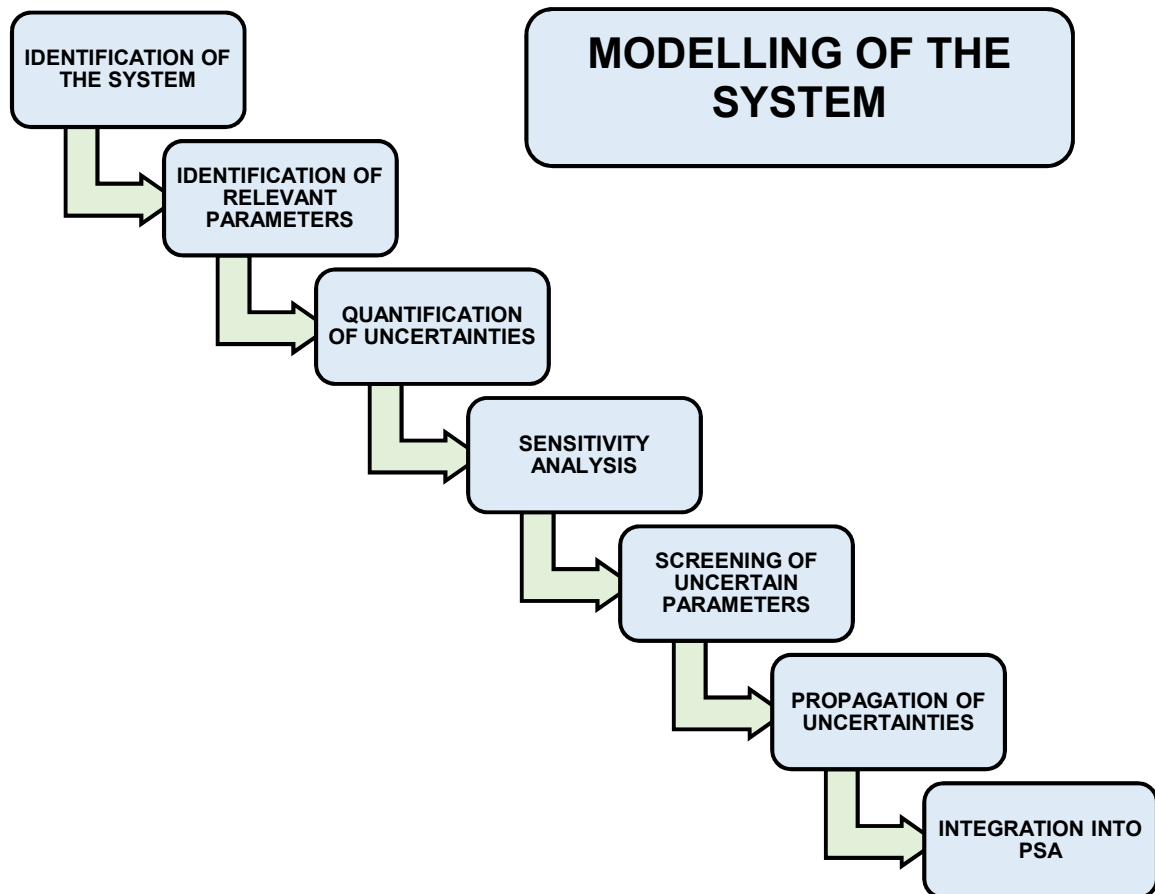


FIG. 9. Demonstration analysis methodology for nuclear systems [10].

TABLE 3. DOMINANT CONTAINMENT EVENT TREE SEQUENCES FOR AP1000

CET SEQ	REL CAT	PDS	FREQ	%	SEQUENCE DESCRIPTION
23	BP	3A	4.08×10^{-9}	20.9	Containment bypass
23	BP	6	3.78×10^{-9}	19.4	Containment bypass
21	CFE	2E	2.67×10^{-9}	13.7	Sump flooding fails
21	CFE	3D	2.05×10^{-9}	10.5	Sump flooding fails
23	BP	1A	2.04×10^{-9}	10.5	Containment bypass
10	CFE	3C	9.97×10^{-10}	5.1	Vessel failure
12	CFE	3D	9.71×10^{-10}	5.0	Core reflooding fails, diffusion flame
23	BP	1P	6.05×10^{-10}	3.1	Containment bypass
22	CI	2L	5.83×10^{-10}	3.0	Containment isolation fails
21	CFE	6	1.86×10^{-10}	2.4	Hydrogen igniters fail, early deflagration to detonation transition
22	CI	3D	3.62×10^{-10}	1.9	Containment isolation fails
21	CFE	6	1.86×10^{-10}	1.0	Sump flooding fails
4	CFI	2E	1.82×10^{-10}	0.9	Hydrogen igniters fail, intermediate deflagration to detonation transition

2.2. OPERATIONAL STATES

Key parameters of interest for a normally operating WCR can be assessed by evaluating mass, energy, and momentum balances at key locations. The most significant parameters of interest include thermodynamic efficiencies, peak clad and pin temperatures, pump power and reactor coolant pump flow rate, reactor pressure, and steam generator heat exchange properties. Appropriate margins are then applied to assure safe performance during normal operation of the reactor.

2.2.1. Normal operation parameters

2.2.1.1. Operational limits and conditions

Operational limits and conditions (OLCs) set boundaries for key operation parameters to prevent fuel failure or plant damage and minimize radiation releases. The OLCs include [11]:

- Safety limits, which are based on the prevention of radioactive material release by limiting fuel and cladding temperatures, coolant pressure, and other parameters necessary to maintain pressure boundary integrity.
- Limiting safety system settings, which are based on limiting pressure and temperature transients and are used to initiate trips, automatic actions, and safety systems to prevent reaching of a safety limit.
- Limits and conditions for normal operation, which ensure safe operation under the assumptions of a safety analysis report and includes considerations such as minimum staffing or amount of equipment and discharge limits for radioactive material release.
- Surveillance requirements, which ensure that all operating limits and conditions are met through inspections, monitoring, calibration, and testing.

OLCs are based on an individual plant's analysis and are incorporated into that plant's operating procedures and inspection programme. The key operation parameters which they describe are applied in areas such as reactivity control, core cooling, and radiation containment capabilities of the reactor. Brief descriptions of these three applications and some examples of the key parameter OLCs are included.

Reactivity control consists of negative reactivity capabilities and positive reactivity limits. It is essential to maintain the capability to put the reactor in a subcritical state from any operational or accident condition for an indefinite period of time. Reactor criticality must be controlled and remain within a window of acceptable values. Operators are able to add negative reactivity by way of control rod position and adjustment of soluble neutron absorber concentrations while taking consideration of other factors such as reactivity coefficients (e.g. fuel temperature, coolant density, etc.). In operations such as reactor startup, limits on the rate of positive reactivity insertion must be set to prevent unplanned neutron excursions, excessive temperatures, or undesirable neutron or heat flux distributions.

Core cooling must be maintained in all conditions, operating or accident, to prevent melting of fuel or damage to the plant. Key operation parameters often focus on thermodynamic properties, such as reactor coolant system temperature and pressure. Temperature and pressure of the coolant system are important to maintain as they have a direct relation to the effectiveness of heat transfer from the fuel to coolant. As a result, operators have a number of available mechanisms to adjust these parameters to keep the reactor (fuel, cladding, coolant) within acceptable temperature ranges.

Radiation releases are minimized in several ways. Boundaries such as fuel cladding, the reactor pressure vessel, and containment are maintained by way of operating within set boundaries (i.e. minimizing thermal stress and maintaining safe coolant pressures) and undergo scheduled inspections. Additional considerations are made to limit the anticipated leaks and releases which result from operation (e.g. use of pressure release valves).

Some of the key parameters which are not directly measured, such as fuel cladding temperature, may have an associated OLC in other closely related parameters such as coolant temperature. FIG. 10 demonstrates the interrelationship of safety limits, safety system settings, and operational limits for fuel cladding temperature.

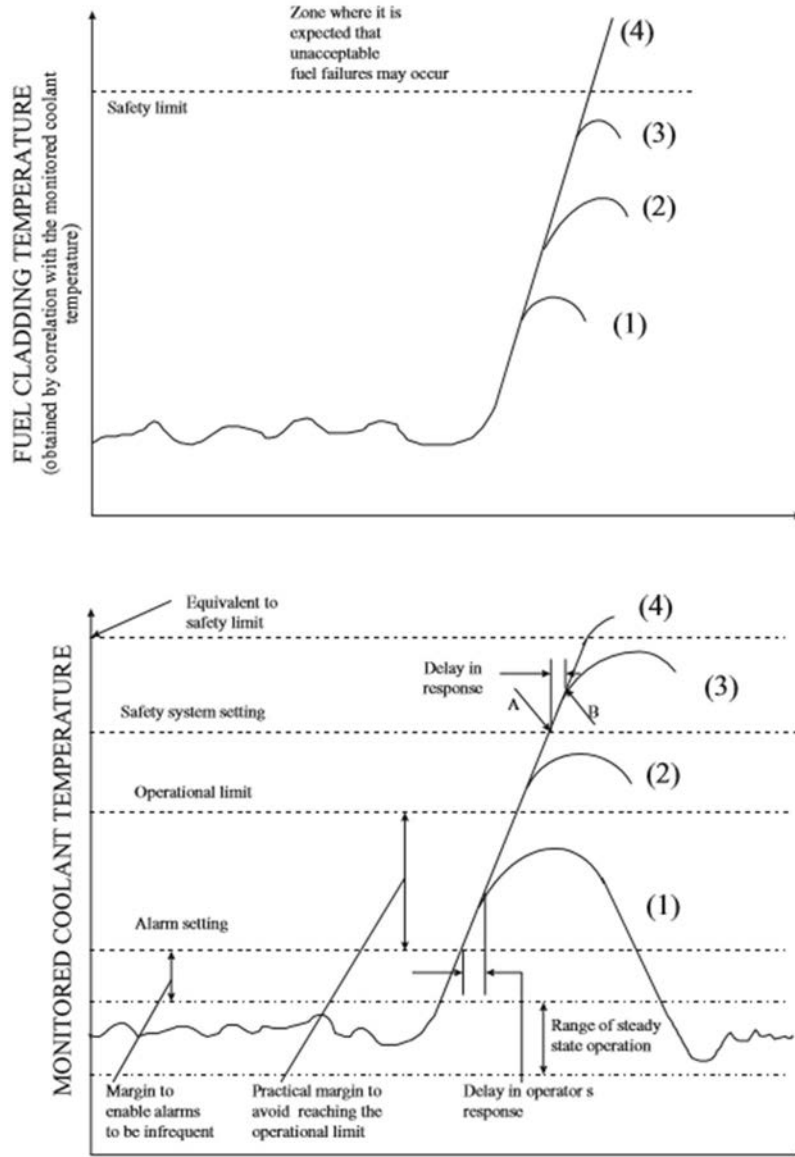


FIG. 10. Interrelationship of safety limits, safety system settings, operational limits [11].

Curve (1) shows the point where an alarm setting is exceeded. At this point an operator is required to take action to return the plant to steady state operation. A delay is shown to represent the response time necessary for the operator to take action.

Curve (2) shows the parameter in excess of the operational limit and ends with operator action to prevent the safety system setting from being reached.

Curve (3) shows the safety system setting being reached, with safety systems (possibly supplemented by operator action) preventing the safety limit being exceeded. A delay is shown to represent the instrumentation delay of safety systems, which should be considered in defining OLCs.

Curve (4) shows the parameter pass the safety limit. Fuel melting may result in core damage or damage to the plant above this value.

2.2.1.2. Safety and operational margins

Safety margin assures that the nuclear power plants operate safely in all modes of operation and at all times. As part of the design process for light water reactors, safety margins are established to ensure that reactors operate safely in all modes of operation at all times. The most significant and effective safety margins are related to the physical barriers against release of radioactive material including the fuel, the cladding, the reactor coolant system (RCS) boundary, and the containment as well as the dose to the surrounding public. FIG. 11 illustrates the concept of safety margins as they apply to key parameter values and regulatory body limitations.

Unfortunately, these values cannot be measured directly and are often not precisely known. Thus, the margin is given in terms of the difference between the regulatory acceptance criteria and the result of given calculations regarding the plant parameter of interest. With this definition in mind, it is of interest to note that reducing the safety margin does not indicate that an accident has occurred, but rather that the legally defined limits have been reached. These limits are generally given based on complex computations and conservative assumptions.

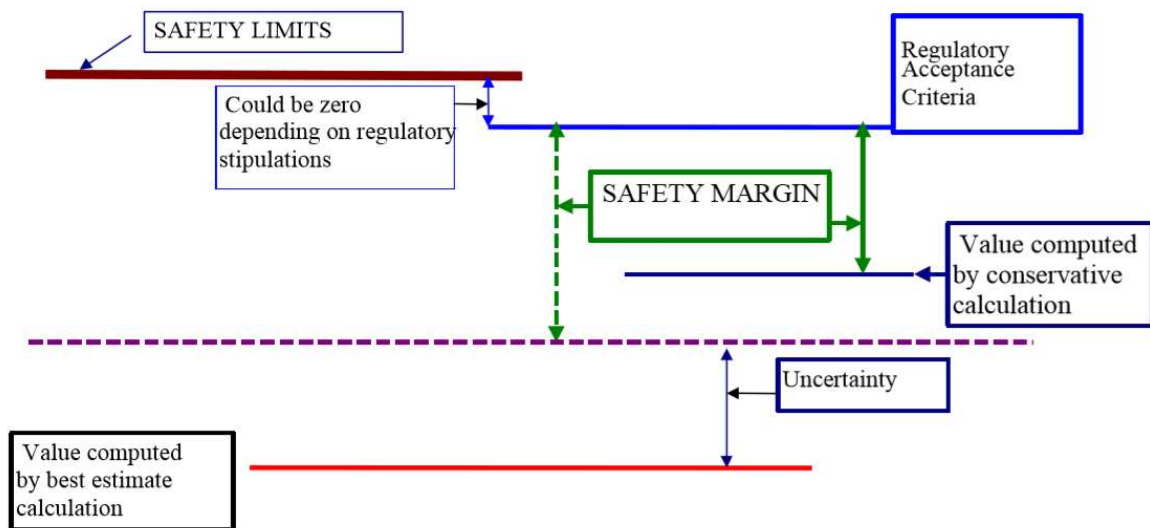


FIG. 11. Illustration of safety margins [12].

To ensure that a plant operates within the safety margins required by licensing documents, OLCs are established and summarized within a plant's technical specifications (tech specs). In addition to OLCs, plant technical specifications also set requirements for design features (e.g. fuel enrichment and fuel storage requirements) and administrative controls (e.g. staffing requirements, staff qualifications, reporting requirements, etc.). The plant must adhere to these tech specs so as to avoid inadvertent operation outside the parameters established by the safety margins. However, it is possible to increase the safety margins by improving analytical methods used in the design of reactors as well as by updating and improving key plant equipment. This allows enhancements in both plant performance and longevity. There are primarily two classes of limits used in the evaluation of safety margins: deterministic safety limits and probabilistic safety targets.

(a) Deterministic safety margin

Deterministic safety margins focus primarily on the conservative limits based upon international standards that are generally accepted by national regulatory bodies such as the US Nuclear Regulatory Commission (NRC). These margins vary depending on the design basis accident (DBA) in consideration. For example, the standards for a loss of coolant accident (LOCA) in a PWR are:

- (i) Peak clad temperature of less than 1200 °C;
- (ii) Maximum clad oxidation of less than 17% clad thickness;
- (iii) Hydrogen generation of less than that required for the deflagration limits for containment integrity;
- (iv) Less than 1% clad strain or a minimum departure from nucleate boiling ratio of ≤ 1.0 .

Other transient conditions facilitate different safety margin limits, each defined by the standards given by the national regulatory body. Often, since these limits cannot be measured directly, it is possible describe them in terms of their effect on factors that can then be measured or controlled directly.

(b) Probabilistic safety targets

Probabilistic safety targets are goals for the safety margin that are determined from an increased focus on PSA, rather than on conservatively defined deterministic safety limits. This concept is illustrated in FIG. 12. Several advanced reactor concepts have attempted to shift the focus from deterministic safety margins to probability safety targets in an attempt to eliminate some of the conservatism inherent in the prior approach. The following illustrate a possible set of probabilistic safety targets based on regulatory requirements, which are not universal, but depend on the individual nation's licensing body:

- (i) Shut down system unavailability $\leq 10^{-6}$ per demand;
- (ii) Engineered safety systems unavailability $\leq 10^{-3}$ per demand;
- (iii) Core damage frequency $\leq 10^{-5}$ /reactor year;
- (iv) Probability for large radioactivity release $\leq 10^{-6}$ /reactor year;
- (v) Individual risk of fatality $\leq 10^{-6}$ /reactor year.

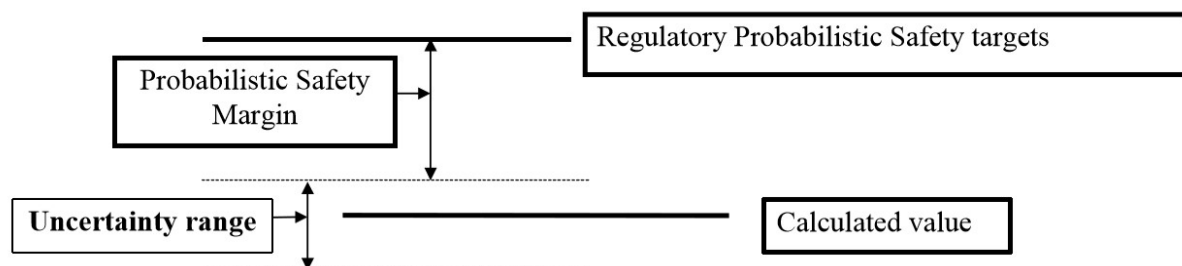


FIG. 12. Illustration of probabilistic safety targets [12].

2.2.2. Example fuel pin temperature analysis

In determining safe OLCs and corresponding margins, a large number and variety of analyses are performed. The following example shows a simple, demonstrational fuel pin temperature analysis. The result of this simple case will provide a non-rigorous determination of the temperature profile across a single fuel pin.

Let us consider a single PWR fuel pin with dimensions as illustrated in FIG. 13. During normal reactor operation, the peak fuel and peak clad temperatures can be assessed by heat balance calculations across the various boundaries of the fuel rod.

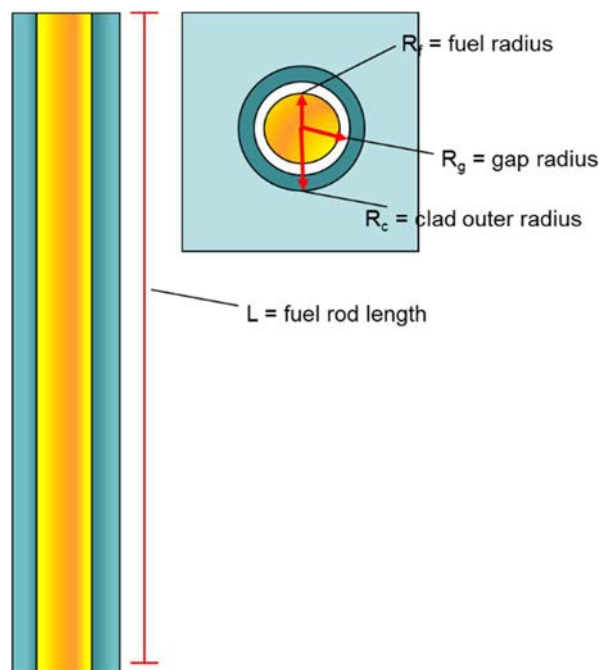


FIG. 13. Standard PWR fuel pin diagram (reproduced courtesy of M. Memmott).

The following assumptions are used in this analysis:

- (1) 1-D radial heat transfer;
- (2) Adjacent fuel pins do not impact mass or heat transfer of the fuel pin cell;
- (3) Isotropic and isothermal heat conductivity for fuel, k_f , and clad, k_c ;
- (4) Single conductance value for the fuel-clad gap, k_g ;
- (5) Infinite fuel rod length;
- (6) Constant coolant temperature which is the same as the clad outer temperature;
- (7) Heat is generated only in the fuel pellet.

Each assumption adds a degree of uncertainty, large or small, to the evaluation, and each of these assumptions can be relaxed to increase the accuracy of this evaluation.

Frequently, a subchannel analysis is undertaken, in which the fuel rods in an assembly or core are evaluated together to determine the radial and axial peaking factors. However, for this example, we will maintain these assumptions to simplify the fuel pin analysis. Given the heat

load, Q , and the total number of fuel pins, N , the pin specific average heat generation rate, $\langle \dot{q} \rangle$, can be calculated via:

$$\dot{Q} = N\langle \dot{q} \rangle \quad (1)$$

Once the fuel pin specific average heat generation rate is determined, the linear heat rate, q' , heat flux at the outer surface of the clad, q'' , and the fuel volumetric heat generation, q''' , can be found through the following equations:

$$\dot{Q} = NL\langle q' \rangle \quad (2)$$

$$\dot{Q} = NL\pi D_{co}\langle q'' \rangle \quad (3)$$

$$\dot{Q} = NL\pi R_{fo}^2\langle q''' \rangle \quad (4)$$

where L is the length of the fuel pin, D is diameter, and R is radius. Subscript 'c' refers to cladding, 'f' refers to fuel, and 'o' means outer radius or diameter. Once these values have been determined, the temperature profile across the fuel, gap, and clad can be evaluated in three separate regions, coupled by the boundary conditions associated with the analysis. We will first evaluate the temperature profile of the fuel pellet. The temperature profile radially across the fuel pellet can be evaluated by applying the following heat equation given the previous assumptions to a single fuel channel:

$$\nabla k_f \nabla T + q''' = 0 \quad (5)$$

Applying assumption (1), the heat equation can be rewritten in cylindrical form:

$$k_f \frac{1}{r} \frac{d}{dr} r \frac{dT}{dr} + q''' = 0 \quad (6)$$

Two boundary conditions are applied for this cylindrical fuel pin as follows:

- (i) The temperature gradient is zero, $\frac{dT}{dr} = 0$, at the centre of the fuel pin ($r = 0$);
- (ii) The centreline temperature of the fuel pin ($r = 0$) is bounded for continuity. Due to symmetry, this is T_{\max} .

Equation (6) is integrated to produce the following:

$$r \frac{dT}{dr} = -\frac{q''' r^2}{2k_f} + C_1 \quad (7)$$

where C_1 is a constant, but is shown to be zero when applying boundary condition (i). Equation (7) is then integrated again to obtain the following:

$$T(r) = -\frac{q''' r^2}{4k_f} + C_2 \quad (8)$$

where C_2 is another constant. Upon applying boundary condition (ii), a temperature profile results:

$$T(r) = T_{\max} - \frac{q'''r^2}{4k_f} \quad (9)$$

No heat is being generated in the fuel-clad gap, this means the temperature profile within this gap is subject to Fick's law, producing the gap heat transfer equation:

$$q'' = \frac{q'}{2\pi r} = -k_g \frac{dT}{dr} \quad (10)$$

where the subscript 'g' refers to the gap between fuel and clad. This equation can be integrated between temperatures at the fuel-gap boundary, T_f , and the gap-clad boundary, T_g , to give the following:

$$T(r) = T_f - \frac{q'}{2\pi k_g} \ln\left(\frac{r}{R_f}\right) \quad (11)$$

Fick's law can again be used to find the temperature profile of the cladding region since, similar to the gap region, it does not produce heat. The equation for heat transfer is:

$$q'' = \frac{q'}{2\pi r} = -k_c \frac{dT}{dr} \quad (12)$$

Integrated this between the temperatures at the inner and outer radius of the cladding gives the following:

$$T(r) = T_g - \frac{q'}{2\pi k_c} \ln\left(\frac{r}{R_g}\right) \quad (13)$$

Solving equations (9), (11), and (13) for q' gives:

$$q' = \frac{T_{\max} - T_c}{\left[\frac{1}{4\pi k_f} + \frac{1}{2\pi k_g} \ln\left(\frac{R_g}{R_f}\right) + \frac{1}{2\pi k_c} \ln\left(\frac{R_c}{R_g}\right)\right]} \quad (14)$$

Rearranging this equation to solve for T_{\max} gives:

$$T_{\max} = q' \left[\frac{1}{4\pi k_f} + \frac{1}{2\pi k_g} \ln\left(\frac{R_g}{R_f}\right) + \frac{1}{2\pi k_c} \ln\left(\frac{R_c}{R_g}\right) \right] + T_c \quad (15)$$

Substituting T_{\max} from equation (15) into equation (9) results in the temperature as a function of radius across the fuel pin similar to that shown in FIG. 14.

In reality, the coolant temperature changes axially as heat is transferred to the coolant from the fuel rod cladding outer surface. In this case, rather than solving for an average linear heat rate, a heat rate as a function of elevation should be utilized. The resulting radial profiles, similar in form to those illustrated in FIG. 14, now include axial variation, indicated (qualitatively) in FIG. 15 for the bulk coolant, T_b , the cladding, T_c , and the middle (centre) of the fuel, T_m .

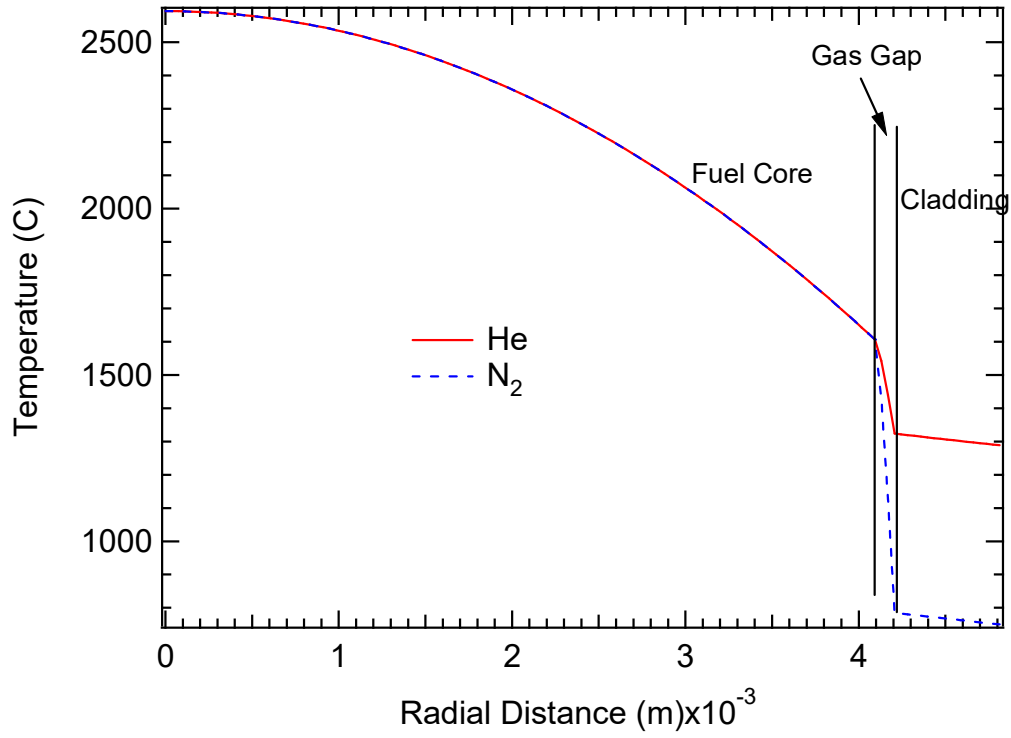


FIG. 14. Radial temperature profile across fuel, gap, and clad regions for N₂ and He filled gap regions (reproduced courtesy of M. Memmott).

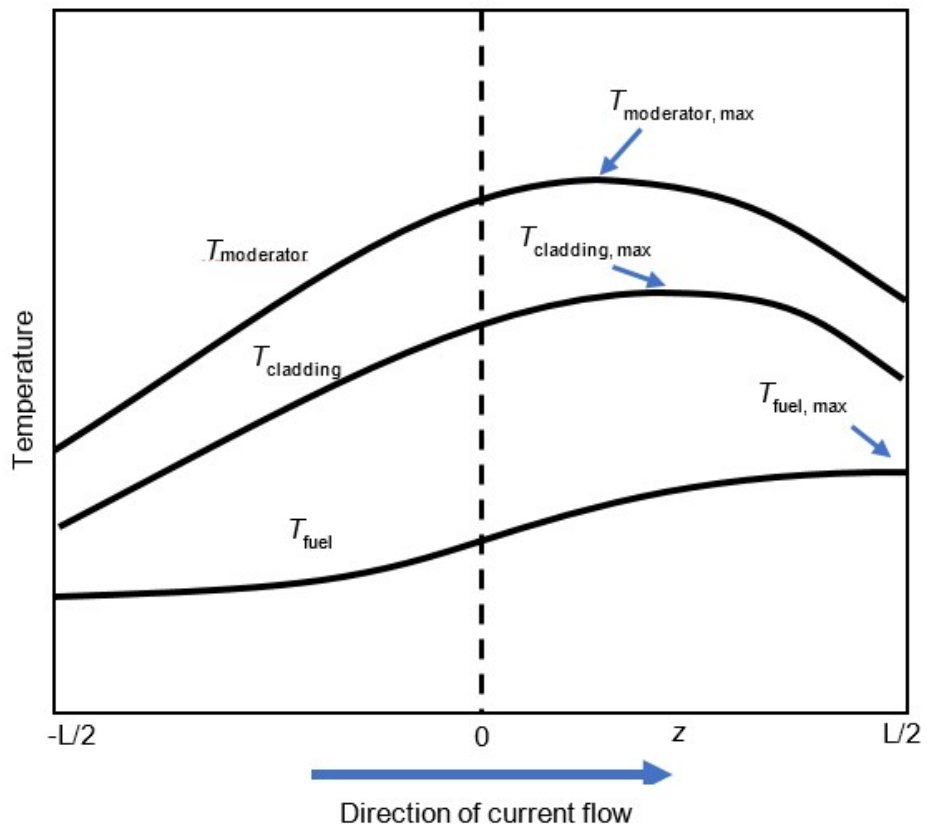


FIG. 15. Depiction of axial variation in temperatures for the coolant, clad, and fuel [2].

Nomenclature used in 3.1.3

D	diameter
k	heat conductivity
L	length
N	total number of fuel pins
\dot{q}	heat generation rate
q'	linear heat rate
q''	heat flux
q'''	volumetric heat generation
Q	heat load
R	radius
T	temperature
b	bulk coolant
c	cladding
f	fuel
g	gap
m	middle (centre)
o	outer

2.3. ACCIDENTS CONDITIONS

To enhance safety, designs measures are taken to (a) prevent accidents with harmful consequences, (b) ensure all accidents accounted for during design have minimal radiological consequences, and (c) ensure those accidents with the most serious radiological consequences are very unlikely to occur and mitigated as much as possible. This section describes plant states, established by the IAEA on the basis of frequency of occurrence in plants [13]. Descriptions of the Three Mile Island (TMI) and Fukushima Daiichi accidents are included and used to provide a basis of lessons learned and ongoing developments in reactor safety.

2.3.1. Accident classifications

The IAEA defines a series of plant states, related as in Table 4, and described in the following paragraphs [13].

TABLE 4. IAEA PLANT STATE CLASSIFICATIONS

OPERATIONAL STATES		ACCIDENT CONDITIONS		
Normal operation	Anticipated operational occurrences	Design basis accidents	Design extension conditions	
			Without significant fuel degradation	With core melting

Operational states include both normal operation and anticipated operational occurrences. Normal operation is defined as operation within the specified plant limits and includes normal

procedures such as startup, planned shutdown, steady state operation, maintenance, testing, and refuelling. Anticipated operational occurrences are deviations from normal operation that are expected to occur once or more during the operating lifetime of the plant. These events cause no damage to the plant and progression to accident conditions should be prevented by system design.

Accident conditions consist of any deviation from normal operation more significant than anticipated operational occurrences. There are two categories of accident conditions: design basis accidents and design extension conditions. Design basis accidents are postulated accident scenarios for which a reactor facility is designed to mitigate and for which only an acceptable amount of radioactive material may potentially be released. Design extension conditions are those postulated conditions not considered under design basis accidents but are considered for the design of a facility according to best estimate uncertainty. These conditions may or may not result in significant fuel degradation, however release of radioactive material must remain within an acceptable limit. This term may include severe accidents, provided the radioactive material release is within the acceptable limit. Severe accidents are accidents more severe than design basis accidents which involve significant core degradation.

A controlled state condition follows either an anticipated operational occurrence or any accident condition once safety functions may be maintained for a long enough time to reach a safe state. A safe state refers to the plant condition upon recovering from either an anticipated operational occurrence or any accident condition. This is achieved once the reactor is subcritical and for which safety functions are maintained for extensive periods.

2.3.2. Examples of accident progression

2.3.2.1. Three Mile Island accident

Though not the only means of initiating events promulgating in radioactive releases, the Three Mile Island Nuclear Generating Station accident illustrates both the strengths and weaknesses present in reactor designs at the time of the accident, and thus presents an important case study for accident progression of PWRs in general.

The following is a basic timeline of the accident:

- (1) December 31, 1978 — Unit 2 begins commercial operation.
- (2) Thursday, March 28, 1979 — Unit 2 experiences equipment and procedure failures resulting in partial core meltdown.
- (3) Saturday March 30, 1979 — Gas (hydrogen) bubble in reactor leads to evacuation readiness plans, suggested evacuation for pregnant women and children within 5 miles (approximately 8 km), and voluntary evacuation of 140 000 people.
- (4) April 6, 1979 — Evacuation order lifted.

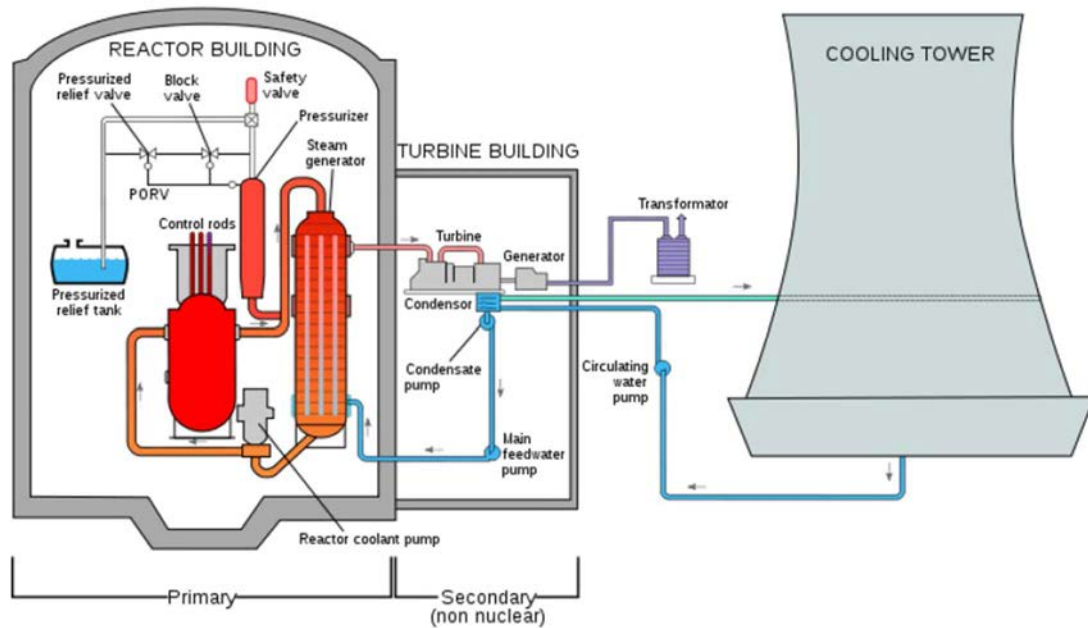


FIG. 16. A schematic of the Three Mile Island Nuclear Generating Station Unit 2 [14].

FIG. 16 illustrates a schematic of TMI Unit 2 to aid in visualization of accident progression. The following points describes the sequence of events leading up to the meltdown, while a depiction of the final state of the melted fuel is illustrated in FIG. 17.

- (1) Running at 97% full load with TMI Unit 1 shut down for refuelling.
- (2) Pumps in condensate polishing system failed, either mechanically or electrically (still not known), followed immediately by main feed water pump failure.
- (3) Automatic scram triggers and turbine is shutdown.
- (4) All control rods fully inserted.
- (5) Pilot operated relief valve (PORV) in the primary system stuck open, allowing reactor coolant to escape.
- (6) Operators did not recognize the loss of coolant condition and overrode an automatic emergency coolant response because of mistaken belief that the reactor had too much coolant.
- (7) Reactor continues generating decay heat, no heat removal occurs since turbines tripped.
- (8) Three auxiliary feedwater pumps activated, but valves had been closed for maintenance, so no water flowed. Closing valves while the reactor is operational is a severe rule violation.

TMI-2 Core End-State Configuration

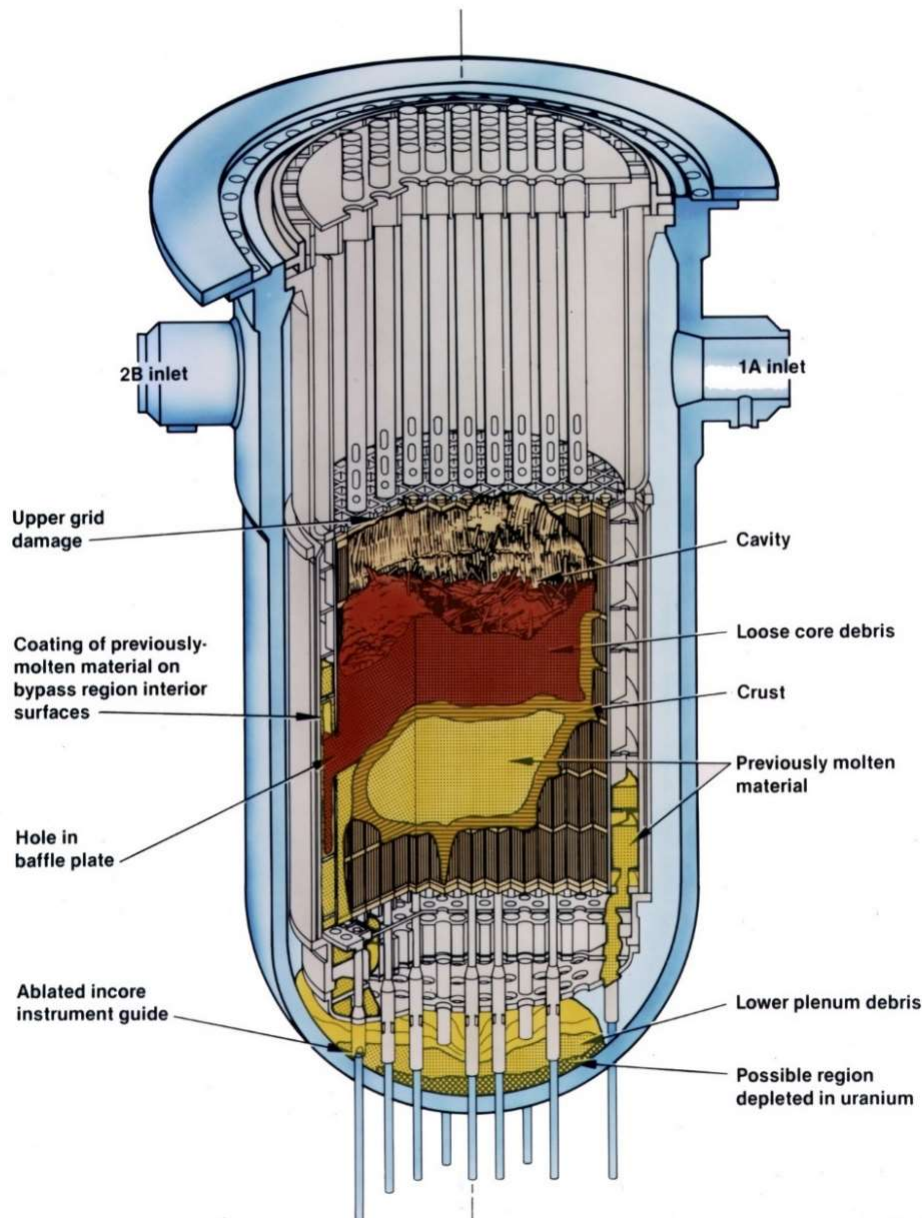


FIG. 17. A depiction of the end core state of the Unit 2 reactor vessel and fuel [15].

The final results of the accident sequence are as follows [14][16]:

- (a) Estimated between 2.5–10 million curies (93–370 PBq) of radioactive noble gases, mainly Xe and Kr, and 10 to 20 curies (370–740 GBq) of radioiodine were released to the environment, primarily through the PORV;
- (b) Voluntary evacuation of the area near the plant.
- (c) Approximately 1 mrem (10 μ Sv) dose to 2 million people near plant (for reference, a chest X ray will result in a 6 mrem dose);
- (d) No perceptible effect on cancer occurrence or other health issue incidence in residents near the plant;
- (e) Significant impact on industry, regulation, and safety.

2.3.2.2. Fukushima Daiichi accident

On 11 March 2011, a 9.0 magnitude earthquake struck 112 miles (180 km) off the coast of Japan. FIG. 18 shows the main event sequence of the ensuing accident.

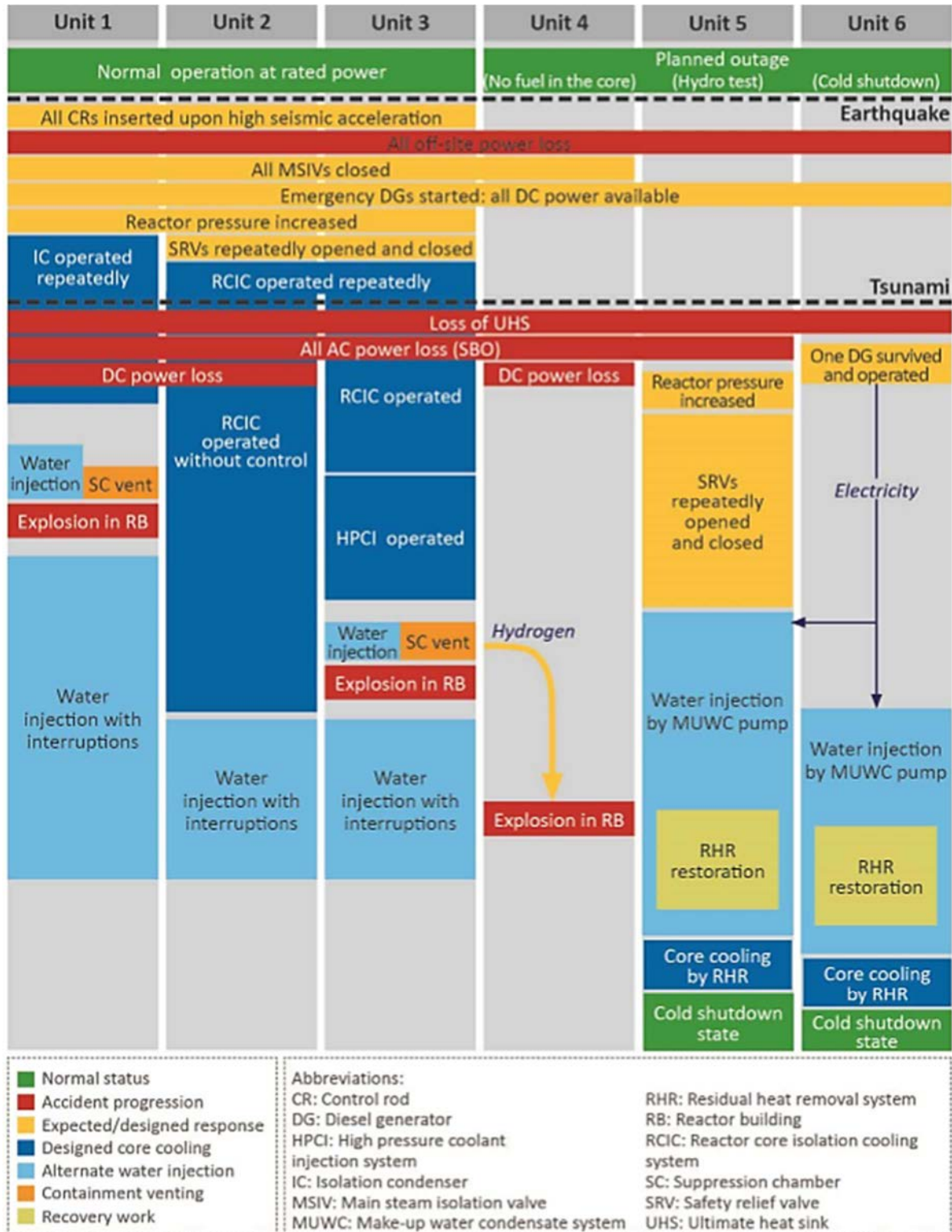


FIG. 18. Main event sequence of Fukushima Daiichi accident [17].

The earthquake caused the operating units, 1 through 3, of Fukushima Daiichi Nuclear Power Plant to automatically scram on seismic reactor protection system trips. Units 4, 5, and 6 were already shut down for refuelling and maintenance. The earthquake damaged switchyard breakers and distribution towers, causing a loss of all off-site electrical power sources. The emergency diesel generators automatically started and provided AC power to emergency systems.

Shortly after the earthquake, a series of large tsunamis struck the site. Some of the tsunamis significantly exceeded the assumptions used in determining the plant's design basis. As a result, flooding disabled safety related equipment including emergency diesel generators, seawater pumps associated with the ultimate heat sink, and switchgear. Flooding also resulted in a complete loss of all AC and DC power at units 1 and 2, while Unit 3 retained limited DC power. Although Unit 4 was shut down, it lost all AC and DC power. One air cooled emergency diesel generator remained functional on Unit 6 and this diesel generator was used to stabilize units 5 and 6.

Ultimately, losses of core cooling resulted in severe damage to three reactor cores and hydrogen explosions damaged secondary containment buildings, contributing to an uncontrolled release of radioactive material. The event at Fukushima Daiichi was rated level 7 on the International Nuclear and Radiological Event Scale with the 1986 accident at Unit 4 of the Chernobyl Nuclear Power Plant being the only other nuclear accident to have a level 7 rating.

2.3.3. Lessons learned

Sustainable operation of nuclear installations and power plants worldwide depend as much on how procedures and standards are implemented as on how the human-machine interface is responsive to sudden mechanical failures, natural disasters or human mistakes. These environments are best managed within the established practices defined and known as safety culture. Following the Fukushima accident, there is an urgent need to rebuild public trust that has been lost regarding the safety of nuclear power. Science and technology should be linked to the welfare of human beings and assurance in safety and reliability of industrial facilities to prevent accidents should be provided. Engineering safety training and education is especially important to build and enhance safety culture in society and workplaces.

There is a need to establish leadership actions and employee engagement that, in acknowledgement that an extreme external event may occur, rigorous preparations are made to respond to such an event through senior management action. This can be accomplished, in part, by the following senior manager actions:

- (i) Periodically reinforce the role that all employees have in emergency preparedness;
- (ii) Participate in and reinforce high standards during emergency drills;
- (iii) Advocate active involvement in related industry activities;
- (iv) Provide case studies on the Fukushima Daiichi event and other events that involve similar factors or behaviours.

Prepare personnel responsible for performing emergency response duties with the required knowledge and skills to execute their role. A combination of training and realistic drills, as well as procedure guidance and human factoring, should be used to prepare the staff for emergency response duties. Emergency response duties to be considered include the following:

- (i) Execute emergency and accident procedures;
- (ii) Assign the highest priority to maintaining core cooling and containment integrity;
- (iii) Interpret post-event data and indications given a sound knowledge of plant operations, safety systems and design basis;
- (iv) Perform tasks associated with the installation and use of portable equipment during emergency conditions;
- (v) Determine expected plant conditions when essential plant status information is uncertain or unavailable;
- (vi) Cope with the unavailability of primary communication methods as well as methods for monitoring critical plant parameters and emergency response functions.

Safety action is especially important in building a safety culture. Safety activities for the future generation are the following:

- (i) Safety responsibilities concerning individuals and organizations;
- (ii) Share information for having a mutual understanding and willingness about risk and safety;
- (iii) Promoting the inheritance of technology and safety knowledge.

Effective leadership is essential when nuclear power plants are undergoing and experiencing abnormal and accident events. Responding to a crisis, a quick decision is often required. The information, including risk, must be shared by all stakeholders. Safe actions must have the positive result of utilizing interactions and networking to control severe situations. This should be strengthened through technical knowledge and safety training.

In addition to human factors, the Fukushima Daiichi accident highlighted needs to improve plant safety through design and enhanced safety assessments [18]. Specifically, these include:

- (i) Conservative assessment of natural hazards, including the potential of simultaneous or sequential occurrence and for the combined effect on multiple unit sites;
- (ii) Periodic reassessment of safety in light of new knowledge gained and implementation of identified corrective actions;
- (iii) Improvement of defence in depth by application of independent, redundant, and diverse protection against both internal and external hazards;
- (iv) Reliable instrumentation and control systems to maintain functionality during design extension conditions;
- (v) Reliable cooling systems which can function during both design basis accidents and design extension conditions;
- (vi) Reliable confinement systems to prevent significant releases of radioactive material in design extension conditions.

3. NATURAL CIRCULATION

Natural circulation is the driving force behind several passive safety systems utilized in advanced WCRs. This section provides an overview of the phenomena of natural circulation flow and computational fluid dynamics (CFD) as one method for modelling of natural circulation flow.

3.1. NATURAL CIRCULATION FLOW

One of the primary challenges associated with nuclear reactor operation is that of accident mitigation. Nuclear power plants differ from other baseload power plants in that even after power operations are halted and the reactor is shut down, a fraction of the operational heat continues to be produced. This residual heat, known as decay heat, continues to be produced indefinitely and must be removed to prevent a build up of heat which could result in fuel heating and eventual meltdown. Current decay heat removal systems often require operator action, external power, and at times actuating mechanical components to provide cooling capabilities. In most scenarios, this is acceptable. However, as the event at Fukushima demonstrated, a station blackout or other event in which operator action and external power are unavailable are possible scenarios where the cooling systems can be bypassed. In these events, natural circulation offers an alternative or redundant option for decay heat removal and understanding of the related phenomena is essential for the further implementation of natural circulation in reactor safety systems.

3.1.1. Overview of natural circulation flow

This overview of natural circulation flow is largely adapted from IAEA-TECDOC-1677 [19].

3.1.1.1. Modes of cooling

Natural circulation describes the complex physical phenomena that occur when a geometrically distinct heat sink and heat source are connected by a fluid flow path in a gravity environment. Natural circulation takes place in a few different configurations in a nuclear plant:

- (a) Inside the primary coolant loop: the core (source) and a steam generator (sink) or the primary side of a heat exchanger (sink), with the core (source) located at a lower elevation.
- (b) Inside the pressure vessel: the core (source) and the vessel downcomer (sink). ‘Steady state’ natural circulation between the core and downcomer occurs due to cooling of downcomer fluid by a heat exchanger (boiler or steam generator) or by inlet of feedwater liquid at a temperature lower than the core outlet temperature.
- (c) Inside the containment atmosphere.

Natural circulation typically results in smaller driving forces than coolant pumps, however remains an important consideration. For example, pressure drops caused by vertical bends and siphons in piping, or heat losses to environment are a secondary design consideration when a

pump is installed and drives the flow; however, a significant influence on overall system performance may be expected due to the same pressure drops and thermal power release to the environment when natural circulation flow. Therefore, a deeper level of knowledge of thermal hydraulic phenomena of specific geometric conditions and governing heat transfer conditions is necessary to describe the impact of natural circulation.

“Natural circulation will occur in a PWR primary loop (in the absence of pumped flow) whenever buoyant forces caused by differences in loop fluid densities are sufficient to overcome the flow resistance of loop components (steam generators, primary coolant pumps, etc.). The fluid density differences occur as a result of fluid heating in the core region (causing the liquid to become less dense) and cooling fluid in the steam generators (causing the fluid to become more dense). The buoyant forces resulting from those density differences cause fluid to circulate through the primary loops, providing a means of removing the core decay heat. Depending on the primary loop fluid inventory, natural circulation consists of three distinct modes of cooling:

- (a) Single phase;
- (b) Two phase (liquid continuous);
- (c) Reflux condensation (or boiler–condenser mode for once through steam generators).

Progression from the single phase mode through the two phase and reflux condensation modes occurs as primary system liquid inventory decreases. Natural circulation flow in PWR is driven by temperature induced density gradients, enhanced by a thermal centre elevation difference between the hot (core) and cold (steam generator) regions in the primary loop. This density gradient produces a buoyancy force that drives the natural circulation flow. Thus, single phase natural circulation is the flow of an essentially subcooled primary liquid driven by liquid density differences within the primary loop.

Two phase natural circulation is normally defined as the continuous flow of fluid and vapour. In this mode of natural circulation, vapour generated in the core enters the hot leg and flows along with the saturated liquid to the steam generator, where at least some of the vapor is condensed. Hence, density gradients are affected in two phase mode not only by temperature differences but also mainly by the voids in the primary loop. In both single phase and two phase natural circulation, the mass flow rate is the most important heat removal parameter.

In the reflux condensation, the vapour generated in the core flows through the hot leg, is condensed in the steam generator and flows back to the core as a liquid. In this mode, the loop mass flow rate has a negligible effect because the primary mechanism of heat removal is vapour condensation.

In summary, the three modes of natural circulation are distinguishable based upon characteristic mass flow rates, loop temperature difference, and basic phenomenological differences. The dominant heat transfer mechanism in single phase natural circulation cooling is convection, making the loop flow rate the most important parameter governing heat removal. Heat generated by the core is transported away from the reactor vessel through the hot leg to

steam generators (heat sink) via the subcooled primary liquid. Heat is transferred from the primary side to the secondary side in the steam generator.

The cooling cycle is completed when the cooled primary fluid flows back to the reactor vessel. The amount of heat removed from the core through single phase natural circulation cooling is normally the amount produced by decay heat power levels (about 5% core power)” [19].

3.1.1.2. Mass inventory and flow patterns

“Since the study of natural circulation cooling in PWR systems became of interest, work on the characterization of natural circulation has been focused in several areas, including effects of both primary and secondary liquid inventory and distribution on natural circulation effectiveness, the stability of the various natural circulation flow interruption due to instabilities, counter-current flow limiting in the hot leg and steam generator tubes, and the effects of non-condensable gases on natural circulation process [19].

With respect to the primary side liquid inventory issue, natural circulation will provide decay heat removal at significantly reduced primary side inventory. The concern here is identifying the minimum primary side liquid inventory at which natural circulation will continue to provide adequate cooling of the core. Similarly, the steam generator secondary will continue to be a heat sink for the primary at significantly reduced secondary liquid inventories. Again, the concern is identifying the minimum secondary inventory that will ensure continued natural circulation flow in the primary loop.

An additional concern with respect to the secondary inventory is the instabilities in primary side natural circulation flow caused by severely reduced secondary side liquid levels. These secondary side induced flow instabilities could reduce the effectiveness of natural circulation cooling. Generally, the stability of the different modes of natural circulation cooling, as well as the stability of transients between modes, is of concern because natural circulation will be the primary mechanism for core decay heat rejection for certain kinds of PWR accidents or transients, and instabilities in natural circulation process could lead to an interruption of natural circulation flow with a corresponding reduction in the removal of core decay heat. Thus, an understanding of factors that influence the onset of flow instabilities and of the effects of the instabilities on decay heat removal is necessary” [19].

3.1.2. Governing equations of single phase flow

Natural circulation flow arises from the interplay of the viscous and the buoyant forces present in a system of water. The details surrounding natural circulation systems may change, however the force balance between the viscous and buoyant forces will indicate the magnitude and direction of flow in a natural circulation system. In other words, the driving force for natural circulation flow is the density difference associated with temperature gradients for the fluid of interest and is countered by the viscous and frictional forces which resist this flow. The flow rate is the velocity of the fluid in which the viscous and the buoyant forces are equal.

As a demonstration single phase flow, a simplistic example is included here where a single flow loop is created that consists of a heat source and sink as illustrated in FIG. 19.

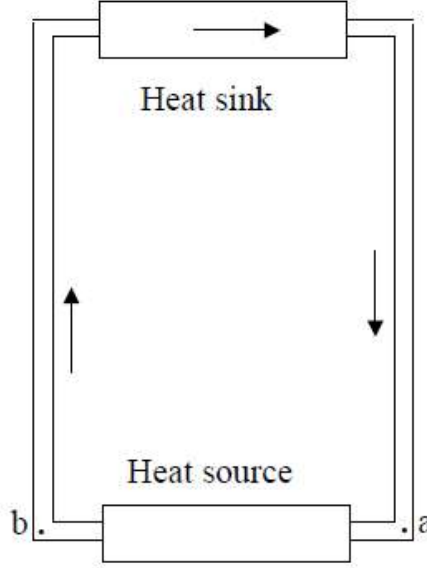


FIG. 19. Rectangular closed natural circulation loop [20].

In this scenario, the buoyant forces, F_B , are based upon the thermal expansion of the fluid, which is a function of temperature. If an equation of state is known that describes how the density, ρ , changes as a function of temperature, T , then the buoyant forces from heat source to heat sink of the hot leg can be expressed as:

$$F_{B,H} = \int_{\rho_{T_1}}^{\rho_{T_2}} g H_H A d\rho(T) \quad (166)$$

where T_1 and T_2 refer to the temperatures at points 'a' and 'b' respectively, g is the gravitational constant, H_H is the height of the hot leg, and A is loop flow cross-sectional area. The buoyant forces of the cold leg, heat sink to heat source, $F_{B,C}$, can be expressed as:

$$F_{B,C} = \int_{\rho_{T_2}}^{\rho_{T_1}} g H_C A d\rho(T) \quad (17)$$

where H_C is the height of the cold leg. By summing these equations, the total buoyant driving force for the loop illustrated in FIG. 19 is:

$$F_{B,C} = \int_{\rho_{T_2}}^{\rho_{T_1}} g \Delta H A d\rho(T) \quad (18)$$

where ΔH is the height difference between the point heater (heat source) and point cooler (heat sink).

Conversely, the viscous or friction losses can be evaluated based upon the same relationship as is used for active flow losses:

$$F_f = \left(f \frac{L}{D} + K\right) A \frac{\rho(T)u^2}{2} \quad (17)$$

where f is the friction factor for natural circulation flow, L is the total flow length of the pipe, D is the pipe diameter, K is the loss coefficient, and u is the velocity of the fluid. By setting these equations equal to each other and solving for velocity, one can determine the steady state fluid flow rate for the simple loops system by finding the product of the velocity and area:

$$\dot{V} = uA = A \sqrt{\frac{2 \int_{\rho T_2}^{\rho T_1} g \Delta H d\rho}{\left(f \frac{L}{D} + K\right) \rho(T)}} \quad (18)$$

Although this works for simple loops, most circumstances where natural circulation flows will be used in lieu of active flows, the flow paths, resistances, heated and cooled lengths, and cross-sectional areas are far more complicated than in a simple flow loop, and this simplistic expression is inadequate. An appropriate expression can be developed for natural circulation flow by performing mass, momentum, and energy balances across the entire loop.

Reyes developed one and two phase natural circulation governing equations for a Multi-Application Small Light Water Reactor integral SMR as part of a scaling analysis, with parameters as indicated in FIG. 20. Scaling analyses provide a method for understanding the relationship between a full scale system phenomena with experiments using a downscaled test facility. Specifically, this type of analysis identifies what factors are accurately modelled in a scaled down test facility as well as defines physical dimensions and conditions must be used to replicate the flow phenomena and heat transfer behaviour of the full scale system.

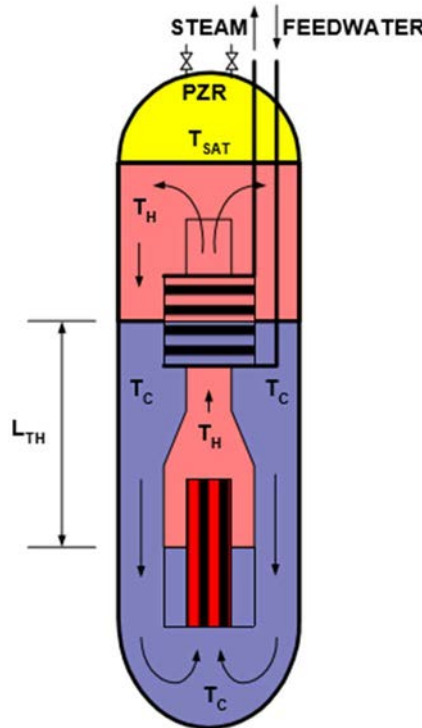


FIG. 20. Natural circulation flow in an integral reactor system [20].

The single phase flow equations as provided [20]:

Loop momentum balance equation:

$$\sum_{i=1}^N \left(\frac{l_i}{a_i} \right) \cdot \frac{d\dot{m}}{dt} = \beta g \rho (T_H - T_C) L_{th} - \frac{\dot{m}^2}{\rho_i a_c^2} \sum_{i=1}^N \left[\frac{1}{2} \left(\frac{fl}{d_h} + K \right)_i \left(\frac{a_c}{a_i} \right)^2 \right] \quad (19)$$

Loop energy balance equation:

$$C_{vl} M_{sys} \frac{d(T_M - T_C)}{dt} = \dot{m} C_{pl} (T_H - T_C) - \dot{q}_{SG} - \dot{q}_{loss} \quad (20)$$

where l is length, a is the flow area, \dot{m} is the mass flow rate, L_{th} is the distance between the heat source and heat sink, d_h is the hydraulic diameter, C is specific heat, \dot{q} is the heat transport rate, t is time, and τ is the residence time constant. Subscripts ‘H’ and ‘C’ are used to denote hot and cold side average temperatures. M_{sys} refers to the mass of the system while subscript ‘M’ is used for the system mixed mean temperature. Subscript ‘SG’ is used for the heat transfer to the steam generator and ‘loss’ is used for heat lost in the flow. Subscripts for specific heat ‘vl’ and ‘pl’ refer to constant volume and constant pressure of liquid.

The following initial and boundary conditions are may be applied:

$$t^+ = \frac{t}{\tau_{loop}} \quad (21)$$

$$\dot{m}^+ = \frac{\dot{m}}{\dot{m}_0} \quad (22)$$

$$\left\{ \sum_{i=1}^N \left[\frac{1}{2 \left(\frac{fl}{d_h} + K \right)_i \left(\frac{a_c}{a_i} \right)^2} \right] \right\}^+ = \frac{\sum_{i=1}^N \left[\frac{1}{2} \left(\frac{fl}{d_h} + K \right)_i \left(\frac{a_c}{a_i} \right)^2 \right]}{\sum_{i=1}^N \left[\frac{1}{2} \left(\frac{fl}{d_h} + K \right)_i \left(\frac{a_c}{a_i} \right)^2 \right]_0} \quad (23)$$

$$(T_M - T_C)^+ = \frac{(T_M - T_C)}{(T_M - T_C)_0} \quad (24)$$

$$(T_H - T_M)^+ = \frac{(T_H - T_C)}{(T_H - T_C)_0} \quad (25)$$

$$\dot{q}_{SG}^+ = \frac{\dot{q}_{SG}}{\dot{q}_{SG0}} \quad (26)$$

$$\dot{q}_{loss}^+ = \frac{\dot{q}_{loss}}{\dot{q}_{loss0}} \quad (27)$$

Dimensionless groups are defined in equations (28) through (35):

Ratio of specific heats:

$$\gamma = \frac{C_{pl}}{C_{vl}} \quad (28)$$

Loop reference length number:

$$\Pi_L = \sum_{i=1}^N \frac{l_i}{l_{ref}} \frac{a_c}{a_i} \quad (29)$$

where

$$l_{ref} = \frac{M_{sys}}{\rho_l a_c}$$

Loop Richardson number:

$$\Pi_{Ri} = \frac{\beta g (T_H - T_C)_0 L_{th}}{u_{c0}^2} \quad (30)$$

or

$$\Pi_{Ri} = \frac{\beta g \dot{q}_{c0} L_{th}}{\rho_l a_c C_{pl} u_{c0}^3} \quad (31)$$

Loop resistance number:

$$\Pi_{Fl} = \sum_{i=1}^N \left\{ \frac{1}{2} \left(\frac{fl}{d_h} + K \right)_i \left(\frac{a_c}{a_i} \right)^2 \right\} \quad (32)$$

Loop energy ratio:

$$\Pi_T = \frac{(T_H - T_C)_0}{(T_M - T_C)_0} \quad (33)$$

Steam generator heat transport number:

$$\Pi_{SG} = \frac{\dot{q}_{SG0}}{\rho_l u_{c0} a_c C_{pl} (T_M - T_C)_0} \quad (34)$$

Loop heat loss number:

$$\Pi_{loss} = \frac{\dot{q}_{loss,0}}{\rho_l u_{c0} a_c C_{pl} (T_M - T_C)_0} \quad (35)$$

where u is the velocity; γ is the ratio of specific heats as shown in equation (28); and Π is the characteristic time ratio for subscripts ‘L’, ‘Ri’, ‘Fl’, ‘T’, ‘SG’, and ‘loss’ corresponding to loop reference length number, Richardson number, loop resistance number, loop energy ratio, steam generator transport number, and heat loss number respectively.

By applying the boundary conditions and dimensionless groups to equations (19) and (20), the dimensionless balance equations (36) and (37) result, and equation (38) shows the characteristic time constant.

Loop momentum balance equation:

$$\Pi_L \frac{d\dot{m}^+}{dt^+} = \Pi_{Ri}(T_H - T_C)^+ - \Pi_{Fl}(\dot{m}^+)^2 \left\{ \sum_{i=1}^N \left[\frac{1}{2} \left(\frac{fl}{d_h} + K \right)_i \left(\frac{a_c}{a_i} \right)^2 \right] \right\}^+ \quad (36)$$

Loop energy balance equation:

$$\frac{1}{\gamma} \frac{d(T_M - T_C)^+}{dt^+} = \Pi_T \dot{m}^+(T_H - T_C)^+ - \Pi_{SG} \dot{q}_{SG}^+ - \Pi_{loss} \dot{q}_{loss}^+ \quad (37)$$

Characteristic time constant:

$$\tau_{loop} = \sum_{i=1}^N \frac{l_i}{u_i} = \sum_{i=1}^N \tau_i = \frac{M_{sys}}{\dot{m}_0} = \frac{M_{sys}}{\rho_l u_{c0} a_c} \quad (38)$$

The steady state solution is provided in equation (39) with the core inlet velocity as indicated in equation (40). The steady state condition is found by setting the time dependent portions of the balance equations to zero and the ‘+’ terms to unity. The result shows the steady state solution is found where the loop Richardson number is equal to the loop resistance number. The equivalent meaning of this is that the buoyancy of fluid is equal to the resistance; therefore, no acceleration of fluid through the system occurs and a steady flow is maintained. The core inlet velocity, or velocity of fluid through the system, is obtained by substituting equation (31) into equation (39) and solving for u_{c0} .

Steady state solution:

$$\Pi_{Ri} = \Pi_{Fl} \quad (39)$$

Core inlet velocity:

$$u_{c0} = \left(\frac{\beta \dot{q}_{c0} L_{th} g}{\rho_l a_c C_{pl} \Pi_{Fl}} \right)^{\frac{1}{3}} \quad (40)$$

Time, fluid velocity, and loop length scale ratios are obtained by the characteristic time constant ratio and the steady state solution for the core inlet velocity. The scale ratio for flow

are must be set to unity to preserve kinematic behaviour in the system. Scaling ratios resulting from this analysis are as follow:

Time scale ratio:

$$\tau_{\text{loop,R}} = \left(\frac{\rho_l C_{\text{pl}}}{\beta} \right)_R \left(\frac{a_c \Pi_{\text{Fl}} l^2}{\dot{q}_{c0}} \right)_R^{\frac{1}{3}} \quad (41)$$

Fluid velocity scale ratio

$$u_R = \left(\frac{\beta}{\rho_l C_{\text{pl}}} \right)_R^{\frac{1}{3}} \left(\frac{\dot{q}_{c0} l}{a_c \Pi_{\text{Fl}}} \right)_R^{\frac{1}{3}} \quad (42)$$

Loop length scale ratio:

$$l_R = (L_{\text{th}})_R \quad (43)$$

Flow area scale ratio:

$$\left(\frac{a_i}{a_c} \right)_R = 1 \quad (44)$$

Loop energy scale ratio:

$$\left[\frac{(T_H - T_C)_0}{(T_M - T_C)_0} \right]_R = 1 \quad (45)$$

Steam generator power scale ratio:

$$\left(\frac{\dot{q}_{\text{SG0}}}{\dot{q}_{c0}} \right)_R = 1 \quad (46)$$

Heat loss scale ratio:

$$\left(\frac{\dot{q}_{\text{loss},0}}{\dot{q}_{c0}} \right)_R = 1 \quad (47)$$

Nomenclature used in 3.1.2

a	flow area
A	cross-sectional flow area
C	specific heat
d_h	hydraulic diameter
D	pipe diameter
f	friction factor
F	force
g	gravitational constant

K	loss coefficient
l	length
L	flow length
\dot{m}	mass flow rate
M_{sys}	system mass
\dot{q}	heat transport rate
T	temperature
u	velocity
β	thermal expansion coefficient
γ	ratio of specific heats
ρ	density
τ	residence time constant
Π	characteristic time constant
C	cold side
f	friction loss
Fl	loop resistance number
H	hot side
loss	lost across flow
L	loop reference length number
M	system mixed
pl	constant pressure liquid
R	ratio
Ri	Richardson number
SG	steam generator
T	loop energy ratio
vl	constant volume liquid

3.1.3. Governing equations of two phase flow

3.1.3.1. Geometry

The most important feature of gas–liquid two phase flows, when compared to single phase flows, is the existence of deformable interfaces. This, coupled with the naturally occurring turbulence in gas–liquid flows, makes them highly complex. Some simplification is possible by classifying the types of interfacial distributions or topology under various headings, known as flow regimes or flow patterns. The two phase flow regimes for gas–liquid flow in vertical tubes are illustrated in FIG. 21 and range from bubble flow to wispy annular flow. Vertical flows are, on average, axially symmetric but with horizontal flows, gravity induces the liquid to move preferentially towards the bottom of the channel as shown in FIG. 22. The two phase flow regimes can be classified according to the geometry of the interfaces into three main classes, namely, separated flow, mixed or transitional flow, and dispersed flow as shown in Table 5 [21].

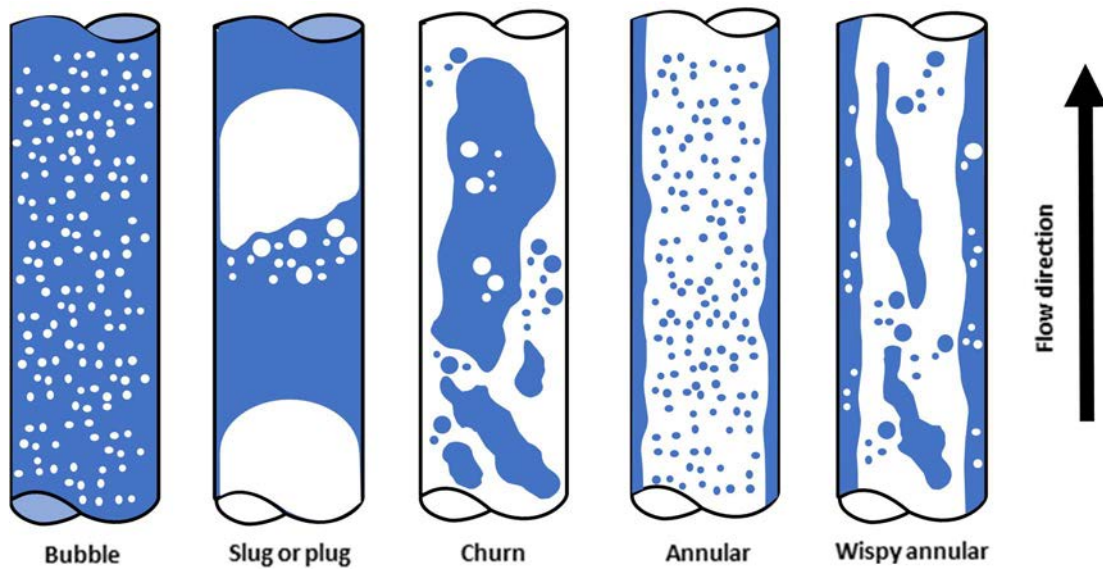


FIG. 21. Main flow regimes in upwards gas-liquid flow in vertical tubes [22].

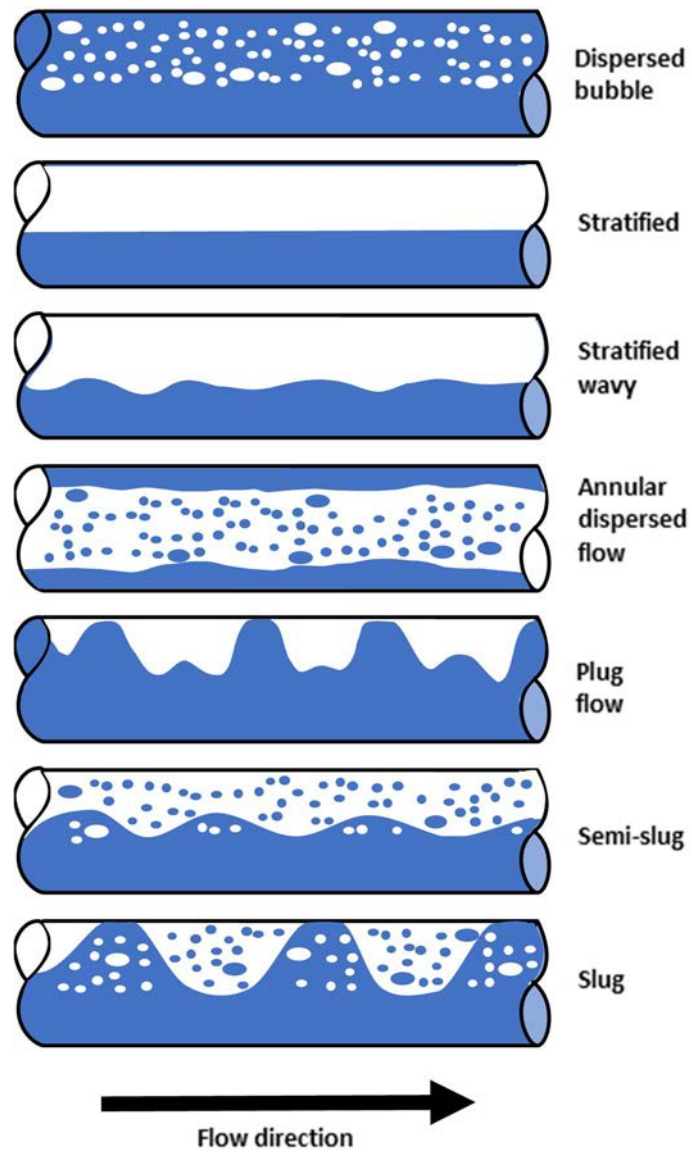




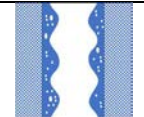
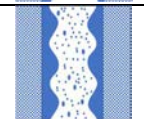

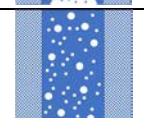
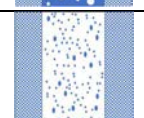
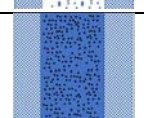


FIG. 22. Main flow regimes in gas-liquid flow in horizontal tubes [22].

TABLE 5. CLASSIFICATION OF TWO PHASE FLOW

CLASS	TYPICAL REGIMES	GEOMETRY	CONFIGURATION	EXAMPLES
Separated flows	Film flow		Liquid film in gas, gas film in liquid	Film condensation, film boiling
	Annular flow		Liquid core and gas film, gas core and liquid film	Film boiling, boilers
	Jet flow		Liquid jet in gas, gas jet in liquid	Atomization, jet condenser
Mixed or transitional flows	Cap, slug, or churn-turbulent flow		Gas pocket in liquid	Sodium boiling in forced convection
	Bubbly annular flow		Gas bubbles in liquid film with gas core	Evaporators with wall nucleation
	Droplet annular flow		Gas core with droplets and liquid film	Steam generator
	Bubbly droplet annular flow		Gas core with droplets and liquid film with gas bubbles	Boiling nuclear reactor channel
Dispersed flows	Bubbly flow		Gas bubbles in liquid	Chemical reactors
	Droplet flow		Liquid droplets in gas	Spray cooling
	Particulate flow		Solid particles in gas or liquid	Transportation of powder

Different two phase flow models have been developed to accurately describe the transport of mass, momentum and energy while at the same time keeping the computer memory requirement for a calculation within available limits. For nuclear reactor safety analysis, the one dimensional equations are generally used, which make the systems of equations relatively simple. However, when the mass, heat, or momentum transfer between different phases is involved the problem becomes complex. We need specific models for such processes occurring at the interface between the phases. The following presents various two phase flow models, and their equations, which are generally employed in nuclear power plant safety codes. The models and their equations given below are one dimensional and based on the Euler–Euler approach.

The fluid phase parameters given in the equations described below have been averaged over the cross-sectional flow area, A . That is, given a fluid phase parameter ϕ_k , corresponding to the k^{th} phase, area averaging is performed as follows:

$$\{\phi_k\} \equiv \frac{1}{A} \iint_A \phi_k dA \quad (48)$$

3.1.3.2. One dimensional two fluid model

The most complex two phase flow model is the two fluid model (discussed in references [23][24]). This model treats the general case of modelling each phase or component as a separate fluid with its own set of governing equations. In general, each phase has its own velocity, temperature and pressure. The velocity difference between the phases is induced by density differences as is done in separated flow. The temperature difference is fundamentally induced by the time lag of energy transfer between the phases at the interface as thermal equilibrium is reached. The modelling of pressure non-equilibrium is much more complex and will not be discussed [23]. For most applications of two fluid modelling this pressure non-equilibrium is negligibly small and usually neglected.

In the two fluid case, several interfacial transport models are required to complete the overall model. This approach has an advantage in that the actual transport processes can be rigorously defined; however, the disadvantage is that these kinetic processes must be modelled in detail, which implies a much greater depth of experimental data and insight.

These interfacial kinetic models are also dependent on the flow pattern. The model one would develop for the interfacial shear stress or heat flux is significantly different for a dispersed flow pattern in contrast to a stratified flow pattern. Similarly, the interfacial models would be different if one had gas bubbles in a liquid versus liquid droplets in a gas. In the two fluid model formulation, the transfer processes of each phase are expressed by their own balance equations, thus it is anticipated that the model can predict more detailed changes and phase interactions than the mixture model. However, this means that the two fluid model is far more complicated not only in terms of the number of field equations involved, but also in terms of the necessary equations for interface transport processes.

It is evident that these interface transport equations should be accurate to display the usefulness of the model. This is particularly true with the interaction terms Γ_k , M_k , and E_k (the mass, momentum, and energy transfers to the k^{th} phase from the interface) since without these interfacial exchanges in the field equations the two phases are essentially independent. These interaction terms determine the degree of coupling between phases, thus the transfer processes in each phase are greatly influenced by these terms. The major benefit of using the two fluid model is that it can take into account the dynamic and thermal non-equilibrium interactions between phases.

The differential formulation of the one dimensional, two fluid, full non-equilibrium transport equations is given below. The details of these equations are given by Todreas and Kazimi [25].

The first transport equation considered is for the conservation of mass in each phase given by:

$$\{\rho_k \alpha_k\} + \frac{\partial}{\partial z} \{\rho_k v_k \alpha_k\} = \Gamma_k \quad (49)$$

where ρ represents density, α the volume fraction, and v the phase velocity. The subscript k indicates either liquid phase — when the subscript is ‘l’, or vapour phase — when the subscript is ‘v’. The leftmost bracketed term represents the rate of change in the area averaged mass for a fluid phase k . In this equation, and those that follow, the fluid phase parameters are averaged over the cross-sectional flow area. The second term represents the change in mass along the axis of flow. Γ_k is the liquid or vapour mass generated by phase change or the interfacial mass transfer rate per unit volume. Thus, Γ_v is the rate at which vapour mass is generated per unit volume from liquid evaporation and Γ_l is the rate at which liquid mass is generated per unit volume from vapour condensation. For steady state flow the first term of equation (49) will vanish, resulting in equation (50):

$$\frac{\partial}{\partial z} \{\rho_k v_k \alpha_k\} = \Gamma_k \quad (50)$$

If each phase is incompressible the density of each phase is constant and equation (49) becomes:

$$\{\alpha_k\} + \frac{\partial}{\partial z} \{v_k \alpha_k\} = \frac{\Gamma_k}{\rho_k} \quad (51)$$

And furthermore, if there is no change of phases, the continuity equation reduces to:

$$\frac{\partial}{\partial t} \{\alpha_k\} + \frac{\partial}{\partial z} \{v_k \alpha_k\} = 0 \quad (52)$$

Equation (52) can be used in a low speed two phase flow without phase changes. Under these conditions the kinematics of the two phase system is completely governed by the phase redistribution, namely, by the convection and diffusion. The form of the above equation is analogous to that of a single phase incompressible flow. The conservation of momentum for each phase is given by:

$$\begin{aligned} \frac{\partial}{\partial t} \{\rho_k v_k \alpha_k\} + \frac{\partial}{\partial z} \{\rho_k v_k^2 \alpha_k\} &= \{\Gamma_k v_{sk} \cdot \mathbf{n}_z\} + \sum_{i=1}^N \{\mathbf{F}_{wk} \cdot \mathbf{n}_z\}_i \\ &- \frac{\partial}{\partial z} \{p_k \alpha_k\} + \{\mathbf{F}_{sk} \cdot \mathbf{n}_z\} + \{\rho_k \alpha_k\} \mathbf{g} \cdot \mathbf{n}_z \end{aligned} \quad (53)$$

where \mathbf{n}_z is the outward normal vector, \mathbf{F} is the force vector, p is pressure, and \mathbf{g} is the gravitational constant vector with g representing the scalar gravitational constant in some of

the following equations. Subscript ‘s’ means the surface of the interface, and subscript ‘w’ means the wall. The first term indicates the rate of change of the area averaged momentum for a fluid phase. The second term is the change in momentum along the flow axis. The first term on the right is the rate of momentum transfer due to phase change. The term $\mathbf{v}_{ks} \cdot \mathbf{n}_z$ is the interface velocity of phase k along the z coordinate and is either a positive or negative scalar value. The second term on the right is the sum of fluid phase drag forces on structures located in the flow. The third term on the right is the pressure gradient along flow axis. The vapour and liquid phases are typically assumed to have equal pressures; however, stability studies by Ransom and Hicks [26] this may result in numerical instabilities. The fourth term gives the drag forces which act on the fluid phase interface. The final term gives the gravitational force acting in the direction of flow. The conservation of energy for each phase is given by:

$$\begin{aligned} \frac{\partial}{\partial t} \{ \rho_k u_k^\circ \alpha_k \} + \frac{\partial}{\partial z} \{ \rho_k h_k^\circ v_k \alpha_k \} = & \Gamma_k h_{sk}^\circ - \left\{ p_k \frac{\partial \alpha_k}{\partial t} \right\} \\ & + \sum_{i=1}^N \left\{ q_k'' \alpha_k \frac{P}{A} \right\}_i - \{ \rho_k g v_k \alpha_k \} + \{ Q_{sk} \} \end{aligned} \quad (54)$$

where u° is the stagnation internal energy, h° is the stagnation enthalpy, q'' is the heat flux, P is the interphase perimeter, and Q_{sk} is the interfacial heat transfer rate. This equation is an energy balance expressed in terms of the stagnation internal energy and stagnation enthalpy, which are defined as follows:

$$u_k^\circ = u_k + \frac{v_k^2}{2} \quad (55)$$

$$h_k^\circ = u_k^\circ + \frac{p_k}{\rho_k} \quad (56)$$

The stagnation internal energy is defined as the sum of the thermodynamic internal energy and the kinetic energy of the fluid phase. The stagnation enthalpy has the usual definition; however, it is expressed in terms of the stagnation internal energy.

The first term on the left side of the energy conservation equation represents the time rate of change of the area averaged energy for a given fluid phase. The second term on the left side represents the change in the energy along the flow axis. The first term on the right side of the equation represents the rate of energy transfer due to phase change. The second term on the right represents the pressure work associated with changes in void fraction. The third term on the right represents the sum of the heat transfer between the fluid phase and structures in the flow. The fourth term on the right represent work due to gravity and the last term on the right side represents interfacial heat transfer.

Equations (49), (53), and (54) for each phase of the liquid–vapour system, represent the six conservation equations that serve as a starting point for two phase flow computer models.

The balance at an interface that corresponds to the field equation is called a jump condition. In analysing two phase flow, it is evident that we first follow the standard method of continuum mechanics. Thus, a two phase flow is considered as a field that is subdivided into single phase regions with moving boundaries between phases. The standard differential balance equations hold for each sub region with appropriate jump conditions to match the solutions of these differential equations at the interfaces. As there is no mass source or sink at the interface, all the vapour added by change of phase should appear as a loss to the liquid and vice versa. This describes the interphase jump conditions:

Mass:

$$\sum_{k=1}^2 \Gamma_k = 0 \quad (57)$$

Momentum:

$$\sum_{k=1}^2 (\Gamma_k \mathbf{v}_{sk} \cdot \mathbf{n}_z + \mathbf{F}_{sk} \cdot \mathbf{n}_z) = 0 \quad (58)$$

Energy:

$$\sum_{k=1}^2 (\Gamma_k h_{sk}^\circ + Q_{sk}) = 0 \quad (59)$$

3.1.3.3. One dimensional two phase mixture model

There is a separate set of governing equations for each phase in the two fluid model that complicates the solution of the governing equations. To reduce the number of governing equations we can adopt the strategy of treating the two phase system as a mixture. This treatment will reduce the number of equations but the accuracy of the results will depend on the validity of the assumption that the two phase system is behaving like a mixture. The mixture model accounts for the transport processes which occur at the interface. However, to obtain the two phase fluid mixture transport equations using the transport equations given below, “one must first recognize that interfacial transfer inside the mixture would not impact the overall mixture behaviour” [20]. This can be readily realized from the interfacial jump conditions mentioned previously. There are two well known mixture models for two phase flow named:

- (a) Two phase homogeneous equilibrium mixture (HEM) model;
- (b) Two phase drift flux model.

These two mixture models will be discussed in detail after developing the general mixture model equations. By summing the balance equations (49), (53), and (54) for each phase and applying the interfacial jump conditions in equations (57) through (59), the six equations are reduced to the following three conservation equations:

Mixture mass:

$$\frac{\partial \rho_m}{\partial t} + \frac{\partial G_m}{\partial z} = 0 \quad (60)$$

Mixture momentum:

$$\frac{\partial G_m}{\partial t} + \frac{\partial}{\partial z} \left(\frac{G_m^2}{\langle \rho_m \rangle} \right) = - \sum_{i=1}^N F_{wi} - \frac{\partial p_m}{\partial z} - \rho_m g \cos \theta \quad (61)$$

Mixture enthalpy:

$$\frac{\partial}{\partial t} \{ \rho_m h_m - p_m \} + \frac{\partial}{\partial z} \{ G_m \langle h_m \rangle \} = \sum_{i=1}^N q_i'' \frac{P_i}{A_i} + \frac{G_m}{\rho_m} \left(\sum_{i=1}^N F_{wi} + \frac{\partial p_m}{\partial z} \right) \quad (62)$$

In addition to these conservation equations, material properties may be defined as follows:

$$\rho_m = \{ \rho_v \alpha + \rho_l (1 - \alpha) \} \quad (63)$$

$$\langle \rho_m \rangle = \frac{G_m^2}{\{ \rho_v v_v^2 \alpha + \rho_l v_l^2 (1 - \alpha) \}} \quad (64)$$

$$\rho_m G_m = \{ \rho_v v_v \alpha + \rho_l v_l (1 - \alpha) \} \quad (65)$$

$$h_m = \frac{\{ \rho_v h_v \alpha + \rho_l h_l (1 - \alpha) \}}{\rho_m} \quad (66)$$

$$\langle h_m \rangle = \frac{\{ \rho_v h_v v_v \alpha + \rho_l h_l v_l (1 - \alpha) \}}{G_m} \quad (67)$$

$$(v^2)_m = \frac{\{ \rho_v \alpha v_v^2 + \rho_l (1 - \alpha) v_l^2 \}}{\rho_m} \quad (68)$$

$$\langle v^2 \rangle_m = \frac{\{ \rho_v \alpha v_v^3 + \rho_l (1 - \alpha) v_l^3 \}}{G_m} \quad (69)$$

$$p_m = \{ p_v \alpha + p_l (1 - \alpha) \} \quad (70)$$

where G is the mass flux, h is the heat transfer coefficient, and the subscript ‘m’ refers to the mixture of phases. With these general mixture model equations and conservation equations, the two mixture models may be explained.

(a) Two phase homogeneous equilibrium mixture (HEM) model

“The homogeneous equilibrium mixture (HEM) model is the simplest of the two phase fluid transport models. The HEM transport equations are derived from the two phase mixture equations by assuming that the velocity of each fluid phase is homogenous and that both phases

are at saturated conditions. The assumption of equilibrium means that the thermodynamic properties of each fluid phase can be expressed as a function of saturation pressure. The HEM transport equations are as follow” [20].

Necessary conditions:

- (i) Thermal equilibrium ($T_l = T_v = T_{SAT}$) or saturated enthalpies ($h_l = h_f$ and $h_v = h_g$)
- (ii) Equal phase pressures ($p_l = p_v = p$)
- (iii) Equal velocities ($v_l = v_v = v_m$)

where T refers to the temperature, subscript ‘SAT’ refers to a saturated parameter (i.e. T_{SAT} is the saturated temperature), subscript ‘f’ denotes liquid side, and subscript ‘g’ denotes vapour side.

Mixture mass:

$$\frac{\partial p_m}{\partial t} + \frac{\partial}{\partial z}(\rho_m v_m) = 0 \quad (71)$$

Mixture momentum:

$$\frac{\partial}{\partial t}(\rho_m v_m) + \frac{\partial}{\partial z}(\rho_m v_m^2) = - \sum_{i=1}^N F_{wi} - \frac{\partial p}{\partial z} - \rho_m g \cos \theta \quad (72)$$

Mixture energy:

$$\begin{aligned} \frac{\partial}{\partial t} \left\{ \rho_m \left[h_m + \frac{v_m^2}{2} \right] - p \right\} + \frac{\partial}{\partial z} \left\{ \rho_m v_m \left[h_m + \frac{v_m^2}{2} \right] \right\} \\ = \sum_{i=1}^N \left(q_i'' \frac{P_i}{A_i} \right) - \rho_m v_m g \cos \theta \end{aligned} \quad (73)$$

Mixture properties for this model are given by:

$$\rho_m = \{\rho_v \alpha + \rho_l(1 - \alpha)\} \quad (74)$$

$$v_m = \frac{\{\rho_v v_v \alpha + \rho_l v_l(1 - \alpha)\}}{\rho_m} \quad (75)$$

$$h_m = \frac{\{\rho_v h_v \alpha + \rho_l h_l(1 - \alpha)\}}{\rho_m} \quad (76)$$

where θ is the angle from vertical z axis.

(b) Two phase drift flux model

“The drift flux model, developed by Zuber and Findlay [27] in 1965, provides a simple, yet reasonably accurate, method of introducing the relative velocity between fluid phases into the mixture equations. The basic idea is that the relative velocity between phases, v_r , is related to a flow regime dependent drift velocity, V_{vj} ” [20]. This relation is given by equation (77). In v_r , the ‘r’ subscript denotes ‘relative’; in the drift velocity the subscript ‘vj’ refers to the component velocity ‘v’ in a frame of reference moving with superficial velocity ‘j’. Equations (78) through (79) present several empirical correlations developed for the drift velocity.

The two phase fluid mixture transport equations given above can be written in terms of the relative velocities between phases. Introducing equation (77) in the mixture equations below and rearranging results in the drift flux model conservation equations and mixture properties given in equations (81) through (87).

Relationship between relative velocity and drift velocity:

$$v_r = (v_v - v_l) = \frac{V_{vj}}{1 - \{\alpha\}} \quad (77)$$

Drift velocity equation for churn turbulent flow regime:

$$V_{vj} = 1.41 \left(\frac{\sigma g (\rho_l - \rho_g)}{\rho_l^2} \right)^{1/4} \quad (78)$$

Drift velocity equation for slug flow regime:

$$V_{vj} = 0.35 \left(\frac{g (\rho_l - \rho_g) D}{\rho_l} \right)^{1/2} \quad (79)$$

Drift velocity equation for annular flow regime:

$$V_{vj} = 23 \frac{\Delta \rho}{\rho_l} \left(\frac{\mu_l (1 - \{\alpha\}) v_l}{\rho_v D} \right)^{1/2} \quad (80)$$

where σ is the surface tension, D is the pipe diameter, and μ represents the dynamic viscosity. The conservation equations are given, with u representing the internal energy:

Mixture mass:

$$\frac{\partial \rho_m}{\partial t} + \frac{\partial}{\partial z} (\rho_m v_m) = 0 \quad (81)$$

Drift flux momentum:

$$\begin{aligned} & \rho_m \frac{\partial v_m}{\partial t} + \rho_m v_v \frac{\partial v_m}{\partial z} + \frac{\partial}{\partial z} \left(\frac{\rho_v \rho_l \{\alpha\} V_{vj}^2}{\rho_m (1 - \{\alpha\})} \right) \\ &= - \sum_{i=1}^N F_{wi} - \frac{\partial \rho_m}{\partial z} - \rho_m g \cos \theta \end{aligned} \quad (82)$$

Drift flux internal energy:

$$\begin{aligned} & \frac{\partial}{\partial t} \{\rho_m u_m\} + \frac{\partial}{\partial z} \{\rho_m u_m v_m\} + \frac{\partial}{\partial z} \left[\frac{\{\alpha\} \rho_l \rho_v (u_v - u_l) V_{vj}}{\rho_m} \right] + p_m \frac{\partial v_m}{\partial z} \\ &+ p_m \frac{\partial}{\partial z} \left[\frac{\{\alpha\} (\rho_l - \rho_v) V_{vj}}{\rho_m} \right] = \sum_{i=1}^N q_i'' \frac{P_i}{A_i} + v_m \left(\sum_{i=1}^N F_{wi} \right) \end{aligned} \quad (83)$$

Mixture properties:

$$\rho_m = \{\rho_v \alpha + \rho_l (1 - \alpha)\} \quad (84)$$

$$v_m = \frac{\{\rho_v v_v \alpha + \rho_l v_l (1 - \alpha)\}}{\rho_m} \quad (85)$$

$$u_m = \frac{\{\rho_v u_v \alpha + \rho_l u_l (1 - \alpha)\}}{\rho_m} \quad (86)$$

$$p_m = \{p_v \alpha + p_l (1 - \alpha)\} \quad (87)$$

“Because of the difficulty of working with a 6-equation model, a variety of simplified models have been developed. These models are derived by using mixture equations, or mixture equations in conjunction with individual phase equations, to obtain a reduced number of balance equations. Using this approach, it is possible to obtain 5-equation, 4-equation or 3-equation models for two phase flow. Of course, the simpler models result in a reduced number of calculated parameters as dictated by the restrictions that have been imposed. One of the following three restrictions is typically imposed on the phase velocities” [20].

- (1) Homogeneous flow, which assumes that the velocity of both phases is equal:

$$v_l = v_v = v_m \quad (88)$$

- (2) Phase slip, which assumes that there is a relative velocity between the phases. The ratio of the vapour velocity to the liquid velocity is defined as the slip ratio, given a flow dependent correlation. Thus, the slip ratio S equals:

$$S = \frac{v_v}{v_l} \quad (89)$$

- (3) Drift flux, which assumes that there is a relative velocity between the phases. The relative velocity is determined from a known drift flux correlation, v_{vj} , that is flow regime dependent:

$$\{v_v - v_l\} = \frac{v_{vj}}{\{1 - \alpha\}} \quad (90)$$

One of the following two restrictions is typically applied to the phase temperatures or enthalpies.

- (1) Full thermal equilibrium, which refers to the assumption that both fluid temperatures are equal and at the saturation temperature corresponding to the local pressure:

$$T_l = T_v = T_{SAT}(p) \quad (91)$$

- (2) Partial thermal equilibrium, which assumes that one of the two phases is at the saturation temperature corresponding to the local pressure:

$$T_l = T_{SAT}(p); T_v = T_{SAT}(p) \quad (92)$$

“In addition to the balance equations, a two phase flow model requires constitutive equations and thermodynamic property equations or tables to obtain a closed set of equations. The constitutive equations include fluid–structure and interfacial transport equations. These are as follows” [20]:

- (a) A wall friction correlation for a mixture or for each of the phases. One such equation is needed for each momentum balance equation.
- (b) A wall heat transfer correlation for a mixture or for each of the phases. One such equation is needed for each energy balance equation.
- (c) An interfacial mass transport equation.
- (d) An interfacial momentum transport equation.
- (e) An interfacial energy transport equation.

“The numerical methods used to solve the flow equations play a major role in the accuracy and stability of the predictions. The topic can easily fill an entire course and will not be discussed here.

Lastly, the number of parameters calculated by each model depends on the number of balance equations. The 6-equation model can be used to calculate 6 unknowns; $\alpha, p, v_l, v_v, T_l, T_v$ ” [20].

Table 6 [25] “provides the details of different types of two phase flow models that have been used for nuclear reactor safety analyses. Eleven different models are presented, including their restrictions, types of constitutive equations and calculated parameters. It is important to recognize that, for any model formulation, a mixture conservation equation plus a phase

conservation equation can be used in place of the two conservation equations for the phases” [20]. An example is provided in FIG. 23.

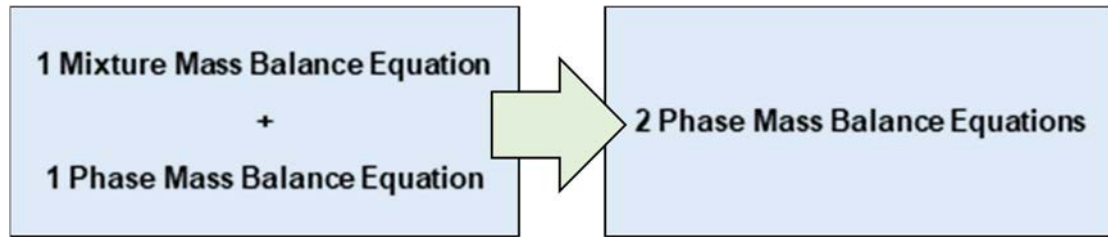


FIG. 23. Equivalent approaches to developing model mass balance equations [25].

Nomenclature used in 3.1.3

A	cross-sectional flow area
\mathbf{F}	force vector
D	pipe diameter
g	gravitational constant scalar
\mathbf{g}	gravitational constant vector
G	mass flux
h	heat transfer coefficient
h°	stagnation enthalpy
\mathbf{n}_z	outward normal vector
p	pressure
Q	heat transfer rate
S	slip ratio
T	temperature
u	internal energy
u°	stagnation internal energy
v	velocity
α	volume fraction
μ	dynamic viscosity
ρ	density
σ	surface tension
Γ	interfacial mass transfer density
ϕ	fluid phase parameter
θ	angle from vertical z axis
f	liquid side
g	vapour side
k	phase variable
l	liquid phase
m	mixture of phases
v	vapour phase
s	surface
SAT	saturated
w	wall

TABLE 6. TWO PHASE FLOW MODELS WITH EQUAL PHASE PRESSURES

CONSERVATION EQUATIONS	RESTRICTIONS	CONSTITUTIVE LAWS	CALCULATED PARAMETERS
SIX EQUATION MODELS			
Two fluid non-equilibrium	None	Phase wall friction	α, p, v_l v_v, T_l, T_v
Mass phase balance		Phase heat flux friction	
Momentum phase balance		Interfacial mass	
Energy phase balance		Interfacial momentum	
		Interfacial energy	
FIVE EQUATION MODELS			
Two fluid partial non-equilibrium	$T_l = T_{SAT}$ or $T_v = T_{SAT}$	Phase wall friction	α, p, v_l, v_v $(T_l \text{ or } T_v)$
Mass phase balance		Mixture wall heat flux	
Momentum phase balance		Interfacial mass	
Mixture energy balance		Interfacial momentum	
Two fluid partial non-equilibrium	$T_l = T_{SAT}$ or $T_v = T_{SAT}$	Phase wall friction	α, p, v_l, v_v $(T_l \text{ or } T_v)$
Mixture mass balance		Phase heat flux friction	
Momentum phase balance		Interfacial mass	
Energy phase balance		Interfacial momentum	
		Interfacial energy	
Slip or drift non-equilibrium	Slip or drift velocity	Mixture wall friction	α, p, T_l T_v, v_m
Mass phase balance		Phase heat flux friction	
Mixture momentum balance		Interfacial mass	
Energy phase balance		Interfacial energy	
		Slip velocity or Drift flux	
Homogeneous non-equilibrium	Equal velocity $v_l = v_v = v_m$	Mixture wall friction	α, p, T_l T_v, v_m
Mass phase balance		Phase heat flux friction	
Mixture momentum balance		Interfacial mass	
Energy phase balance		Interfacial energy	
FOUR EQUATION MODELS			
Two fluid equilibrium model	$T_l = T_v = T_{SAT}$	Phase wall friction	α, p, v_l, v_v
Mixture mass balance		Mixture heat flux friction	
Momentum phase balance		Interfacial mass	
Mixture energy balance		Interfacial momentum	
Drift partial non-equilibrium	Drift velocity $T_l \text{ or } T_v = T_{SAT}$	Mixture wall friction	$\alpha, p, v_m,$ $T_l \text{ or } T_v$
Mass phase balance		Mixture wall heat flux	
Mixture momentum balance		Interfacial mass	
Mixture energy balance		Drift flux correlation	
Slip partial non-equilibrium	Slip ratio $T_l \text{ or } T_v = T_{SAT}$	Mixture wall friction	$\alpha, p, v_m,$ $T_l \text{ or } T_v$
Mixture mass balance		Mixture wall heat flux	
Mixture momentum balance		Interfacial mass	
Phase energy balance		Drift flux correlation	
Homogeneous partial non-equilibrium	$u_l = u_v = u_m$ $T_l \text{ or } T_v = T_{SAT}$	Mixture wall friction	$\alpha, p, v_m,$ $T_l \text{ or } T_v$
Mixture mass balance		Phase wall heat flux	
Mixture momentum balance		Interfacial mass	
Phase energy balance		Interfacial energy	
THREE EQUATION MODELS			
Homogeneous equilibrium (HEM):	$u_l = u_v = u_m$ $T_l = T_v = T_{SAT}$	Mixture wall friction	α, p, u_m
Mixture mass balance		Mixture wall heat flux	
Mixture momentum balance			
Mixture energy balance			
Slip or drift equilibrium:	Slip or drift velocity $T_l = T_v = T_{SAT}$	Mixture wall friction	α, p, u_m
Mixture mass balance		Mixture wall heat flux	
Mixture momentum balance		Slip velocity or drift flux	
Mixture energy balance			

3.2. CHALLENGES TO NATURAL CIRCULATION

This lesson describes the impact of stagnation and thermal stratification within natural circulation loops. These example calculations are based on and adapted from annexes of IAEA-TECDOC-1474 [20] and several figures from this lecture, consisting of experiments using test facilities at Oregon State University (OSU), are used to illustrate concepts.

3.2.1. Examples for loss of natural circulation flow

A schematic of the APEX-CE test facility, shown in FIG. 24, models a PWR system. The facility includes a reactor vessel, a pressurizer, two U tube steam generators, reactor coolant pumps, and a safety injection system. Simulated decay heat is introduced to the system by electrically heating a ‘rod bundle’. The facility has a 1:4 length scale and 1:274 volume scale compared to a typical PWR.

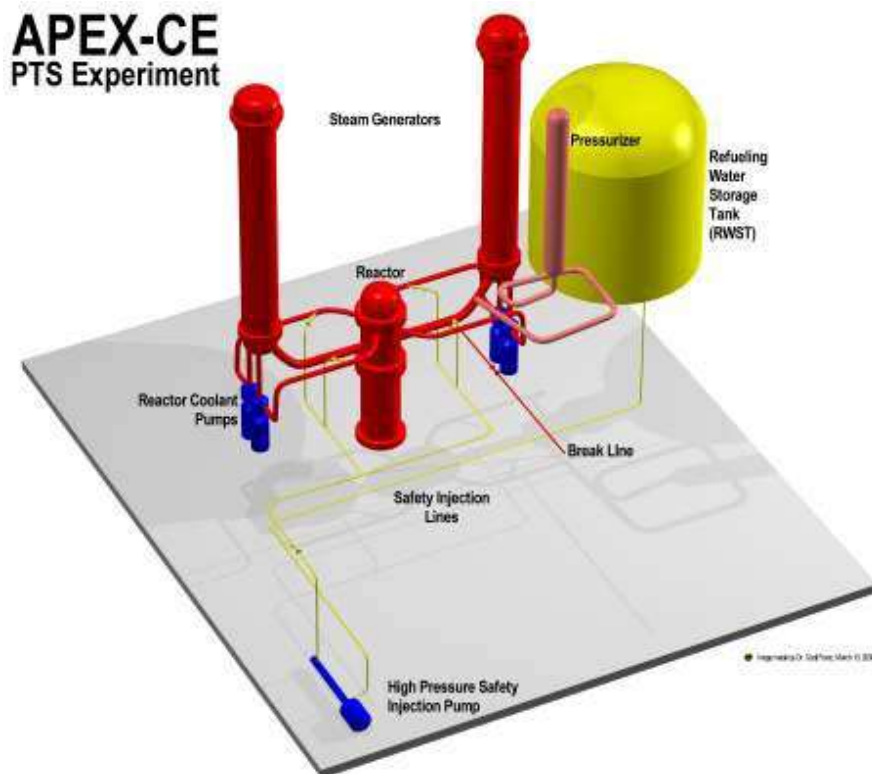


FIG. 24. Schematic of the APEX-CE test facility [20].

3.2.1.1. Loss of heat sink

Loss of heat sink may occur on loss of feedwater supply or by a main steam line break (MSLB) in one of multiple steam generators. Operators isolate feedwater in the steam generator affected by the MSLB and close steam isolation valves. However, the steam generator with a MSLB will depressurize on continued venting of steam and result in the simultaneous cooling of the primary system. It is possible for the primary fluid to then reach temperatures below that of the secondary fluid in functioning steam generators. If this occurs, there is no longer a heat sink driving force for natural circulation to these other steam generators.

In an APEX-CE test to demonstrate this mechanism the stagnation of cold legs 1 and 3, which are connected to a functioning steam generator, is shown in FIG. 25. This is indicated by drop in temperature of the hot leg below the steam generator temperature. The result of stagnation in this test is shown in FIG. 26, where flow rate through the working steam generator drops over the period of stagnation.

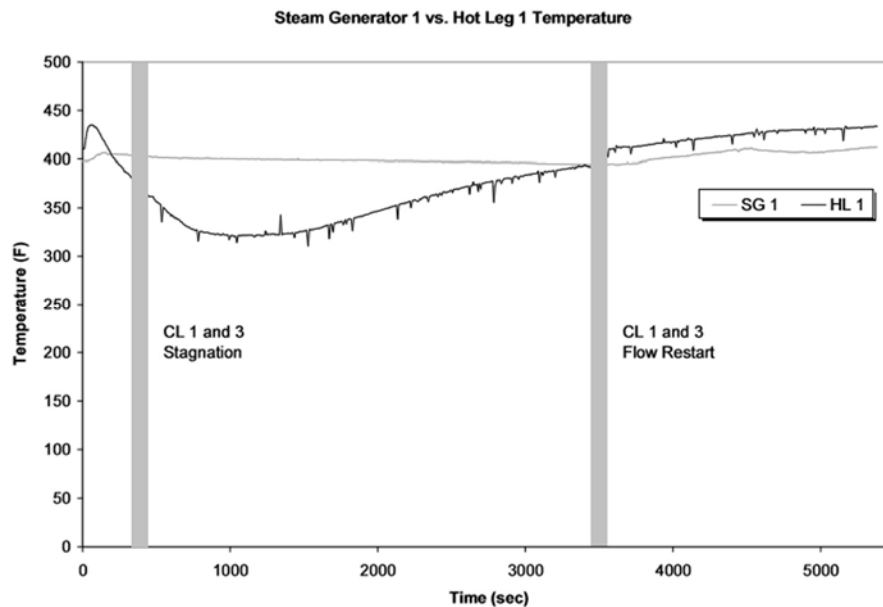


FIG. 25. Reverse heat transfer and recovery during a MSLB simulation [20].

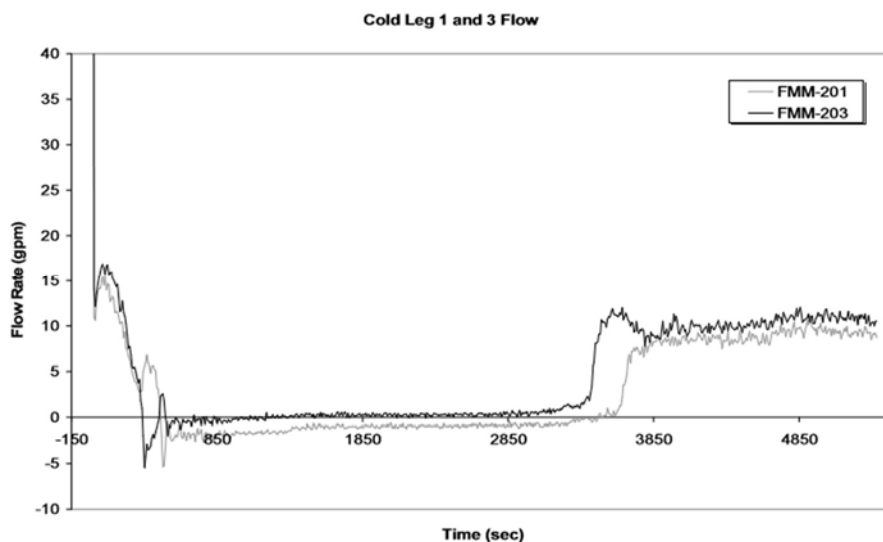


FIG. 26. Loss of flow and recovery during a MSLB simulation [20].

3.2.1.2. Loop seal cooling

The reactor crossover leg or pump loop seal is the region of piping returning from the steam generator and connecting to reactor coolant pumps in the cold leg. In the event of overcooling, such as that caused by a MSLB and described previously, pressure drops in the primary coolant system. If pressure drops beneath the setpoint, cold borated water is injected into the region of the cold leg between the reactor coolant pumps and the reactor vessel. The injected water has

a higher density than the coolant and will create a negative buoyancy region in the loop which will reduce the coolant flowrate. In plants which have multiple coolant loops, flow may be diverted from the steam generator to adjacent cold legs which are not have negatively buoyant regions.

FIG. 27 shows the Separate Effects Test Loop at OSU and visualizes mixing of fluorescent salt water injected in the cold leg. FIG. 28 shows that APEX-CE loop seal 2 and 4 are cooling asymmetrically, despite being connected to the same steam generator. FIG. 29 shows stagnation of loop 4 earlier than loop 2 as a result of loop seal cooling.



FIG. 27. Injected coolant mixing with fluid in a transparent loop seal [20].

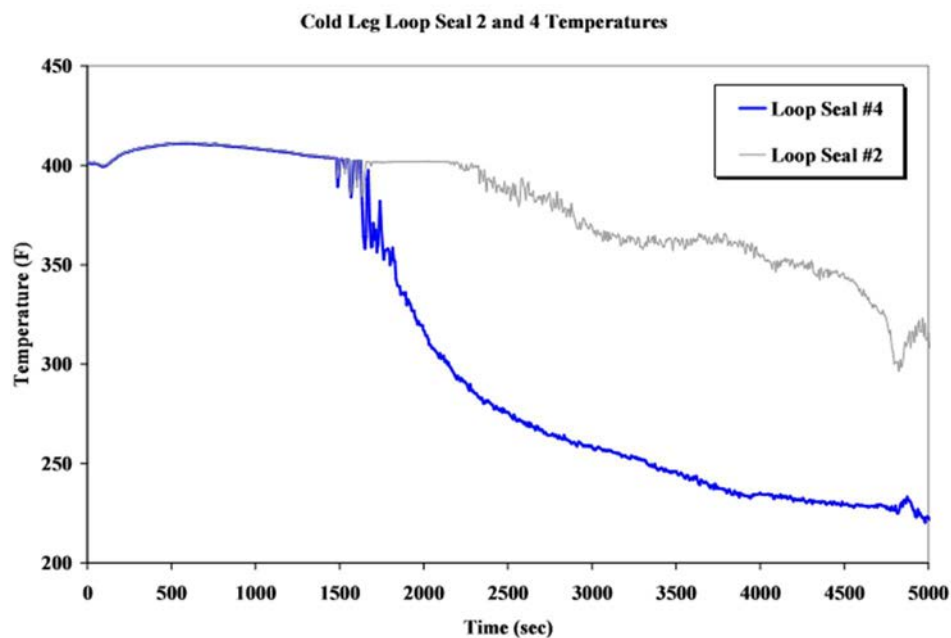


FIG. 28. Asymmetric loop seal cooling [20].

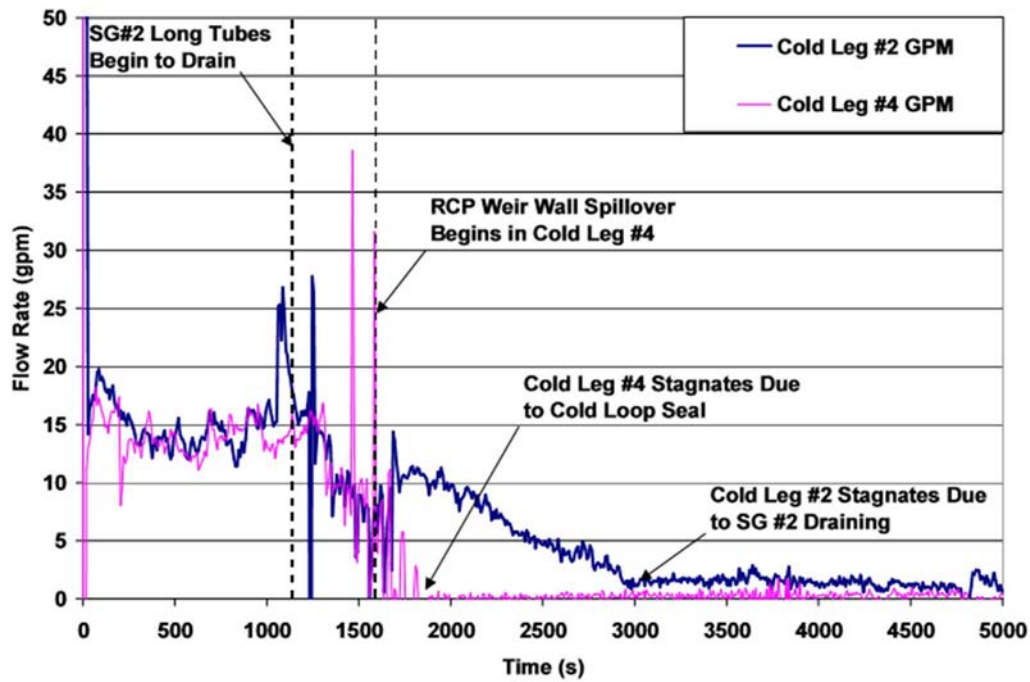


FIG. 29. Stagnation of primary loop due to loop seal cooling [20].

During a PWR small break loss of coolant accident (SBLOCA), or similar event where primary water inventory is reduced, the void fraction of the system increases, resulting in a rise in flow rate up to a maximum value where two phase flow has maximum driving buoyancy. The natural circulation flow in the primary system will gradually decrease from this point because of draining in the steam generator tubes. The time it takes for a steam generator tube to drain is heavily dependent on the length of the tubes, with longer tubes taking less time to drain.

FIG. 30 shows the results of an APEX-CE test in which a break valve was opened and closed in stepped intervals to remove primary system fluid, rising to a maximum before decreasing again. Idaho National Engineering Laboratory performed similar tests with their Semiscale facility and compare in FIG. 31. FIG. 32 shows the significant different in draining times between the longest and shortest tubes of a steam generator U tube bundle.

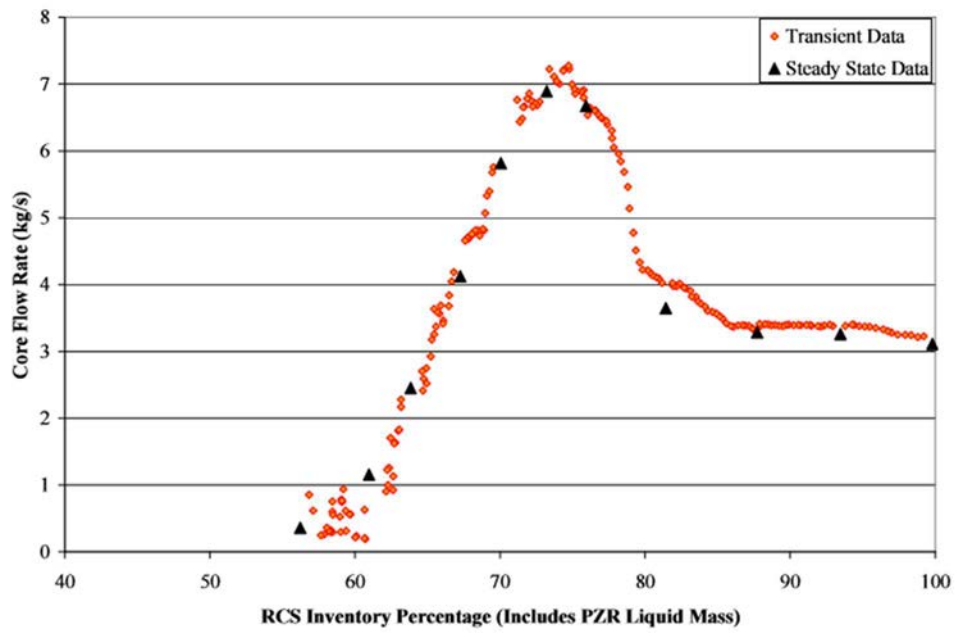


FIG. 30. Cold leg flow rates during a stepped inventory reduction [20].

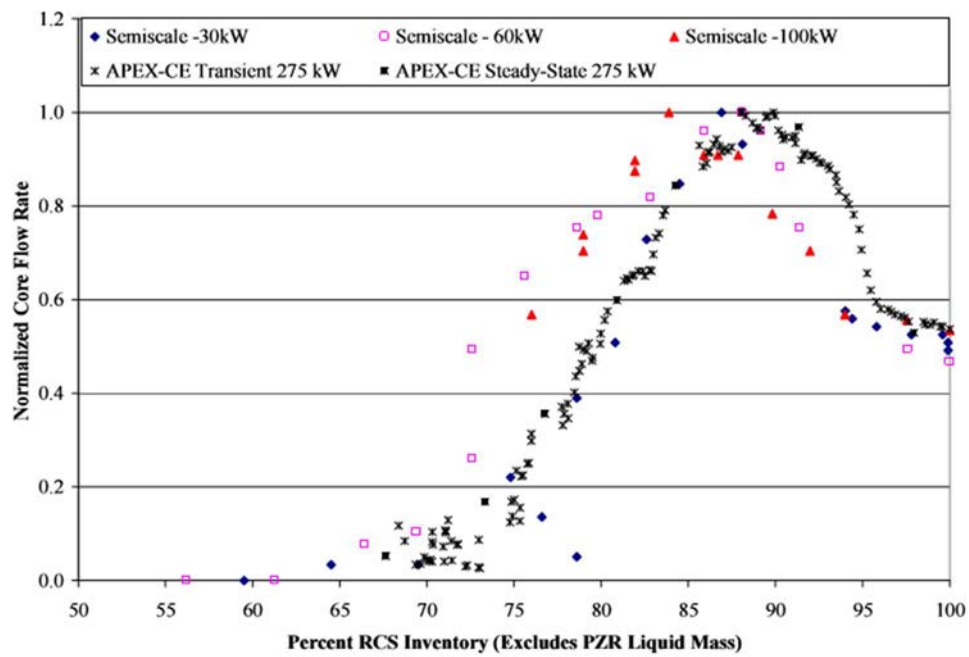


FIG. 31. Cold leg flow rates during a stepped inventory reduction [20].

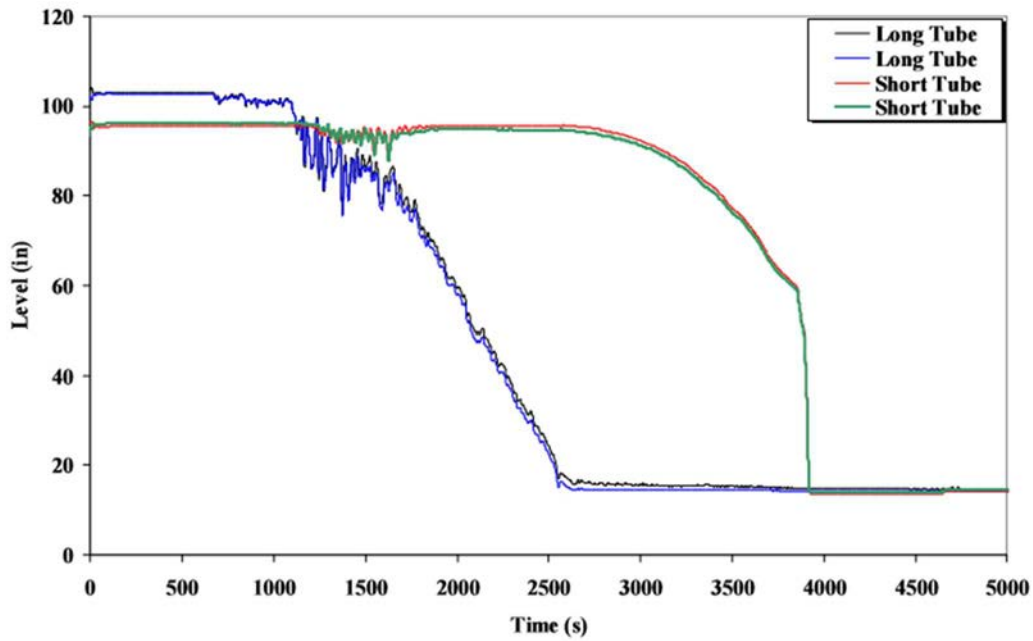


FIG. 32. Liquid levels in tubes of steam generator 2 during SBLOCA test [20].

3.2.2. Examples calculations for thermal stratification

Natural circulation flow is an important factor during safety system operation as it mixes the coolant into a relatively uniform temperature and pressure. When this uniformity is interrupted, a phenomenon known as thermal stratification may occur, in which distinct regions of fluid form. In a thermally stratified system, a column of fluid known as a plume may form and flow through other fluid regions. The governing equations of such a flow will be discussed. FIG. 33 visualizes thermal stratification and shows some of the regions of a PWR system in which thermal stratification may occur.

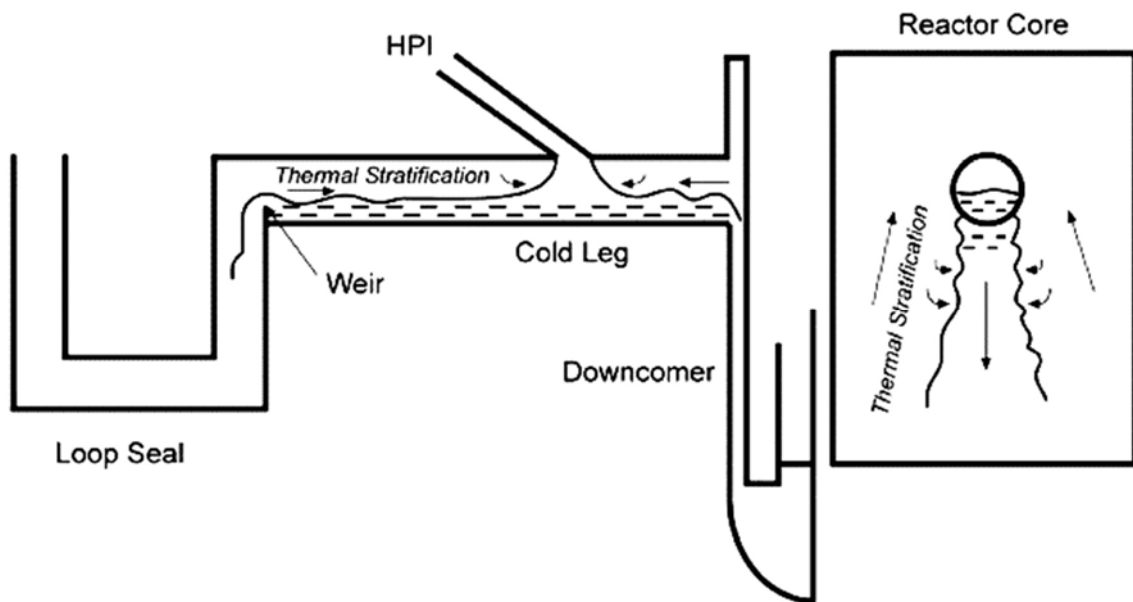


FIG. 33. Regions of thermal stratification in the primary loop of a PWR [20].

In geometries such as the left example in FIG. 33, consisting of thermal stratification in a horizontal cold leg by injection, the following criterion may be applied [28]:

$$Fr_{HPI/CL} = \left[1 + \frac{Q_{CL}}{Q_{HPI}} \right]^{-7/5} \quad (93)$$

where Q is volumetric flow rate, subscript 'CL' denotes cold leg, subscript 'HPI' denotes injection nozzle, and $Fr_{HPI/CL}$ is a modified Froude number, defined as:

$$Fr_{HPI/CL} = \frac{Q_{HPI}}{a_{CL} \left[g D_{CL} \frac{\rho_{HPI} - \rho_{CL}}{\rho_{HPI}} \right]^{1/2}} \quad (94)$$

where D represents diameter. Reyes developed a similar criterion in equation (93) using a hydraulic jump analysis as follows [29]:

$$Fr_{HPI/CL} = \left[1 + \frac{\rho_{CL} Q_{HPI}}{\rho_{HPI} Q_{CL}} \right]^{-1/2} \left[1 + \frac{Q_{CL}}{Q_{HPI}} \right]^{-3/2} \quad (95)$$

FIG. 34, shows the results of the criteria given by equations (93) and (95). It is shown that the two equations evolve similarly in the region where there is a large volumetric flow in the cold leg with a relatively small injection flow, $Q_{CL}/Q_{HPI} \gg 1$. The two, however, differ greatly as Q_{CL}/Q_{HPI} approaches 1. It is in this region where thermal stratification occurs, as volumetric flow rate through the cold leg is minimal.

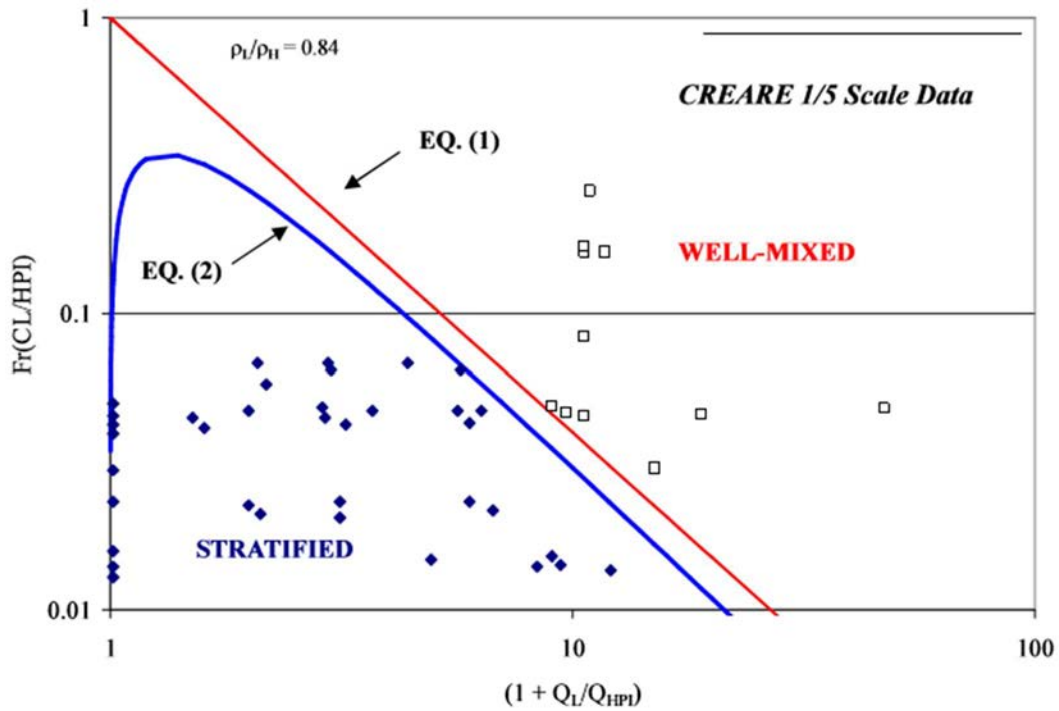


FIG. 34. Comparison of thermal stratification criteria in a horizontal cold leg [20].

FIG. 35 shows the injection of cold water from the top of the cold leg such that a plume is generated. Coolant system water mixes with the injection fluid at the plume boundaries through entrainment, indicated as region 1, and at free shear layers, indicated as region 2, shown by arrows in the figure. The plume results in cold water spreading in both directions, eventually resulting in a stagnant layer on the reactor coolant pump side of the cold leg. Once this stagnant layer forms, the injection flow is fully directed toward the reactor vessel side. Experiments at various scale test facilities have shown that, at least for top injection plumes, free shear mixing is negligible to entrainment mixing (CREARE 1/5 [30], CREARE 1/2 [31] and Purdue 1/2 [32]).

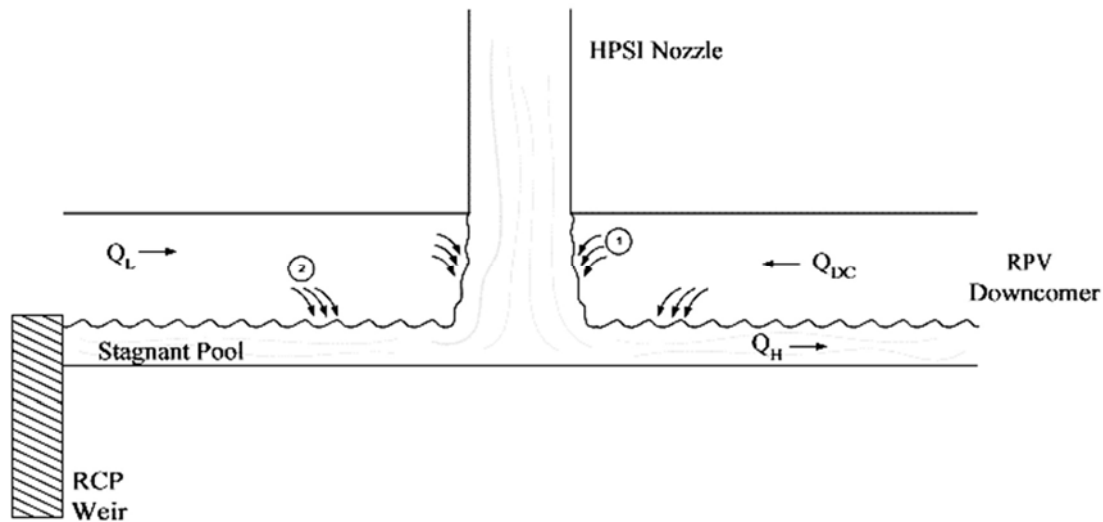


FIG. 35. Thermally stratified conditions for top injection [20].

3.2.2.1. Fundamental assumptions

The shearing motion caused by friction, known as vorticity, is restricted to the plume and its boundary, and does not occur in the bulk of fluid outside of the plume. The vorticity of the plume will cause turbulence in the fluids which in turn leads to fluctuating boundaries. However, this turbulence may not be forceful enough to collapse the plume and lead to fluids mixing. Rouse, Yih and Humphreys [33], Batchelor [34], Morton [35] and Turner [36] each studied the details of forced plume behaviour and have made progress in the development of governing equations.

Several assumptions may be made in characterizing the governing conservation equations of plume formation, and these are as follow:

(a) Taylor's entrainment assumption

Taylor [37] recognized that the plume spread and the position along the plume's height may be used to characterize velocity of fluid inflow across the plume boundary as proportional to the local mean velocity of the plume:

$$-v_E = \alpha_E u_p \quad (96)$$

where v_E is the ratio of mean inflow velocity, α_E is an entrainment constant, and u_p is the plume axial velocity. Taylor's entrainment assumption is that, at least for pure plumes, the entrainment constant is a known value which may be correlated to the momentum flux and the buoyancy flux.

(b) Similarity of velocity and buoyancy profiles

Morton made the assumption that the velocity and buoyancy profiles are the same across the height of the plume, and this assumption is supported by experimental data. A Gaussian profile is typically used to describe the velocity and buoyancy profiles as a function of horizontal position, allowing for mass and momentum flux to be described by mean values corresponding to integrals across the horizontal length of the profile.

(c) Gaussian profile

The Gaussian relationships typically used to describe the velocity and buoyancy profiles are as follow:

$$u(r, z) = u_p(z) \exp\left(-\frac{r^2}{b_u^2}\right) \quad (97)$$

$$g\Delta\rho(r, z) = g\Delta\rho(z) \exp\left(-\frac{r^2}{b_g^2}\right) \quad (98)$$

where u is velocity, g is the gravitational constant, and r is the distance from the plume centre; b_u and b_g are empirical constants, of length units, characterizing the Gaussian profiles. In equation (98), $g\Delta\rho$ is the plume buoyancy where $\Delta\rho$ is defined as the difference in density between the plume and its surroundings:

$$\Delta\rho = (\rho - \rho_m) \quad (99)$$

where ρ_m is the density of the fluid medium external to the plume. The equation of fluid state, defining the difference in temperature, is shown:

$$(T - T_m) = \frac{(\rho - \rho_m)}{\beta_o \rho_o} \quad (100)$$

where β_o and ρ_o are reference values of thermal expansion coefficient and density respectively. A temperature profile can be found by substituting this fluid state equation into the buoyant force from equation (98) as follows:

$$(T - T_m) = (T - T_m)_p \exp\left(-\frac{r^2}{b_g^2}\right) \quad (101)$$

The result of these profiles are several regions of dominance in the plume, as visualized in FIG. 36.

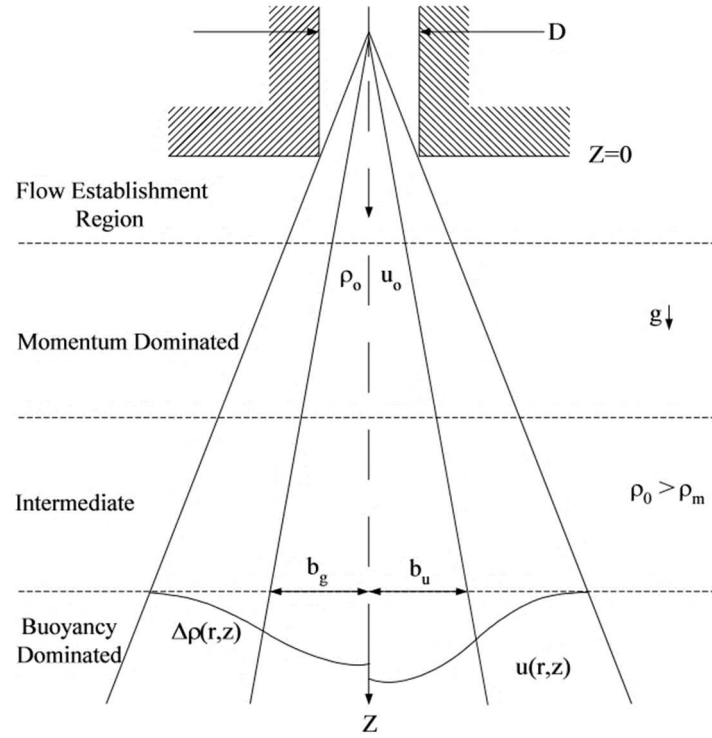


FIG. 36. Gaussian profiles in forced plumes [20].

3.2.2.2. Axisymmetric plumes

Following these assumptions, governing equations can be found for flow in axisymmetric, top injection plumes into a horizontal flow. Chen and Rodi used boundary layer assumptions and made the Boussinesq approximation for steady flow conditions to develop the following conservation equations [38]:

Mass conservation:

$$\frac{\partial}{\partial z}(\rho u r) + \frac{\partial}{\partial r}(\rho v r) = 0 \quad (102)$$

Momentum conservation:

$$\frac{\partial}{\partial z}(\rho u^2 r) + \frac{\partial}{\partial r}(\rho u v r) = g(\rho - \rho_m)r - \frac{\partial}{\partial r}(\rho u' v' r) \quad (103)$$

Thermal energy conservation:

$$\frac{\partial}{\partial z}(\rho u T r) + \frac{\partial}{\partial r}(\rho v T r) = -\frac{\partial}{\partial r}(r \rho v' T') \quad (104)$$

where v is the horizontal flow velocity of the fluid medium. The term $\rho u' v'$ is used to describe the shear stress. An equation for the thermal energy can also be written as:

$$\frac{\partial}{\partial z}[\rho u r (T - T_m)] + \frac{\partial}{\partial r}[\rho v r (T - T_m)] = -\rho u r \frac{\partial T_m}{\partial z} - \frac{\partial}{\partial r}(r \rho v' T') \quad (105)$$

Plume volume flux can be found by taking a spatial integral (eliminating common terms) and rearranging equation (102) as follows:

$$\begin{aligned}
\int_0^R \left[\frac{\partial}{\partial z} (\rho u r) + \frac{\partial}{\partial r} (\rho v r) \right] dr &= 0 \\
\int_0^R \frac{\partial}{\partial z} (\rho u r) dr &= - \int_0^R \frac{\partial}{\partial r} (\rho v r) dr \\
\frac{d}{dz} \int_0^R u r dr &= -v_E R
\end{aligned} \tag{106}$$

where v_E is the entrainment velocity. The density ρ is cancelled through the Boussinesq approximation, which removes differences in density except in the presence of the gravitational constant.

A momentum flux balance equation, equation (103), can similarly be found by integrating the momentum conservation equation as follows:

$$\begin{aligned}
\int_0^R \left[\frac{\partial}{\partial z} (\rho u^2 r) + \frac{\partial}{\partial r} (\rho u v r) \right] dr &= \int_0^R \left[g(\rho - \rho_m) r - \frac{\partial}{\partial r} (\rho u' v' r) \right] dr \\
\frac{d}{dz} \int_0^R \rho u^2 dr + \rho u v R &= g \int_0^R (\rho - \rho_m) r dr - \rho u' v' R \\
\frac{d}{dz} \int_0^R \rho u^2 dr &= g \int_0^R (\rho - \rho_m) r dr
\end{aligned} \tag{107}$$

The final step assumes that the second term on each side is small at $r = R$ due to the relatively low plume velocity and shear stress at this extremum.

Yet another equation, this one for thermal energy flux, can be found by integrating the energy conservation equation as it appears in equation (105):

$$\begin{aligned}
\int_0^R \left\{ \frac{\partial}{\partial z} [\rho u r (T - T_m)] + \frac{\partial}{\partial r} [\rho v r (T - T_m)] \right\} dr \\
= \int_0^R \left[-\rho u r \frac{\partial T_m}{\partial z} - \frac{\partial}{\partial r} (r \rho v' T') \right] dr \\
\frac{d}{dz} \int_0^R \rho u r (T - T_m) dr &= -\rho \frac{dT_m}{dz} \int_0^R u r dr \\
\frac{d}{dz} \int_0^R u (T - T_m) r dr &= -\frac{dT_m}{dz} \int_0^R u r dr
\end{aligned} \tag{108}$$

In moving from the first step to the second, the terms $(T - T_m)$ and $\rho v'T'$ are approximated as zero at r equal to R . In moving from the second to the third, the Boussinesq approximation is again used to eliminate the density term.

These three new equations, found by integrating the conservation equations, can be evaluated in consequence of profiles such as the Gaussian profiles presented prior. The evaluated result of these three equations yields a set of differential equations to create scaling groups. Substituting equation (97) into (106) and solving will result in a volume flux balance equation:

$$\begin{aligned}\frac{d}{dz} \int_0^R u_p \exp\left(-\frac{r^2}{b_u^2}\right) r dr &= -v_E R \\ \frac{d}{dz} \left[u_p \frac{b_u^2}{2} \left(1 - \exp\left(-\frac{R^2}{b_u^2}\right)\right) \right] &= -v_E R \\ \frac{d}{dz} (b_u^2 u_p) &= -2R v_E\end{aligned}\tag{109}$$

In this derivation, $\exp(-R^2/b_u^2)$ is approximated to be zero. A momentum flux balance equation can be found similarly by substituting equation (98) into (107) and solving:

$$\begin{aligned}\frac{d}{dz} \int_0^R \rho u_p^2 \exp\left(-\frac{2r^2}{b_u^2}\right) dr &= g \int_0^R (\rho - \rho_m) \exp\left(-\frac{r^2}{b_g^2}\right) r dr \\ \frac{d}{dz} \left[\frac{\rho u_p^2 b_u^2}{4} \left(1 - \exp\left(-\frac{2R^2}{b_u^2}\right)\right) \right] &= g(\rho - \rho_t)_p \frac{b_u^2}{2} \left(1 - \exp\left(-\frac{R^2}{b_u^2}\right)\right) \\ \frac{d}{dz} (\rho b_u^2 u_p^2) &= 2g(\rho - \rho_t)_p b_g^2\end{aligned}\tag{110}$$

Substituting equation (101) into (108) results in a balance equation for thermal energy flux:

$$\begin{aligned}\frac{d}{dz} \int_0^R u_p \exp\left(-\frac{b_g^2 + b_u^2}{b_g^2 b_u^2} r^2\right) (T - T_m)_p r dr \\ = -\frac{dT_m}{dz} \int_0^R u_p \exp\left(-\frac{r^2}{b_u^2}\right) r dr \\ \frac{d}{dz} \left[\frac{b_g^2 b_u^2 u_p \Delta T}{2(b_g^2 + b_u^2)} \left(1 - \exp\left(-\frac{R(b_g^2 + b_u^2)}{b_g^2 b_u^2}\right)\right) \right] \\ = \frac{b_u^2 u_p}{2} \frac{dT_m}{dz} \left(1 - \exp\left(-\frac{R^2}{b_u^2}\right)\right) \\ \frac{d}{dz} \left(\frac{b_g^2 b_u^2 u_p \Delta T_p}{b_g^2 + b_u^2} \right) = b_u^2 u_p \frac{dT_m}{dz}\end{aligned}\tag{111}$$

Equations (109) through (111) are can be compared to those developed by Rodi [39]. These equations can also be written using volumetric flow rates; the plume's volumetric flow rate is:

$$Q_p = 2\pi \int_0^R ur dr \quad (112)$$

The substitution of Gaussian profile equation (97) is shown:

$$\begin{aligned} Q_p &= 2\pi \int_0^R u_p \exp\left(-\frac{r^2}{b_u^2}\right) r dr \\ Q_p &= \pi b_u^2 u_p \left(1 - \exp\left(-\frac{R^2}{b_u^2}\right)\right) \\ Q_p &= \pi b_u^2 u_m \end{aligned} \quad (113)$$

Taking a derivative and making the substitution of equation (109) gives the following relationship for entrainment volumetric flow rate:

$$\frac{dQ_E}{dz} = 2\pi R v_E \quad (114)$$

The governing equations for the forced plume are found by substituting equations (113) and (114) into (109) through (111). The three produced governing equations are as follow:

Volume balance:

$$\frac{dQ_p}{dz} = -\frac{dQ_E}{dz} \quad (115)$$

Momentum balance:

$$\frac{d}{dz} \left(\frac{\rho Q_p^2}{b_u^2} \right) = 2\pi^2 g b_g^2 (\rho - \rho_L)_p \quad (116)$$

Energy balance:

$$\frac{d}{dz} \left(\frac{Q_p \Delta T_p \lambda}{\sqrt{1 + \lambda^2}} \right) = -Q_p \frac{dT_m}{dz} \quad (117)$$

where λ is the ratio of b_g to b_u . At the lower position limit, $z = 0$, Q_{HPI} is approximately equal to Q_p , D_{HPI} is approximately $2R$, and ΔT_p is approximately $(T_{HPI} - T_m)$.

Furthermore, the following dimensionless initial and boundary conditions are constructed for the case:

$$z^+ = \frac{2z}{D_{\text{HPI}}} \quad (118)$$

$$Q_p^+ = \frac{Q_p}{Q_{\text{HPI}}} \quad (119)$$

$$Q_E^+ = \frac{Q_E}{Q_{E0}} \quad (120)$$

$$b_u^+ = \frac{2b_u}{D_{\text{HPI}}} \quad (121)$$

$$b_g^+ = \frac{2b_g}{D_{\text{HPI}}} \quad (122)$$

$$\Delta T_p^+ = \frac{\Delta T}{T_{\text{HPI}} - T_m} \quad (123)$$

$$\left(\frac{dT_m}{dz}\right)^+ = \frac{\frac{dT_m}{dz}}{\left(\frac{dT_m}{dz}\right)_0} \quad (124)$$

$$\Delta \rho_p^+ = \frac{\Delta \rho_p}{\rho_{\text{HPI}} - \rho_m} \quad (125)$$

Dimensionless groups are defined to characterize various flow behaviours; these are:

$$\Pi_{\text{QE}} = \left(\frac{Q_E}{Q_{\text{HPI}}}\right)_0 \quad (126)$$

$$Fr_{\text{HPI}} = \frac{Q_{\text{HPI}}}{A_{\text{HPI}} \left(\frac{g\Delta\rho_p D_{\text{HPI}}}{\rho_{\text{HPI}}}\right)_0^{\frac{1}{2}}} \quad (127)$$

$$\Pi_{\Delta T} = \frac{D_{\text{HPI}}}{(T_{\text{HPI}} - T_m)_0} \left(\frac{dT_m}{dz}\right)_0 \quad (128)$$

where Π_{QE} is the ratio of volumetric fluxes at the entrance, Fr_{HPI} is a ratio of inertia to buoyancy, A_{HPI} is the cross-sectional area of the injection nozzle, and $\Pi_{\Delta T}$ describes the level of thermal stratification. By substituting equations (118) through (125) into the governing equations (115) through (117) and applying the dimensionless groups from equations (126) through (128), the following dimensionless balance equations are made:

Volume balance:

$$\frac{dQ_p^+}{dz^+} = -\Pi_{\text{QE}} \frac{dQ_E^+}{dz^+} \quad (129)$$

Momentum balance:

$$(Fr_{\text{HPI}})^2 \frac{d}{dz^+} \left(\frac{\rho Q_p}{b_u^2} \right)^+ = \frac{\pi}{2} (b_g^2 \Delta \rho_p)^+ \quad (130)$$

Energy balance:

$$\frac{d}{dz^+} \left(\frac{Q_p \Delta T_p \lambda}{\sqrt{1 + \lambda^2}} \right)^+ = - \frac{\Pi_{\Delta T}}{2} Q_p^+ \left(\frac{dT_m}{dz} \right)^+ \quad (131)$$

Theofanous [40] further characterized decay equations to predict volumetric flow and temperature in the plume as follow:

Entrainment correlation:

$$\Pi_{\text{QE}} = 0.5176 \left(\frac{z}{D_{\text{HPI}}} \right)^{1.236} (Fr_{\text{HPI}})^{-0.414} \quad (132)$$

Temperature decay correlation:

$$\Delta T^+ = 1 - 0.326 \left(\frac{z}{D_{\text{HPI}}} \right)^{0.65} (Fr_{\text{HPI}})^{-0.274} \quad (133)$$

3.2.2.3. Planar plumes

In addition to those discussed for axisymmetric plumes, governing equations have been developed for planar plumes as illustrated in FIG. 37.

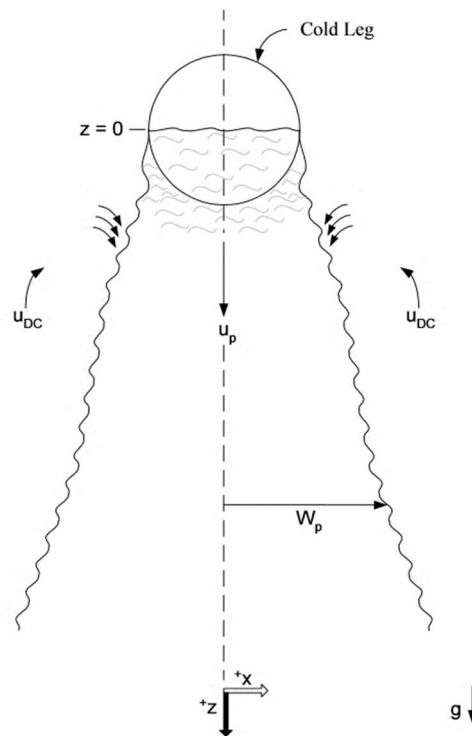


FIG. 37. Schematic of a single planar plume in the RPV downcomer.

The same assumptions are made as with axisymmetric plumes including Taylor's entrainment assumption, similarity of profiles, and Gaussian profiles. The following are the profiles for the planar case:

$$u(x, z) = u_p(z) \exp\left(-\frac{x^2}{b_u^2}\right) \quad (134)$$

$$g\Delta\rho(x, z) = g\Delta\rho(z) \exp\left(-\frac{x^2}{b_u^2}\right) \quad (135)$$

$$(T - T_m) = (T - T_m)_p \exp\left(-\frac{x^2}{b_g^2}\right) \quad (136)$$

The conservation equations were developed for this case as [38]:

Mass conservation:

$$\frac{\partial}{\partial z}(pu) + \frac{\partial}{\partial x}(pv) = 0 \quad (137)$$

Momentum conservation:

$$\frac{\partial}{\partial z}(pu^2) + \frac{\partial}{\partial x}(puv) = g(\rho - \rho_m)r - \frac{\partial}{\partial x}(\rho u'v') \quad (138)$$

Thermal energy conservation:

$$\frac{\partial}{\partial z}[pu(T - T_m)] + \frac{\partial}{\partial x}[pv(T - T_m)] = -\rho u \frac{\partial T_m}{\partial x} - \frac{\partial}{\partial x}(\rho v'T') \quad (139)$$

where equation (139) is written in the same form as equation (105). These three equations are integrated to produce flux balance equations. Equation (137) results in the volume flux balance equation as follows:

$$\begin{aligned} \int_0^{W_p} \left[\frac{\partial}{\partial z}(\rho u) + \frac{\partial}{\partial x}(\rho v) \right] dx &= 0 \\ \int_0^{W_p} \frac{\partial}{\partial z}(\rho u) dx &= \int_0^{W_p} \frac{\partial}{\partial x}(\rho v) dx \\ \frac{d}{dz} \int_0^{W_p} u dx &= -v_E W_p \end{aligned} \quad (140)$$

where W_p is the plume halfwidth. The Boussinesq approximation is used to eliminate density terms in the final step of this evaluation. The momentum flux balance equation is found in a similar integration of equation (138):

$$\begin{aligned}
\int_0^{W_p} \left[\frac{\partial}{\partial z} (\rho u^2) + \frac{\partial}{\partial x} (\rho u v) \right] dx &= \int_0^{W_p} \left[g(\rho - \rho_m) - \frac{\partial}{\partial x} (\rho u' v') \right] dx \\
\frac{d}{dz} \int_0^{W_p} \rho u^2 dx + \rho u v W_p &= g \int_0^{W_p} (\rho - \rho_m) dx - \rho u' v' W_p \\
\frac{d}{dz} \int_0^{W_p} \rho u^2 dx &= g \int_0^{W_p} (\rho - \rho_m) dx
\end{aligned} \tag{141}$$

In the final step, the approximation that the velocity and buoyancy are zero at $x = W_p$. Finally, the thermal energy flux balance equation is found by integrating equation (139):

$$\begin{aligned}
\int_0^{W_p} \left\{ \frac{\partial}{\partial z} [\rho u (T - T_m)] + \frac{\partial}{\partial x} [\rho v (T - T_m)] \right\} dx \\
= \int_0^{W_p} \left[-\rho u \frac{\partial T_m}{\partial z} - \frac{\partial}{\partial x} (\rho v' T') \right] dx \\
\frac{d}{dz} \int_0^{W_p} \rho u (T - T_m) dx = -\rho \frac{dT_m}{dz} \int_0^{W_p} u dx \\
\frac{d}{dz} \int_0^{W_p} u (T - T_m) dx = -\frac{dT_m}{dz} \int_0^{W_p} u dx
\end{aligned} \tag{142}$$

The Boussinesq approximation is again used to eliminate the density terms in the final step of this evaluation.

Equations (140) through (142) can be solved using the planar plume Gaussian profiles found in equations (134) (136). The volume flux is found by substituting equation (134) into equation (140) as follows:

$$\begin{aligned}
\frac{d}{dz} \int_0^{W_p} u_p \exp\left(-\frac{x^2}{b_u^2}\right) dx &= -v_E W_p \\
\frac{d}{dz} \left(\frac{b_u u_p \sqrt{\pi}}{2} \right) &= -v_E W_p \\
\frac{d}{dz} (b_u u_p) &= -\frac{2}{\sqrt{\pi}} v_E
\end{aligned} \tag{143}$$

Momentum flux is solved by substitution of (134) and (135) into (141) as follows:

$$\frac{d}{dz} \int_0^{W_p} \rho u_p^2 \exp\left(-\frac{2x^2}{b_u^2}\right) dx = g \int_0^{W_p} \Delta \rho_p \exp\left(-\frac{x^2}{b_u^2}\right) dx \tag{144}$$

$$\frac{d}{dz} \left(\frac{\rho b_u u_p^2 \sqrt{\pi}}{4} \right) = \frac{g \Delta \rho_p b_g \sqrt{\pi}}{2}$$

$$\frac{d}{dz} (\rho b_u u_p^2) = 2g \Delta \rho_p b_g$$

Substituting equations (124) and (126) into equation (142) yields the equation for thermal energy flux:

$$\begin{aligned} \frac{d}{dz} \int_0^{W_p} u_p (T - T_m)_p \exp \left(-\frac{b_g^2 + b_u^2}{b_g^2 b_u^2} x^2 \right) dx \\ = -\frac{dT_m}{dz} \int_0^{W_p} u_p \exp \left(-\frac{x^2}{b_u^2} \right) dx \\ \frac{d}{dz} \left(\frac{b_g b_u u_p \Delta T_p \sqrt{\pi}}{2 \sqrt{b_g^2 + b_u^2}} \right) = -\frac{dT_m}{dz} \frac{b_u u_p \sqrt{\pi}}{2} \\ \frac{d}{dz} \left[b_u u_p \Delta T_p \left(\frac{\lambda^2}{1 + \lambda^2} \right)^{1/2} \right] = -b_u u_p \frac{dT_m}{dz} \end{aligned} \quad (145)$$

The plume volumetric flow rate can be represented as:

$$Q_p = 2s \int_0^{W_p} u dx \quad (146)$$

where s is the downcomer gap size. Substituting the Gaussian velocity profile, given by equation (134), and integrating is shown:

$$\begin{aligned} Q_p &= 2s \int_0^{W_p} u_p \exp \left(-\frac{x^2}{b_u^2} \right) dx \\ Q_p &= \sqrt{\pi} b_u u_p s \end{aligned} \quad (147)$$

Entrainment volumetric flow rate is related to entrainment velocity by the following expression:

$$\frac{dQ_E}{dz} = s W_p v_E \quad (148)$$

The governing equations for the forced plume are found by substituting equations (147) and (148) into (143) through (145). The three produced governing equations are as follow:

Volume balance:

$$\frac{dQ_p}{dz} = -\frac{dQ_E}{dz} \quad (149)$$

Momentum balance:

$$\frac{d}{dz} \left(\frac{\rho Q_p^2}{b_u^2} \right) = 2\pi^2 s^2 g \Delta \rho_p b_g \quad (150)$$

Energy balance:

$$\frac{d}{dz} \left(\frac{Q_p \Delta T_p \lambda}{\sqrt{1 + \lambda^2}} \right) = -Q_p \frac{dT_m}{dz} \quad (151)$$

Furthermore, the following dimensionless initial and boundary conditions are constructed:

$$z^+ = \frac{2z}{D_{CL}} \quad (152)$$

$$Q_p^+ = \frac{Q_p}{Q_{p0}} \quad (153)$$

$$Q_E^+ = \frac{Q_E}{Q_{E0}} \quad (154)$$

$$b_u^+ = \frac{2b_u}{D_{CL}} \quad (155)$$

$$b_g^+ = \frac{2b_g}{D_{CL}} \quad (156)$$

$$\Delta T_p^+ = \frac{\Delta T}{T_{p0} - T_m} \quad (157)$$

$$\left(\frac{dT_m}{dz} \right)^+ = \frac{\frac{dT_m}{dz}}{\left(\frac{dT_m}{dz} \right)_0} \quad (158)$$

$$\Delta \rho_p^+ = \frac{\Delta \rho_p}{\rho_{p0} - \rho_m} \quad (159)$$

The dimensionless groups for this problem are defined as:

$$\Pi_{QE} = \left(\frac{Q_E}{Q_p} \right)_0 \quad (160)$$

$$Fr_{DC} = \frac{Q_{p0}}{sD_{CL} \left(\frac{g\Delta\rho_p D_{CL}}{\rho_p} \right)^{\frac{1}{2}}_0} \quad (161)$$

$$\Pi_{\Delta T} = \frac{D_{CL}}{(T_p - T_m)_0} \left(\frac{dT_m}{dz} \right)_0 \quad (162)$$

where Π_{QE} , Fr_{DC} and $\Pi_{\Delta T}$ are the same as presented for the axisymmetric plume, though with the subscript ‘DC’ referring to the downcomer. Applying the conditions given in equations (152) through (159) and the dimensionless groups in (160) through (162) to the governing equations (149) through (151) yields the following dimensionless balance equations:

Volume balance:

$$\frac{dQ_p^+}{dz^+} = -\Pi_{QE} \frac{dQ_E^+}{dz^+} \quad (163)$$

Momentum balance:

$$(Fr_{DC})^2 \frac{d}{dz^+} \left(\frac{\rho Q_p}{b_u^2} \right)^+ = \frac{\pi}{2} \Delta\rho_p^+ b_g^+ \quad (164)$$

Energy balance:

$$\frac{d}{dz^+} \left(\frac{Q_p \Delta T_p \lambda}{\sqrt{1 + \lambda^2}} \right)^+ = -\frac{\Pi_{\Delta T}}{2} Q_p^+ \left(\frac{dT_m}{dz} \right)^+ \quad (165)$$

Kotsovinos [41] further characterizes mean planar fluid velocity at the plume axis by the following correlation:

Plume velocity correlation:

$$u_p = 1.66 \left(\frac{Q_{p0} g (\rho_{HPI} - \rho_m)}{s \rho_m} \right)^{\frac{1}{3}} \quad (166)$$

Dimensionless plume velocity:

$$Nu_p = C \cdot Re_p^{0.8} Pr^{0.4} \quad (167)$$

Nomenclature used in 3.2

A	cross-sectional area
b_g	empirical constant, length units
b_u	empirical constant, length units
D	diameter
Fr	modified Froude number
g	gravitational constant

Q	volumetric flow rate
r	distance from plume centre
s	downcomer gap size
T	temperature
u	velocity
v	velocity, horizontal flow velocity
W	halfwidth
x	distance from plume centre
α	constant
β	thermal expansion coefficient
λ	ratio of empirical constants
ρ	density
Π	dimensionless group, ratio
CL	cold leg
DC	downcomer
E	entrainment
HPI	pressure injection nozzle
m	fluid medium external to plume
p	plume
QE	volumetric flux at entrance
ΔT	thermal stratification

3.3. COMPUTATIONAL FLUID DYNAMICS MODELLING

In fluid mechanics, fluid flows are governed by partial differential equations which represent conservation laws such as mass, momentum, and energy. CFD replaces these partial differential equations with algebraic equations which are then solved numerically on digital computers using computer programs or commercial software packages to obtain a numerical solution to the governing equations. Examples of PIEAS applications of CFD to a range of reactor phenomena are included to provide further context to CFD concepts and applications in WCR.

3.3.1. Computational fluid dynamics concepts

3.3.1.1. Basic CFD procedure

In fluid mechanics, fluid flows are governed by partial differential equations which represent conservation laws such as mass, momentum and energy. CFD replaces these partial differential equations with algebraic equations which are then solved numerically on digital computers using computer programs or commercial software packages to give governing equations. In CFD, fluid flows are predicted and analysed using mathematical models, numerical techniques and software tools. The main interest in industrial CFD is to gain valuable information of a physical phenomenon at lower cost, and at less time compared to experimental approach. Moreover, in experimental approach detailed knowledge of the phenomenon cannot be obtained due to in-built limitations of measurements at selected points. CFD usage is increasing

in many industrial fields where it is used to predict flow and performance of process industry equipment and hence helps in improving the design of the product. The majority of fluid flows involved in practical engineering problems have complex flow features such as three dimensional, unsteady, turbulent, and may include combustion, and many CFD software have the capabilities to capture these flow features. The fundamental equations for any CFD problem are the Navier–Stokes (NS) equations which relate the pressure, velocity, density and temperature of the moving fluid. In many cases, CFD simulations give approximate solution to the fluid flow problem which might be due to inadequate representation of the mathematical model and limited computing power.

In the case of nuclear reactor safety analysis, system codes are extensively used to analyse the fluid flows. These codes provide one dimensional analysis and do not give fine details of the flow due to coarse nodalization. However, in many instances during nuclear reactor safety analysis, fine details and full three-dimensional flow effects are desired which have a significant influence on the safety criteria. One such feature is turbulent mixing which is always present in safety related thermal hydraulic phenomenon. CFD codes are then required to simulate mixing phenomenon using fine resolution with millions of mesh points. The problem becomes even more complex if the number of phases present is more than one and size of the geometry is large which require complex modelling and huge number of mesh points to resolve fine scale flow features.

In order to produce reliable results, both in house and commercial codes for thermal hydraulic analysis of nuclear reactors and other industrial problems have been developed and validated. Commercial codes such as ANSYS-CFX and FLUENT are widely and increasingly used for nuclear reactor safety applications. In the nuclear reactor community, for example, the SATURNE code is developed at EDF and the TRIO-U code and CAST3M code are developed at CEA for single phase flow whereas the NEPTUNE platform developed by CEA and EDF includes a two phase flow CFD tool. Two phase models are also available in commercial codes. All these codes are engaged in a qualification process in the field of nuclear thermal hydraulics to ensure that the software is effectively able to produce relevant results in a clearly defined application field [42].

The approximation of a continuously varying quantity in terms of values at a finite number of points is called discretization.

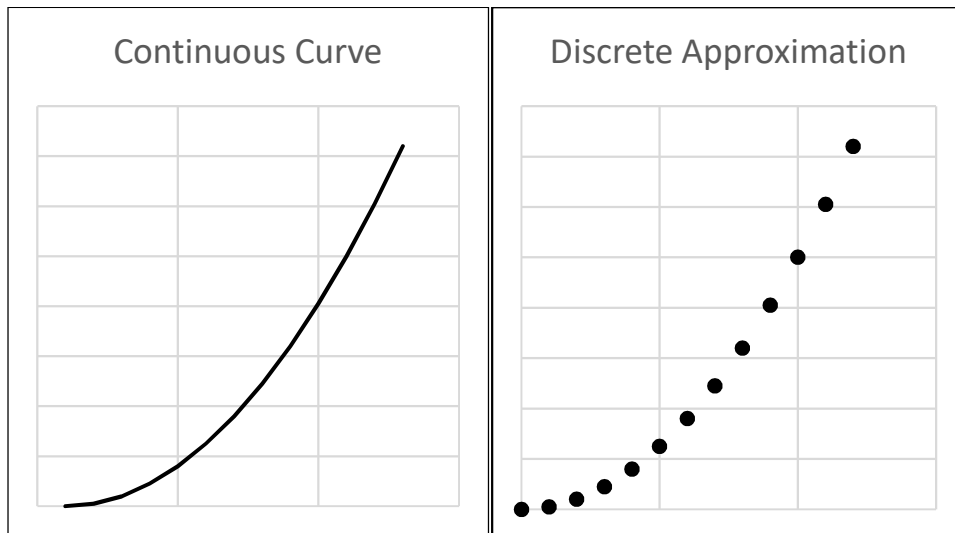


FIG. 38. Continuous function and its discrete approximation [43].

The fundamental elements of CFD simulation are:

- (a) Discretized flow field — field variables (ρ, u, v, w, p, \dots) are approximated by values at a finite number of nodes.
- (b) The equations of motion are discretized — approximated in by values at a finite number of nodes where the following conversion has been made:
differential or integral equations \rightarrow algebraic equations (as shown in FIG. 38)
(continuous) (discrete)
- (c) The resulting system of algebraic equations is solved to give values at the nodes.

CFD codes provide a complete CFD analysis consisting of following three main elements:

- (1) Pre-processing;
- (2) Solver;
- (3) Post-processing.

FIG. 39 shows the framework that illustrates the interconnectivity of elements within CFD analysis.

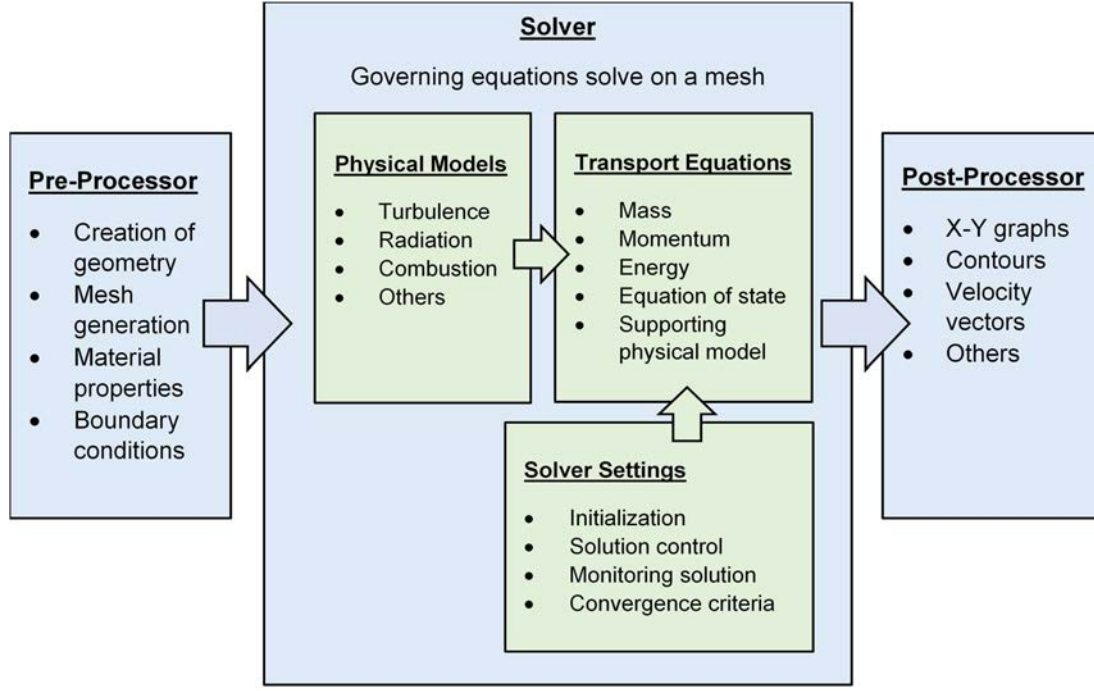


FIG. 39. Interconnectivity function of the three main elements within CFD analysis framework [44].

3.3.1.2. Governing equations of fluid flows

Navier–Stokes equations for a single phase flow in spacetime (x, t) domain describing the motion of fluids can be expressed in differential form as [45]:

Continuity:

$$\frac{\partial \rho}{\partial t} + \nabla \cdot (\rho \mathbf{u}) = 0 \quad (168)$$

Momentum conservation:

$$\rho \frac{\partial \mathbf{u}}{\partial t} + \rho \mathbf{u} \cdot \nabla \mathbf{u} = -\nabla p + \nabla \cdot \boldsymbol{\tau} + \rho \mathbf{f} \quad (169)$$

Energy conservation:

$$\begin{aligned} \rho \frac{\partial}{\partial t} \left(e + \frac{1}{2} u^2 \right) + \rho \mathbf{u} \cdot \nabla \left(e + \frac{1}{2} u^2 \right) \\ = -\nabla \cdot (p \mathbf{u}) + \nabla \cdot (\boldsymbol{\tau} \cdot \mathbf{u}) - \nabla \cdot \mathbf{q} + \rho \mathbf{f} \cdot \mathbf{u} + \dot{q} \end{aligned} \quad (170)$$

where ρ , \mathbf{u} , p , and e represent density, velocity, thermodynamic pressure, and specific internal energy, respectively while \mathbf{f} and \dot{q} are body force per mass and internal heating per volume. For the Newtonian fluid, shear stress tensor $\boldsymbol{\tau}$ is given as:

$$\boldsymbol{\tau} = \lambda (\nabla \cdot \mathbf{u}) \boldsymbol{\delta} + \mu (\nabla \mathbf{u} + \nabla \mathbf{u}^T) \quad (171)$$

where δ is a unit tensor and where μ and λ are absolute viscosity and second coefficient of viscosity, respectively. $\nabla \mathbf{u}^T$ is the transpose of the velocity gradient tensor. Also, according to Fourier's law of heat conduction, heat flux \mathbf{q} is given by:

$$\mathbf{q} = -\kappa \nabla T \quad (172)$$

where T and κ are temperature and thermal conductivity, respectively.

3.3.1.3. Discretization methods in CFD

Governing equations in CFD are discretized using the following methods:

(a) Finite difference method (FDM)

In FDM, Taylor series expansion is used to discretize the derivatives of the flow variables. This method is directly applied to the differential form of the governing equations e.g.

$$0 = \frac{\partial \mathbf{u}}{\partial x} + \frac{\partial \mathbf{v}}{\partial y} \approx \frac{u_{i+1,j} - u_{i-1,j}}{2\Delta x} + \frac{v_{i,j+1} - v_{i,j-1}}{2\Delta y} \quad (173)$$

The advantage of FDM include its simplicity and high degree of accuracy in spatial discretization, however it requires coordinate transformation and is limited to only simple geometries.

(b) Finite volume method (FVM)

FVM is applied directly to the integral formulation of the governing equations e.g.

$$net\ mass\ outflow = (\rho u A)_e - (\rho u A)_w + (\rho v A)_n - (\rho v A)_s \quad (174)$$

where subscripts e, w, n, and s are representing the east, west, north, and south faces of a volume cell, respectively.

FVM is flexible, suitable for complex geometries, and maintains conservation of mass, momentum, and energy. Unlike FDM, it does not require coordinate transformation. However, high order approximation of spatial derivatives cannot be obtained in FVM.

FIG. 43 shows the concept of FDM and FVM.

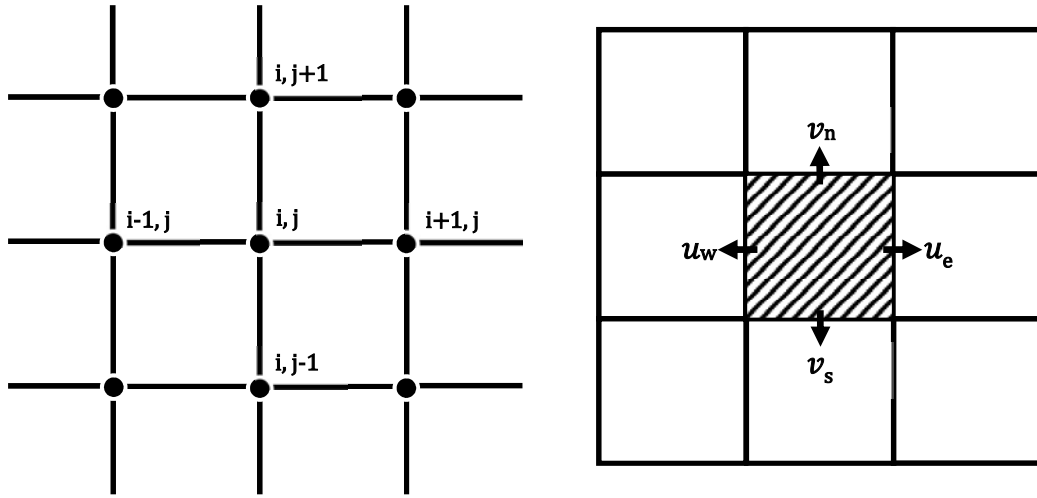


FIG. 40. Concept of FDM and FVM [43].

(c) Finite element method (FEM)

In FEM, the physical domain is subdivided into triangular or tetrahedral elements. Inside each element shape functions are defined which gives the variation of the solution inside element. In FEM, the governing equations are transformed from differential to equivalent integral form.

This can be done in two different ways. The first one is based on the variational principle and the second one is the method of weighted residuals. FEM is very popular in solid mechanics. This is attractive because of its integral formulation and unstructured grids which are important factors for simulating flows around complex geometries [46].

In addition to these methods, there are other discretization methods which include boundary element method, spectral method etc.

3.3.1.4. Verification and validation

V&V procedures are the primary means of assessing accuracy in computational simulations. These procedures serve as tools with which we build confidence and reliability in computational simulations. In the case of nuclear reactor safety, the validation of computationally simulated results is of critical importance as these affect the safety of the system under consideration and wrong predication may cause catastrophic failure of the nuclear system.

It is important to know the different terminologies used in the context of V&V [47]:

- Conceptual model: the conceptual model is composed of all information, mathematical modelling data, and mathematical equations that describe the physical system or process of interest. In CFD, the conceptual model is dominated by the partial differential equations for conservation of mass, momentum, and energy.

- Computerized model: the computerized model is an operational computer program that implements a conceptual model.
- Qualification: Determination of adequacy of the conceptual model to provide an acceptable level of agreement for the domain of intended application.

Verification is the process of assessing quality of performance to an intended function. Verification is performed either through code verification or solution verification. In code verification, the focus is on finding and removing mistakes in the source code; and finding and removing errors in the numerical algorithms. While solution verification assures the accuracy of input data; estimates the numerical solution error; and assures the accuracy of output data for the problem of interest. Verification can also be described as solving the equation right. It is concerned more with mathematics rather than physics. FIG. 41 shows the verification process for comparing the numerical simulation with various types of highly accurate solutions.

Validation is the process of determining whether the intended function is performed satisfactorily. To this end, validation assures that the computational simulation performed using CFD agrees well with real physics. In validation, simulations are compared with experimental results in order to identify and quantify errors and uncertainties. Validation can also be described as solving the right equations. FIG. 42 shows the validation process.

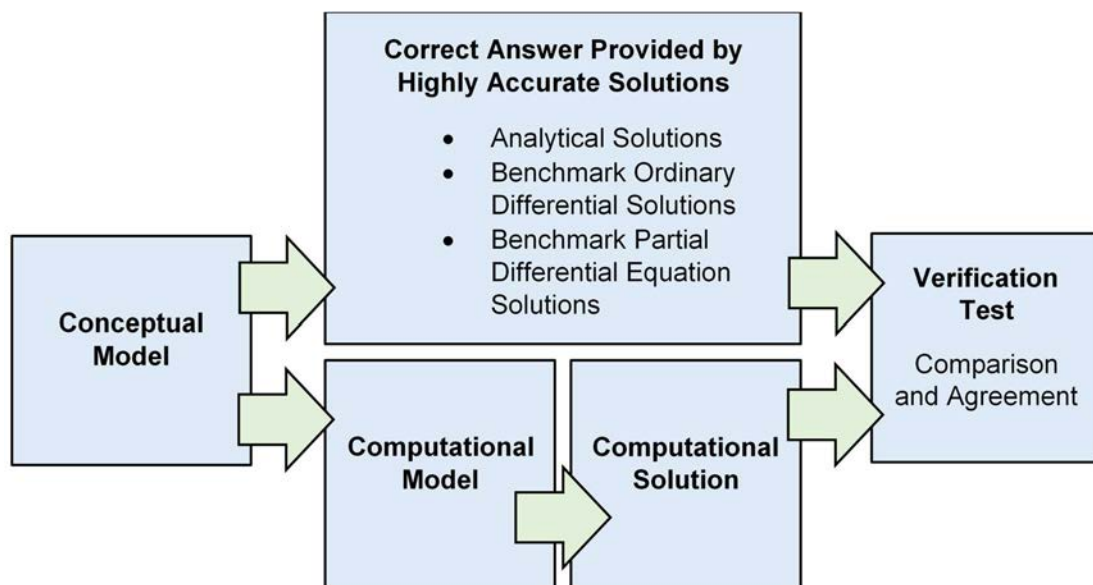


FIG. 41. Verification process [47].

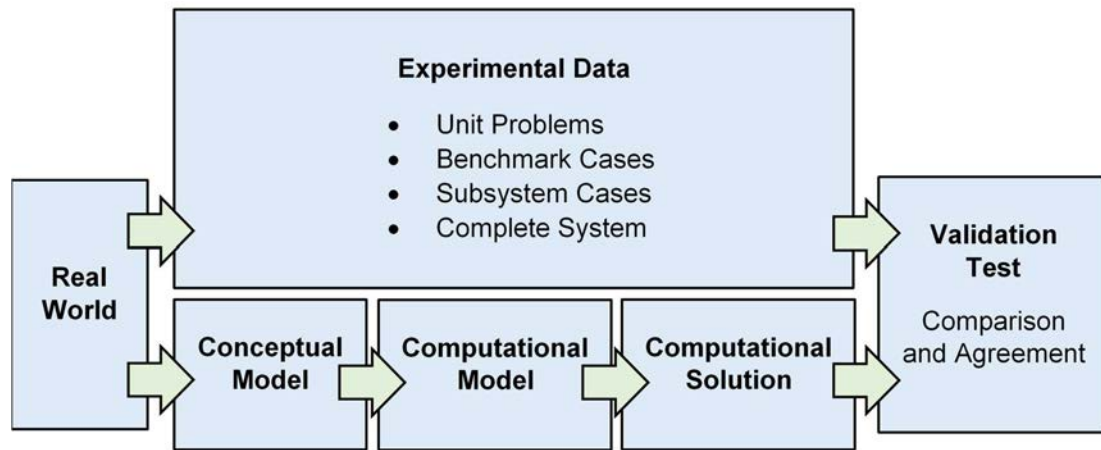


FIG. 42. Validation process [47].

A prediction is concerned with the computational simulation of a specific problem of interest which is different from the problems that have been validated before. The relationship between prediction and validation is shown in FIG. 43.

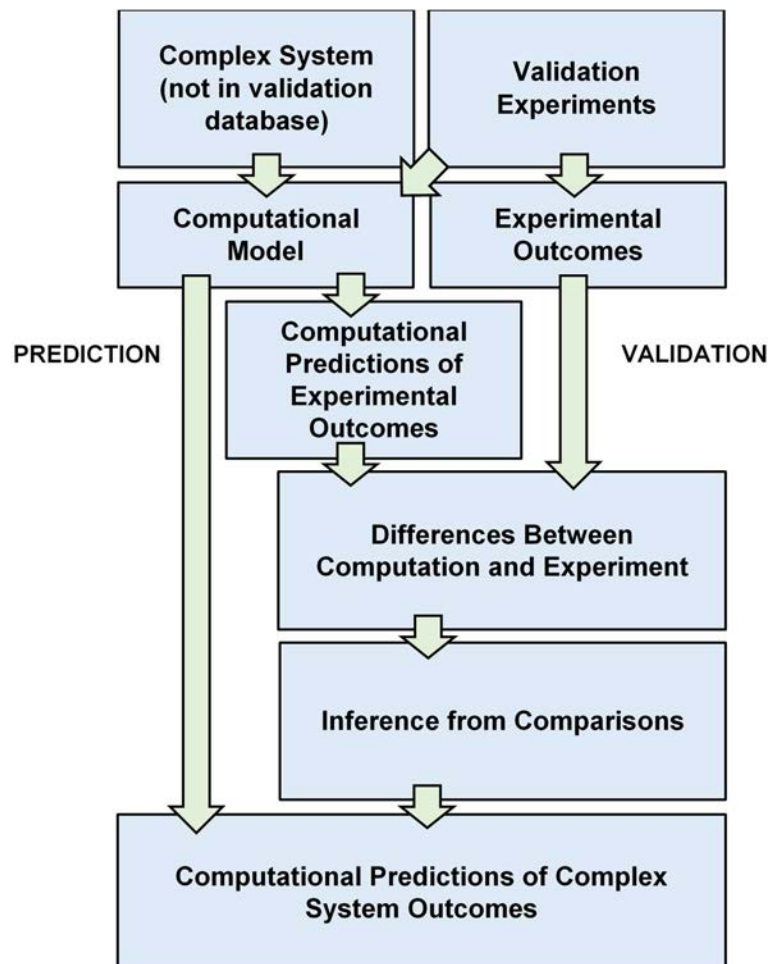


FIG. 43. Relationship between prediction and validation [47].

3.3.1.5. Turbulent flow

The majority of fluid flows are turbulent in nature. The main motivation behind studying turbulent flows is that in many industrial engineering problems the transport and mixing of matter, momentum, and heat in flows is of great practical importance and turbulence greatly enhances the rates of these processes. In turbulent flow adjacent layers continually mix. A net transfer of momentum occurs because of the mixing of fluid elements from layers with different mean velocity. This mixing is a far more effective means of transferring momentum than viscous stresses. Consequently, the mean velocity profile tends to be more uniform in turbulent flow.

Turbulence is difficult to define. Turbulent flows are usually described by listing some of features such as irregular, diffusive, rotational, occur at high Reynolds numbers, dissipative, and non-local. Turbulence is a continuum phenomenon and it is a property of fluid flow, not fluid itself. Physical processes which are involved in turbulence include unsteadiness, convection, production, diffusion and dissipation [48].

Turbulent flows are characterized by an infinite number of time and length scales. Turbulence can be considered to be composed of eddies of different sizes. These sizes range from the flow length scale L to the smallest eddies. Each eddy of length size l has a characteristic velocity $u(l)$ and timescale $t(l)=u(l)/l$. The largest eddies have length scales comparable to L . Each eddy has a Reynolds number, Re . For large eddies, Re is large, i.e. viscous effects are negligible. The idea is that the large eddies are unstable and break up transferring energy to the smaller eddies. The smaller eddies undergo the same process and so on. This energy cascade continues until the Reynolds number is sufficiently small that energy is dissipated by viscous effects: the eddy motion is stable, and molecular viscosity is responsible for dissipation. The smallest scales in the flow at which energy is dissipated are known as Kolmogorov length, velocity and time scales and are respectively given as:

$$\eta = \left(\frac{v^3}{\epsilon} \right)^{\frac{1}{4}} \quad (175)$$

$$u_\eta = (\epsilon v)^{\frac{1}{4}} \quad (176)$$

$$\tau_\eta = \left(\frac{v}{\epsilon} \right)^{\frac{1}{2}} \quad (177)$$

where v is the kinematic fluid velocity and ϵ is the average rate of dissipation. computation of turbulent flows is a challenging task because of the unsteady and 3D nature of the flow; strong dependence on initial conditions; and the presence of a wide range of eddies. All of these features need to be captured accurately.

In CFD, different predication methods are used for computing turbulent flows which include direct numerical simulation (DNS), Reynolds Averaging Navier–Stokes (RANS) equation, large eddy simulation (LES), and hybrid method.

(a) Direct numerical simulation

It is believed that physics of all fluid flow problems including turbulent flows is embodied in the Navier–Stokes equations under continuum hypothesis. In DNS, the idea is to solve time dependent Navier–Stokes equations and resolve all the scales of turbulence for a sufficient time interval. However, with this approach there are two major challenges which need to be resolved in order to use it as a routine technique for design and analysis purposes. The first one is the available computational resources. Modern computers do not have the memory, operational speed and data transfer capabilities necessary to perform DNS of complex configurations at high Re numbers. For 2D flows, in order to resolve all scales, the number of grid points should be proportional to $Re_\delta^{(3/4)}$ while for 3D flows it should be proportional to $Re_\delta^{(9/4)}$. One of the approaches to gain higher performance and higher speed of computation is to use parallel processing.

The second important challenge is the solution algorithm which does not contain any numerical errors. This aspect is related with the grid system, numerical scheme and boundary conditions. Higher order grid generation schemes and higher order numerical schemes are recommended for DNS. At present, DNS has limited use in practical problems. However, DNS still provides wide range of valuable data on transition and turbulent flows which is difficult to obtain experimentally. Thus, DNS plays an important role in the understanding of turbulence phenomenon and its importance will increase as more and more powerful computers are available [48].

(b) Reynolds Averaging Navier–Stokes equations

In RANS approach, the solution variables in the original NS equations are decomposed into time averaged (mean) and fluctuating components. For example, for velocity components:

$$u_i = \bar{u}_i + u'_i \quad (178)$$

where \bar{u}_i and u'_i are mean and fluctuating velocity components respectively. Introducing this expression into continuity and momentum equations yields the following time averaged NS equations in Cartesian tensor form:

$$\frac{\partial \bar{\rho}}{\partial t} + \frac{\partial}{\partial x_i} (\bar{\rho} \bar{u}_i) = 0 \quad (179)$$

$$\begin{aligned} \frac{\partial}{\partial t} (\bar{\rho} \bar{u}_i) + \frac{\partial}{\partial x_j} (\bar{\rho} \bar{u}_i \bar{u}_j) \\ = -\frac{\partial \bar{p}}{\partial x_i} + \frac{\partial}{\partial x_j} \left[\mu \left(\frac{\partial \bar{u}_i}{\partial x_j} + \frac{\partial \bar{u}_j}{\partial x_i} + \frac{2}{3} \delta_{ij} \frac{\partial \bar{u}_l}{\partial x_l} \right) \right] \\ + \frac{\partial}{\partial x_j} (-\bar{\rho} u'_i u'_j) \end{aligned} \quad (180)$$

The above equations (178), (179), and (180) are same as original NS equations except that instead of instantaneous variables, the solution variables are now time averaged. In the above

equations, additional terms $-\rho \overline{u'_i u'_j}$ can be seen due to turbulence. This term is known as Reynolds stresses and represents additional unknowns and must be modelled in order to close the systems of governing equations.

In order to close the system of governing equations, additional relations are used which are known as turbulence models. These models relate the fluctuating quantities with the mean flow quantities through some empirical constants. The RANS equations can be closed using two different models:

- (i) Eddy viscosity models. eddy viscosity models employ the Boussinesq hypothesis to relate the Reynolds stresses with mean velocity gradients as:

$$-\rho \overline{u'_i u'_j} = \mu_t \left(\frac{\partial \bar{u}_i}{\partial x_j} + \frac{\partial \bar{u}_j}{\partial x_i} \right) - \frac{2}{3} \left(\rho k + \mu_t \frac{\partial \bar{u}_i}{\partial x_i} \right) \delta_{ij} \quad (181)$$

This hypothesis is used in various turbulence models which include the Spalart–Allmaras model, k – ϵ , k – ω models. These models provide low computational cost for computing turbulent viscosity, μ_t . In the Spalart–Allmaras model, one additional transport equation is solved while in k – ϵ and k – ω , two additional transport equations are solved. Eddy viscosity models are suitable for simple turbulent shear flows such as boundary layer, jet flows, mixing layers etc. However, some of these models have been modified to capture complex flow features such as strong adverse pressure gradients etc. (e.g. realizable k – ϵ model). The downside of Boussinesq hypothesis is that it takes μ_t as an isotropic scalar quantity.

- (ii) Reynolds stress models (RSM). RSM computes Reynolds stresses by means of transport equations which are written for each term present in the Reynolds stress tensor. This implies that five additional equations need to be solved in 2D flows and seven additional transport equations must be solved for 3D flows. RSM model requires more computational power compared to eddy viscosity models and are suitable for complex 3D turbulent flows with long streamline curvature and swirl [49].

(c) Large eddy simulation

In DNS, all the effort is directed towards the resolution of all scales of turbulence while in RANS all scales are modelled. LES provides the compromise between DNS and RANS. As 99% of the energy is contained outside the dissipation range i.e. the smallest scales, therefore, one thinks of modelling these small scales that have universal characteristics while fully resolving the larger scales. This is large eddy simulation. In LES, large scales are resolved and the small (subgrid) scales are modelled. Subgrid scale models are used for subgrid turbulent scales and are applicable to wide range of flow regimes and conditions. A filter is introduced that would act as an automation technique that tells the equations what to fully resolve and what to fully model [48].

(d) Hybrid approach

Detached eddy simulation is a hybrid approach which was proposed by Spalart et al. [50] in 1997. In this approach, the regions where turbulent length scales are smaller than grid dimensions are solved using RANS approach and the regions where length scales are larger than the grid dimensions are solved using LES. Therefore, the computation cost is less than LES. The switching between RANS and LES is done at some suitable interface.

3.3.1.6. Computational multiphase fluid dynamics

Multiphase flow is the simultaneous flow of different phases or states of matter such as solid, liquid, or gas. In the analysis of thermal hydraulics of nuclear reactor safety, study of multiphase phenomenon and its computation are very important. Two phases are present during normal operation in BWRs and in accidental conditions leading to loss of coolant accident in both BWR and PWR making the analysis more complex compared to single phase analysis. Such analysis can be performed using CFD as it gives detailed and valuable information which is difficult to measure experimentally because of the harsh environment present in the reactor. In nuclear reactors, computational models are needed to analyse the multiphase flow processes such as boiling, condensation, deposition etc.

Modelling of multiphase flow is a complex task. This is mainly due to the lack of understanding of the flow phenomenon and lack of computational capacity required to simulate such flows. However, different modelling approaches have been proposed which provide different level of information and accuracy for multiphase flow applications. The main approaches are discussed below.

(a) Euler–Lagrange modelling approach

In this approach, the fluid phase is treated continuous and NS equations are used to solve it, while dispersed phase is calculated by tracking a large number of particles, droplets or bubbles throughout the flow domain. The dispersed phase can exchange mass, momentum, and energy with the continuous phase. The conservation equations for continuous phase and dispersed phase are given as [51]:

$$\frac{\partial \alpha_f \rho_f}{\partial t} + \nabla \cdot (\alpha_f \rho_f \mathbf{u}_f) = S_m \quad (182)$$

$$\frac{\partial \alpha_f \rho_f}{\partial t} + \nabla \cdot (\alpha_f \rho_f \mathbf{u}_f \mathbf{u}_f) = \alpha_f \nabla p - \alpha_f \nabla \cdot \boldsymbol{\tau}_f - \mathbf{S}_p + \alpha_f \rho_f \mathbf{g} = 0 \quad (183)$$

$$\frac{\partial \mathbf{u}_p}{\partial t} = \sum F \quad (184)$$

Here α is volume fraction, S_m is a mass source term existing in the case of exchange of mass between the phases, S_p is a momentum source term existing in case of exchange of momentum between the phases and F is force. Subscripts f and p refer to the fluid and particle phases, respectively.

This approach is computationally expensive since it gives information at the level of single particle. Therefore, this approach is limited to flows having low volume fraction of the dispersed phase.

(b) Euler–Euler approach

In this approach all phases are considered continuous. This approach is also known as multi-fluid approach. This approach can also be used to model dispersed flows if overall motion of the particles is of interest. In this case, the volume fraction of the dispersed phase should be high enough to treat it as continuous phase.

This approach treats all the phases separately and transport equations for each phase are solved. In addition to the transport equations, equation of volume fraction is also solved for each phase. A set of conservation equation of two fluid model with two continuous phases is given below [51]:

$$\frac{\partial \alpha_k \rho_k}{\partial t} + \nabla \cdot (\alpha_k \rho_k \mathbf{U}_k) = 0 \quad (185)$$

$$\begin{aligned} \frac{\partial \alpha_k \rho_k \mathbf{U}_k}{\partial t} + \nabla \cdot (\alpha_k \rho_k \mathbf{U}_f \mathbf{U}_f) \\ = -\alpha_k \nabla \mathbf{P} - \alpha_k \nabla \cdot \boldsymbol{\tau}_k + \alpha_k \rho_k \mathbf{g}_k + S_k = 0 \end{aligned} \quad (186)$$

$$\frac{\partial \alpha_k}{\partial t} + \nabla \cdot (\alpha_k \mathbf{U}_k) = 0 \quad (187)$$

where \mathbf{U} represents a mean velocity field, \mathbf{P} the mean shared pressure between phases, and \mathbf{g} gravity. Subscript k refers to the k^{th} continuous phase.

There are other simplified versions of the Euler–Euler approach which include the mixture model and the volume of fluid model. In the mixture model, both phases are treated as interpenetrating continua. The transport equations in this model are based on mixture properties such as mixture viscosity, mixture velocity etc. In addition, the transport equations for volume fraction is also solved in order to track each phase. On the other hand, in the volume to fluid model, both phases are treated as continuous but, like previous approaches, are not treated as interpenetrating continua [49].

Nomenclature used in 3.3.1

e	specific internal energy
\mathbf{f}	body force per mass
F	force
\mathbf{g}	gravity
p	pressure
\mathbf{P}	mean shared pressure between phases
\mathbf{q}	heat flux
\dot{q}	internal heating density
S	source term

T	temperature
\mathbf{u}	velocity, flow variable
u_η	Kolmogorov velocity
\mathbf{U}	mean velocity field
v	kinematic fluid velocity
\mathbf{v}	flow variable
α	volume fraction
δ	unit tensor
ϵ	average rate of dissipation
η	Kolmogorov length
κ	thermal conductivity
λ	second coefficient of viscosity
μ	absolute viscosity
ρ	density
$\boldsymbol{\tau}$	shear stress tensor
τ_η	Kolmogorov time scale
e	east
m	mass
n	north
f	fluid phase
k	phase variable
p	momentum, particle phase
s	south
w	west

3.3.2. CFD applications in reactor safety

In nuclear reactor safety analysis, CFD has been used to perform single phase flow analysis. It is believed that for single phase flow, CFD has reached a good level of maturity and accuracy in terms of turbulence modelling, mesh, boundary conditions and numerical schemes. However, accurate computation of multiphase flows in reactor safety analysis using CFD still needs significant R&D efforts. Furthermore, attention should also be given to the efforts leading to code and model validation.

In water cooled reactors, CFD can be used in number of safety related applications such as given in [52] and [53] which include, among others:

- (a) Boron dilution transient;
- (b) Pressurized thermal shock;
- (c) Hydrogen distribution;
- (d) Aerosol deposition;
- (e) Direct contact condensation;
- (f) Natural circulation in various reactor components;
- (g) Bubble dynamics in suppression pools;

- (h) Flow mixing in lower plenum;
- (i) Steam line break;
- (j) Thermal fatigue;

Following is an explanation of some of these safety related issues, specifically (a) to (e) on the previous list, and why CFD is used to simulate them.

(a) Boron dilution transient

Boron dilution is one of the important transient in PWR. In this transient, slugs of weakly borated water can be formed in one of the primary system loops due to different mechanism such as failure of water makeup system, steam generator tube break etc. As soon as the under borated slug is entered into the reactor core, it results into insertion of positive reactivity and might lead to power excursion. The transport of under borated slug of water in to the core may lead to serious consequences with respect of reactor safety especially after RCP startup or during restart of natural circulation after LOCA.

The boron dilution transient can be assessed in three steps:

- (i) Global scale system code analysis which provide boundary conditions for step (ii);
- (ii) Local scale CFD analysis which provide detailed 3D simulations in cold leg, downcomer, and reactor core;
- (iii) Neutronic analysis using input from step (ii).

For modelling this transient in CFD, the related parts of the reactor are downcomer, the lower plenum, and the piping network used for transporting the slug. The features relevant to CFD simulations are the geometrical complexity of the domain, transient behaviour of the flow, and the need of the precise mixing properties of the flow.

(b) Pressurized thermal shock

PTS in general denotes the occurrence of thermal loads on the reactor pressure vessel under pressurized conditions. PTS is related with the ageing of the RPV as its integrity must need to be assured throughout the lifetime of the vessel. A very severe PTS scenario limiting the RPV life is injection of cold water from emergency core cooling system into the cold leg during a postulated loss of coolant accident. The water after injection gets mixed with the hot water present in the cold leg, and the mixture then flows towards the downcomer resulting into further mixing with the ambient fluid as shown in FIG. 44. As a result, high thermal gradients may occur in the structural components while the primary circuit pressurization is partially preserved.

The main issue in simulating PTS condition is to predict the transient fluid temperature reliably to estimate the loads upon the RPV in order to investigate thermal stresses and thermal fatigue of the vessel. The temperature of the fluid is influenced by turbulence, stratification and by condensation rate in case of two phase flow. It is important to know that the state (single phase

or two phase) of the cooling fluid depends upon the break size, its location, and operational mode of the nuclear power plant.

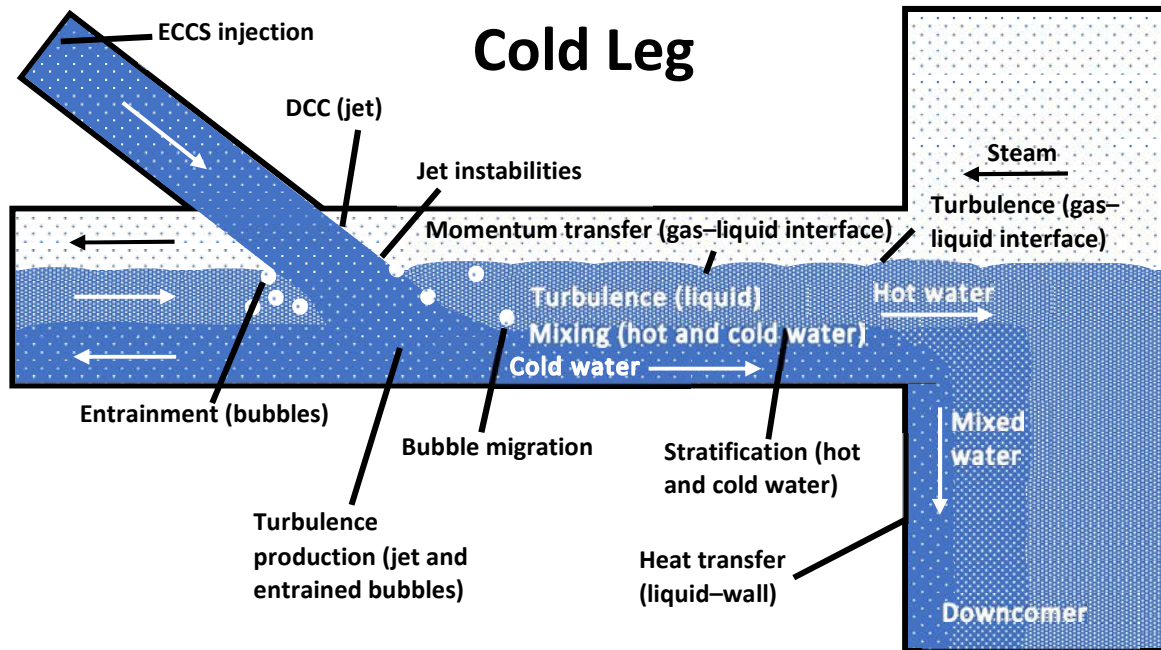


FIG. 44. Flow feature present during PTS condition with partially filled cold leg [53].

As far as CFD simulations for PTS are concerned, it is important to capture above mentioned features for the whole transient which may last for several minutes. Furthermore, complex geometries (downcomer, upper plenum, and pipes) and complex flow patterns (such as stratified flow, jet etc.), and unsteady 3D effects make this a challenging problem for CFD. The existing reported simulations concern single phase flow, whereas simulations of two phase flows in such situations are just beginning. The detailed references on this problem can be found in [52].

(c) Hydrogen distribution

During a severe accident in nuclear power plant containment, large quantities of hydrogen are produced. If the amount of hydrogen exceeds prescribed limit, it can result in deflagration or even detonation putting the integrity of containment at stake, the last and final barrier against the spread of radioactivity. This situation requires the proper distribution and handling of hydrogen inside the containment. Historically, the severe accidents at TMI 1979, Chernobyl 1986 and recently Fukushima Daiichi 2011 all suffered with the core damage and eventually hydrogen generation. In TMI, over 500 kg of hydrogen was produced while in Chernobyl 3000 kg per unit [54]. Consequently, radioactivity was released outside the containment building resulting in the evacuation of public in the immediate periphery of nuclear power plants.

In order to employ the effective hydrogen mitigation methods, it is important to know the detailed thermal hydraulics phenomena associated with the containment. The containment related thermal hydraulics phenomena include condensation and evaporation on walls, pool

surfaces and condensers. These phenomena need to be accurately modelled as the associated heat and mass transfer strongly influence the pressure and mixture composition inside containment. The accurate prediction of this mixture composition is very important as this information is required to determine the burning mode of hydrogen and operation of passive autocatalytic recombiners (PARs) inside the containment.

Since the scale of the problem is large due to the huge size of the containment, capturing all the essential features using CFD require huge computational effort. In case of coarse mesh, accuracy is lost and all the true gradients of velocity and temperature are washed out resulting into a wrong distribution of hydrogen inside the containment. Furthermore, condensation model need to be incorporated as these are not standard to commercial CFD codes. Similarly, in order to simulate realistic accidental scenarios, there is need to run simulations with complete geometrical model including PARs and other containment related systems such as sprays and sumps.

(d) Aerosol deposition and atmospheric transport

In the case of severe accident, fission products are released inside the containment in the form of aerosols. If the containment integrity is not maintained and there is a leak in the containment, these aerosols would be released into the environment and pose a health hazard to the population around the nuclear power plant. In the conservative scenario, all the aerosols eventually are released into the environment. However, an accurate realistic prediction can be made by investigating the detailed processes which include initial core degradation, fission product release, aerosol borne transport and retention in the coolant circuitry, and the aerosol dynamics and chemical behaviour in the containment.

The phenomena of aerosol removal from the containment requires in depth treatment of the forces acting on the aerosol particles. In order to simulate and track their motion, CFD simulations are needed in order to predict their 3-D velocity field. The goal in such simulations is to find out the residence time or life span of the aerosols moving in the containment using CFD. By accurately tracking all the aerosol particles, statistical information on the actual deposition can be obtained.

(e) Direct contact condensation (DCC)

In some nuclear reactor designs, saturated steam is discharged to subcooled water pools where it gets condensed. This phenomenon is known as direct contact condensation and may occur as part of the nuclear reactor emergency core cooling system. When DCC occurs, it causes thermal and pressure oscillations, which may challenge the structural integrity of related equipment and piping. Therefore, investigations of DCC mechanisms have been performed to find the efficiency of the condensation process and thermal mixing in the pool. To perform such investigations for nuclear reactor design and safety, complete 3-D simulations using CFD would be required. However, CFD investigations related to DCC mechanisms are sparse compared to experimental investigations. Some experimental and CFD studies on DCC are given in [55] and [56].

3.3.3. Example CFD simulations

3.3.3.1. Hydrogen distribution in containment

The physical phenomenon related to hydrogen distribution has already been explained in the previous section. A CFD methodology to predict hydrogen distribution inside containment after a severe accident was developed at PIEAS [57] using FLUENT. Two different multiphase approaches were selected to predict the behaviour of hydrogen with results validated by the THAI HM-2 experiment.

THAI vessel is well instrumented experimental facility in Eschborn, Germany operated by Becker technologies. It is dedicated for various experiments such as hydrogen and steam distribution, iodine removal and aerosols behaviour during the course of severe accidents. Test HM-1 was performed with inert helium gas while HM-2 test with hydrogen gas. THAI vessel details are given in [58].

Initially the containment atmosphere consists of 98 vol.% nitrogen gas, 1 vol.% oxygen and 1 vol.% steam at ambient conditions (101 325 Pa, 298 K). HM-2 test consists of two phases:

- (i) Phase 1: Hydrogen and steam injection in containment for a given period (0–4200 s) resulting in the maximum concentration of hydrogen in the dome of containment.
- (ii) Phase 2: Erosion of stratified hydrogen rich gas layers by injecting steam in the containment and mixing of atmosphere in the vessel (4300–6300 s). Physical processes (e.g. natural convection, fluid flow, heat transfer, turbulence effect and concentration of hydrogen) in various zones of containment were predicted through CFD simulation in the first phase of HM-2 (i.e. no steam or condensation is considered).

Two CFD cases have been studied in order to study different effects of the same experimental setup i.e. variation in geometry scale down, use of different multiphase models etc.

(i) Case A

In order to perform a transient CFD simulation, a scaled down model (both with respect to position and time) of THAI vessel was selected. This was done in order to reduce both computation time and problem complexity. To simplify the geometrical model, condensate trays were neglected as these trays do not have any effect on buoyancy, concentration or turbulence. Differences between the actual vessel and CFD model are given in Table 7 [57].

A hybrid mesh was created with the concept of inflation for capturing turbulence effects near the walls. After the generation of mesh, the setup was done in FLUENT software. FLUENT setup for this case is shown in Table 8 [57].

After completing the simulations, converged solutions were obtained. Convergence of solutions can be measured with the help of residuals. Calculated results include volume fraction

contours of nitrogen and hydrogen at different time steps, increase in pressure with time, and increase in mass of hydrogen in the vessel with time.

Volume fraction contours show the amount of gases present in the vessel at different time intervals. In the beginning, the vessel gas composition is of nitrogen only, with no hydrogen present inside the vessel, as shown in FIG. 45 (left). Hydrogen concentration in the vessel increases with time, while nitrogen concentration correspondingly decreases as can be seen in FIG. 45 (middle). Due to hydrogen inlet to the vessel, pressure inside the vessel increases. The hydrogen inlet flow essentially stops at 420 seconds. Hydrogen, being a light gas, accommodates at the top of the vessel and nitrogen concentration accumulates in other portions of the vessel as shown in FIG. 45 (right). The maximum hydrogen concentration inside the vessel is 64%, which is higher than the experimental value of 36%. This difference is due to an assumption disregarding other phases which are also present in phase 1 of the scenario.

Pressure inside the vessel increases linearly with time as can be seen in FIG. 46, and pressure becomes constant because hydrogen inlet is stopped at last 10 seconds as shown in FIG. 46. The pressure increase is the same as that of experimental setup, with differences in values arising from the downscaled model causing an increase in mass flow rate and velocity.

TABLE 7. PARAMETERS COMPARISON OF BOTH ACTUAL AND CFD MODELS.

PARAMETER	ACTUAL MODEL	CFD MODEL
Model	Full scale model	One tenth of original dimension
Inlet	Mixture inlet (upper inlet) Steam inlet (lower inlet)	Hydrogen inlet (upper inlet) No lower inlet
Multiphase	Four Phase model	Two phase model (Hydrogen, and Nitrogen)
Time	Stage 1: 4200 secs with 100 seconds no inlet Stage 2 consists of 2000 secs	Stage 1: 420 seconds with 10 seconds no inlet No Stage 2
Mass flow rate	Hydrogen mass flow rate is 0.3 g/s	Hydrogen mass flow rate is 0.03 g/s

TABLE 8. FLUENT SETUP

PARAMETER	SETTING
Solver	Pressure based
Formulation	Transient
Turbulence approach	RANS with standard $k-\epsilon$ model
Pressure velocity coupling	Phase coupled scheme
Spatial discretization	1st order upwind
Temporal discretization	1st order implicit
Geometry	3D half vessel
Walls	No slip
Near wall treatment	Standard wall function
Conduction	3D
Multiphase model	Mixture model
Time step size	0.1 s for first 2 s and then increased to 0.2 s

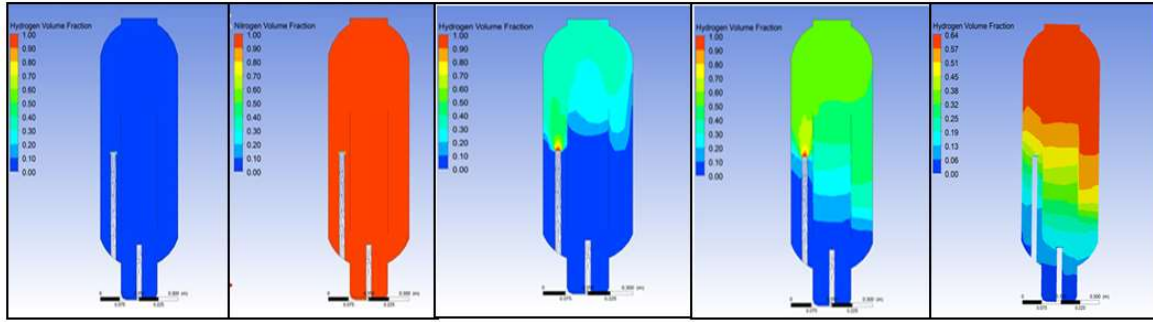


FIG. 45. From left: hydrogen, nitrogen contours at $t = 0$ s, hydrogen contours at $t = 100$ s, 300 s, 430 s (reproduced courtesy of PIEAS, ©Nawaz, R. [57]).

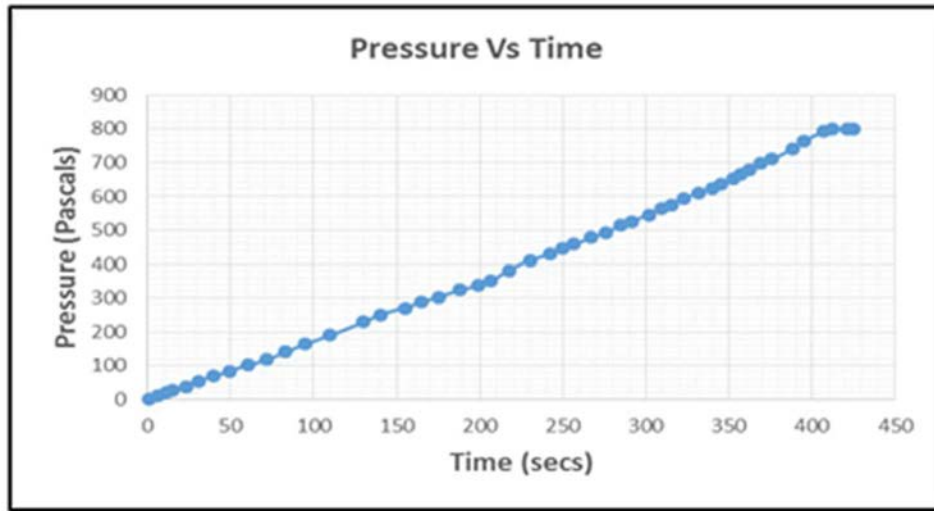


FIG. 46. Pressure with respect to time (reproduced courtesy of PIEAS, ©Nawaz, R. [57]).

(ii) Case B

In this case a temporal downscaled model of THAI vessel was selected to show the pressure variation with respect to time. Geometric dimensions are the same as in the experimental setup. Differences between the actual vessel and the CFD model are given in Table 9 [57]. In the CFD model only the first phase has been simulated and the difference in mass flow inlet which occurs in the first phase is due to the time based downscaling in the model.

For hydrogen and steam distribution in the containment, flow is non-rotating and has a low Mach number. Therefore, an absolute velocity formulation and a pressure based solver were used for this case. The properties of four components used in the analysis are mentioned in Table 10 [57].

For simulating this case, a multispecies model was used. This model is used when the components' densities are very close and there is a significant interaction between them. In this analysis, four components were involved: nitrogen, hydrogen, steam, and water each including interaction and momentum transfer with each other. The Eulerian model was used for modelling multiphase interaction and two components are mixed together to form one phase. Phase 1 consisted of nitrogen and water, while phase 2 consisted of hydrogen and steam, with

mass transfer occurring between the species of phase 1 (water) and phase 2 (steam). The simulation was run after specifying boundary conditions for each component.

Concentration of hydrogen at different time steps (150 s, 300 s, 430 s) are shown in FIG. 47. A strong increase in the concentration gradient exists at an elevation of 4 m. Wide distribution and mixing of hydrogen occurs in the dome of the containment and reaches a constant maximum in this region, while in the base falling below 0.5%. Since hydrogen and steam are light, they accumulate in the dome of containment due to buoyancy driven phenomenon. The maximum hydrogen concentration comes out to be 37.4% which is close to the experimental value of 36%.

TABLE 9. GENERAL SPECIFICATION OF CFD MODEL FOR CASE B

PARAMETER	ACTUAL MODEL	CFD MODEL
Time	Phase 1 has 4200 s with 100 s no inlet Phase 2 has 2000 s (4300 s to 6300 s)	Phase 1 has 420 s with 10 s no inlet Phase 2 not simulated
Mass flow rate	Hydrogen mass flow rate is 0.3 g/s Steam mass flow rate is 0.24 g/s	Hydrogen mass flow rate is 3 g/s Steam mass flow rate is 2.4 g/s

TABLE 10. PROPERTIES OF GASES

FLUID	μ (kg/m s)	C_p (J/kg k)	ρ (kg/m ³)	K (W/m k)
Water	Constant	Mixing law	Ideal	Constant
Nitrogen				
Hydrogen	Constant	Mixing law	Incompressible ideal	Constant
Steam				

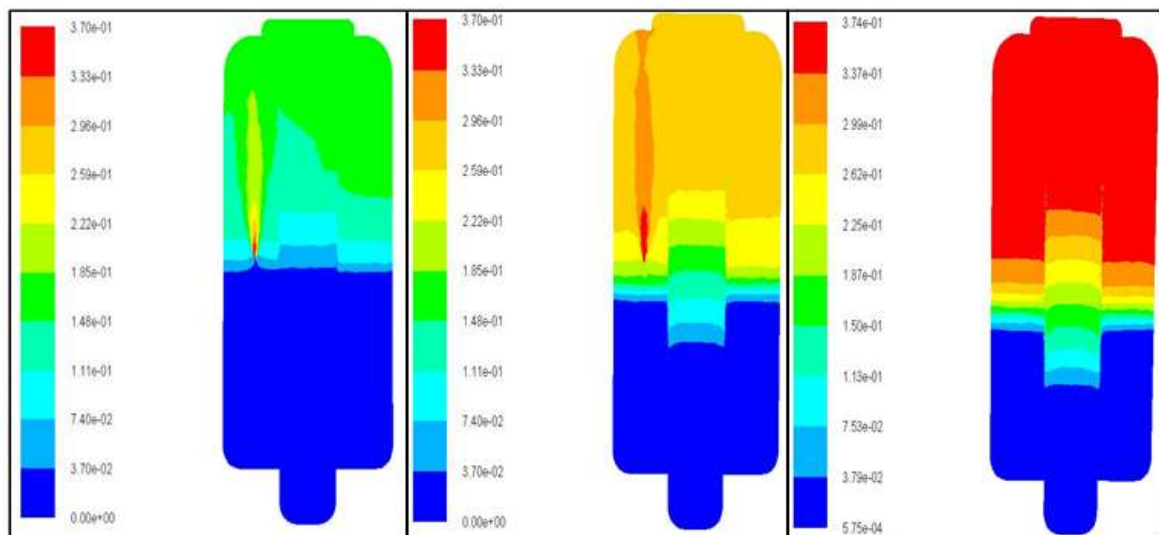


FIG. 47. From left: hydrogen contour at $t = 150$ s, 300 s, 430 s.

3.3.3.2. Aerosol removal through venturi scrubber

The Fukushima accident has raised concerns over the safety of nuclear power plants and the integrity of release barriers, the last of which is the containment. In cases of a severe accident, pressure inside the containment builds up due to release of hydrogen gas and fission fragments. To avoid any damage due to the increased pressure, a filtered containment venting system

(FCVS) is employed to mitigate the consequences of a severe accident [59]. Major components of FCVS are shown in FIG. 48.

Aerosol removal from contaminated air using a venturi scrubber is an important aspect of the FCVS. A study of this process was carried out at PIEAS in 2016 [60] in which dust particle removal efficiency was calculated using CFD from a self priming venturi scrubber. A CFD methodology using ANSYS CFX was developed and validated using the geometry and conditions given by Pak and Chang [61] for a forced feed venturi scrubber. The geometric dimensions of the venturi are shown in FIG. 49 and given in Table 11 [61].

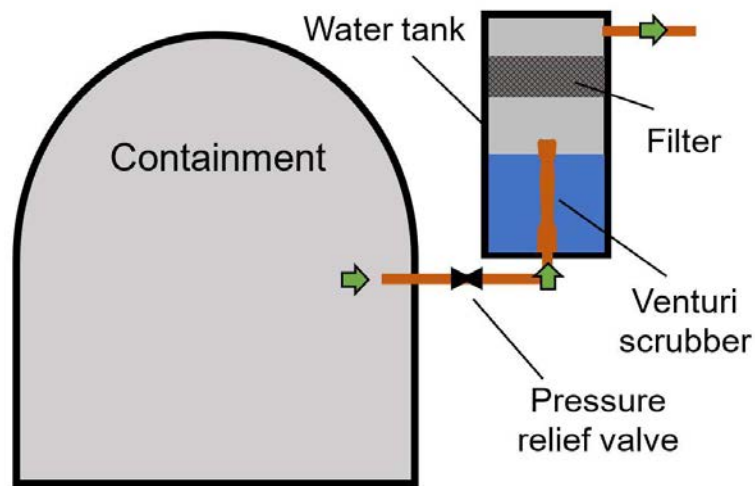


FIG. 48. Schematic of FCVS with main components [60].

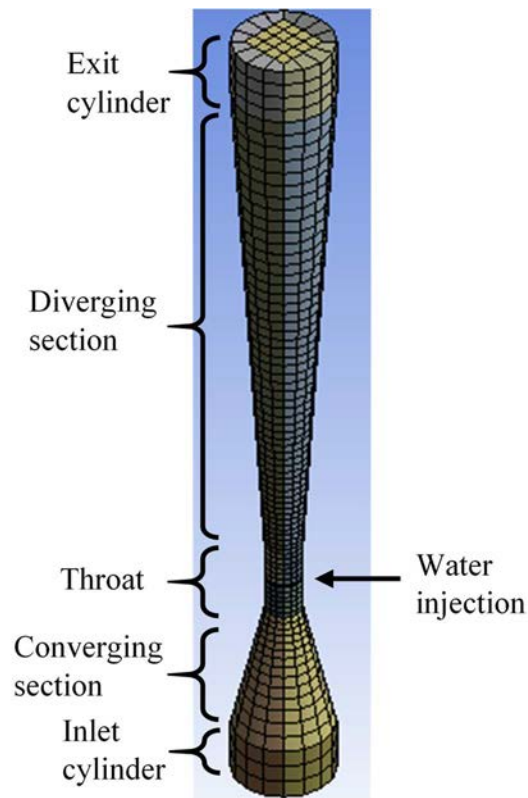


FIG. 49. Meshing of venturi scrubber (reproduced courtesy of PIEAS, ©Ahmed, S. [60]).

TABLE 11. GEOMETRY DIMENSIONS

PARAMETER	DIMENSION
Pipe diameter (D)	0.192 m
Inlet cylinder length (L_e)	0.1 m
Converging section length (L_c)	0.253 m
Throat length (L_t)	0.14 m
Throat diameter (d_t)	0.07 m
Diverging section length (L_d)	0.997 m
Exit cylinder length (L_o)	0.112 m
Number of orifices	12

An Eulerian–Lagrangian approach was used to create a multiphase (air, water, dust) model with hydrophobic TiO_2 dust particles were used to simulate aerosols. A Lagrangian approach was used to track water and dust particles while air was modelled through an Eulerian approach as continuous fluid in the forced feed venturi scrubber. The RNG $k-\varepsilon$ model was used to capture turbulent effects [59] and the Schiller Nauman model was used to estimate particles drag coefficient. The cascade atomization and breakup model was used to simulate the deformation of water droplet. Removal efficiency of the dust particles was calculated by inertial impaction mechanism for which single particle collection efficiency, η , is defined as [61]:

$$\eta = \left(\frac{\Psi}{\Psi + 0.7} \right)^2 \quad (188)$$

where Ψ denotes the Stoke's number defined by Pak and Chang as:

$$\Psi = \frac{\rho_p d_p^2 (v_p - v_d)}{9\mu_g d_d} \quad (189)$$

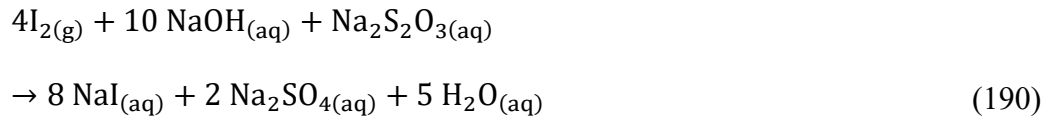
where ρ_p is the density of the particle, d_p the diameter of the particle, v_p the velocity of the particle, v_d the velocity of the droplet, μ_g the viscosity of the gas, and d_d the diameter of the droplet.

After performing a mesh independence study, 95 000 mesh elements were calculated. Using the throat velocity, the inlet air flow rate was calculated. Then, using the liquid to gas flow ratio, liquid flow rate was calculated. Removal efficiency was calculated for two liquid–gas flow rate ratios of 2 L/m^3 and 2.5 L/m^3 and results were compared to Pak and Chang's results as shown in Table 12 [60].

TABLE 12. COMPARISON OF DUST PARTICLES REMOVAL EFFICIENCY

LIQUID TO GAS FLOW RATE RATIO (L/m^3)	PAK AND CHANG RESULTS REMOVAL EFFICIENCY (%)	CURRENT CFX SIMULATION REMOVAL EFFICIENCY
2	98	97
2.5	99	98

Currently, at PIEAS, ongoing research is being done which replaces the dust particles with gaseous iodine (I_2). This offers a different approach to calculating removal efficiency using CFD since mass transfer would occur between the air and scrubbing solution where iodine gets absorbed. In a FCVS, the scrubbing solution is a mixture of sodium thiosulphate and sodium hydroxide and following reaction takes place:



It was assumed that the above reaction is fast, so that chemical kinetics must be considered [61]. Therefore, only mass transfer was considered; however, no such model was available in FLUENT. A separate UDF, based on the mathematical model proposed in [62], was written for calculating the mass transfer. The results have been calculated for the same geometry with air and iodine inlet flow rate of 0.07 kg/s and water inlet velocity at orifices of 1.8 m/s for droplet diameters of 10^{-3} m, 10^{-4} m, 10^{-5} m and 10^{-6} m respectively. The results are shown in FIG. 50.

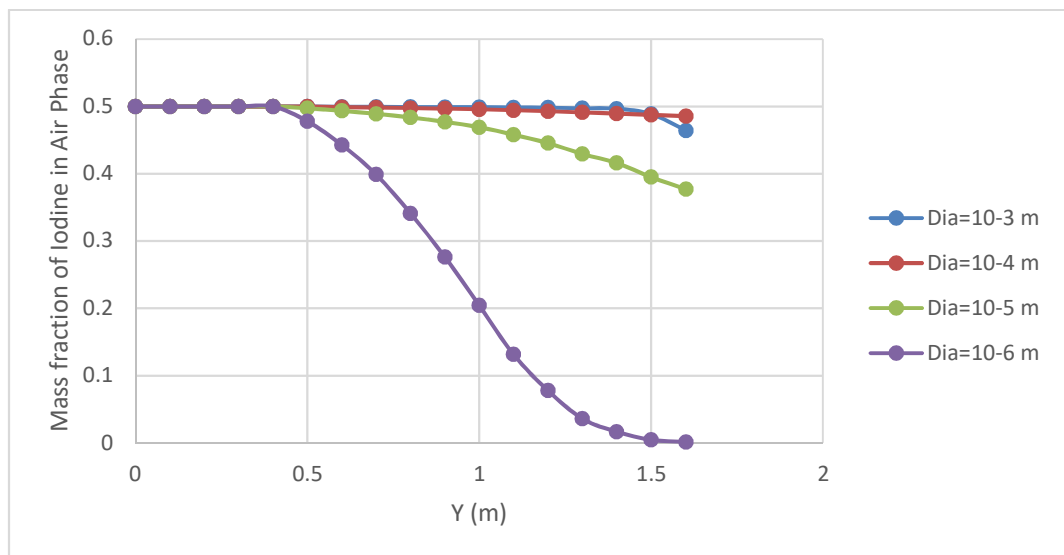


FIG. 50. Change in mass fraction of iodine in air due to change of diameter of water droplet (reproduced courtesy of PIEAS, ©Ashfaq, T. [63]).

The following conclusions can be drawn from FIG. 50:

- (i) There is no transfer of iodine to the water phase before 0.4 m which is the point where water is injected.
- (ii) The mass fraction of iodine in the air phase decreases in all cases. This is due to transfer of iodine to the water phase.
- (iii) The mass transfer of iodine (from air phase to water phase) increases with decreased droplet diameter. As diameter decreases, surface area to volume ratio increases. Thus, more surface area is available on the water droplets for iodine transfer.
- (iv) There is a dip at 1.6 m for the 10^{-3} m diameter droplet due to reverse flow at the outlet.

The scrubbing tank is an important component of the FCVS which removes radioactive iodine from an incoming stream of contaminated air. Heat is added by the stream of air and steam from the containment into the scrubbing solution at around 180 °C. Steam present in the incoming flow is also being condensed in the solution. To remove heat from the solution, a jacketed heat exchanger was provided around the scrubbing tank of FCVS pilot scale setup being developed at PIEAS. It is essential to keep the scrubbing solution below its boiling temperature in order to efficiently remove iodine and other aerosols from the incoming stream.

The direct contact condensation phenomenon can occur in various components of a nuclear power plant including in the drain tank of a PWR or in a BWR pressure suppression pool during either normal operation or accidental conditions. Understanding of DCC phenomena is especially important in the design of a scrubbing tank since steam is expected to come into contact with solution inside the tank through the sparger-venturis and intended to condense inside tank so that only clean air is released into the environment.

There is an ongoing research project at PIEAS to investigate this aspect of DCC inside a scrubbing tank through CFD. To investigate DCC phenomena and to find the major related parameters, the condensation of a simplified 2D axially symmetric case are considered. The tank is 2824 mm in height with a jacketed heat exchanger with a diameter of 30 mm. A stainless steel wall of 10 mm separates the tank and jacket. An inlet of diameter 20 mm is provided at the centre of the tank. This is equivalent to 378 holes of a sparger assembly with each hole having a diameter of 1 mm. The water inside the tank is initially at room temperature. A two phase Eulerian model is used for simulation, in which phases are dealt with as interpenetrating continua. The steam has been treated as incompressible fluid. As the flow was expected to be highly turbulent, the standard $k-\epsilon$ model has been used. A SIMPLE coupled implicit solver has been used to solve the non-linear governing equations. Steady state simulations are carried out using upwind discretization schemes for all equations. For modelling the condensation phenomenon, the model proposed by Shah et al. [64] was used. After a mesh independence study, 21 500 mesh elements were selected.

Results were obtained for temperature and volume fraction of steam. FIG. 51 shows the variation of volume fraction of steam at the centre of tank with axial distance, and corresponding contours. The volume fraction of the steam becomes zero after 1.5 m from the bottom of the tank. The condensation of steam can be observed around the steam plume. FIG. 52 shows the phase interaction (i.e. mass transfer of vapour phase into liquid phase). It can be observed that all of the steam is condensed inside the tank, with none escaping. FIG. 53 represents the temperature variation inside the tank. The average temperature inside the tank is around 340 K, which can be seen in FIG. 53 and FIG. 54 where the axial temperature distribution is shown at different radial positions. FIG. 54 also shows turbulence eddies inside tank, which is evidence that heat is transferred from the tank to the heat exchanger by means of convection.

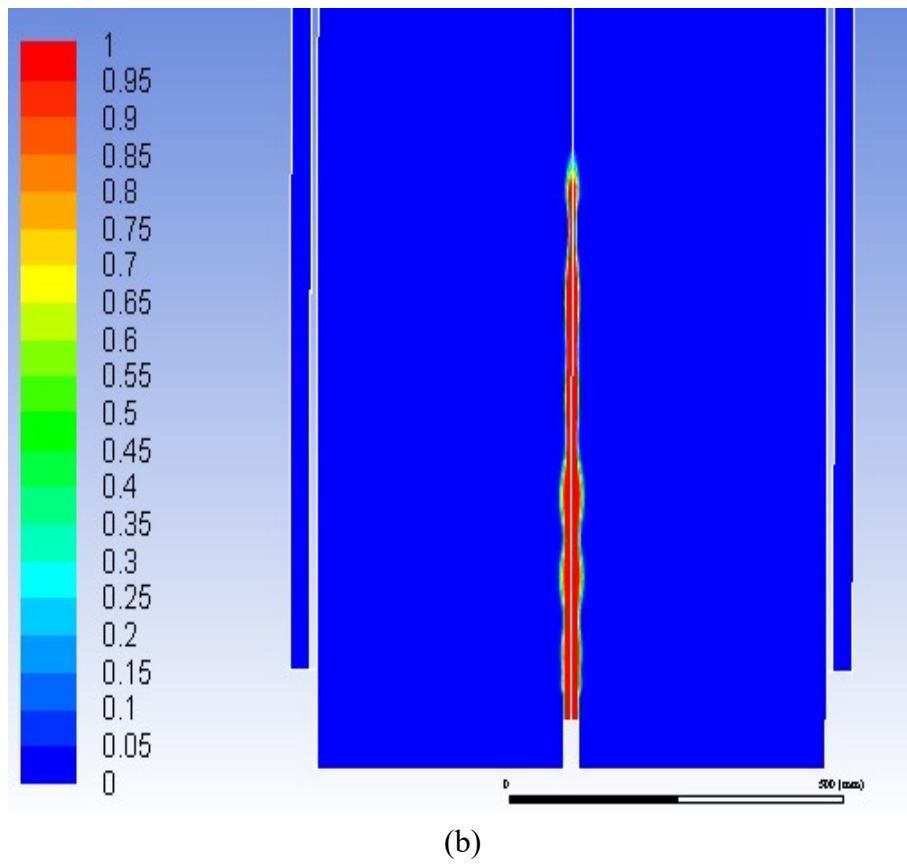
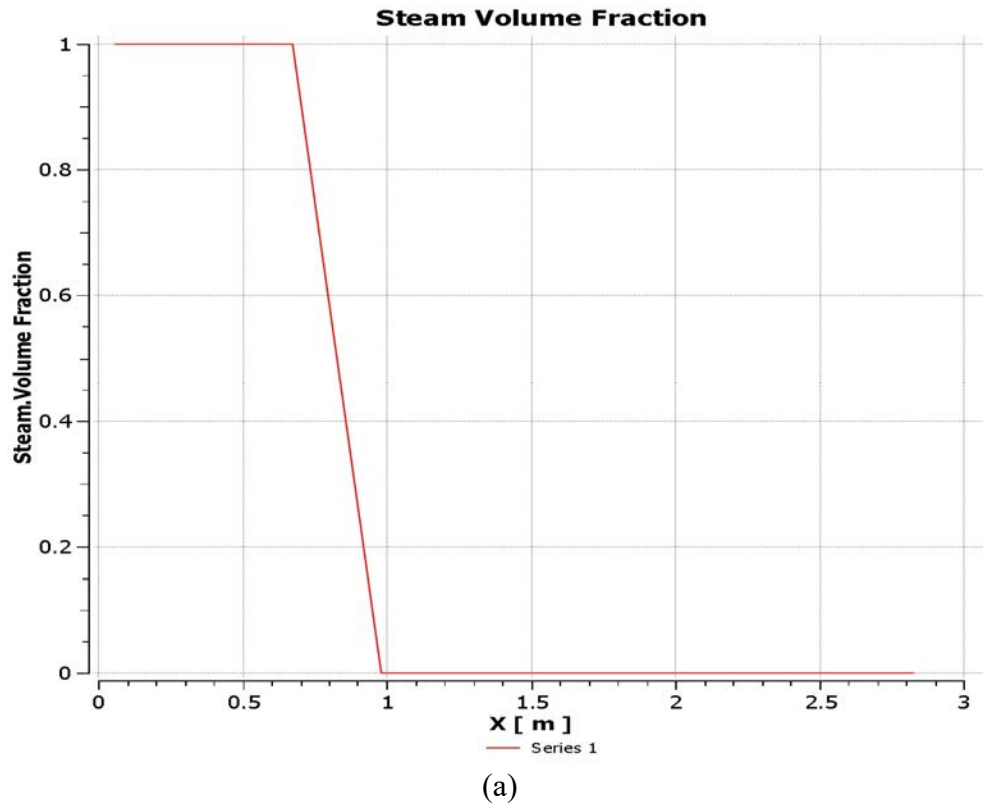


FIG. 51. (a) Plot of volume fraction and (b) contours of steam at the centre of tank (reproduced courtesy of PIEAS, ©Nadeem, A.M. [65]).

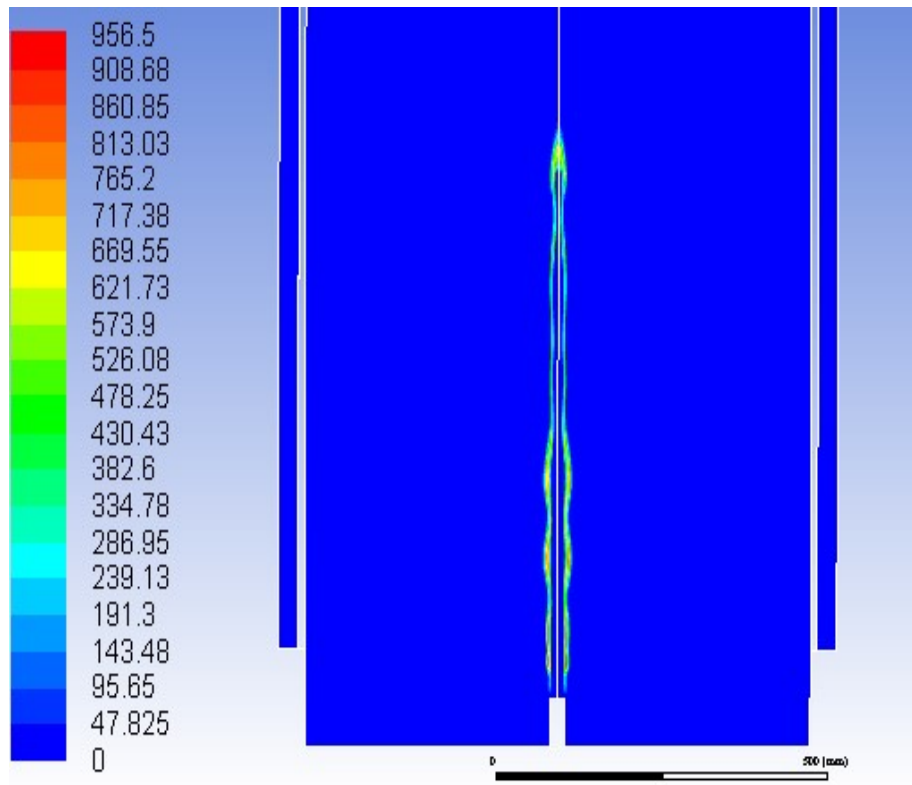


FIG. 52. Contours for phase interaction (mass transfer steam to water) (reproduced courtesy of PIEAS, ©Nadeem, A.M. [65]).

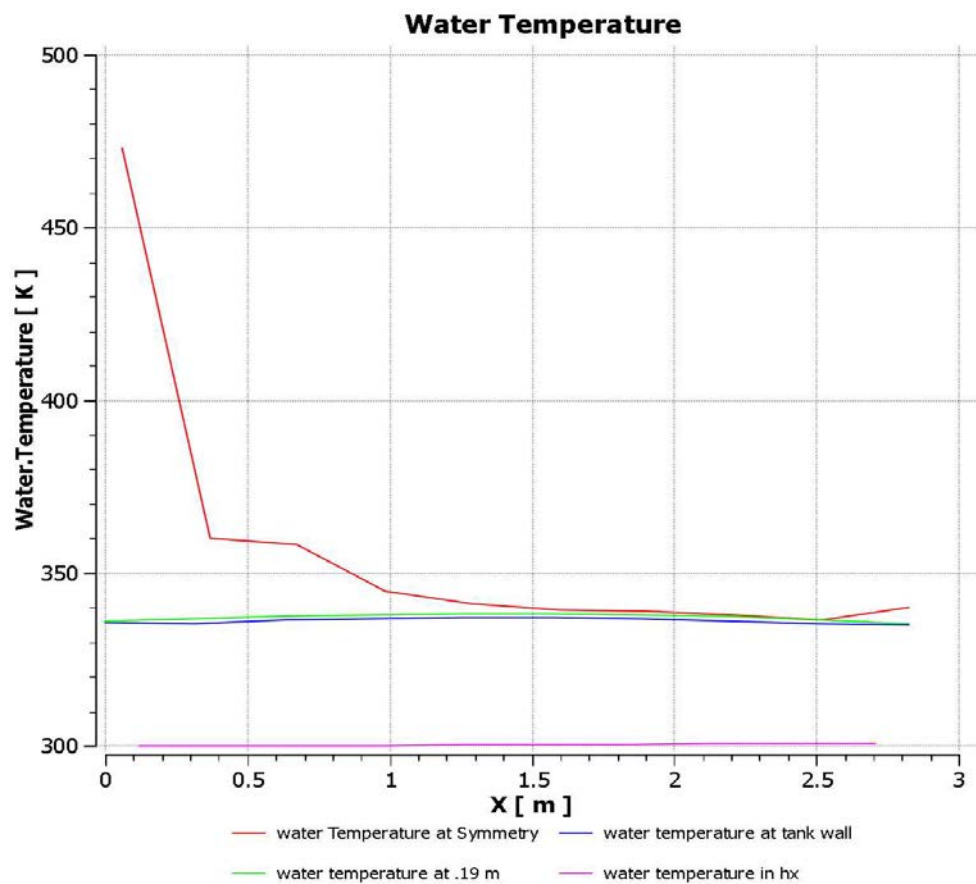
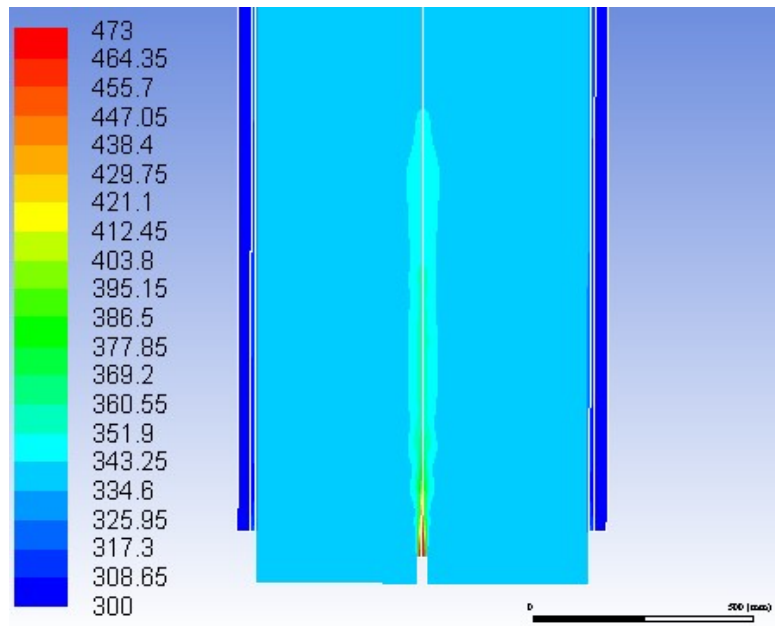
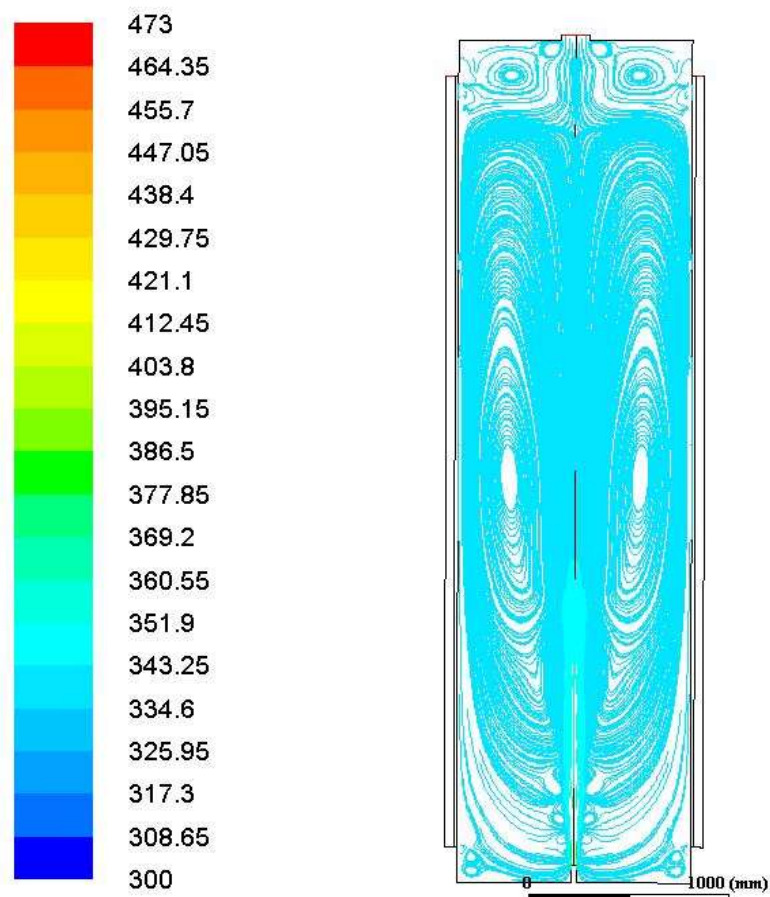


FIG. 53. Temperature distribution inside tank at different radial locations (reproduced courtesy of PIEAS, ©Nadeem, A.M. [65]).



(a)



(b)

FIG. 54. (a) Contours of water temperature inside tank and (b) corresponding flow pattern (reproduced courtesy of PIEAS, ©Nadeem, A.M. [65]).

4. PASSIVE SAFETY SYSTEMS IN ADVANCED WATER COOLED REACTORS

Passive safety systems utilize passive processes such as natural circulation or evaporation, which occur without external power or force, to perform safety related functions. This lesson provides information on the motivating factors in the development of passive safety system and the application of various passive concepts to reactor safety systems. Included are example safety systems from advanced designs in each of the following major categories of WCRs: PWRs, BWRs, and SMRs.

4.1. OVERVIEW AND ASSESSMENT OF PASSIVE SAFETY SYSTEMS

Passive safety systems are being used to meet many of the goals, both economic and safety related, which are motivating the further development of advanced WCRs. This lesson provides an overview of the motivation for development, classification, and challenges in application of these passive safety systems as an adaptation of IAEA-TECDOC-1474 [20]. Several specific common passive safety systems are briefly discussed and explained in context of their ‘passivity’.

4.1.1. Design goals of advanced WCRs and passive safety systems

4.1.1.1. Economic aspects of advanced WCRs

“Economic competitiveness with other energy sources is an obvious goal of new plant development. Both private sector and state owned electricity generating organizations carefully examine the costs of their operations, and focus on supply technologies that are of low cost and low risk.

Capital costs for nuclear plants generally account for 50–75% of the total nuclear electricity generation costs, compared to 25–60% for coal plants and 15–40% for gas plants. This high capital cost presents a significant challenge to the addition of new nuclear power capacity. Until recently, nuclear power’s advantage in having a small share of its generating costs in fuel costs could offset the disadvantage of its high capital costs in regulated markets, since investment costs could be recovered over several decades through regulated rates. Now, with increased competition in the electric power industry, short term profitability has become a criterion for successful generation along with long term economic viability. With deregulation, owners are not guaranteed cost recovery through regulated rates; with privatization, investors seek appropriately rewarded risk, which often translates into seeking small capital investments and high returns, and the minimization of their economic risks. For nuclear plants to form a significant part of the future generating mix in competitive electricity markets, capital cost reduction through simplified designs must be an important focus. Reductions in operating, maintenance and fuel costs should also be pursued.

Design organizations are challenged to develop advanced nuclear power plants with lower capital costs and shorter construction times (e.g. by simplification, standardization, modularization, etc.) and sizes suitable for various grid capacities and owner investment

capabilities. This includes large sizes for some markets and small and medium sizes for others” [20].

“The nuclear community must continue to move forward in identifying and implementing new approaches for further reducing the costs of new nuclear plants... In summary, these are:

- (a) Modularization, factory fabrication, and series production;
- (b) Development of highly reliable components and systems, including ‘smart’ (instrumented and monitored) components and methods for detecting incipient failures to improve system reliability so that dependence on costly redundancy and diversity practices could be reduced. Development is also required to correlate signals from the ‘smart’ components with reliability, and criteria must be developed for when to do maintenance and replacement;
- (c) Further development of passive safety systems where the safety function can be met more cheaply than with active systems. This would include development of reliability models for passive systems;
- (d) Development of computer based advanced technologies for design, procurement, manufacture, construction and maintenance with a focus on coordination of activities to reduce costs and schedules;
- (e) Further development of PSA methods and data bases to support plant simplification and to support examination of potential risk informed regulatory requirements for new plants leading to more economical designs with very high safety levels. PSA assessments must:
 - (i) Be capable of assessing the total risk including full power, low power, shutdown, fires and external events;
 - (ii) Be capable of accounting for safety culture and human factors;
 - (iii) Accurately account for ageing effects; and
 - (iv) Include capability to quantify uncertainties.

The challenge will be to establish PSA methods, including understanding of uncertainties in predicted results, to demonstrate that sufficient defence in depth, and sufficient balance among the various levels of defence in depth, can be achieved through simpler and cheaper technical solutions;

- (f) Improvement of the technology base for eliminating overdesign (e.g. improved understanding of thermohydraulic phenomena, more accurate data bases of thermohydraulic relationships and thermophysical properties, better neutronic and thermohydraulic codes, and further code validation). The focus could be on removing the need to incorporate excessively large margins into the design simply for the purpose of allowing for limitations of calculational methodology and uncertain data;
- (g) Reduction of number of components and materials requiring nuclear grade standards;
- (h) Design for higher temperature (higher thermal efficiency);
- (i) Design for multiple applications (e.g. cogeneration of electricity and heat; seawater desalination);

- (j) Achieving international consensus regarding commonly acceptable safety requirements that would facilitate development of standardized designs which can be built in many countries without requiring significant redesign efforts” [20].

New reactor designs are making more extensive use of passive safety features for a variety of purposes, for instance in: core cooling during transients, design basis accidents or even severe accidents or for containment cooling. These applications are done with the claim that passive systems are highly reliable and reduce the cost associated with the installation and maintenance of systems requiring multiple trains of equipment requiring expensive pumps, motors and other equipment as well as redundant safety class power supplies.

4.1.1.2. Safety design goals of advanced WCRs

“In the course of nuclear power development in the latter part of the twentieth century, there have been significant developments in technology for reactor safety. These include:

- (a) Advances in the application of PSA;
- (b) Introduction of more rigorous quality assurance programmes for plant design, licensing, construction and operation;
- (c) Increased attention to the effect of internal and external hazards — in particular the seismic design and qualification of buildings;
- (d) Major advances in fracture mechanics and non-destructive testing and inspection;
- (e) Increased emphasis on the man-machine interface including improved control room design, and plant design for ease of maintenance;
- (f) Rapid progress in the field of control and instrumentation — in particular, the introduction of microprocessors into the reactor protection system;
- (g) Increased emphasis on prevention and mitigation of severe accidents at the design stage.

New nuclear plant designs are being developed to meet stringent safety requirements. While there are differences in safety requirements among countries developing new designs, the stringent requirements are generally reflected in the IAEA’s Safety Standards Series. See for example [13], [66], and [67] which consists of the following categories:

- (a) Safety Fundamentals present basic objectives, concepts and principles of safety and protection in the development and application of nuclear energy for peaceful purposes;
- (b) Safety Requirements establish the requirements that must be met to ensure safety. These requirements, which are expressed as ‘shall’ statements, are governed by the objectives and principles presented in the Safety Fundamentals;
- (c) Safety Guides recommend actions, conditions or procedures for meeting safety requirements. Recommendations in Safety Guides are expressed as ‘should’ statements, with the implication that it is necessary to take the measures recommended or equivalent alternative measures to comply with the requirements.

The IAEA's Safety Standards are not legally binding on Member States but may be adopted by them, at their own discretion, for use in their national regulations.

Technical aspects of safety including principles are discussed in Reference [66] for siting, design and construction, commissioning, operation and maintenance, and radioactive waste management and decommissioning.

In 2000 the IAEA published the report 'Safety of Nuclear Power Plants: Design' [13] establishes nuclear plant safety design requirements applicable to safety functions and associated structures, systems and components, as well as to procedures important to nuclear plant safety. It recognizes that technology and scientific knowledge will continue to develop, and that nuclear safety is not a static entity; however, these requirements reflect the current consensus. They are expressed as 'shall' statements, and are governed by the objectives and principles in the Safety Fundamentals report. The Design Requirements report avoids statements regarding the measures that 'should' be taken to comply with the requirements. Rather, Safety Guides are published from time to time by the IAEA to recommend measures for meeting the requirements, with the implication that either these measures, or equivalent alternative measures, 'should' be taken to comply with the requirements.

The new nuclear power plant designs currently under development incorporate various technical features to meet very stringent safety requirements. Specifically, safety objectives for future plants include reducing the likelihood of accidents as well as mitigating their consequences in the extremely unlikely event that they occur. The objectives include the practical elimination of accident sequences that could lead to large early radioactive release, whereas severe accidents that could imply late containment failure are to be considered in the design process so that their consequences would necessitate only protective measures limited in area and in time [67].

In 1996, INSAG-10 [68] noted that prevention of accidents remains the highest priority among the safety provisions for future plants and that probabilities for severe core damage below 10^{-5} per plant year ought to be achievable. INSAG-10 noted that values that are much smaller than this would, it is generally assumed, be difficult to validate by methods and with operating experience currently available. INSAG-10, therefore, considers improved mitigation to be an essential complementary means to ensure public safety. INSAG-10 also stated the need to demonstrate that for accidents without core melt there will be no necessity for protective measures (evacuation or sheltering) for people living in the vicinity of the plant, and for severe accidents that are considered in the design, that only protective measures that are very limited in area and time would be needed (including restrictions in food consumption).

In 1999, INSAG-12 [69] (Revision 1 of INSAG-3), confirmed that the target frequency for core damage frequency (CDF) in existing nuclear power plants is below about 10^{-4} with severe accident management and mitigation measures reducing by a factor of at least 10 the probability of large off-site releases requiring short term off-site response. INSAG-12 continued by noting that for future plants, improved accident prevention (e.g. reduced common mode failures, reduced complexity, increased inspectability and maintainability, extended use

of passive features, optimized human–machine interface, extended use of information technology) could lead to achievement of an improved CDF goal of not more than 10^{-5} per reactor year. With regard to offsite release for future plants, INSAG-12 stated that an objective for future plants is ‘the practical elimination of accident sequences that could lead to large early radioactive releases, whereas severe accidents that could imply a late containment failure would be considered in the design process with realistic assumptions and best estimate analyses so that their consequences would necessitate only protective measures limited in area and in time’.

From the IAEA’s Safety Standards Series and INSAG publications, a number of safety goals for future nuclear plants can be identified:

- (a) A reduction in CDF relative to current plants;
- (b) Consideration of selected severe accidents in the design of the plants;
- (c) Ensuring that releases to the environment in the event of a severe accident are kept as low as practicable with the aim of providing a technical basis for simplification of emergency planning;
- (d) Reduction of the operator burden during an accident by an improved man–machine interface;
- (e) The adoption of digital instrumentation and control;
- (f) The introduction of passive components and systems.

Technological advances are being incorporated into advanced designs to meet the stringent safety goals and objectives, see [4] and [70]. Design features both to improve prevention of severe accidents involving core damage, as well as for mitigating their consequences are being incorporated. Considerable development has been carried out worldwide on new systems for heat removal during accidents. Progress has been made in containment design and in instrumentation and control systems. To further reduce the probability of accidents and to mitigate their consequences, designers of new plants are adopting various technical measures. Examples are:

- (a) Larger water inventories (large pressurizers, large steam generators), lower power densities, negative reactivity coefficients to increase margins and grace periods thereby reducing system challenges.
- (b) Redundant and diverse safety systems with proven high reliability with improved physical separation between systems.
- (c) Passive cooling and condensing systems.
- (d) Stronger containments large enough to withstand the pressure and temperatures from design basis accidents without fast acting pressure reduction systems, and with support systems to assure their integrity during severe accidents (for example, to control hydrogen concentrations). In some designs there is an outer second containment that provides protection against external events, and allows for detection and filtration of activity that potentially would leak from the inner containment.

Some new designs rely on well proven and highly reliable active safety systems to remove decay heat from the primary system and to remove heat from the containment building during accidents. Other new designs incorporate safety systems that rely on passive means using, for example, gravity, natural circulation, and compressed gas as driving forces to transfer heat from the reactor system or the containment to either evaporating water pools or to structures cooled by air convection. Considerable development and testing of passive safety systems has been and is being carried out in several countries. In other designs a coupling of active safety systems and passive safety systems is adopted. For each of these approaches, the main requirement is that the proposed safety systems fulfil the necessary functions with appropriate reliability” [20].

4.1.2. Classification of passive safety systems

“The use of passive safety systems such as accumulators, condensation and evaporative heat exchangers, and gravity driven safety injection systems eliminate the cost associated with the installation, maintenance and operation of active safety systems that may require multiple pumps with independent and redundant electric power supplies. Another motivation for the use of passive safety systems is the potential for enhanced safety through increased safety system reliability” [20].

Passive safety features (i.e., those that take advantages of natural forces or phenomena such as gravity, pressure differences or natural heat convection) have been used to accomplish safety functions in operating reactors for many decades. Traditionally however, the use of such passive features, for instance in a reactor scram, were of limited extent and safety systems heavily relied on active driving devices (e.g. electrical or diesel motors).

Passive safety systems are considered in new and advanced reactor designs for enhanced safety and reliability, and with the goal to reduce human intervention. Because of the reliance of currently operating safety systems on operator action, electrical power, or mechanical actuation, it is possible that a station blackout event or even severe natural disasters previously classified as BDBA, could potentially disable safety systems leading to a core melt and or significant releases. Thus, significant effort has gone into developing passive safety systems which do not require electrical energy, operator action, mechanical actuation, or other input in order to cool the core and protect the public from release.

The IAEA defines a passive safety system as “a system which is composed entirely of passive components and structures or a system which uses active components in a very limited way to initiate subsequent passive operation” [71]. Due to the wide range of systems which may meet this definition, the IAEA has further defined four categories corresponding to the degree of system passivity. Characterizing features and examples of passive systems falling into these categories are summarized in Table 13 [72].

TABLE 13. CATEGORIES OF SAFETY SYSTEM PASSIVITY

CATEGORY	SYSTEMS IN THIS CATEGORY:	EXAMPLE SYSTEMS OR COMPONENTS INCLUDE:
A	<ul style="list-style-type: none"> — Do not receive external signal inputs of intelligence; — Do not receive electrical power or force as external inputs; — Do not have any moving or mechanical parts; — Do not have any moving working fluid. 	<ul style="list-style-type: none"> — Physical barriers against release of fission products (e.g. fuel cladding, pressure boundary systems); — Building structures which protect the nuclear power plant from external events (e.g. earthquakes, tsunamis, and other natural disasters); — Conductive and radiative heat transfer mechanisms for core heat removal; — Static components of safety systems (e.g. static components of pressurizer, accumulator, or surge tanks).
B	<ul style="list-style-type: none"> — Do not receive external signal inputs of intelligence; — Do not receive electrical power or force as external inputs; — Do not have any moving or mechanical parts; — Have a moving working fluid. 	<ul style="list-style-type: none"> — Systems based on pressure boundaries (e.g. emergency borated water injection from an external pool); — Systems based on natural circulation (e.g. coolant system which continues to remove core heat through natural circulation).
C	<ul style="list-style-type: none"> — Do not receive external signal inputs of intelligence; — Do not receive electrical power or force as external inputs; — Do have moving or mechanical parts; — May or may not have a moving working fluid. 	<ul style="list-style-type: none"> — Systems utilizing check valves (e.g. check valve equipped accumulators or storage tanks); — Automatic pressure relief valves; — Rupture disks in filtered venting systems.
D	<ul style="list-style-type: none"> — May receive inputs of intelligence to begin passive processes; — Energy used to initiate the passive process comes from stored sources (e.g. batteries, elevated fluid); — May only have active components in the form of controls, instrumentation, and valves which are used to initiate passive processes; — May not be manually initiated. 	<ul style="list-style-type: none"> — Gravity driven, battery initiated systems (e.g. gravity based injection systems); — Gravity or pressure driven shutdown systems (e.g. gravity driven control rod insertion).

4.1.3. Challenges to passive safety systems

Despite benefits surrounding their reliability, there are several setbacks facing the design and implementation of passive safety systems. The following paragraphs discuss several of the major issues.

(a) Design limitations

Many passive safety systems which exist today have design limits which impede their capability to serve a function efficiently. The weak driving forces, such as natural circulation and small pressure differences, pose significant challenges to the design and safety demonstration of passive systems for a broad range of accident conditions and additional loads that can be imposed by internal or external hazards.

Additionally, several passive safety systems utilize a working fluid. Because of this, current passive safety systems typically can only last three to seven days before significant cooling water is lost and further action is required. While this remains a significant improvement over many active systems, which often cannot operate longer than a few hours before significant damage to the plant or dose to the public occurs, the creation of a 'walk away safe' reactor is beyond current design capabilities. In this way, factors, such as the limited size of an economically justifiable reserve coolant tank, pose a design limitation for the extended functionality periods of passive safety systems.

(b) System integrity

Performance of passive safety systems is dependent upon structural and functional integrity remaining intact. There remain, as with many active systems, several ways in which passive systems may fail. The following represent commonly postulated initiators of passive safety system abnormal operation or functional degradation:

- (i) Inadvertent actuation;
- (ii) Boron chemical concentration shifts;
- (iii) Through wall cracks or ruptures;
- (iv) Flange leaks;
- (v) Flow reversal;
- (vi) Temperature stratification;
- (vii) Valve failures (check, PORV, or motor operated).

In addition to these, there exist conceivable scenarios which could arise locally (e.g. flooding, forceful impact, fires) to inhibit or disable not only active systems, but also those systems which do not rely on external input. The assessment of passive safety systems should thusly consider possible failure mechanisms.

(c) Obscurity of definition

There has been little uniformity in the definition ascribed to passive safety systems in the nuclear industry. As a result, confusion and often misunderstanding regarding the capacity, function and even reliability of passive safety systems. The IAEA has developed a convention for passive safety systems, as previously indicated in Table 13. This table alleviates the confusion of passivity levels, but there is still a large degree of uncertainty distinguishing passive safety systems reliability.

Within the framework of IAEA definition, full passivity does not necessarily correspond to a safer, more reliable design. For example, relying on a gravity or natural circulation system as opposed to an active alternative may not be the best option due to the relatively weak driving force of natural circulation. While natural circulation is more reliable to function in certain accidents, it may not be sufficiently effective to mitigate the effects of others. The use of a higher passivity design, in this way, should not be considered as a direct association to a wholly superior design; in this example, natural circulation should instead be considered as an

alternative which may be more reliable in dealing with certain accident scenarios where active system failure is possible.

Additional confusion can arise from the broad definition of system passivity due to its extension to systems which often exhibit inherent passivity. For example, structural components acting as barriers to fission product release, such as fuel cladding or reactor containment, are considered to exhibit the highest level of passivity. The underlying concept of fuel cladding is far removed from the innovation and functional complexity of designs utilizing natural circulation cooling loops, gravity drain tanks, and accumulators; however, defining the degree of passivity make no distinction to this effect.

(d) Insufficient data and operating experience

Despite large interest in passive safety systems, there is a shortage of experimental data, phenomena identification and ranking, and even understanding of operating conditions. This indicates that passive safety systems require significant investments in assessment and licensing before integration with a new or existing plant can be attempted.

Passive safety systems are well understood under standard operating modes and conditions. However, early licensing efforts indicate significant interest exists for the operation of these safety systems in nonstandard transient conditions and alternative modes. Further, conditions that lead to and permeate accident conditions are often unknown and obscure. Thus, an understanding of conditions surrounding non-standard operation is essential to passive safety system technologies application.

Very few operating plants utilize passive safety system concepts. Thus, the response of regulators in the face of implementing a new technology is largely unknown with a large degree of uncertainty. If a passive safety system developer can validate increased safety at decreased cost and licensing uncertainties, they will likely be able to secure a significant portion of the market for nuclear reactor safety systems.

4.1.4. Examples of common passive safety systems

Natural circulation is important for advanced water cooled reactors as a passive core heat removal mechanism. These passive mechanisms are often initiated by limitedly active components or integrated as passive modes of operation in normally active systems and structural components.

Presented are several passive safety systems commonly used in advanced reactor designs. The information given, and any figure of a system or component appearing in this subsection, is adapted in part or in whole from IAEA-TECDOC-1624 [72]. This reference also includes discussion of passive safety systems used in specific reactor designs and correlates these to the driving passive phenomena. Technologies included for description include:

- (a) Pre-pressurized core flooding tank (accumulator);
- (b) Elevated tank natural circulation loop (core makeup tank);

- (c) Elevated gravity drain tank;
- (d) Passively cooled steam generator;
- (e) Passive residual heat removal heat exchanger;
- (f) Isolation condenser;
- (g) Sump natural circulation;
- (h) Containment pressure suppression pool;
- (i) Containment heat removal and pressure suppression systems;
- (j) Containment spray.

Descriptions are accompanied by explanations of typical passivity categories, within the IAEA definition, associated with each system.

(a) Pre-pressurized core flooding tank (accumulator)

Pre-pressurized core flooding tanks, or accumulators, are used in both conventional and advanced reactor designs and typically consists of a large tank filled with cold borated water and a pressurized fill gas. These tanks are isolated from the reactor coolant system (RCS) by check valves, when the pressure in the RCS drops below the fill gas pressure as a result of an event such as a loss of coolant accident (LOCA). Once the check valve is opened, the fill gas will force borated water through the RCS to the reactor core. FIG. 55 shows an example accumulator. Due to the check valves, which are considered ‘moving mechanical parts’, accumulators are classified as Category C passive safety systems.

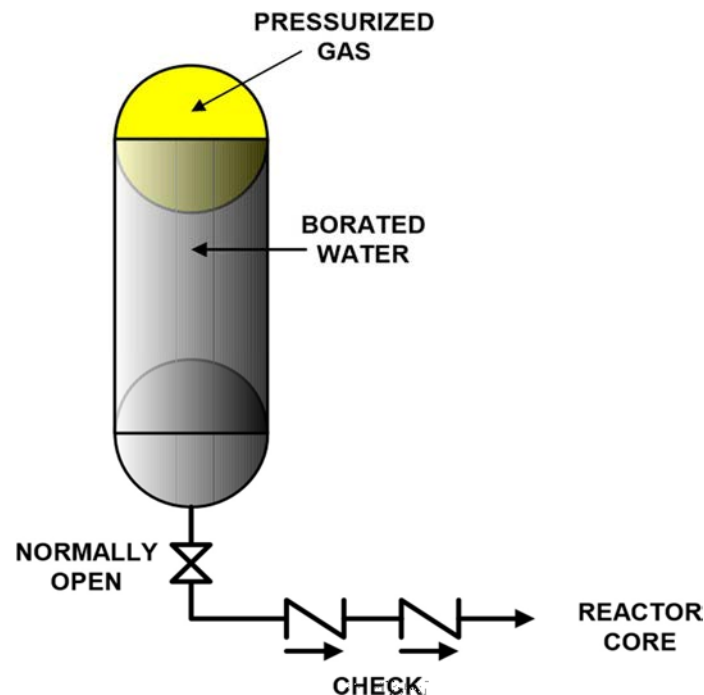


FIG. 55. Pre-pressurized core flooding tank (accumulator) [72].

Accumulators are used in many of the currently operating nuclear power plants as part of the emergency core cooling system (ECCS).

(b) Elevated tank natural circulation loop (core makeup tank)

Natural circulation loops such as a core makeup tank (CMT) provide a passive core heat removal mechanism. Similar to an accumulator, a CMT is filled with borated water and isolated from the reactor vessel by a series of check valves and an additional, typically closed valve. However, CMT are not pressurized by gas, instead being connected to the RCS as shown in FIG. 56. In an accident scenario, a signal will be sent to open the closed valve to create a natural circulation loop. Following natural circulation, cold borated water will flow to the reactor core. Because this system only operates passively following the signal to open the isolation valve, it is classified as a Category D passive safety system.

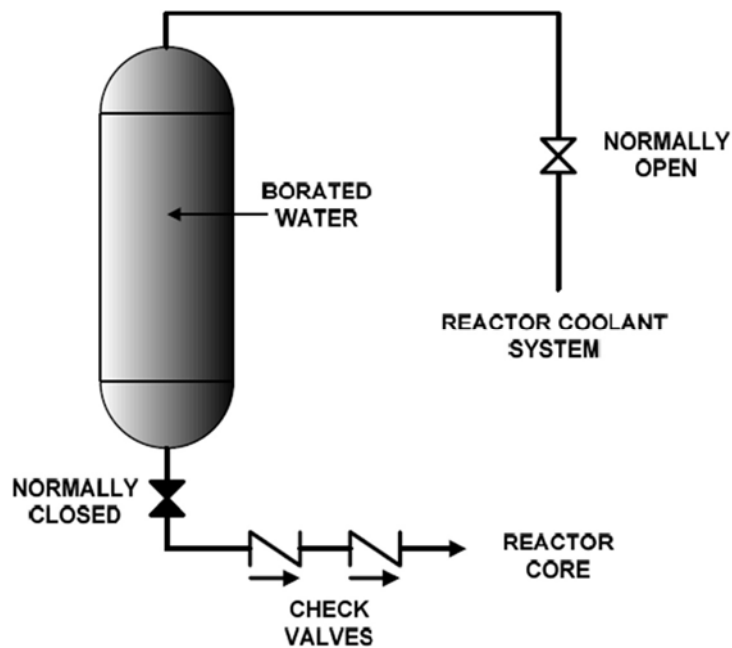


FIG. 56. Elevated tank natural circulation loop (core makeup tank) [72].

Many advanced reactor designs make use of natural circulation loops as a method for reactor cooling and an effective method for boron injection. These systems are normally connected to the ECCS to reduce the number of pipes. In a design such as this, flow rate through the CMT can be affected by the injection of borated water from an accumulator.

(c) Elevated gravity drain tank

Elevated gravity drain tanks are elevated tanks full of cold borated water, separated from the reactor system by an isolation valve and a series of check valves as shown in FIG. 57. On loss of pressure in the reactor, a signal is sent to open the normally close isolation valve and the water drains into the reactor system by gravity. Because the system relies on a signal to open the isolation valve, it is classified as a Category D passive safety system.

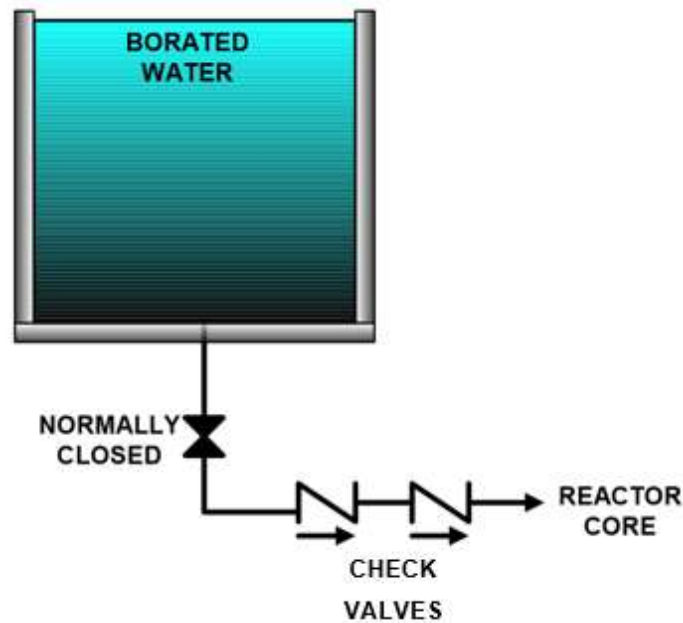


FIG. 57. Elevated gravity drain tank [72].

(d) Passively cooled steam generator

Steam generators may be used to remove core heat through natural circulation. This is done by tying the steam generator to an external cooling system, either a cooling tower or cooling tank, which is normally isolated by closed valves. Upon opening these valves, reactor vessel water will continue to generate steam in the steam generator, which condenses when passing through the external cooling system. Because the valves must be signalled to open, this is categorized as a Category D passive safety system. FIG. 58 shows both a water cooled and an air cooled example of passively cooled steam generators.

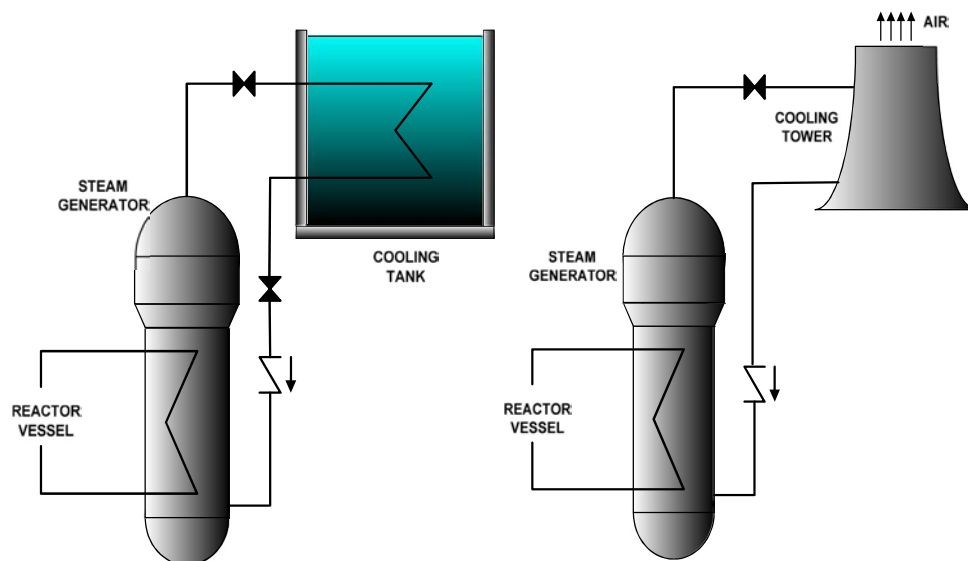


FIG. 58. Passively cooled steam generators; left — water cooled, right — air cooled [72].

(e) Passive residual heat removal heat exchanger

Passive residual heat removal (PRHR) heat exchangers consist of cooling tanks attached to the reactor vessel where the flow loop is broken by a typically closed valve as shown in FIG. 59. In an accident scenario, a signal may be sent to open the valve to allow water to flow through the PRHR tubes and allow core decay heat to be removed by heat transfer to the cooling pool. Because it is reliant on a signal to open the valve, this is considered a Category D passive safety system.

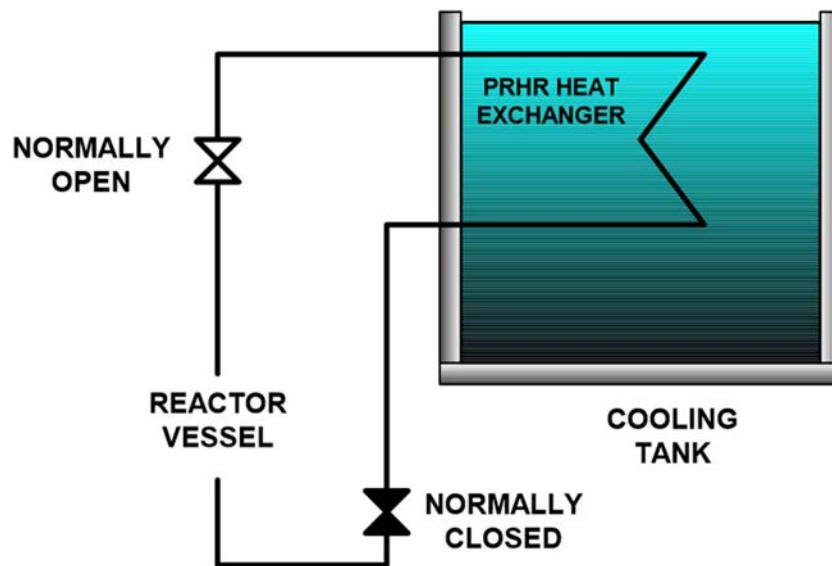


FIG. 59. Passive residual heat removal heat exchanger [72].

Several advanced designs use cooling tanks filled with water as passive heat exchangers for core cooling. The effectiveness of PRHR systems can be affected by natural circulation flow rate and the material properties of the fluid and the heat exchanger.

(f) Isolation condenser

Isolation condensers (ICs), as shown in FIG. 60, perform passive core decay heat removal in a similar way to PRHR systems. However, they are designed for heat transfer by condensation of steam produced in a BWR and are typically closed off from the reactor vessel. On opening of the valves in an accident, steam will flow through the IC line and condense when passing through the cooling tank before flowing back to the reactor vessel. Because the valves must be signalled to open, this is a Category D passive safety system.

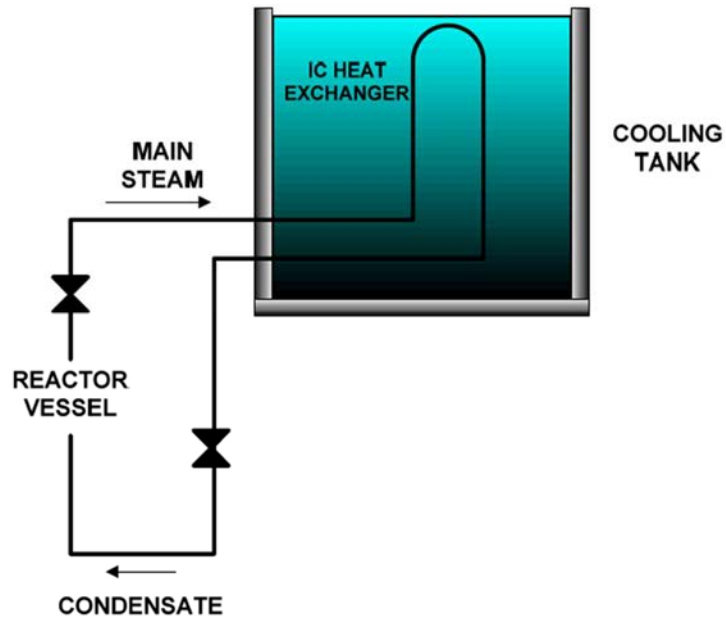


FIG. 60. Isolation condenser cooling system [72].

(g) Sump natural circulation

Sump natural circulation utilizes water lost from the reactor coolant system to perform core decay heat removal. In an event such as a loss of coolant accident (LOCA), water released into the reactor containment is collected and stored as shown in FIG. 61. A signal will open the normally closed valve, allowing natural circulation to pull water through the sump screen and into the reactor vessel where it boils and is released as steam through the ADS, and in some designs recirculated through water storage tanks. Because of the initiating signal, this is a Category D passive safety system.

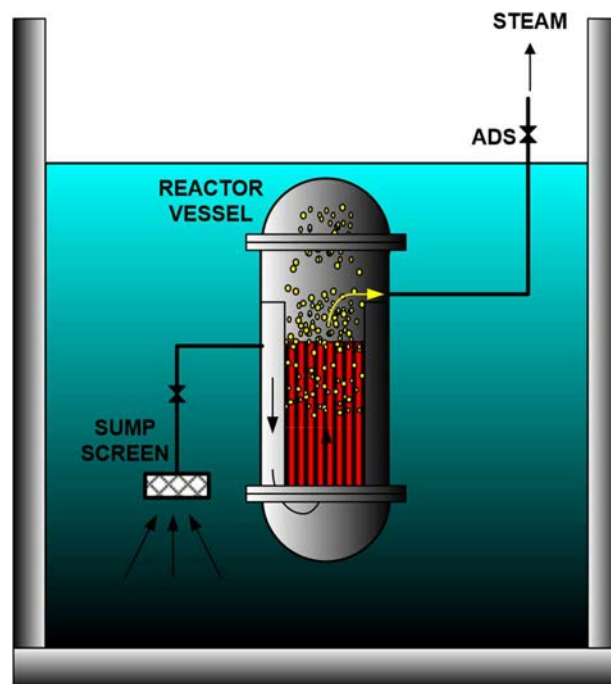


FIG. 61. Sump natural circulation cooling [72].

(h) Containment suppression pool

Containment suppression pool systems are used to mitigate pressure increase in BWRs and consist of a drywell and wet well separated by suppression pools as shown in FIG. 62. In the event of a loss of coolant, steam is released into the drywell. As pressure continues to increase, steam is forced through vent lines into the suppression pools where it is condensed. Because this system only uses a working fluid, without mechanical moving parts and does not have initiating signals or power, it is a Category B passive safety system.

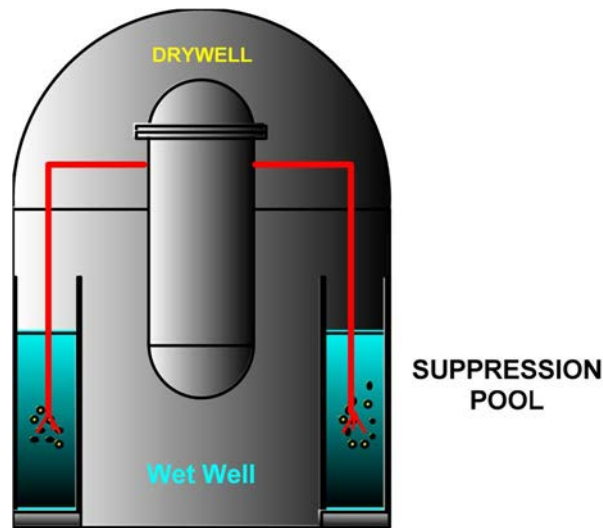


FIG. 62. Containment suppression pool system [72].

(i) Containment heat removal and pressure suppression systems

Containment heat and pressure can be removed through utilization of elevated cooling tanks. There are significantly different approaches to this, and three concepts will be discussed. All of these systems utilize working fluid and in their most basic form do not have mechanical parts or externally initiated signals. In this simplest situation they would be considered Category B passive safety systems; however externally signalled valves are included in many designs, often classifying them as Category D passive safety systems.

The first method utilizes an angled heat exchanger attached to a storage pool as shown in FIG. 63. Water is forced by natural circulation through the condenser, making use of the gravity gradient caused by the angle.

The second method connects a loop from a heat exchanger in containment to a heat exchanger in an external storage pool as shown in FIG. 64. As heat is produced in the containment, natural circulation will drive fluid flow in the loop where it will release heat to the storage pool.

A third method separates containment into a drywell and a wet well, with a connection between the two through a condenser in an external pool as shown in FIG. 65. In an accident scenario, steam produced in the drywell will increase pressure. This pressure forces steam through piping to the water storage pool where it is condensed. Condensate is then returned to the containment wet well.

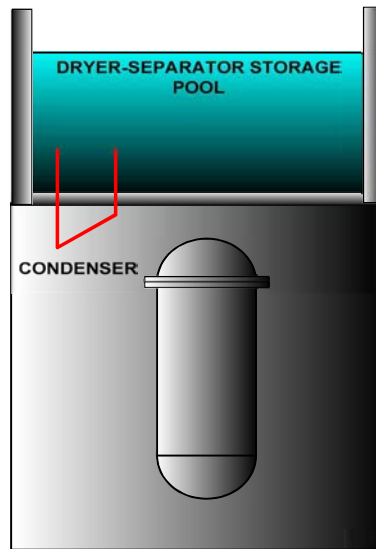


FIG. 63. Containment heat and pressure removal by gravity driven condenser [72].

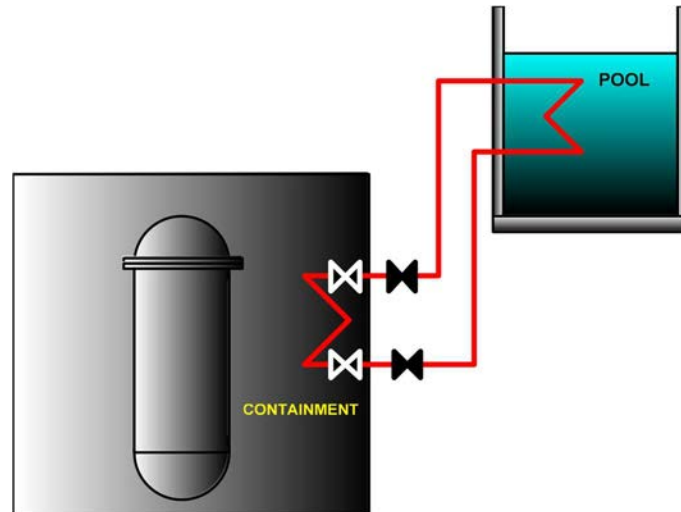


FIG. 64. Containment heat and pressure removal by closed loop heat exchangers [72].

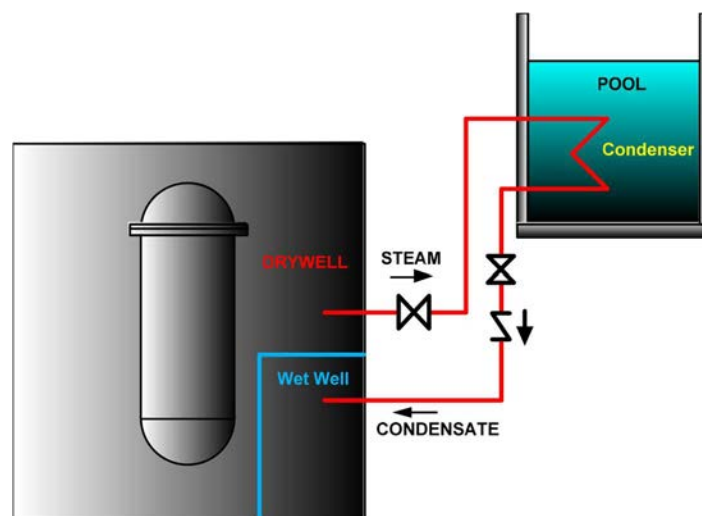


FIG. 65. Containment heat and pressure removal by pressure driven condenser [72].

(j) Containment spray systems

Passive containment spray systems utilize natural draft air to cool the containment. This is done, as shown in FIG. 66, by condensation of steam on the inside surface of the containment. Heat from the containment air is transferred to air outside the containment shell and allowed to flow out of the system. This alone is a Category B passive safety system; however, containment sprays are commonly used in combination. Containment sprays are signalled to spray cold water on the outside of the containment, cooling the surface and allowing further condensation and cooling inside. Because these sprays receive an initiating signal, they are a Category D passive safety system.

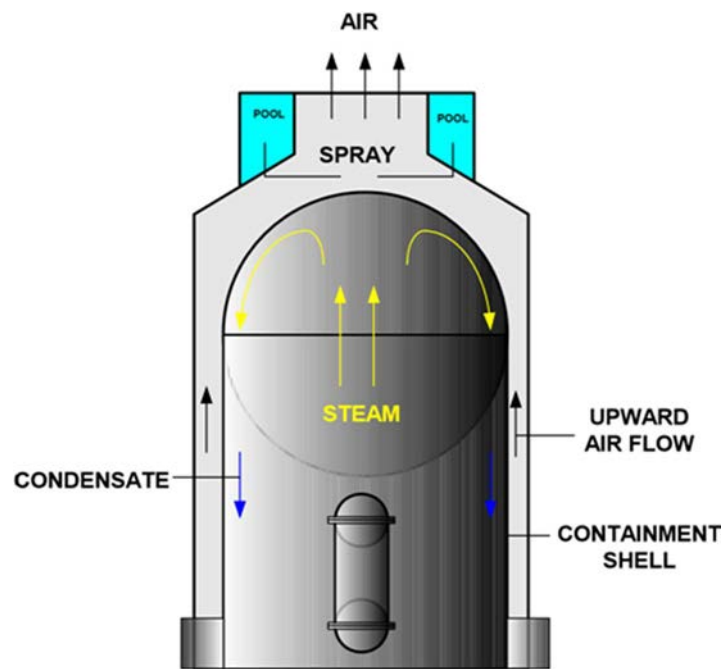


FIG. 66. Containment heat and pressure reduction by natural draft air and containment spray [72].

The effectiveness of heat exchange on the containment shell is affected by several factors. Non-condensable gases in the containment may act as insulation to reduce heat transfer and vapour condensation. The internal geometry of containment can also have an effect on how effective condensation on the surface is and external geometry can have an effect on heat transfer rate to air. The material properties of containment can also affect the conduction of heat through the containment and determine how much energy the shell will absorb during initial heating.

4.2. EXAMPLES OF PASSIVE SAFETY IN ADVANCED REACTOR SYSTEM DESIGNS

This section contains descriptions of passive safety systems as utilized in select WCR designs. These descriptions are extracted from the IAEA Advanced Reactors Information System (ARIS) database [4] and adapted to the scope of taught concepts. Descriptions include the direct application of passive safety systems, including many which were previously described, to actual advanced WCR designs.

4.2.1. PWR design example: VVER-1000 (V-466B)

The VVER-1000 (V-466B) was designed to meet Russian safety requirements with consideration of both IAEA recommendations and European utility requirements. The strategy for management of design basis accidents utilizes both active and passive safety systems, while the strategy for beyond design basis accidents is mainly based on the use of passive safety systems. The following paragraphs describe some of the included passive safety systems.

4.2.1.1. Quick boron injection system

The quick boron injection system is specially reserved for use in beyond design basis accident management where a scram did not, or failed to, occur. The main idea of this system is to put the reactor core in a subcritical state by the injection of high concentration boric acid solution into the primary coolant loop.

The quick boron injection system consists of four independent channels, each consisting of a tank filled with boric acid and connected to the primary coolant loop and isolated from the system by valves. The flow of boric acid through these valves is initiated by a pressure differential across the valves.

4.2.1.2. Core flooding system

The core flooding system is intended to provide a passive supply of boron solution into the reactor core to simultaneously remove decay heat and maintain the core at a subcritical state. It is designed to function in the event a primary system leak during a station blackout (including the loss of diesel generators) and function for as long as possible (at least 24 hours).

The system consists of eight hydro accumulators, combined into four groups. Each group of the system consists of two second stage hydro accumulators (each with a volume of 120 m³), piping, and valves. The hydro accumulators are subjected to atmospheric pressure under normal operating conditions and contain a boric acid solution. The result is a total water inventory of 960 m³ available for supply to the core.

The second stage hydro accumulators are connected via a discharge line to the piping of the first stage hydro accumulators. The first stage hydro accumulators are, in turn, connected to non-isolated collection chambers of the RPV. The boric acid solution flows from the hydro accumulators to the RPV when the coolant pressure drops.

4.2.1.3. Passive heat removal system

The VVER-1000 system is designed to maintain heat removal from the reactor core during accidents with total loss of AC sources of electric power when either the primary loop is sealed or when leaks occur in the primary or secondary loops.

The decay heat removal system consists of four independent natural circulation loops, one for each coolant loop. Each steam generator has piping to carry and distribute steam into the

two heat exchangers. The steam is condensed in the heat exchangers and is returned to the steam generator.

The steam is condensed as a result of cooling by atmospheric air taken from outside the containment building. Air naturally flows into an annular corridor around the containment building and passes through air ducts to the heat exchangers. Air gate valves are included upstream and downstream of each heat exchanger in the direction of the air flow. Between the heat exchanger and the upper air gate valve, a regulating device limits the flowrate of air. Opening these air gates facilitates the heat exchanging process and closing returns the system to a standby mode of operation to minimize heat loss. During normal operation the system is permanently connected to steam generators.

4.2.2. BWR design example: Economic Simplified Boiling Water Reactor

The basic Economic Simplified Boiling Water Reactor (ESBWR) safety design philosophy is built on utilization of inherent margins (e.g. larger volumes and water inventory) to eliminate system challenges. The first line of defence is to enhance the normal operating system's ability to handle transients and accidents through design features such as adjustable speed, motor driven feedwater pumps and higher capacity pumps with backup power. As a second line of defence, passive safety systems are used in the design to provide confidence in the plant's ability to handle transients and accidents. All safety related systems are designed such that no operator actions are needed to maintain safe, stable conditions for 72 hours following a design basis accident. A view of the passive safety system configuration is shown in FIG. 67. Descriptions of some important passive safety systems are provided in the following paragraphs.

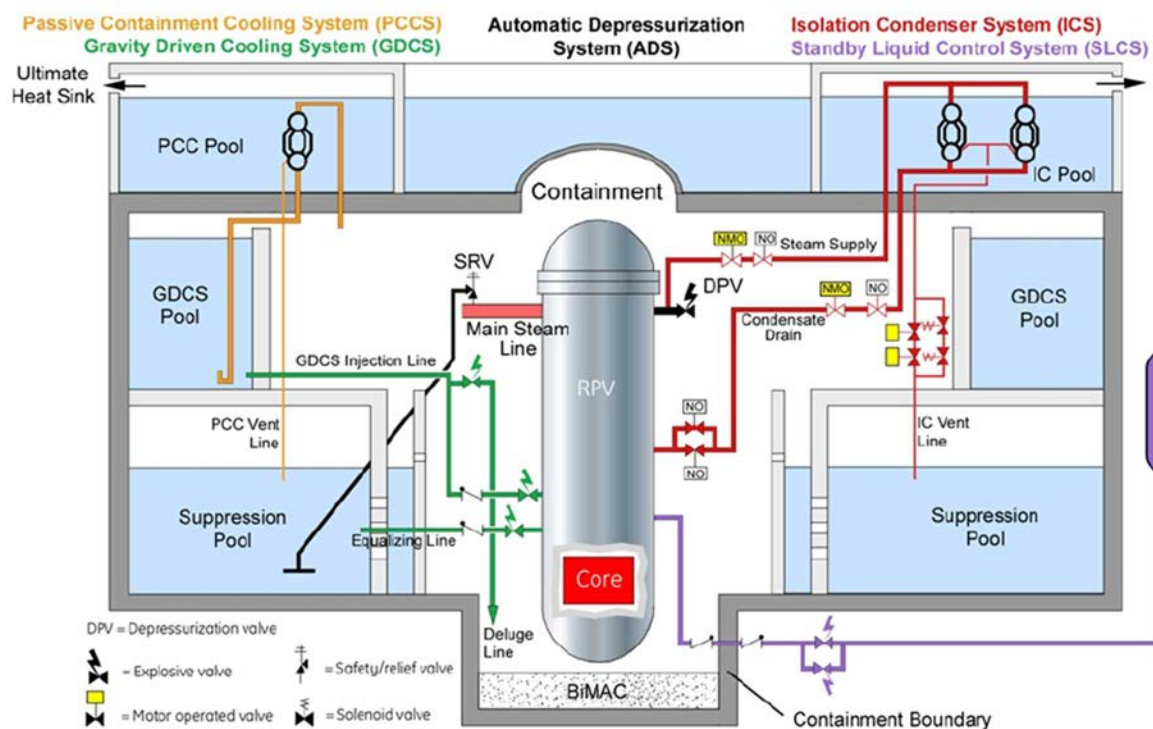


FIG. 67. ESBWR safety system configuration [4].

4.2.2.1. Isolation condenser system

The isolation condenser system removes decay heat after any reactor isolation during power operations. Decay heat removal limits further increases to steam pressure, keeping the RPV pressure below the safety relief valve setpoint. The IC system consists of four independent loops, each containing a heat exchanger that transfers heat by condenses steam in the tube and heating water in the IC pool; evaporated water from the IC pool is then vented to the atmosphere. The arrangement of the IC heat exchanger is shown in FIG. 68.

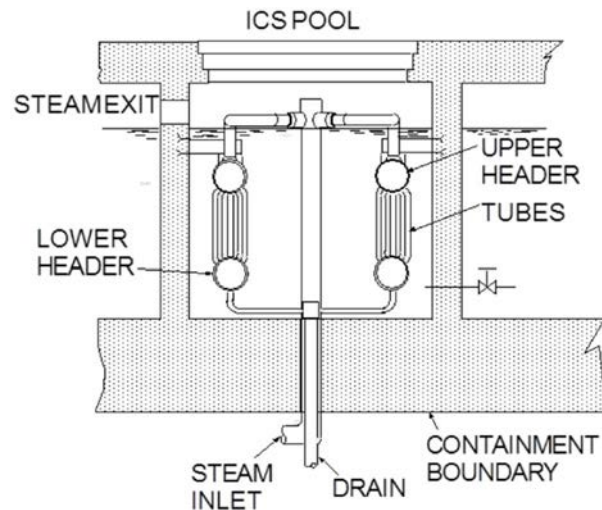


FIG. 68. Isolation condenser arrangement [4].

The IC system is initiated automatically by any of the following signals: high reactor pressure, main steam isolation valve closure, or an RPV water level signal. To start IC operation, the condensate return valve is opened whereupon the standing condensate drains into the reactor and the steam water interface in the IC tube bundle moves downward below the lower headers. The ICS can also be initiated manually by the operator from the control room by opening the IC condensate return valve.

The IC pool has an installed capacity that provides approximately 72 hours of reactor decay heat removal capability. The heat rejection process can be continued indefinitely by replenishing the IC pool inventory. Heat transfer from the IC tubes to the surrounding IC pool water is accomplished by natural convection, and no forced circulation equipment is required.

4.2.2.2. Gravity driven cooling system

The gravity driven cooling system (GDCS), in conjunction with the ADS, comprises the emergency core cooling system for ESBWR. Following a confirmed RPV water level signal and depressurization of the reactor to near ambient pressure conditions indicated by the ADS, the GDCS will inject large amounts of water into the reactor. The water flows to the RPV through simple, passive, gravity draining.

The GDCS is composed of four identical divisions. For short term cooling needs, each division takes suction from three independent GDCS pools positioned in the upper elevations of the

containment (see FIG. 69). Flow from each division is controlled by pyrotechnic type ECCS injection valves, which remain open after initial actuation. Each division of the short term subsystem feeds two GDCS injection nozzles on the RPV.

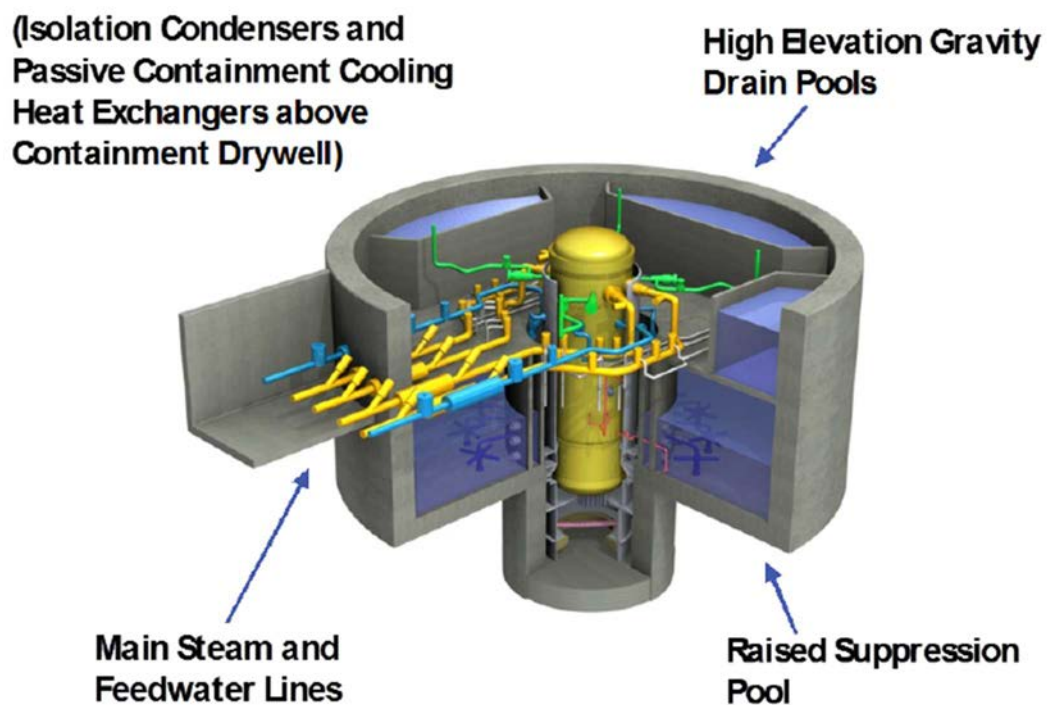


FIG. 69. Gravity driven cooling system diagram [4].

Backup flooding capabilities are also provided by a second GDCS subsystem fed by water from the suppression pool. Pyrotechnic type ECCS injection valves are also used in this subsystem, which feeds one RPV injection nozzle per division. These nozzles are placed at a lower elevation on the RPV than those of the short term subsystem.

In the event of a postulated severe accident that results in core melting where the molten core reaches the lower drywell region, the three upper GDCS pools have sufficient inventory to flood the lower drywell cavity to a level equal to the top of the active fuel.

The GDCS is completely automatic in actuation and operation. The ability to actuate the system manually is provided as a backup, but the operator cannot close any valves in the system.

4.2.2.3. Passive containment cooling system

The PCCS is a passive system that removes the decay heat and maintains the containment within its pressure limits for design basis accidents such as a LOCA. It consists of six low pressure, independent, loops. Each loop contains a steam condenser in a pool of water, as shown in FIG. 70, with the steam inlet coming from the drywell area surrounding the RPV.

The steam condenser condenses steam on the tube side and transfers heat to the water in the IC-PCCS pool. The IC-PCCS pool is vented to the atmosphere. Each PCCS condenser is located in an individual compartment of the IC-PCCS pool, and all pool compartments

communicate at their lower elevations. This allows full use of the collective water inventory, independent of the operational status of any given PCCS loop.

The PCCS loops are driven by the pressure difference created between the containment drywell and the suppression pool during a LOCA. PCCS operation requires no sensing, control, logic or power actuated devices for operation. Together with the pressure suppression containment system, the four PCCS condensers limit containment pressure to less than the design pressure for at least 72 hours after a LOCA, without inventory makeup to the IC-PCCS pool. The PCCS condensers are a closed loop integral part of the containment pressure boundary and are designed for twice the containment design pressure. Since there are no containment isolation valves between the PCCS condensers and the drywell, they are always in ‘ready standby’ mode.

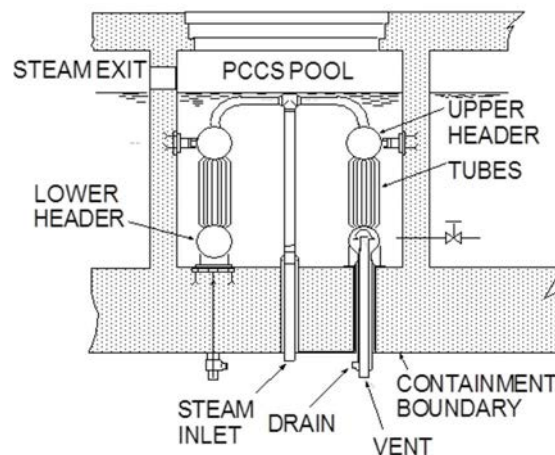


FIG. 70. Passive containment cooling condenser arrangement [4].

4.2.3. SMR design example: NuScale Power Modular and Scalable Reactor

The NuScale plant includes a comprehensive set of engineered safety features designed to provide stable long term nuclear core cooling under all conditions, as well as severe accident mitigation. They include a high pressure containment vessel, two passive decay heat removal and containment heat removal systems, and severe accident mitigation. These safety systems are briefly described in the following paragraphs.

4.2.3.1. Containment system design

The containment vessel has several features that distinguish it from existing containment designs. During normal power operation, the containment atmosphere is evacuated to provide an insulating vacuum that significantly reduces heat loss from the reactor vessel. As a result, the reactor vessel does not require surface insulation. This eliminates the potential for sump screen blockage. Furthermore, the deep vacuum improves steam condensation rates during any sequence where safety valves vent steam into this space. Further, by eliminating containment air (little to no oxygen), it prevents the creation of a combustible hydrogen mixture in the unlikely event of a severe accident, and eliminates corrosion and humidity problems inside containment, and eliminates the need for hydrogen recombiners. Finally, because of its relatively small diameter, it has been designed for a maximum pressure of approximately

5.5 MPa (800 psia). As a result, the equilibrium pressure between the reactor and the containment vessels in the event of a small break LOCA is achieved within a few minutes and will always be below the containment design pressure.

4.2.3.2. Decay heat removal

Each NuScale module has its own set of independent passive safety systems. As shown in FIG. 71, the entire NSSS including its containment, is immersed in a pool of water capable of absorbing all decay heat generated following a reactor shutdown for greater than 30 days followed by air cooling for an unlimited length of time. The water is contained in a stainless steel lined concrete structure that is entirely below grade.

Each NuScale module includes two redundant passive safety systems to provide pathways for decay heat to reach the containment pool: the decay heat removal system (DHRS) and the emergency core cooling system (ECCS). These systems do not require external power for actuation. The DHRS uses either of the two independent helical coil steam generator tube bundles to transfer heat generated within the core to the containment pool.

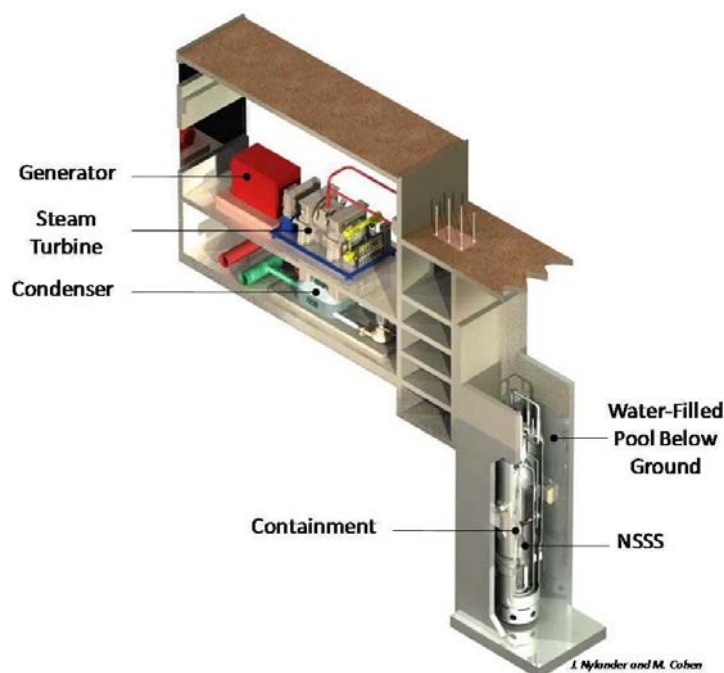


FIG. 71. Independent NuScale module shown submerged in water in a steel lined concrete pool [4].

The ECCS, shown in FIG. 72, provides a means of removing core decay heat in the event the steam generator tube bundles are not available. It operates by opening the vent valves located on the reactor head. Primary system steam is vented from the reactor vessel into the containment where it condenses on the containment surfaces. The condensate collects in the lower containment region (sump). When the liquid level in the containment sump rises above the top of the recirculation valves, the recirculation valves are opened to provide a natural circulation path from the sump through the core and out of the reactor vent valves.

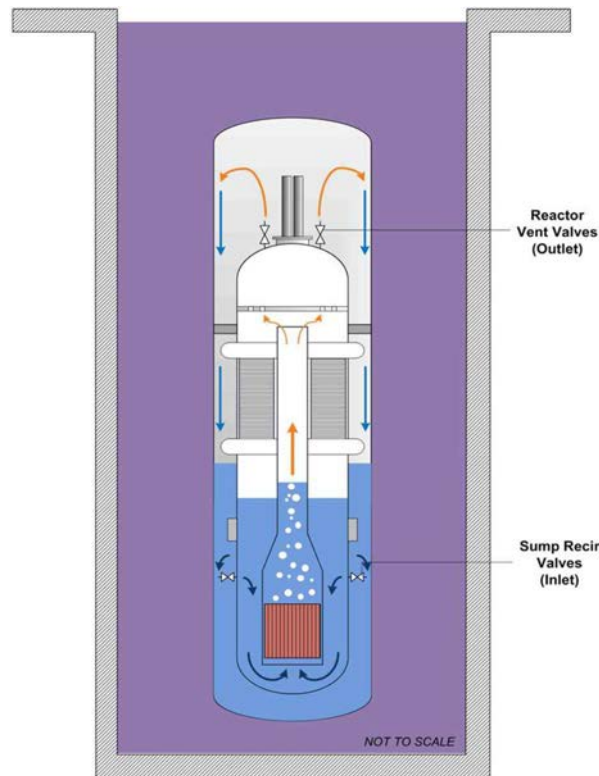


FIG. 72. Description of the containment heat removal system [4].

The integral configuration eliminates the possibility of a large break loss of coolant accident (LBLOCA) by design. For design basis small break assumptions, there is no scenario in which the core becomes exposed or uncovered as it will always be under water. As a result, cooling pathways are always available to remove decay heat. Because of the assured heat removal path and the failsafe nature of the ECCS valves, which passively open upon loss of power, the reactor can be safely cooled for an indefinite period of time without AC or DC power, without operator action, and without additional water.

4.2.3.3. Plant design inherent safety

The NuScale plant design offers significant severe accident mitigation features. First, each module has a smaller fuel inventory than a traditional reactor and therefore has a reduced source term. The containment vacuum eliminates the need for combustible gas control inside containment since there is little or no oxygen. The steel containment immersed in a stainless steel lined pool eliminates the potential for molten concrete coolant interactions. The ability to reliably equilibrate containment and reactor pressure prevents the possibility of a high pressure corium melt ejection. Lastly, the NuScale plant builds on defence in depth by including additional fission product barriers. As with conventional large light water designs, the fuel pellet, cladding, reactor vessel, and containment prevent transport of fission products to the outside atmosphere. The NuScale design provides additional barriers which further reduce the potential for severe accident releases, including: the containment cooling pool, the stainless steel lined containment pool structure, biological shield, and finally the reactor building.

5. SUMMARY

Reliable safety systems play an essential role in mitigating the effects of an accident scenario. In the currently operating reactor fleet, core decay heat removal is largely performed by active safety systems, such as safety injection pumps or feedwater pumps, which rely on a continuous supply of electricity. In events which may render these active systems inoperable, alternative options should be in place. One way in which many reactors can continue core heat removal is by supplying active safety systems with electricity from on-site emergency generators; however, as demonstrated at Fukushima by damage to and failure of these generators, this is not a perfect solution. Advanced water cooled reactor designs take steps to improve safety system reliability for accident scenarios through the use of passive safety systems.

Advanced reactor designs apply passive safety concepts to reduce the need for external power or operator action in accident events. Many passive phenomena utilized in these safety systems are inherent to generic reactor design and operation. For example, natural circulation forces are present within the primary coolant loop of PWRs due to the system's pressure and temperature distribution; however, the observable effect during normal reactor operation is relatively small as it is typical for coolant pumps to operate with significantly greater force. This natural circulation flow becomes a dominant mechanism upon events such as station blackout and continues to remove core decay heat without any external power or operator action. In addition to these inherent passive mechanisms, safety systems such as natural circulation cooling loops or gravity drain tanks can be implemented in a reactor design to take advantage of energy stored in the system (e.g. pressure differences, gravity). Many passive safety systems make use of partially active components; for example, valves which receive an emergency signal to open and complete a natural circulation loop or to inject coolant. Because passive safety systems utilize natural forces and existing energy, with limited active components, they operate with high reliability.

Despite this reliable nature when compared to active safety systems, the design and implementation of passive safety systems face many challenges. The driving forces behind passive systems such as natural circulation, gravity, and evaporation are often weaker than their active counterparts (e.g. safety injection pumps, feedwater pumps). Additionally, many passive safety system designs included in advanced WCRs still rely on a continual supply of working fluids, such as coolant water which may be lost during operation, and thus only function for a limited time. Beyond these technical challenges, the integration of passive safety systems into reactor designs faces administrative and regulatory challenges. Many of these system designs have yet to accumulate significant operational experience and their effectivity and reliability are difficult to quantify. These issues are major barriers to the design, licensing, and construction of passively safe, enhanced reliability reactors.

Regardless of these challenges, passive safety systems yield enough benefits for their application and further development. Passive safety systems are seeing wide use in many new reactor designs and will likely play a major role in the advancement of the nuclear energy industry in the years to come.

Appendix I

PCTRAN TWO-LOOP PWR SIMULATOR

I.1. INTRODUCTION

PCTRAN is a basic principle reactor simulator of a generic conventional two-loop PWR plant. It is one of a series of simulators available from the IAEA for Member State use in training and education. Access can be requested through the IAEA simulator website [73]. A brief overview of the simulator is given in the website, and a user manual is available online for download [74]. An additional IAEA Training Course Series publication on the PCTran Two-loop PWR Simulator, with exercises, is available [75].

The following assumes the user is familiar with the basic operation of the PCTran simulator. Users should refer to the aforementioned literature for basic instruction and additional exercises.

The plant simulated by PCTran is of conventional design. As a result, few passive safety systems are included. Of note, however, are accumulators. In addition to this, natural circulation flow may be established in the reactor coolant system in certain accident scenarios.

This exercise demonstrates a cold leg LBLOCA accident, which highlights the functionality of accumulators and natural circulation. LBLOCAs are considered to be a DBA for PWRs. This particular simulation is that of a 'double ended guillotine break', in which a cold leg pipe connection is entirely severed and water is discharged freely. It should be noted that active systems remain operational for this simulation.

I.2. DEMONSTRATION

- (1) Load initial condition #1 (100% POWER EOC).

Initial condition #2 (100% POWER MOC) or #3 (100% POWER BOC) may also be used, and exhibit slightly different behaviour, however figures and plots in this demonstration were created using initial condition #1.

- (2) Run the simulator for about 5 seconds to achieve a steady state condition.
- (3) 'Freeze' the simulator.
- (4) Select malfunction #2 with a 2800 failure fraction and set to 'active'.

Malfunction #2 is a cold leg LBLOCA. The 2800 failure fraction will result in a 2800 cm² break in the cold leg.

- (5) Manually trip the reactor coolant pumps.

By tripping the pumps, coolant loss through the break is minimized. Reactor operators would typically perform this step as a manual response to a LOCA.

(6) Resume the simulator and observe the system response to the break.

A rupture appears in cold leg A, and a coolant loss rate in t/hr is now shown. The reactor coolant system pressure drops rapidly, as shown in FIG. 73, and the pressurizer water level decreases. This rapid loss of coolant is the 'blowdown' phase. Reactor building temperature and pressure increase as coolant escapes, initiating reactor building sprays once pressure reaches the setpoint at 1.3 bar. Escaped water begins to accumulate in the sump. Water level drops in the coolant system, uncovering the reactor core. Fuel temperature begins to rise. The reactor trips due to low pressure in the pressurizer, followed by a turbine trip.

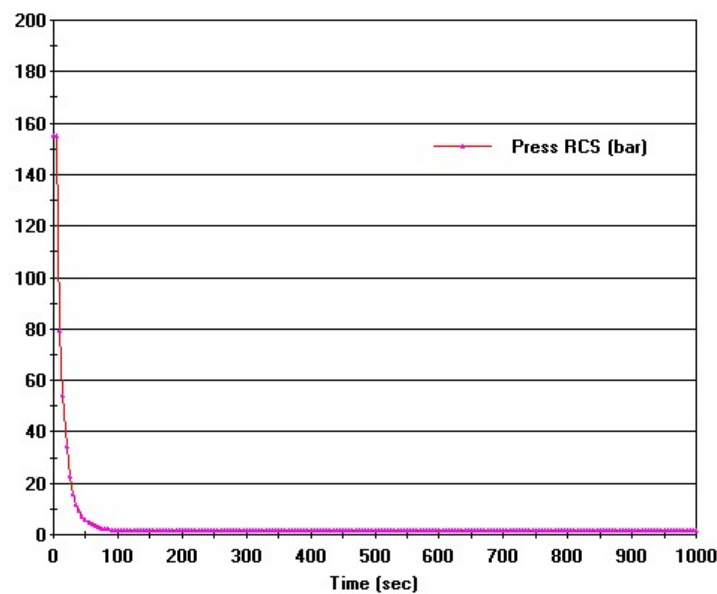


FIG. 73. Reactor coolant system pressure (bar).

The ECCS responds to coolant pressure dropping below the setpoint of 129.6 bar by starting high pressure injection pumps. The amount of water provided by the high pressure injection is not enough to compensate for the water losses through the break. Pressure continues to fall and the accumulator begins functioning once the pressure drops below the nitrogen pressure of 44.32 bar in the accumulator tank. The low pressure injection system begins operating once pressure drops below the 11.3 bar setpoint.

Once all three of these systems are operating, the reactor begins to successfully refill. FIG. 74 shows the uncovered core with ECCS operating, and FIG. 75 shows recovery of the core. These are the 'refill' and 'reflood' phases of the accident. Once water level stabilizes (at the height of the leaking cold leg), long term cooling is provided by natural circulation driving ECCS water through the core and fuel temperature stops rising. FIG. 74 shows the stabilization of leak rate and ECCS injection rate, resulting in the state shown in FIG. 76. FIG. 77 shows the fuel temperature rapidly dropping as a result of the reactor trip, but rising briefly as the core is uncovered before stable cooling is provided by natural circulation flow. As time progresses, the ECCS drains the water tank and switches to sump recirculation.

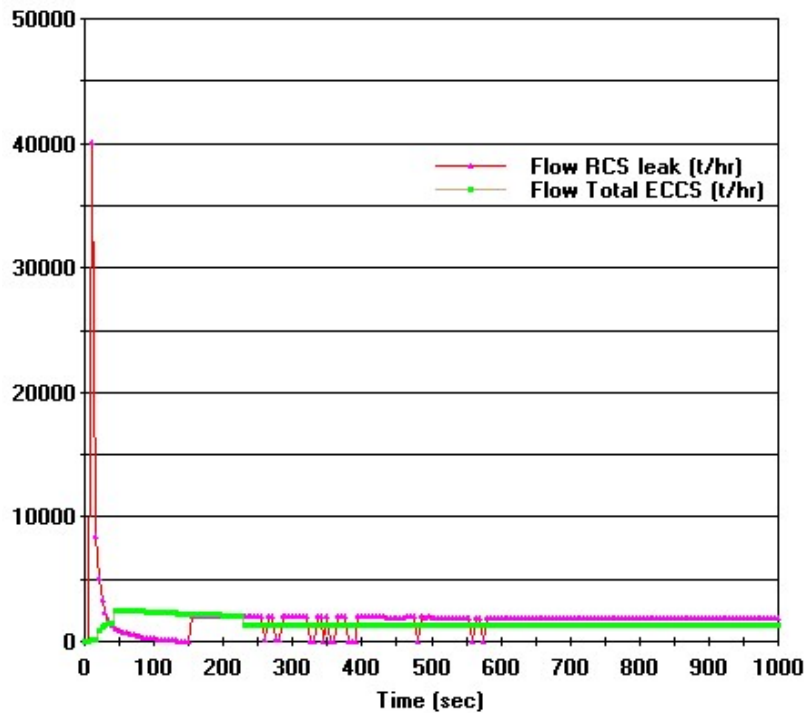


FIG. 74. Reactor coolant leaking rate and total ECCS flow rate (t/hr).

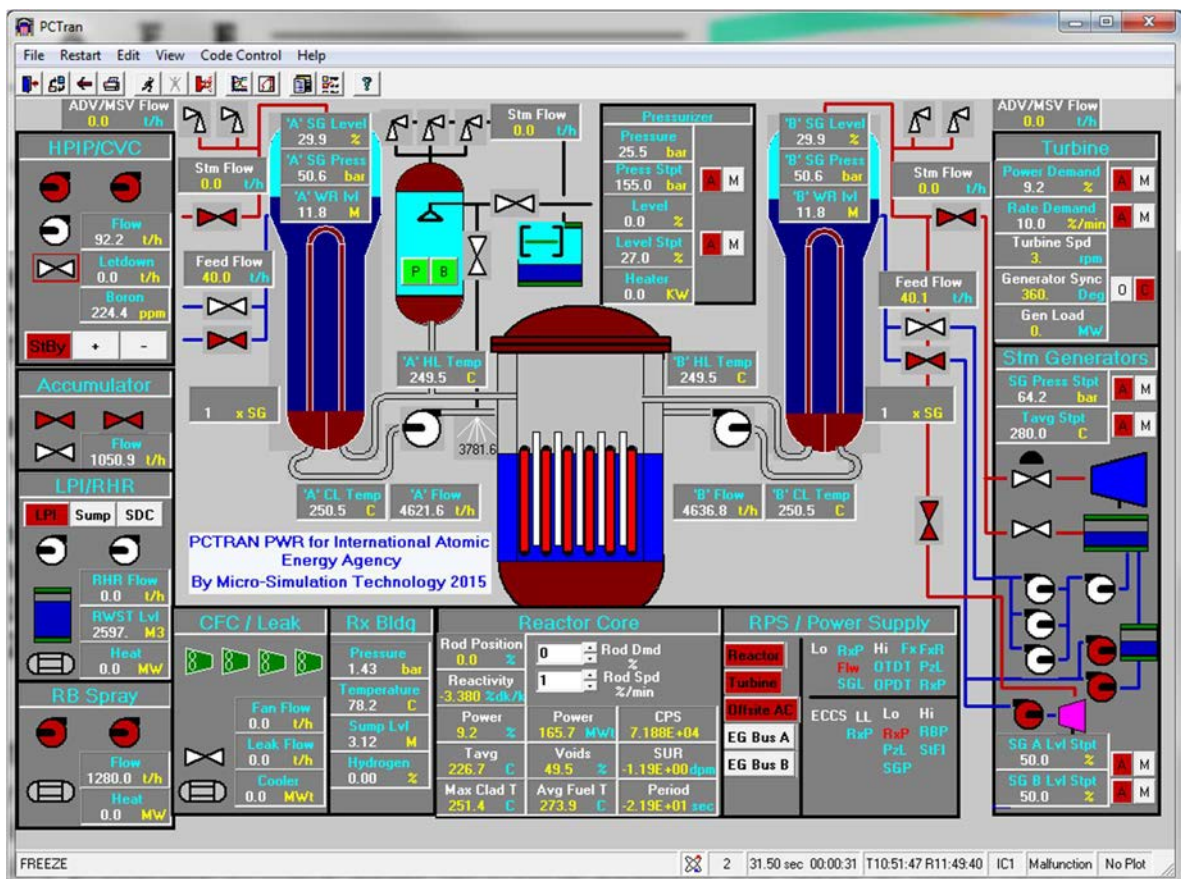


FIG. 75. Reactor core uncovering, accumulators and reactor building spray operational.

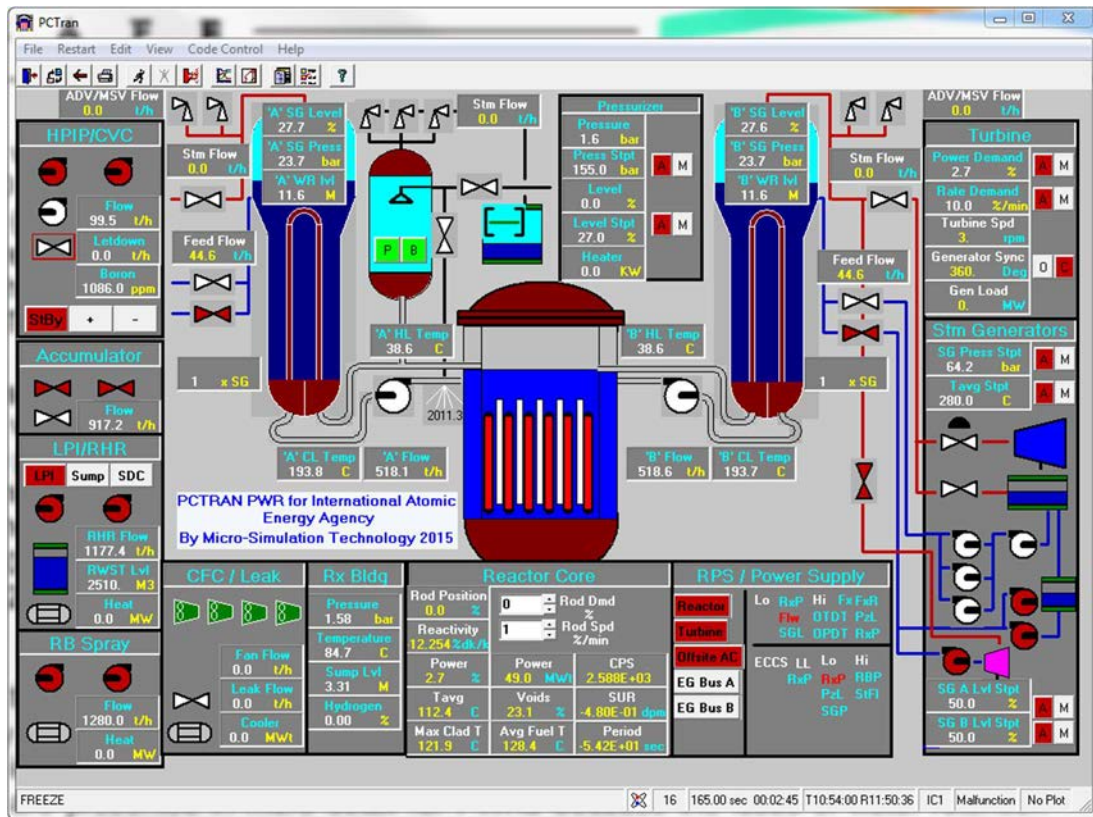


FIG. 76. Water level stabilized, cooling provided by natural circulation flow.

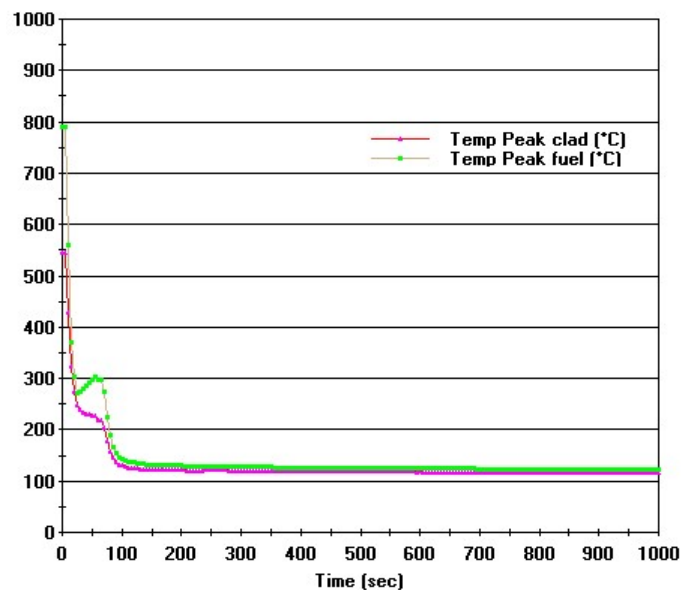


FIG. 77. Peak fuel and cladding temperatures (°C).

There are a few considerations that are either non-observable or not simulated in PCTRAN. In a typical LBLOCA, ECCS water may be blocked by reverse flowing steam from the downcomer annulus for some time following the blowdown phase. The period of time which it is blocked is the 'bypass' phase. The refill phase refers to the filling of the lower plenum following the bypass phase, where the reflood phase is the actual recovering of the core. Because there is no bypass phase, and there is no visible refilling of the lower plenum, the refill and reflood phases are indistinguishable.

Appendix II

ADVANCED PASSIVE PWR SIMULATOR

II.1. INTRODUCTION

The Advanced Passive PWR Simulator is a basic principle reactor simulator based on a 600 MW(e) advanced PWR design. The simulated reactor is similar to the AP-600 design, though with some differences. It is one of a series of simulators available from the IAEA for Member State use in training and education. Access can be requested through the IAEA simulator website [73]. A brief overview of the simulator is given in the website, and a user manual is available online for download [76].

The following exercise assumes the user is familiar with the basic operation of the Advanced Passive PWR Simulator. Users should refer to the aforementioned literature for basic instruction and additional exercises.

The Advanced Passive PWR Simulator utilizes several passive safety systems. These include accumulators, core makeup tanks, a PRHR system, an in-containment refuelling water storage tank (IRWST), a sump recirculation path, and a PCCS.

This exercise demonstrates a cold leg LOCA. In addition to accumulators, which are common in conventional designs, this accident highlights several passive heat removal systems used in advanced reactor designs. Active systems are left operable for the following example.

II.2. DEMONSTRATION

- (1) Load 'Full Power' initial condition.
- (2) Load 'RC Cold Leg #4 LOCA Break' malfunction.
- (3) Run the simulator.

Immediately a rupture appears in cold leg #4. Coolant drains out of the reactor, and the accumulator begins to operate. Though the accumulators do slow the loss of coolant inventory, it is unable to keep up with the loss from the break. As a result, pressure continues to drop until the low liquid level in the pressurizer reaches a setpoint. At this point, the reactor is scrammed, valves to the PRHR removal inlet valves are opened, core makeup tank outlet valves are opened, steam generators are isolated, and coolant pumps are tripped. In this process, several natural circulation loops allowing passive heat removal have been opened.

The PRHR exchanger allows coolant to naturally circulate to a heat exchanger submerged in the an IRWST. Over time this leads to evaporation within the IRWST.

The core makeup tanks use a natural circulation loop to provide additional, borated coolant to the system. Over time, these core makeup tanks will also drain over time.

FIG. 78 shows the simulator in the condition where these passive processes are operable. Flow through both the PRHR and the two core makeup tanks is observable, and further water supply can be seen from the accumulators and active systems.

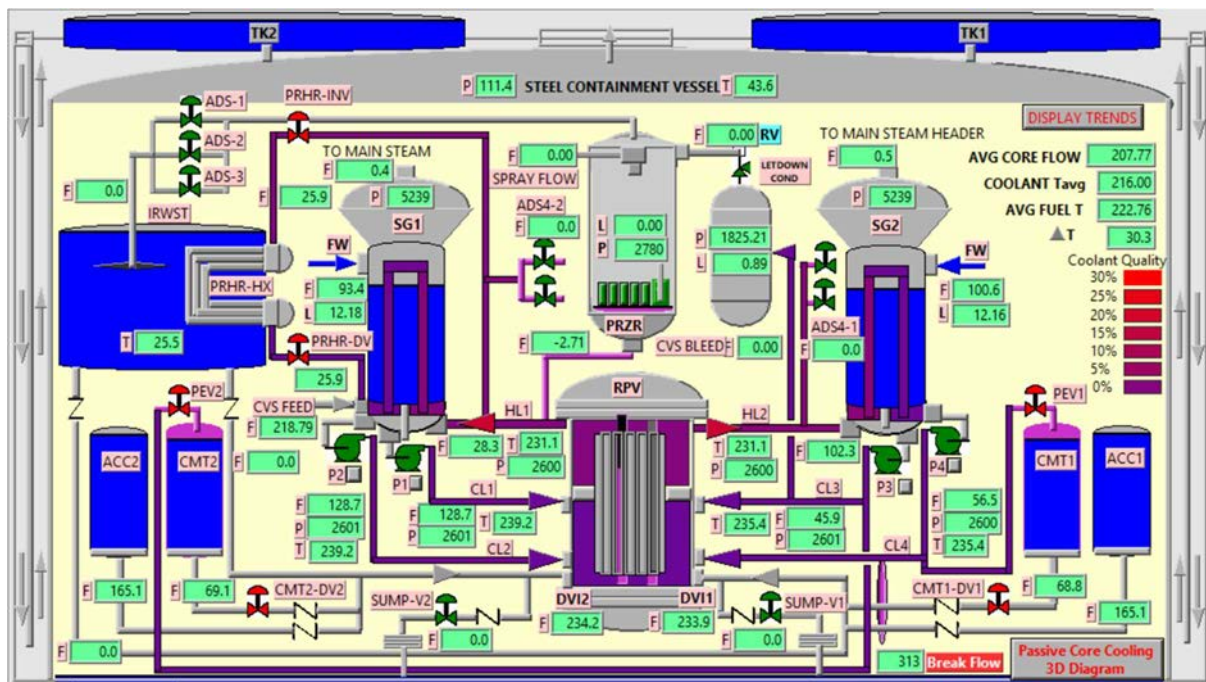


FIG. 78. System status following low pressurizer level signal.

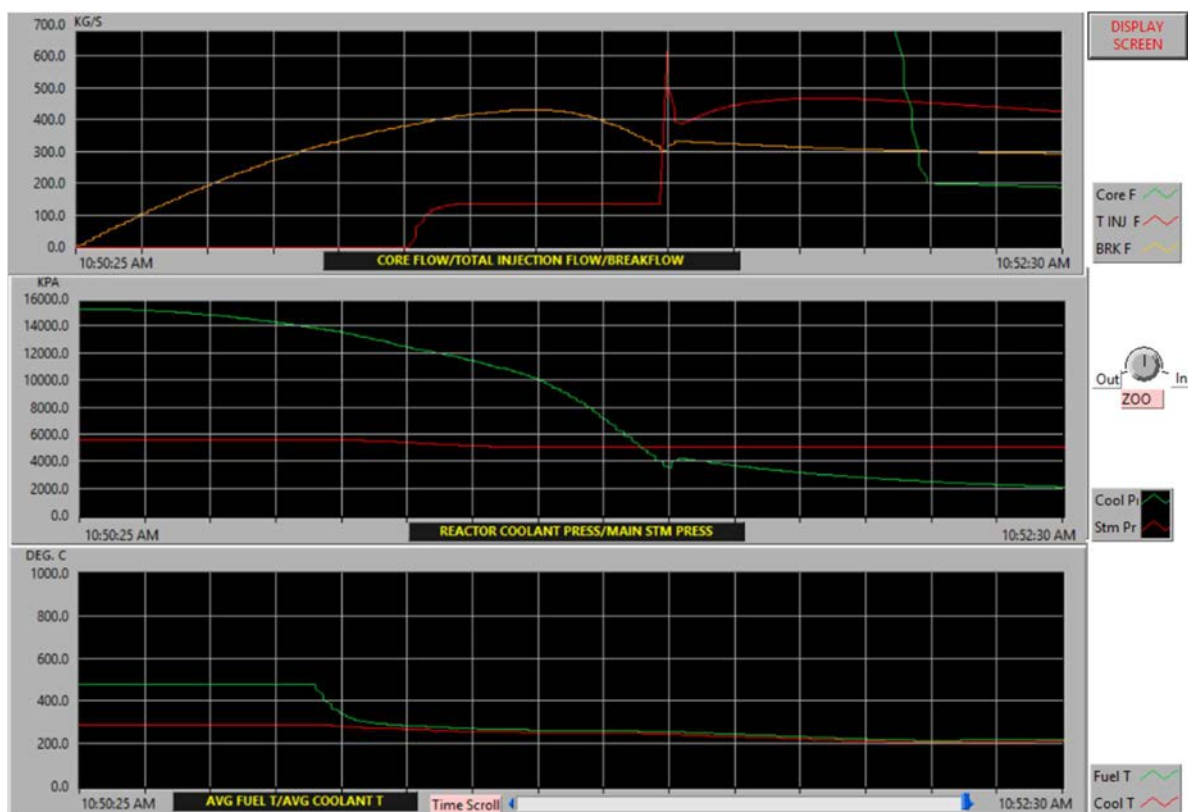


FIG. 79. Passive core cooling screen.

FIG. 79 show various flow rates, the reactor coolant and main steam pressure, and the fuel and coolant temperatures up to this point. The coolant pressure can be seen to drop until safety systems start to supply coolant. The fuel temperature can be seen dropping where the reactor was scrammed. Injection flow can be seen at a stable rate from the accumulator, and once pressure reaches a low setpoint, other safety systems kick in to provide additional injection. Core flow can be seen dropping and will continue at a relatively steady rate as natural circulation flow stabilizes the decay heat removal process.

The reactor reaches a stable coolant level during operation of all of these systems. However, over time the accumulators and core makeup tanks will drain. FIG. 80 shows a later progression of the accident at a point where the accumulators have drained and core makeup tank flow is being reduced. Fuel temperatures have additionally increased, but so has the flow through the PRHR system. Water has been visibly accumulated in the sump region of the containment vessel and will recirculate water on further draining of coolant. Once all other systems have reached a low water level, a stable natural circulation flow may be established between the sump and IRWST.

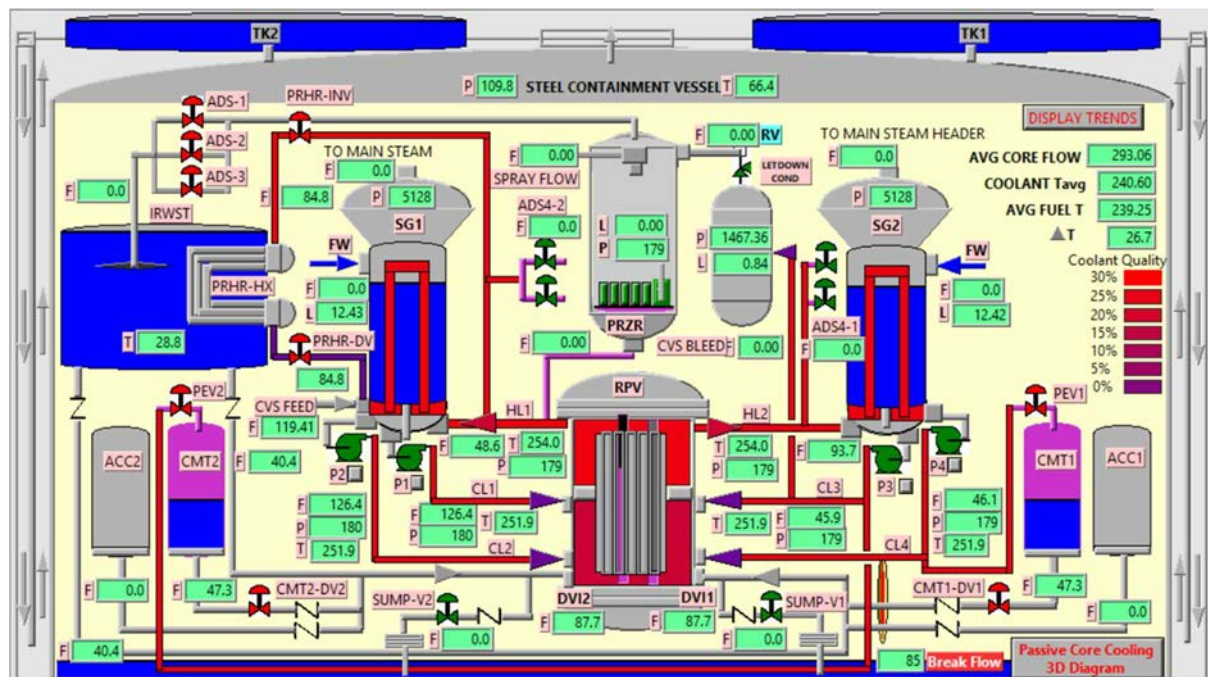


FIG. 80. System status following extensive makeup injection.

Some additional safety features can be observed in the simulator which were not visibly used in this simulation. One notable example is the spray system. Above the containment vessel are two large spray storage tanks, which may be used to cool the outside of the containment vessel. Additionally, an air flow path for natural circulation can be seen around the edges of FIG. 80. Air comes in from the sides, flows past the containment vessel, and flow out the top of the structure.

Appendix III

INTEGRAL PRESSURIZED WATER REACTOR SIMULATOR

III.1. INTRODUCTION

The Integral Pressurized Water Reactor (iPWR) simulator is a basic principle reactor simulator of an SMR design. It is one of a series of simulators available from the IAEA for Member State use in training and education. Access can be requested through the IAEA simulator website [73]. A brief overview of the simulator is also given in the website. An IAEA Training Course Series publication describing the operation of the iPWR simulator, and an accompanying exercise booklet, have been published and are available online from [77] and [78].

The following exercise assumes the user is familiar with the basic operation of the iPWR simulator. Users should refer to the aforementioned literature for basic instruction and additional exercises.

The iPWR reactor features several passive systems. Those which are important for this demonstration are the passive decay heat removal (PDHR) system, two accumulators, and the gravity injection system (GIS).

This exercise demonstrates a large steam generator tube rupture. In this accident, coolant is able to flow from the primary to the secondary system.

III.2. DEMONSTRATION

- (1) Load initial condition #1 (100% BOL natural circulation).
- (2) Load 'Steam generator tube failure 1' malfunction (SM-MSS-2), severity = 100.0%.
- (3) Run the simulator.

Immediately, a high radiation alarm (¹⁶N in the main steam system under the 'Systems' tab) sounds in response to primary coolant water leaking into secondary. Coolant system pressure drops, lowering the water level in the pressurizer. After approximately a minute and a half, a reactor trip occurs, followed by a turbine trip. Steam no longer flows to the turbine, and flow to the condenser system increases. FIG. 81 shows the ¹⁶N radiation alarm, reactor and turbine trips, low steam flow to the turbine, and increased flow to condensers in comparison to normal conditions.

Reactor coolant pressure continues to drop, actuating the ADS once below 9.00 MPa. The rapid depressurization allows low pressure systems (e.g. accumulators and gravity injection system) to maintain coolant level.

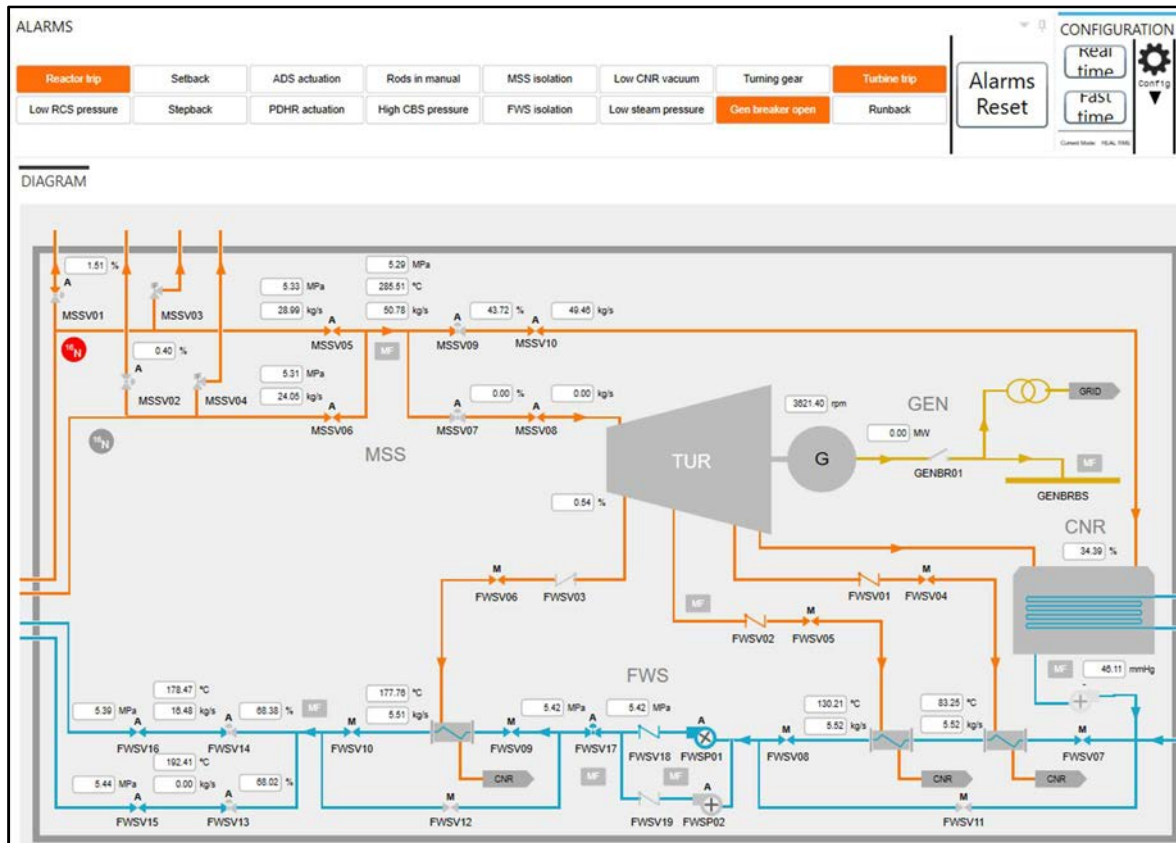


FIG. 81. Main steam and condenser systems following main steam line break.

(4) Manually actuate the PDHR system and observe the system responses.

The PDHR is the same as the PRHR system described in the main text. Actuating the passive decay heat removal system isolates the feedwater lines. Valves to the PDHR open, creating flow loops for heat removal. Feedwater isolation valves close. The main steam system is isolated when its pressure falls below 2.5 MPa and the decay heat removal system is operating.

With the isolation of the main steam system, the reactor is provided by natural circulation in the PDHR alone and no more coolant is lost through the steam generator rupture. As a result, reactor coolant pressure stabilizes, and the temperature in the PDHR cooling pool (heat sink) rises. FIG. 82 shows the flow, caused by natural circulation, through the PDHR system and increased (compared to normal operating) pool temperature.

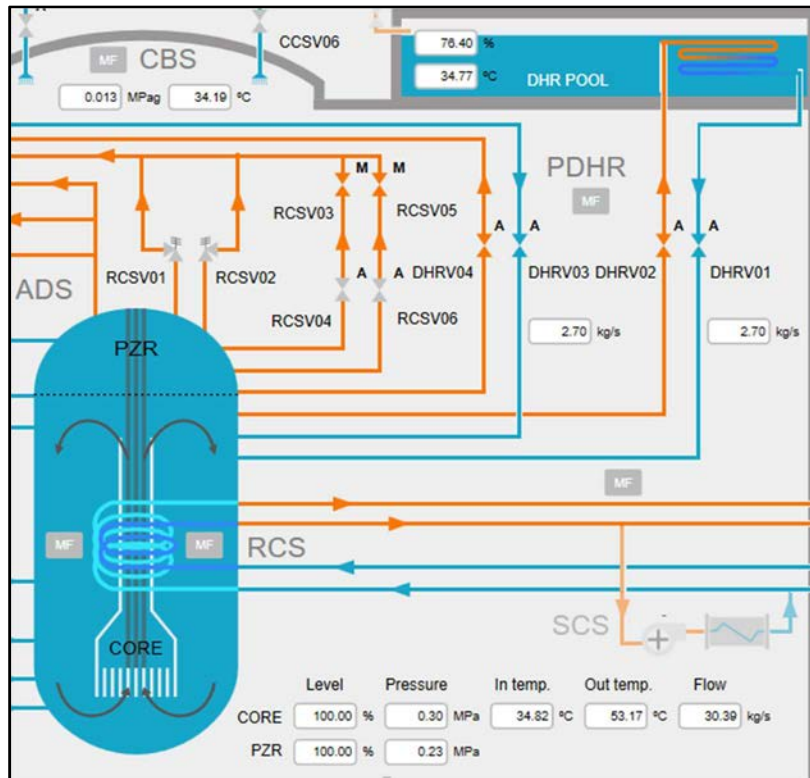


FIG. 82. PDHR system operating under natural circulation flow.

When coolant pressure falls below 5.0 MPa, the accumulators add to the coolant inventory. The GIS, or elevated gravity drain tank as described in the main text, actuates when coolant pressure falls below 0.5 MPa. FIG. 83 shows the now emptied accumulators and the now operating GIS.

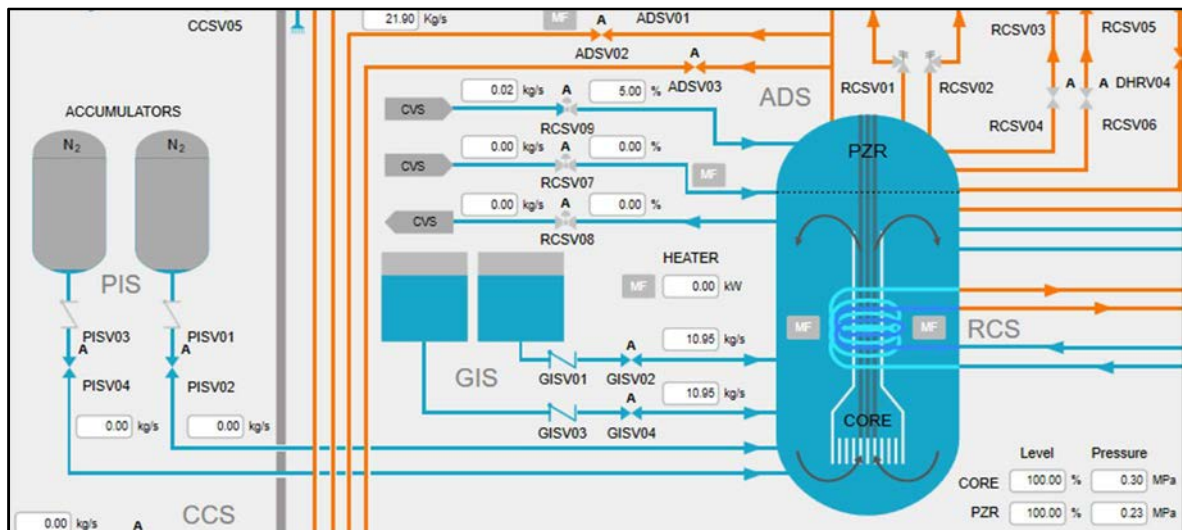


FIG. 83. Accumulators and GIS.

The reactor remains shutdown as a result of the insertion of control rods during the trip, and fuel temperature is stabilized by the natural circulation loop of the PDHR.

REFERENCES

- [1] INTERNATIONAL ATOMIC ENERGY AGENCY, Terms for Describing New, Advanced Nuclear Power Plants, IAEA-TECDOC-936, IAEA, Vienna (1997).
- [2] SHULTZ, J.K., FAW, R.E., Fundamentals of Nuclear Science and Engineering Second Edition, CRC Press, Boca Raton (2008).
- [3] NUCLEAR REGULATORY COMMISSION, Pressurized Water Reactors, <https://www.nrc.gov/reactors/pwrs.html>
- [4] INTERNATIONAL ATOMIC ENERGY AGENCY, Advanced Reactor Information System (ARIS) Database.
- [5] NUCLEAR REGULATORY COMMISSION, Boiling Water Reactors, <https://www.nrc.gov/reactors/bwrs.html>
- [6] INTERNATIONAL ATOMIC ENERGY AGENCY, Design Safety Considerations for Water Cooled Small Modular Reactors Incorporating the Lessons Learned from the Fukushima Daiichi Accident, IAEA-TECDOC-1785, IAEA, Vienna (2016).
- [7] INTERNATIONAL ATOMIC ENERGY AGENCY, Advances in Small Modular Reactor Technology Developments 2016 Edition, IAEA, Vienna (2016).
- [8] WESTINGHOUSE ELECTRIC COMPANY LLC., ML113560390, Federal Register Notice - AP1000 Design Certification Amendment, 10 CFR Part 52 (RIN 3150-AI81) NRC-2010-0131, (2011).
- [9] INTERNATIONAL ATOMIC ENERGY AGENCY, Development and Application of Level 1 Probabilistic Safety Assessment for Nuclear Power Plants, IAEA Safety Standards Series No. SSG-3, IAEA, Vienna (2010).
- [10] BUCKNOR M., GRABASKAS, D., BRUNETT, A. J., GRELLE, A., Advanced reactor passive system reliability demonstration analysis for an external event, Nucl. Eng. Tech. **49** (2017) 360, 372.
- [11] INTERNATIONAL ATOMIC ENERGY AGENCY, Operational Limits and Conditions and Operating Procedures for Nuclear Power Plants, IAEA Safety Standards Series No. NS-G-2.2, IAEA, Vienna (2000).
- [12] INTERNATIONAL ATOMIC ENERGY AGENCY, Safety Margins of Operating Reactors, Analysis of Uncertainties and Implications for Decision Making, IAEA-TECDOC-1332, IAEA, Vienna (2003).
- [13] INTERNATIONAL ATOMIC ENERGY AGENCY, Safety of Nuclear Power Plants: Design, Safety Standards Series No. SSR-2/1 (Rev.1), IAEA, Vienna (2016).
- [14] NUCLEAR REGULATORY COMMISSION, NRC Backgrounder on the Three Mile Island Accident.
- [15] NUCLEAR REGULATORY COMMISSION, TMI-2 Core End-State Configuration (2007).
- [16] ELECTRIC POWER RESEARCH INSTITUTE, Analysis of Three Mile Island – Unit 2 Accident, EPRI-NSAC--80-1, EPRI, Palo Alto (1980).
- [17] INTERNATIONAL ATOMIC ENERGY AGENCY, The Fukushima Daiichi Accident, Technical Volume 1/5: Description and Context of the Accident, IAEA, Vienna (2015).
- [18] INTERNATIONAL ATOMIC ENERGY AGENCY, The Fukushima Daiichi Accident, Report by the Director General, IAEA, Vienna (2015).
- [19] INTERNATIONAL ATOMIC ENERGY AGENCY, Natural Circulation Phenomena and Modelling for Advanced Water Cooled Reactors, IAEA-TECDOC-1677, IAEA, Vienna (2012).
- [20] INTERNATIONAL ATOMIC ENERGY AGENCY, Natural Circulation in Water Cooled Nuclear Power Plants, IAEA-TECDOC-1474, IAEA, Vienna (2005).

- [21] ISHII, M., HIBIKI, T., Thermo-Fluid Dynamics of Two-Phase Flow, 2nd edition, Springer-Verlag, New York (2011).
- [22] YADIGAROGLU, G., HEWITT, G.F. (Eds), Introduction to Multiphase Flow, Basic Concepts, Applications and Modelling, Springer International Publisher, (2018).
- [23] ISHII, M., Thermo-fluid Dynamic Theory of Two-phase Flow, Eyrolles, Paris (1974).
- [24] ISHII, M., MISHIMA, K., Two-fluid model and hydrodynamic constitutive relations, Nucl. Eng Des. **82** (1984) 107, 126.
- [25] TODREAS, N.E., KAZIMI, M.S., Nuclear Systems I Thermal Hydraulic Fundamentals, Taylor and Francis, Milton Park (1993).
- [26] RANSOM, V.H., HICKS, D.L., Hyperbolic two-pressure models for two-phase flow, J. Comp. Phys. **53** (1984) 124, 151.
- [27] ZUBER, N., FINDLAY, J.A., Average volumetric concentration in two-phase flow systems, J. Heat Transf. **87** (1965) 453.
- [28] THEOFANOUS, T.G., NOURBAKHS, H.P., GHERSON, P., IYER, K., Decay of Buoyancy Driven Stratified Layers with Applications to Pressurized Thermal Shock (PTS), NUREG/CR-3700, U.S. Nuclear Regulatory Commission, (1984).
- [29] REYES, J., A transition criterion for the onset of slugging or mixing in horizontal conduits, Experimental Heat Transfer, Fluid Mechanics, and Thermodynamics 2001, Vol. 2, Eddizoni ETS, Pisa (2001).
- [30] FANNING, M.W., ROTHE, P.H., Transient Cooldown in Model Cold Leg and Downcomer, Interim Report EPRI NP-3118, Electric Power Research Institute, Palo Alto (1983).
- [31] VALENZUELA, J.A., DOLAN, F.X., Thermal and Fluid Mixing in a 1/2 –Scale Test Facility, NUREG/CR-3426, U.S. Nuclear Regulatory Commission, (1985).
- [32] THEOFANOUS, T.G., IYER, K., NOURBAKHS, H.P., GHERSON, P., Buoyancy effects of overcooling transients calculated for the NRC pressurized thermal shock study, driven stratified layers with applications to pressurized thermal shock (PTS), NUREG/CR-3702, U.S. Nuclear Regulatory Commission, (1986).
- [33] ROUSE, H., YIH, C.S., HUMPHREYS, H.W., Gravitational convection from a boundary source, Tellus **4** (1952) 201, 210.
- [34] BATCHELOR, G.K., Heat convection and buoyancy effects in fluids, Q. J. R. Meteorol. Soc. **80** (1954) 339, 358.
- [35] MORTON, B.R., Forced plumes, J. Fluid Dyn. **5** (1959) 151, 163.
- [36] TURNER, J.S., Buoyancy Effects in Fluids, Cambridge University Press, Cambridge (1979).
- [37] MORTON, B.R., TAYLOR, G., TURNER, J.S., Turbulent gravitational convection from maintained and instantaneous sources, Proc. R. Soc. Lond. A **234** (1956) 1, 23.
- [38] CHEN, C.J., RODI, W., Vertical Turbulent Buoyant Jets: A Review of Experimental Data, HMT, Vol. 4, Pergamon Press, New York (1980).
- [39] RODI, W., Turbulent Buoyant Jets and Plumes, HMT, Vol. 6, Pergamon Press, New York (1982).
- [40] YER, K. NOURBAKHS, H.P., THEOFANOUS, T.G., REMIX: A computer program for temperature transients due to high pressure injection after interruption of natural circulation, NUREG/CR-3701, Purdue University, U.S. Nuclear Regulatory Commission, (1986).
- [41] KOTSOVINOS, N.E., Plane Turbulent Buoyant Jets, PhD. Thesis, Calif. Inst. Technol. (1975).
- [42] BESTION, D., et al., Recommendation on Use of CFD Codes for Nuclear Reactor Safety Analysis, ECORA, (2004).
- [43] APSLEY, D., Introduction to CFD, (2008).

- [44] TU, J., et al., Computational Fluid Dynamics- A Practical Approach, Butterworth Heinemann, Oxford (2008).
- [45] BIRD, R., STEWART, W., LIGHTFOOT, E., Transport Phenomena, John Wiley & Sons Inc., Hoboken (2007).
- [46] BLAZEK, J., Computational Fluid Dynamics: Principles and Applications, Elsevier, New York (2001).
- [47] OBERKAMPF, W.L., TRUCANO, T.G., Verification and validation in computational fluid dynamics, Prog. Aerosp. Sci. **38** (2002) 209, 272.
- [48] HOFFMAN, K.A., CHIANG, S.T., Computational Fluid Dynamics, Vol. 3, Engineering Education System, Wichita (2000).
- [49] ANSYS, ANSYS Fluent Theory Guide, Canonsburg (2013).
- [50] SPALART, P.R., JOU, W.H., STRELETS, M., ALLMARAS, S.R., “Comments on the Feasibility of LES for Wings and on a Hybrid RANS/LES Approach”, paper presented at 1st AFOSR Int. Conf. on DNS/LES, Ruston, 1997.
- [51] STENMARK, E., On Multiphase Flow Models in ANSYS CFD Software, MS Thesis, Chalmers Univ. Technol. (2013).
- [52] NUCLEAR ENERGY AGENCY, Extension of CFD Codes Application to Two Phase Flow Problems, NEA/CSNI/R(2010)2, Organisation for Economic Co-operation and Development, Paris (2010).
- [53] LUCAS, D., et al., An overview of the pressurized thermal shock issue in the context of the NURESIM project, Sci. Tech. Nucl. Install. **2009** (2009).
- [54] LEYSE, M., Preventing Hydrogen explosions in Severe Nuclear Accidents, R:14-02-B, The Natural Resources Defense Council, New York (2014).
- [55] NUCLEAR ENERGY AGENCY, Assessment of CFD Codes for Nuclear Reactor Safety Problems, NEA/CSNI/R(2014)12, Organisation for Economic Co-operation and Development, Paris (2015).
- [56] LI, S.Q., et al., CFD based approach for modelling steam-water direct condensation in sub-cooled water flow in tee junction, Prog. Nucl. Energy **85** (2015) 729, 746.
- [57] NAWAZ, R., Numerical Investigation of Hydrogen Distribution in Advanced NPP Containment Using FLUENT, MS Thesis, Pak. Inst. Eng. Appl. Sci. (2015).
- [58] HOUKEMA, M., SICCAM, N.B., KOMEN, E.M.J., VISSER, D.C., Validation of a FLUENT CFD model for hydrogen distribution in a containment, Nucl. Eng. Des. **245** (2012) 161, 171.
- [59] ALI, M., YAN, C., SUN, Z., GU, H., MEHBOOB, K., Dust particle removal efficiency of a venturi scrubber, Ann. Nucl. Energy **54** (2013) 178, 183.
- [60] AHMED, S., Numerical Computation of Dust Particle Removal Efficiency in a Self-priming Venturi Scrubber, MS Thesis, Pak. Inst. Eng. Appl. Sci. (2016).
- [61] PAK, S., CHANG, K., Performance estimation of a venturi scrubber using a computational model for capturing dust particles with liquid spray, J. Hazard. Mater. **138** 3 (2006) 560, 573.
- [62] ALI, M., YAN, C., SUN, Z., GU, H., WANG, J., MEHBOOB, K., Iodine removal efficiency in non-submerged and submerged self-priming venturi scrubber, Nucl. Eng. Technol. **45** 2 (2013) 203, 210.
- [63] ASHFAQ, T., Mass Transfer Investigation of Iodine in Venturi Scrubbing Solution of Filtered Containment Venging System, MS Thesis, Pak. Inst. Eng. Appl. Sci. (2017).
- [64] SHAH, A., CHUGHTAI, I.R., INAYAT, M.H., Numerical simulation of direct-contact condensation from a supersonic steam jet in subcooled water, Chin. J. Chem. Eng. **18** (2010) 577, 587.
- [65] NADEEM, A.M., Parametric Study for Jacketed Heat Exchanger used in Scrubber Tank using CFD, MS Thesis, Pak. Inst. Eng. Appl. Sci. (2017).

- [66] INTERNATIONAL ATOMIC ENERGY AGENCY, Fundamental Safety Principles, Safety Standards Series No. SF-1, IAEA, Vienna (2006).
- [67] INTERNATIONAL ATOMIC ENERGY AGENCY, Safety Assessment for Facilities and Activities, Safety Standards Series No. GSR Part 4 (Rev. 1), IAEA, Vienna (2016).
- [68] INTERNATIONAL NUCLEAR SAFETY ADVISORY GROUP, Defence in Depth in Nuclear Safety, 75-INSAG-3 Rev. 1, INSAG-10, IAEA, Vienna (1996).
- [69] INTERNATIONAL NUCLEAR SAFETY ADVISORY GROUP, Basic Safety Principles for Nuclear Power Plants, INSAG-12, IAEA, Vienna (1999).
- [70] INTERNATIONAL ATOMIC ENERGY AGENCY, Advanced Applications of Water Cooled Nuclear Power Plants, IAEA-TECDOC-1584, IAEA, Vienna (2008).
- [71] INTERNATIONAL ATOMIC ENERGY AGENCY, Safety Related Terms for Advanced Nuclear Plants, IAEA-TECDOC-626, IAEA, Vienna (1991).
- [72] INTERNATIONAL ATOMIC ENERGY AGENCY, Passive Safety Systems and Natural Circulation in Water Cooled Nuclear Power Plants, IAEA-TECDOC-1624, IAEA, Vienna (2009).
- [73] INTERNATIONAL ATOMIC ENERGY AGENCY, Nuclear Reactor Simulators for Education and Training.
- [74] MICRO-SIMULATION TECHNOLOGY, PCTran Personal Computer Transient Analyzer For a Two-loop PWR and TRIGA Reactor, USA (2011).
- [75] INTERNATIONAL ATOMIC ENERGY AGENCY, PCTran Generic Pressurized Water Reactor Simulator Exercise Handbook, Training Course Series 68, IAEA, Vienna (2019).
- [76] CASSIOPEIA TECHNOLOGIES INC., Advanced Pressurized Water Reactor Simulator User Manual, Canada (2011).
- [77] INTERNATIONAL ATOMIC ENERGY AGENCY, Integral Pressurized Water Reactor Simulator Manual, Training Course Series 65, IAEA, Vienna (2017).
- [78] INTERNATIONAL ATOMIC ENERGY AGENCY, Integral Pressurized Water Reactor Simulator Manual: Exercise Handbook, Training Course Series 65, IAEA, Vienna (2017).

Annex

OVERVIEW OF RELATED IAEA LITERATURE

A-1. INTRODUCTION

The following IAEA publications provide useful reference and further information on passive safety, natural circulation, and training/education with basic principle simulators. Many of the listed publications were used as sources for the creation of this Training Course Series. These may be useful for extending taught lessons either in further detail or in a somewhat broader scope than this publication alone. Summaries are included to provide a basic overview of the content of each publication.

A-2. IAEA-TECDOC-1474: NATURAL CIRCULATION IN WATER COOLED NUCLEAR POWER PLANTS

This publication was developed as a part of the coordinated research project on Natural Circulation Phenomena, Modelling and Reliability of Passive Systems that Utilize Natural Circulation, launched in 2004. It provides detailed information on the phenomena, modelling, and experiments which are used in support of the design and analysis of natural circulation systems. Provided is an overview of advanced reactors, with examples of natural circulation systems in advanced designs, followed by a listing of the advantages of using and challenges facing the use of natural circulation systems. Further presented are the governing equations for natural circulation flow, an overview of the analysis tools used, and a description of several experimental natural circulation test facilities. The main publication gives a high level overview of natural circulation flow, though supports this with specific system and facility examples. However, this publication includes 22 annexes of additional material, presented at the IAEA training course on Natural Circulation in Water Cooled Reactors, which provide detailed studies and descriptions of natural circulation flow. These annexes provide a significant amount of information from individual Member States in support of the main publication.

A-3. IAEA-TECDOC-1624: PASSIVE SAFETY SYSTEMS AND NATURAL CIRCULATION IN WATER COOLED NUCLEAR POWER PLANTS

This publication provides information on passive safety systems in advanced water cooled reactor designs as the second report from the coordinated research project on Natural Circulation Phenomena, Modelling and Reliability of Passive Safety Systems that Utilize Natural Circulation. The aim of this project was to further understand natural circulation related phenomena of advanced WCRs and to assess the reliability of passive safety systems which utilize natural circulation. It describes common advanced reactor passive safety systems which focus on core heat removal such as accumulators and gravity drain tanks among others. This is followed by a description of containment temperature and pressure suppression passive safety systems. Following the component descriptions, the underlying phenomena of passive safety

systems are discussed and described in terms of their thermohydraulic effects. The publication goes on to identify examples of passive safety systems in advanced designs, identifying which of the phenomena are utilized in each. Extensive descriptions of passive safety systems of a variety of specific reactor designs are included as annexes. This publication provides a useful reference for understanding the phenomena utilized in passive safety systems, as well as informing on the utilization of passive safety systems in various advanced designs.

A-4. IAEA-TECDOC-1677: NATURAL CIRCULATION PHENOMENA AND MODELLING FOR ADVANCED WATER COOLED REACTORS

This publication is the third and final report from the coordinated research project on Natural Circulation Phenomena, Modelling, and Reliability of Passive Safety Systems that Utilize Natural Circulation and summarizes the research projects of participating institutes. It advises on the characterization of natural circulation phenomena with accompanying experimental details, describes a variety of test facilities and plant analyses for natural circulation and passive safety systems, and provides methodologies for the assessment of passive system reliability and application. This publication provides a useful reference for technical and experimentally supported understanding of natural circulation phenomena in advanced WCRs.

A-5. IAEA-TECDOC-1705: PASSIVE SAFETY SYSTEMS IN ADVANCED WATER COOLED REACTORS (AWCRs)

This publication summarizes the results of the IAEA/INPRO collaborative project titled Advanced Water Cooled Reactor Case Studies in Support of Passive Safety Systems. It describes a series of case studies surrounding the phenomena of natural circulation and thermal stratification in three advanced WCR designs: Advanced Heavy Water Reactor (AHWR), Advanced Power Reactor Plus (APR+) and Central Argentina de Elementos Modulares (CAREM). After discussing each of the reactor designs, it provides descriptions of natural circulation and thermal stratification, the phenomena of interest. This is followed by a detailed description of the case studies performed in investigating each of the reactor designs, which utilize both theoretical and experimental methods. This is a useful reference for understanding assessment processes for passive safety systems in advanced WCRs.

A-6. IAEA-TECDOC-1836: DEVELOPING A SYSTEMATIC EDUCATION AND TRAINING APPROACH USING PERSONAL COMPUTER BASED SIMULATORS FOR NUCLEAR POWER PROGRAMMES

This publication contains the proceedings of a Technical Meeting, held in Vienna, 15–19 May 2017 on the use of PC based simulators for nuclear power programmes. The publication is split into three sections, corresponding to the three topical sessions of the meeting: the topic of the first session was on the experiences of simulator use in education and training of national nuclear power programmes; the second topical session covered the use of simulators in teaching reactor technology fundamentals; the third topical session highlighted various available simulator software and their uses for education. This publication provides further information on the application of simulators to education and training.

A-7. IAEA-TCS-65: INTEGRAL PRESSURIZED WATER REACTOR SIMULATOR MANUAL

This Training Course Series publication gives a thorough description of the Integral Pressurized Water Reactor (iPWR) Simulator. This simulator is one of a series of basic principle reactor simulators provided by the IAEA to interested Member States, and is one of those used in support of this present publication. The manual provides users with a more complete description of the simulator's functionality and operation than is present within this publication. The accompanying exercise book additionally provides a series of demonstrational procedures with descriptions of expected simulator responses included.

GLOSSARY

This glossary compiles relevant reference terminology from the IAEA Safety Glossary (2016 Revision), the US NRC Glossary, and other IAEA publications.

accident conditions. Deviations from normal operation that are less frequent and more severe than anticipated operational occurrences.

advanced reactor design. An advanced plant design is a design of current interest for which improvement over its predecessors and/or existing designs is expected. Advanced designs consist of evolutionary design and designs requiring substantial development efforts. The latter can range from moderate modifications of existing designs to entirely new design concepts. They differ from evolutionary designs in that a prototype or demonstration plant is required, or that not sufficient work has been done to establish whether such a plant is required.

anticipated operational occurrence. A deviation of an operational process from normal operation that is expected to occur at least once during the operating lifetime of a facility but which, in view of appropriate design provisions, does not cause any significant damage to items important to safety or lead to accident conditions.

beyond design basis accident. Postulated accident with accident conditions more severe than those of a design basis accident.

boiling water reactor. A common nuclear power reactor design in which water flows upward through the core, where it is heated by fission and allowed to boil in the reactor vessel. The resulting steam then drives turbines, which activate generators to produce electrical power.

controlled state. Plant state, following an anticipated operational occurrence or accident conditions, in which fulfilment of the main safety functions can be ensured and which can be maintained for a time sufficient to implement provisions to reach a safe state.

decay heat. The heat produced by the decay of radioactive fission products after a reactor has been shut down.

defence in depth. A hierarchical deployment of different levels of diverse equipment and procedures to prevent the escalation of anticipated operational occurrences and to maintain the effectiveness of physical barriers placed between a radiation source or radioactive material and workers, members of the public or the environment, in operational states and, for some barriers, in accident conditions.

departure from nucleate boiling. The point at which the heat transfer from a fuel rod rapidly decreases due to the insulating effect of a steam blanket that forms on the rod surface when the temperature continues to increase.

design basis. The range of conditions and events taken explicitly into account in the design of structures, systems and components and equipment of a facility, according to established criteria, such that the facility can withstand them without exceeding authorized limits.

design basis accident. A postulated accident leading to accident conditions for which a facility is designed in accordance with established design criteria and conservative methodology, and for which releases of radioactive material are kept within acceptable limits.

design extension conditions. Postulated accident conditions that are not considered for design basis accidents, but that are considered in the design process of the facility in accordance with best estimate methodology, and for which release of radioactive material are kept within acceptable limits.

emergency core cooling system. Reactor system components (pumps, valves, heat exchangers, tanks, and piping) that are specifically designed to remove residual heat from the reactor fuel rods in the event of a failure of the normal core cooling system.

event tree. An event tree graphically represents the various accident scenarios that can occur as a result of an initiating event (i.e., a challenge to plant operation).

evolutionary design. An evolutionary design is an advanced design that achieves improvements over existing designs through small to moderate modifications with a strong emphasis on maintaining design proveness to minimize technological risks. The development of an evolutionary design requires at most engineering and confirmatory testing.

fault tree analysis. A deductive technique that starts by hypothesizing and defining failure events and systematically deduces the events or combinations of events that caused the failure events to occur.

innovative design. An innovative design is an advanced design which incorporates radical conceptual changes in design approaches or system configuration in comparison with existing practice. Substantial R&D, feasibility tests, and a prototype or demonstration plant are probably required.

loop. In a pressurized water reactor, the coolant flow path through piping from the reactor pressure vessel to the steam generator, to the reactor coolant pump, and back to the reactor pressure vessel. Large PWRs may have as many as four separate loops.

loss of coolant accident. Those postulated accidents that result in a loss of reactor coolant at a rate in excess of the capability of the reactor makeup system from breaks in the reactor coolant pressure boundary, up to and including a break equivalent in size to the double ended rupture of the largest pipe of the reactor coolant system.

normal operation. Operation within specified operational limits and conditions.

operational limits and conditions. A set of rules setting forth parameter limits, the functional capability and performance levels of equipment and personnel approved by the regulatory body for safe operation of an authorized facility.

operational states. States defined under normal operation and anticipated operational occurrences.

risk assessment. Assessment of the radiation risks and other risks associated with normal operation and possible accidents involving facilities and activities.

passive component. A component whose functioning does not depend on an external input such as actuation, mechanical movement or supply of power.

pressurized water reactor. A common nuclear power reactor design in which very pure water is heated to a very high temperature by fission, kept under high pressure, and converted to steam by a steam generator. The resulting steam is used to drive turbines, which activate generators to produce electrical power

pressurizer. A tank or vessel that acts as a head tank (or surge volume) to control the pressure in a pressurized water reactor.

probabilistic safety assessment. A comprehensive, structured approach to identifying failure scenarios, constituting a conceptual and mathematical tool for deriving numerical estimates of risk.

reactor coolant system. The system used to remove energy from the reactor core and transfer that energy either directly or indirectly to the steam turbine.

reactor protection system. System that monitors the operation of a reactor and which, on sensing an abnormal condition, automatically initiates actions to prevent an unsafe or potentially unsafe condition.

safety assessment. Assessment of all aspects of facilities and activities that are relevant to protection and safety; for an authorized facility, this includes siting, design and operation of the facility.

safety culture. The assembly of characteristics and attitudes in organizations and individuals which establishes that, as an overriding priority, protection and safety issues receive the attention warranted by their significance.

safety limit. Limits on operational parameters within which an authorized facility has been shown to be safe.

safe state. Plant state, following an anticipated operational occurrence or accident conditions, in which the reactor is subcritical and the main safety functions can be ensured and maintained stable for a long time.

safety system. A system important to safety, provided to ensure the safe shutdown of the reactor or the residual heat removal from the reactor core, or to limit the consequences of anticipated operational occurrences and design basis accidents.

safety system setting. Settings for levels at which safety systems are automatically actuated in the event of anticipated operational occurrences or design basis accidents, to prevent safety limits from being exceeded.

scram. A rapid shutdown of a nuclear reactor in an emergency.

severe accident. Accident more severe than a design basis accident and involving significant core degradation.

small modular reactor. Advanced nuclear reactors with electric power of up to 300 MW_e, built as modules in a factory setting then shipped to sites as demand arises, aiming for the economy of multiple by shortening construction schedule.

station blackout. The loss of all on-site and off-site AC power sources.

steam generator. The heat exchanger used in some reactor designs to transfer heat from the primary (reactor coolant) system to the secondary (steam) system. This design permits heat exchange with little or no contamination of the secondary system.

validation. The process of determining whether a product or service is adequate to perform its intended function satisfactorily.

verification. The process of determining whether the quality or performance of a product or service is as stated, as intended or as required.

ABBREVIATIONS

ADS	Automatic depressurization system
ARIS	Advanced Reactors Information System
BDBA	Beyond design basis accident
BWR	Boiling water reactor
CDF	Core damage frequency
CET SEQ	Containment event tree sequence
CFD	Computational fluid dynamics
CMT	Core make up tank
CNR	Condenser system
DBA	Design basis accident
DCC	Direct contact condensation model
DHRS	Decay heat removal system
DNS	Direct numerical simulation
ECCS	Emergency core cooling system
ESBWR	Economic Simplified Boiling Water Reactor
ESWS	Emergency service water system
FCVS	Filtered containment venting system
FDM	Finite difference method
FEM	Finite element method
FREQ	Frequency
FVM	Finite volume method
GDCS	Gravity driven cooling system
GEN	Generator system
GIS	Gravity driven water injection system
HEM	Homogeneous equilibrium mixture model
IAEA	International Atomic Energy Agency
IC	Isolation condenser
IRWST	In-containment refuelling water storage tank
iPWR	Integral Pressurized Water Reactor
LES	Large eddy simulation
LOCA	Loss of coolant accident
LWR	Light water cooled reactor
MSLB	Main steam line break

NRC	Nuclear Regulatory Commission (United States of America)
NS	Navier–Stokes equations
OLC	Operational limits and conditions
OSU	Oregon State University (United States of America)
PCCS	Passive containment cooling system
PDS	Plant damage state
PIEAS	Pakistan Institute of Engineering and Applied Sciences
PORV	Pilot operated relief valve
PRA	Probability risk assessment
PRHR	Passive residual heat removal system
PSA	Probabilistic safety analysis
PTS	Pressurized thermal shock
PWR	Pressurized water reactor
RANS	Reynolds Averaging Navier–Stokes equation
RCS	Reactor coolant system
REL CAT	Release category
RPS	Reactor protection system
RPV	Reactor pressure vessel
RSM	Reynold’s stress model
SBLOCA	Small break loss of coolant accident
SMR	Small (and medium or) modular reactor
TMI	Three Mile Island Nuclear Generating Station
V&V	Verification and validation
VOF	Volume of fluid
WCR	Water cooled reactor

CONTRIBUTORS TO DRAFTING AND REVIEW

Jevremovic, T.	International Atomic Energy Agency
Krause, M.	International Atomic Energy Agency
Memmott, M.	Brigham Young University, United States of America
Qureshi, K.	Pakistan Institute of Engineering & Applied Sciences, Pakistan
Schow, R.	SHINE Medical Technologies, United States of America
Shah, A.	Pakistan Institute of Engineering & Applied Sciences, Pakistan
Takasugi, C.	International Atomic Energy Agency



IAEA

International Atomic Energy Agency

No. 25

ORDERING LOCALLY

In the following countries, IAEA priced publications may be purchased from the sources listed below or from major local booksellers.

Orders for unpriced publications should be made directly to the IAEA. The contact details are given at the end of this list.

CANADA

Renouf Publishing Co. Ltd

22-1010 Polytek Street, Ottawa, ON K1J 9J1, CANADA

Telephone: +1 613 745 2665 • Fax: +1 643 745 7660

Email: order@renoufbooks.com • Web site: www.renoufbooks.com

Bernan / Rowman & Littlefield

15200 NBN Way, Blue Ridge Summit, PA 17214, USA

Tel: +1 800 462 6420 • Fax: +1 800 338 4550

Email: orders@rowman.com Web site: www.rowman.com/bernan

CZECH REPUBLIC

Suweco CZ, s.r.o.

Sestupná 153/11, 162 00 Prague 6, CZECH REPUBLIC

Telephone: +420 242 459 205 • Fax: +420 284 821 646

Email: nakup@suweco.cz • Web site: www.suweco.cz

FRANCE

Form-Edit

5 rue Janssen, PO Box 25, 75921 Paris CEDEX, FRANCE

Telephone: +33 1 42 01 49 49 • Fax: +33 1 42 01 90 90

Email: formedit@formedit.fr • Web site: www.form-edit.com

GERMANY

Goethe Buchhandlung Teubig GmbH

Schweitzer Fachinformationen

Willstätterstrasse 15, 40549 Düsseldorf, GERMANY

Telephone: +49 (0) 211 49 874 015 • Fax: +49 (0) 211 49 874 28

Email: kundenbetreuung.goethe@schweitzer-online.de • Web site: www.goethebuch.de

INDIA

Allied Publishers

1st Floor, Dubash House, 15, J.N. Heredi Marg, Ballard Estate, Mumbai 400001, INDIA

Telephone: +91 22 4212 6930/31/69 • Fax: +91 22 2261 7928

Email: alliedpl@vsnl.com • Web site: www.alliedpublishers.com

Bookwell

3/79 Nirankari, Delhi 110009, INDIA

Telephone: +91 11 2760 1283/4536

Email: bkwell@nde.vsnl.net.in • Web site: www.bookwellindia.com

ITALY

Libreria Scientifica "AEIOU"

Via Vincenzo Maria Coronelli 6, 20146 Milan, ITALY

Telephone: +39 02 48 95 45 52 • Fax: +39 02 48 95 45 48

Email: info@libreriaaeiou.eu • Web site: www.libreriaaeiou.eu

JAPAN

Maruzen-Yushodo Co., Ltd

10-10 Yotsuyasakamachi, Shinjuku-ku, Tokyo 160-0002, JAPAN

Telephone: +81 3 4335 9312 • Fax: +81 3 4335 9364

Email: bookimport@maruzen.co.jp • Web site: www.maruzen.co.jp

RUSSIAN FEDERATION

Scientific and Engineering Centre for Nuclear and Radiation Safety

107140, Moscow, Malaya Krasnoselskaya st. 2/8, bld. 5, RUSSIAN FEDERATION

Telephone: +7 499 264 00 03 • Fax: +7 499 264 28 59

Email: secnrs@secnrs.ru • Web site: www.secnrs.ru

UNITED STATES OF AMERICA

Bernan / Rowman & Littlefield

15200 NBN Way, Blue Ridge Summit, PA 17214, USA

Tel: +1 800 462 6420 • Fax: +1 800 338 4550

Email: orders@rowman.com • Web site: www.rowman.com/bernan

Renouf Publishing Co. Ltd

812 Proctor Avenue, Ogdensburg, NY 13669-2205, USA

Telephone: +1 888 551 7470 • Fax: +1 888 551 7471

Email: orders@renoufbooks.com • Web site: www.renoufbooks.com

Orders for both priced and unpriced publications may be addressed directly to:

Marketing and Sales Unit

International Atomic Energy Agency

Vienna International Centre, PO Box 100, 1400 Vienna, Austria

Telephone: +43 1 2600 22529 or 22530 • Fax: +43 1 2600 29302 or +43 1 26007 22529

Email: sales.publications@iaea.org • Web site: www.iaea.org/books

